AD-760 563

DUAL DIAMETER ROLLER BEARING - 3.5 MILLION DN-600F

John Rumberger, et al

Franklin Institute Research Laboratories

Prepared for:

Air Force Aero Propulsion Laboratory

May 1973

AFAPL-TR-73-23

AD 760563

DUAL DIAMETER ROLLER BEARING - 3.5 MILLION DN-600°F

John Rumbarger
Edmund Filetti
James Dunfee
David Gubernick

Franklin Institute Research Laboratory

TECHNICAL REPORT AFAPL-TR-73-23

May 1973

Approved for public release:
distribution unlimited

Air Force Aero Propulsion Laboratory
Air Force Systems Command
Wright-Patterson Air Force Base, Ohio

Details of illustrations in
this document may be better
studied on microfiche

UNCLASSIFIED

Security Classification

DOCUMENT CONTROL DATA - R & D

(Security classification of title, body of abstract and indexing annotation must be entered when the overall report is classified)

1. ORIGINATING ACTIVITY (Corporate author) The Franklin Institute 20th & The Parkway Philadelphia, Pa. 19103	2a. REPORT SECURITY CLASSIFICATION UNCLASSIFIED 2b. GROUP N/A

3. REPORT TITLE

DUAL DIAMETER ROLLER BEARING - 3.5 MILLION DN-600°F

4. DESCRIPTIVE NOTES (Type of report and inclusive dates)

Final Report, June 23, 1971 - December 31, 1972

5. AUTHOR(S) (First name, middle initial, last name)

John Rumberger, Edmund Filetti, James Dunfee, David Gubernick

6. REPORT DATE	7a. TOTAL NO. OF PAGES	7b. NO. OF REFS
May 1973	173	11

8a. CONTRACT OR GRANT NO. F-33615-71-C-1883	9a. ORIGINATOR'S REPORT NUMBER(S) F-C3132
b. PROJECT NO. 3048	
c. Task No. 304806	9b. OTHER REPORT NO(S) (Any other numbers that may be assigned this report) AFAPL-TR-73-23
d.	

10. DISTRIBUTION STATEMENT

Approval for public release: distribution unlimited

11. SUPPLEMENTARY NOTES	12. SPONSORING MILITARY ACTIVITY
Details of illustrations in this document may be better studied on microfiche	Air Force Aero Propulsion Laboratory Air Force Systems Command Wright-Patterson Air Force Base, Ohio

13. ABSTRACT

Five gas turbine engine mainshaft roller bearing configurations were investigated for capability of sustained performance at DN values (Bore in mm x Speed in RPM) from 2 million to 3.5 million and normal operating temperatures to 600°F. A unique Dual Diameter Roller was selected for the final analysis of stress and lubrication parameters, design and fabrication. A 140 mm Bore Dual Diameter Roller Bearing operated successfully for 30 min. continuous operation at 25,000 RPM (3.5 million DN) with stabilized outer race temperatures above 525°F. Lubrication was with Polyphenyl Ether 5P4E in an air environment.

14 KEY WORDS	LINK A		LINK B		LINK C	
	ROLE	WT	ROLE	WT	ROLE	WT
Elastohydrodynamic Lubrication Dual Diameter Roller Polyphenyl Ether MIL-L-7808 3.5 Million DN 600°F						

DUAL DIAMETER ROLLER

BEARING - 3.5 MILLION DN-600°F

John Rumbarger
Edmund Filetti
James Dunfee
David Gubernick

lc

FOREWORD

This report was prepared by the Franklin Institute Research Laboratories, 20th and Benjamin Franklin Parkway, Philadelphia, Pa. 19103 under USAF Contract F-33615-71-C-1883. The work was administered under the direction of the Air Force Aero Propulsion Laboratory, with Mr. John Jenkins and Mr. M. R. Chasman (AFAPL/SFL) acting as project engineers.

This report covers work conducted from 23 June 1971 - 31 December 1972.

The Franklin Institute Research Laboratories was prime contractor and performed all of the analysis and design. The prototype test bearings were manufactured by the Bower Bearing Div., Federal-Mogul Corp., Detroit, Mich. The prototype testing was accomplished by subcontractor Midwest Aero Industries Div., Pure Carbon Company, Saint Mary's, Pa. The testing was under the direction of Mr. Donald Moyer of MAIC.

Publication of this report does not constitute Air Force Approval of the report's findings or conclusions. It is published only for the exchange and stimulation of ideas.

HOWARD F. JONES, CHIEF
Lubrication Branch
Fuels and Lubrication Division

ABSTRACT

Five gas turbine engine mainshaft roller bearing configurations were investigated for capability of sustained performance at DN values (Bore in mm x Speed in RPM) from 2 million to 3.5 million and normal operating temperatures to 600°F. A unique Dual Diameter Roller was selected for the final analysis of stress and lubrication parameters, design and fabrication. A 140 mm Bore Dual Diameter Roller Bearing operated successfully for 30 min. continuous operation at 25,000 RPM (3.5 million DN) with stabilized outer race temperatures above 525°F. Lubrication was with Polyphenyl Ether 5P4E in an air environment.

CONTENTS

Section	Title	Page
I	INTRODUCTION	1
II	SELECTION OF PRELIMINARY CONFIGURATION	4
	1. Candidate Bearing Configurations	4
	2. Load Life Parametric Study	13
	3. Cage-Slip and Horsepower Loss Study	17
	4. Series Hybrid Bearing	21
	5. Selection of Dual Diameter Roller Bearing	26
III	LUBRICANT SELECTION	27
IV	DUAL DIAMETER BEARING ANALYSIS AND DESIGN	32
	1. Design Considerations	32
	2. Inner Race Stresses	35
	3. Lubrication	36
	4. Performance Analysis	40
	5. EHD Parameters	48
	6. Design Drawings	48
V	DUAL DIAMETER BEARING FABRICATION	57
VI	DUAL DIAMETER BEARING TESTS	65
	1. Test Rig	65
	2. MIL-L-7808, Test Bearing A1	69
	3. 5P4E, Test Bearing A1	69
	4. 5P4E, Test Bearing C3	82
VII	CONCLUSIONS	87
	APPENDIX I - TEST LOGS	88

Preceding page blank

CONTENTS (CONT'D.)

Section	*Title*	*Page*
	APPENDIX II - GAS TURBINE ENGINE MAINSHAFT ROLLER BEARING-SYSTEMS ANALYSIS	111
VIII	REFERENCES	175

FIGURES

Figure No.	Title	Page
1(a)	Solid Rollers - Inner Land Riding Cage.	5
1(b)	Solid Rollers - Outer Land Riding Cage.	6
1(c)	Hollow Roller Concept	7
1(d)	Series Hybrid Bearing	9
2	Dual Diameter Roller Bearing Configuration.	10
3	Kinematics of Dual Diam. Roller	11
4	Relative Kinematics of Two Diameter Roller.	12
5	Bearing Life vs. Roller Diam. (Hollow Rollers).	15
6	Bearing Life vs. Roller Diam. (Dual Diam. Rollers). . . .	16
7	Cage Slip % vs. Radial Load	20
8	Cage Speed in RPM vs. Radial Load	22
9	HP Loss vs. Speed	23
10	Friction Loss vs. Speed Ratio, MIL-L-7808 Oil	25
11	Bearing Life with 5P4E Lubricant.	30
12	Inner Race Maximum Tangetial Stress Vs. Shaft Speed . . .	34
13	Finite Element Analysis of Inner Race Tangential Stresses at 4.0 x 10^6 DN	37
14	Thermal Nodes and Methods of Lubrication.	39
15	Effect of Oil Flow Upon Outlet Temperature and Bearing Power Loss.	42
16	Dual Diameter Roller Bearing Frictional Horsepower Losses	46

FIGURES

Figure No.	*Title*	*Page*
17	Two-Diameter Roller Bearing Assembly	52
18	Inner Ring, Two Diameter Roller Bearing	53
19	Outer Ring, Two Diameter Roller Bearing	54
20	Two Diameter Roller	55
21	Cage, Two Diameter Roller Bearing	56
22	Dual Diameter Roller Bearing Assembly	58
23	Bearing No. C3 Inner Race Circularity	60
24	Bearing No. C3 Inner Raceway Contour	61
25	Bearing No. C3 Outer Race Circularity	62
26	Bearing No. C3 Outer Raceway Contour	63
27	Typical Dual-Diameter Roller Crown Profile Traces	64
28	Dual Diameter Roller Bearing Test Stand	66
29	Dual Diameter Roller Bearing Instrumentation	67
30	Cross Section of Dual Diameter Bearing Test	68
31	Test Bearing No. 1, ΔT vs. Speed, MIL-L-7808 G	71
32	Test Bearing No. 1, ΔT vs. Speed, Polyphenyl Ether, 5P4E	74
33	Test Bearing No. 1, Inner Race Failure	75
34	Test Bearing No. 1, Outer Race Cage Roller Assembly Failure	76
35	Failed Rollers	77
36	Test Bearing No. 1, Outer Ring Failure	78

FIGURES

Figure No.	*Title*	*Page*
37	Test Bearing No. 1 Cage Failure	79
38	Test Bearing No. 2 ΔT vs. Speed, Polyphenyl Ether, 5P4E	84
39	Second Dual Diameter Test Bearing	85

TABLES

Table No.	*Title*	*Page*
I	Bearing Operating Requirements	2
II	Duty Cycle at 4.0 x 10^6 DN	14
III	Schedule of Computer Runs	18
IV	Summary of Computer Results	19
V	Summary of Test Results	28
VI	Properties of Test Lubricants	29
VII	Lubricant Properties Used in the Analysis	31
VIII	Properties of M-50 Hardened to RC-60 Per VASCO Technical Bulletin	35
IX	Inner Race Tangential Stress (ksi)	38
X	Effect of Oil Flow Rate on Bearing Performance	41
XI	Oil Flow Rate vs. Speed (DN)	41
XII	Summary of Performance Analysis Computer Runs	43
XIII	Summary of Temperature Profiles for Dual Diameter Roller Bearing	45
XIV	Symmary of Cage Analysis	47
XV	Traction Values - Outer Race Contact - Unloaded Rollers	49
XVI	Traction Values - Outer Race Contact - Maximum Loaded Rollers	50
XVII	Traction Values - Inner Race Contact - Maximum Loaded Rollers	51
XVIII	Summary of Test Bearing Dimensional Tolerances	59
XIX	Data Summary Sheet First Test Bearing - MIL-L-7808 Oil	70

TABLES

Table No.	*Title*	*Page*
XX	Data Summary Sheet First Test Bearing - Polyphenyl Ether 5P4E	73
XXI	Thermal Analysis of First Test Bearing Conditions with 5P4E	81
XXII	Data Summary Sheet, Second Test Bearing Polyphenyl Ether 5P4E	83

SECTION I

INTRODUCTION

The objective of this research program was to develop a long life, high speed roller bearing design for future high performance turbine engines. The bearing must be capable of sustained performance at DN values from 2.0×10^6 to above 3.5×10^6 and normal operating temperatures to 600 F while maintaining the rotating shafts within the necessary tolerance for optimum compressor and turbine performance.

The trends in turbine engine technology are toward increased rotational speed, larger bearing diameters and increased bearing temperature. It is anticipated that bearing DN requirements (bearing bore mm x rpm) will grow from the current 2×10^6 or less to greater than 3.5×10^6 in the 1980's. Efforts to increase bearing DN capability are currently aimed at ball bearings. Approaches being investigated for ball bearings include hollow balls and compliant races. The roller bearing has received very little attention. Efforts which have focused on roller bearings indicate that variations in roller bearing geometry such as the dual diameter roller and hollow rollers, show promise for significant increases in bearing performance. Improved ball and roller bearing capability is required for future systems.

Known current roller bearing types were investigated in order to select a preliminary configuration for further development. The selection was based on the potential of each type to meet the capabilities shown in Table I. A bearing bore of 140 mm was selected for this preliminary configuration study.

The results of the preliminary configuration study resulted in the selection of the dual diameter roller bearing concept for further consideration. This selection was based upon lower cage speeds obtained in the dual diameter bearing which result in significantly lower [illegible] mechanic losses (viscous loss due to shearing of the oil). These lower drags or losses in turn result in a lower cage slip threshold.

Table I

BEARING OPERATING REQUIREMENTS

Normal Operating Temperature	600°F
Operating Temperature Range	-65 to +800°F
Normal Operating DN (mm x rpm)	4.0×10^6
Operating Radial Load Range (lb.)	0 to 2000
L_{10} Life, Hr. (greater than)	1000
Radial Deflection at Max. Load, (in.)	0.010
Minimum Heat Generation	

The dual diameter roller bearing configuration was subjected to a thorough analysis from which a final design was developed. A complete systems analysis incorporating the latest available elastohydrodynamic lubrication technology and including fluid drag forces and thermal effects was accomplished by means of a digital computer program (Reference 1). This analysis was used to finalize the bearing design and determine operating clearances and oil flow or lubrication requirements of the bearing. Complete detailed working drawings of the prototype test bearings are contained in the body of this report.

Six prototype dual diameter roller bearings were manufactured by the Federal-Mogul Corporation, Bower Bearings Div., Detroit, Michigan, to the drawings and specifications contained in this report. A summary of inspection data relating to dimensional quality of the test bearings is also included.

Two dual diameter prototype roller bearings were tested by the Midwest Aero Industries Div., Pure Carbon Co., St. Mary's, Pa. on a special high speed mainshaft test rig. The test bearings were operated initially with MIL-L-7808 lubricant at 250°F oil inlet and then later with Polyphenyl Ether 5P4E lubricant at 600°F.

SECTION II

SELECTION OF PRELIMINARY CONFIGURATION

1. CANDIDATE BEARING CONFIGURATIONS

Five basic concepts or candidate bearing configurations, as shown on Figure 1(a-d), were investigated. The reasons for considering the various configurations are listed below:

a. Solid rollers - inner land riding cage: The inner land riding cage solid roller concept, Figure 1a, is one of the most commonly used mainshaft roller bearing designs. This design consists of an inner race with two integral shoulders to guide the roller complement. The one piece fully machined cage has close clearance and rides on an oil film in contact with the lands on the inner race. The outer race is a sleeve construction which allows complete axial freedom of the inner race and roller complement. It is common in some designs to provide coolant flow through slots under the inner race since the inner race operating temperature is approximately 50°F hotter than the outer race operating temperature. An advantage of this type of cage construction is the fact that friction in the cage to land areas will help to drive the cage at synchronous or epicyclic speed.

b. Solid roller - outer land riding cage: This outer land riding concept, Figure 1b, is very similar to the concept above; the main difference being that the integral guiding flanges and the cage to race land guidance are on the outer race. This bearing configuration is also common in modern jet engines. The advantage of this type of construction is better retention of oil at the outer race contact (due to centrifugal forces) under momentary oil starvation. Also some engine applications are more easily assembled with this type of roller guidance. It should be noted that in this configuration the friction in the cage to land surfaces is a dissipative effect which will tend to place a drag on the cage and add to the cage slipping tendency.

c. Hollow roller concept: The roller bearing concept is shown in Figure 1c. This concept can be applied to either an inner land riding cage or an outer land riding cage configuration. Basically the use of a hollow roller reduces the outer race to roller loading. The centrifugal force on the outer race due to

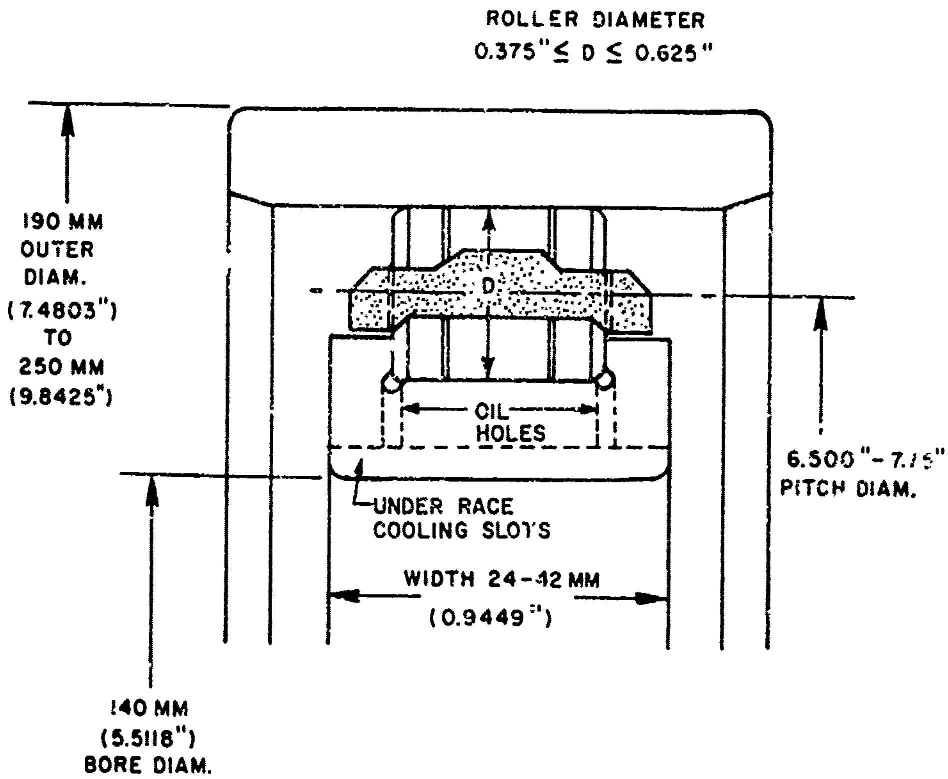

Figure 1(a). Solid Rollers - Inner Land Riding Cage

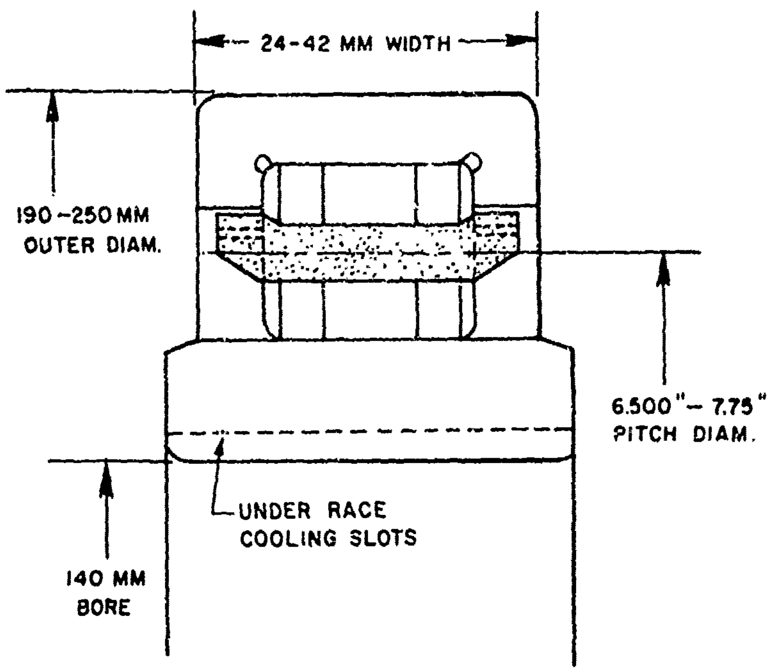

Figure 1(b). Solid Rollers - Outer Land Riding Cage

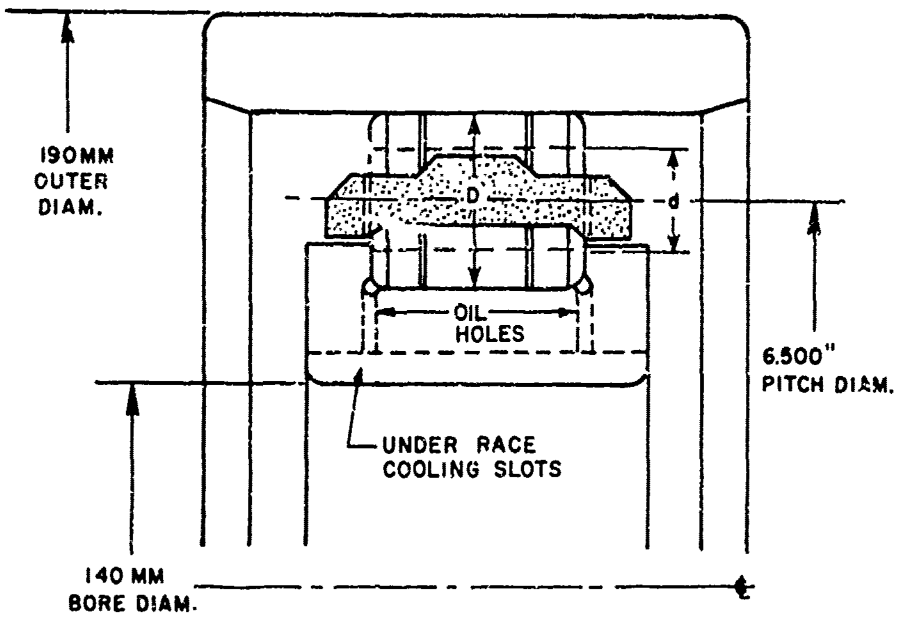

HOLLOW ROLLER CONCEPT
(Reduce Roll Mass)

Figure 1(c). Hollow Roller Concept

the cage and roller complement rotative speed results in significant contact loading. Hollow rollers of less mass than solid rollers are found to be beneficial. A note of caution is indicated in that prior experience shows that too thin a wall section in the hollow rollers will lead to roller breakage due to reverse bending of the rings. Thus mass reduction must be compromised with ring bending fatigue properties. Attempts have been made in the past to use three or more oversized hollow rollers equally spaced in a solid roller complement to provide rollers which are always under load and essentially drives the cages up to cyclic speed. The effect which was analyzed in the preliminary selection of configurations was the mass reduction effect only.

d. Series hybrid bearing: The series hybrid bearing is a relatively new concept, Figure 1d, for reducing the effective speed of rotation at the inner race of a mainshaft roller bearing. This concept consists of a rolling element bearing and an oil film journal bearing in series. The inner race of the roller bearing is separated from the outer surface of the rotating shaft by means of the hydrodynamic oil film bearing. Both bearings carry the full radial load, however, the inner race of the rolling bearing will rotate at some intermediate speed to the shaft speed resulting in a lower effective DN operating regime for the roller bearing. The speed reduction is the main advantage of this configuration. Additional under race cooling of the inner race can also be accomplished if locating oil film thrust bearing surfaces are built as pumps to supply additional coolant flow under the inner race. These locating thrust bearings to maintain the location of the inner race are not shown on Figure 1d. The main disadvantage is the obvious one of mechanical complexity.

e. Dual diameter roller concept: The dual diameter roller concept is shown in Figure 2. This is basically a wagon wheel shaped roller with a large central diameter and two smaller diameters which look very much like an axle through the main wheel. The purpose of this configuration is to reduce cage operating speed. A reduction in cage orbital speed results in a significant reduction of the outer race to roller contact load due to centrifugal effects.

The relative kinematics of a conventional roller bearing and a dual diameter roller bearing are shown in Figure 3. The large outer diameter of the two-diameter roller contacts the inner race surface. The small roller diameters of the two-diameter roller contact the outer race surface. The effects of the relative kinematics are shown graphically in Figure 4. With a small roller (50% of the major roller diameter) it can

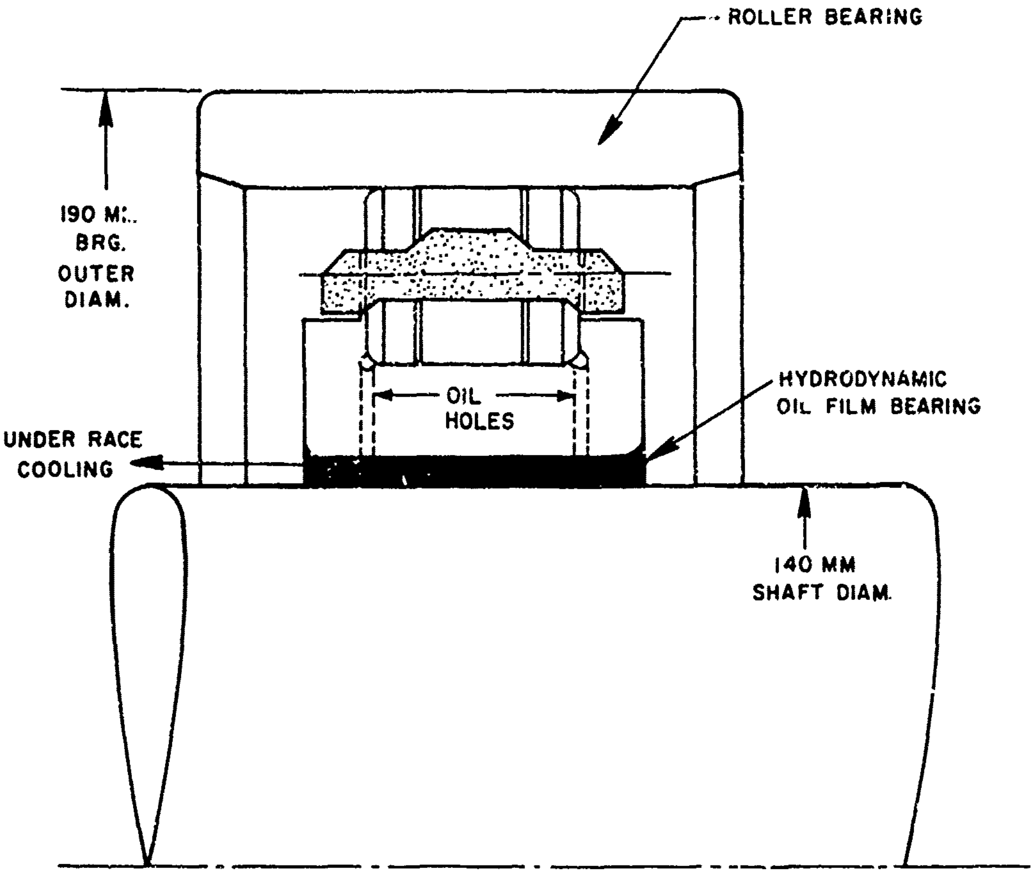

SERIES HYBRID BEARING
(Reduce Roller Bearing
Inner Race Speed)

Figure 1(d). Series Hybrid Bearing

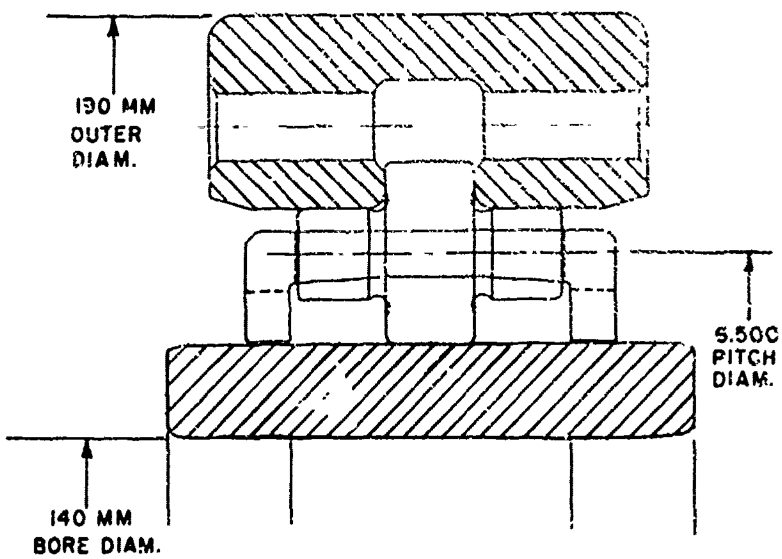

Figure 2. Dual Diameter Roller Bearing Configuration

Solid Roller	Two Diam. Roller
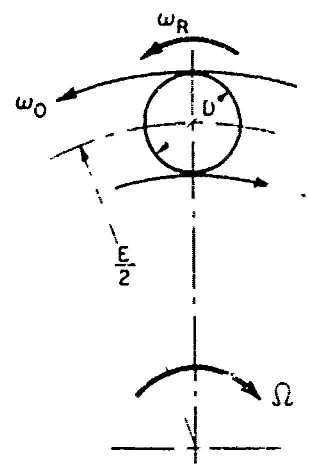 Solid Roller	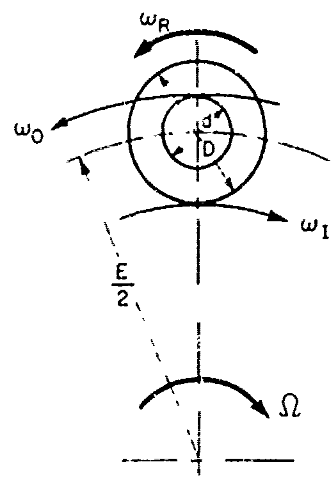 Two Diam. Roller
$\gamma = D/E$	$\gamma' = d/E \quad \phi = d/D$
$\omega_o = \frac{\gamma\ \omega_R}{(1 + \gamma)}$	$\omega_o = \frac{\gamma'\ \omega_R}{(1 + \gamma')}$
$\omega_I = \frac{\gamma\ \omega_R}{(1 - \gamma)}$	$\omega_I = \frac{\gamma\ \omega_R}{(1 - \gamma)}$
$\Omega = \omega_o + \omega_I$	$\Omega = \omega_o + \omega_I$
$\omega_R = \frac{\Omega\ (1 - \gamma^2)}{2\ (\gamma)}$	$\omega_R = \frac{\Omega\ (1 - \gamma)\ (1 + \phi\gamma)}{(1 + \phi)\ (\gamma)}$
$\omega_c = -\ \omega_o$	$\omega_c = -\ \omega_o$
$\omega_c = -\ \frac{\Omega}{2}\ (1 - \gamma)$	$\omega_c = -\ \frac{\phi\ (1 - \gamma)}{(1 + \phi)}\ \Omega$
Assumes Zero Slip	

Figure 3. Kinematics of Dual Diam. Roller

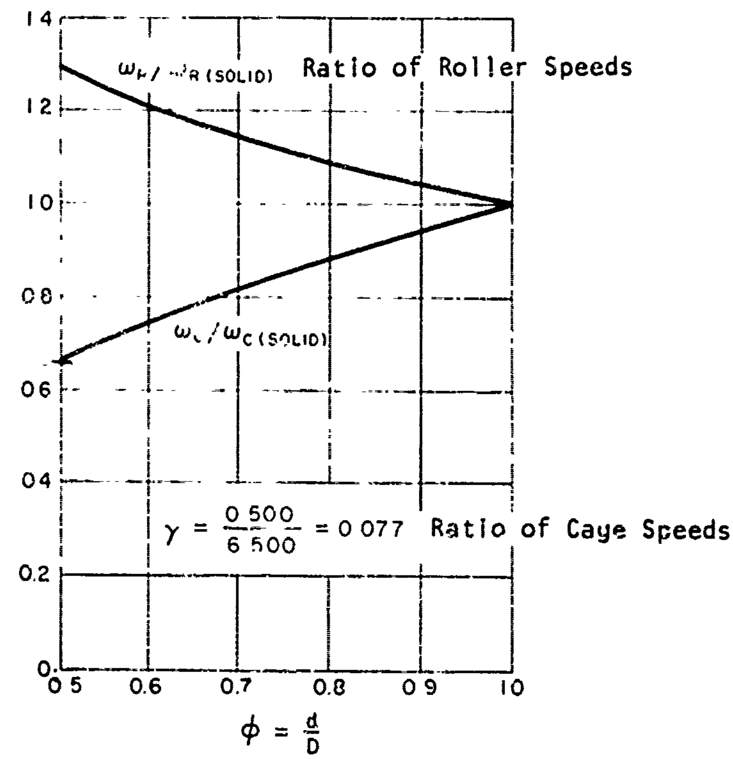

Figure 4. Relative Kinematics of Dual Diameter Roller

be seen that for the same inner race speed, a cage rotative speed 1/3 less than that of the conventional bearing can be achieved. At the same time the roller rotative speed about its own axis is about 1/3 greater in the dual diameter roller than in the conventional roller design. This increased roller rotative speed enhances the entrainment velocity which is important in the development of a full elastohydrodynamic oil film in the contacts. Higher entrainment velocities of the two-diameter roller will essentially result in thicker EHD oil films in the contact. Thus a 4.0×10^6 DN bearing of the two-diameter roller configuration will result in cage rotative speeds and resulting centrifugal effects at the roller to outer race contact comparable to those found in a 2.67×10^6 DN bearing of conventional design.

2. LOAD-LIFE PARAMETRIC STUDY

Initial calculations indicated that the requirements for greater than 1,000 hours L-10 operating life at 4.0×10^6 DN could not be achieved with 2,000 lbs. radial load. The 2,000 lb. load is representative of momentary maneuvering loads and not intended as a long time operating load condition for design of mainshaft bearings. The duty cycle given in Table II was used for the parametric study.

A special short length computer program was used for the parametric study and consisted of a full load deflection analysis of the bearing with elastohydrodynamic films in the race roller contacts. The EHD film thicknesses were computed per the classical isothermal Dowson-Higginson formulas (Reference 2). This is a simplification in that no cage slip was considered. However, for the purposes of load life studies this is a valid assumption especially for preliminary configuration selection. The three radial loads identified in Table II were used to analyze the operating L-10 life and the results were prorated over the percentages of operating times (Reference 3). The figures presented are in terms of the prorated life over the duty cycle.

Table II

DUTY CYCLE AT 4.0 x 10^6 DN

% Time	Radial Load
10	2000 pounds
20	1000 pounds
70	500 pounds

The parametric studies were run with the following assumptions:

- Constant pitch diameter = 6.50 inches ≡ E
- Number of rollers = π times E divided by 1.5 times D
- Effective length of contact = roller diameter (D)
- 4 x 10^6 DN (28,740 shaft rpm at 140 mm bore)
- Dual diameter roller .8D outer length, .5D inner length

The L-10 prorated bearing life over the entire duty cycle in hours for the hollow roller concept is shown in Figure 5 where bearing life is plotted as a function of roller diameter. The bottom curve on Figure 5 represents a solid roller of the configurations described in Figure 1a and 1b. A similar plot of the L-10 prorated bearing life over the duty cycle for the dual diameter roller bearing is shown in Figure 6. An obvious knee in the curves is apparent for all of the roller concepts at a roller diameter of 0.5 inches. This can be explained in terms of the exponential reduction in life with increasing load. The larger diameter rollers have a higher outer race contact load because of increased centrifugal force and over 0.5 inch roller diameter this increase in centrifugal effects is greater than the corresponding increase in dynamic capacity of the roller race contact.

The results of the parametric study in terms of the design goal of more than 1,000 hours L-10 life are (a) roller diameter must be 0.5 inches or less for all configurations, (b) solid rollers are not acceptable in any diameter size, (c) hollow rollers should be 0.5 to 0.7 hollow, (d) dual diameter rollers with 0.5 to 0.6 small to large diameter roller ratio

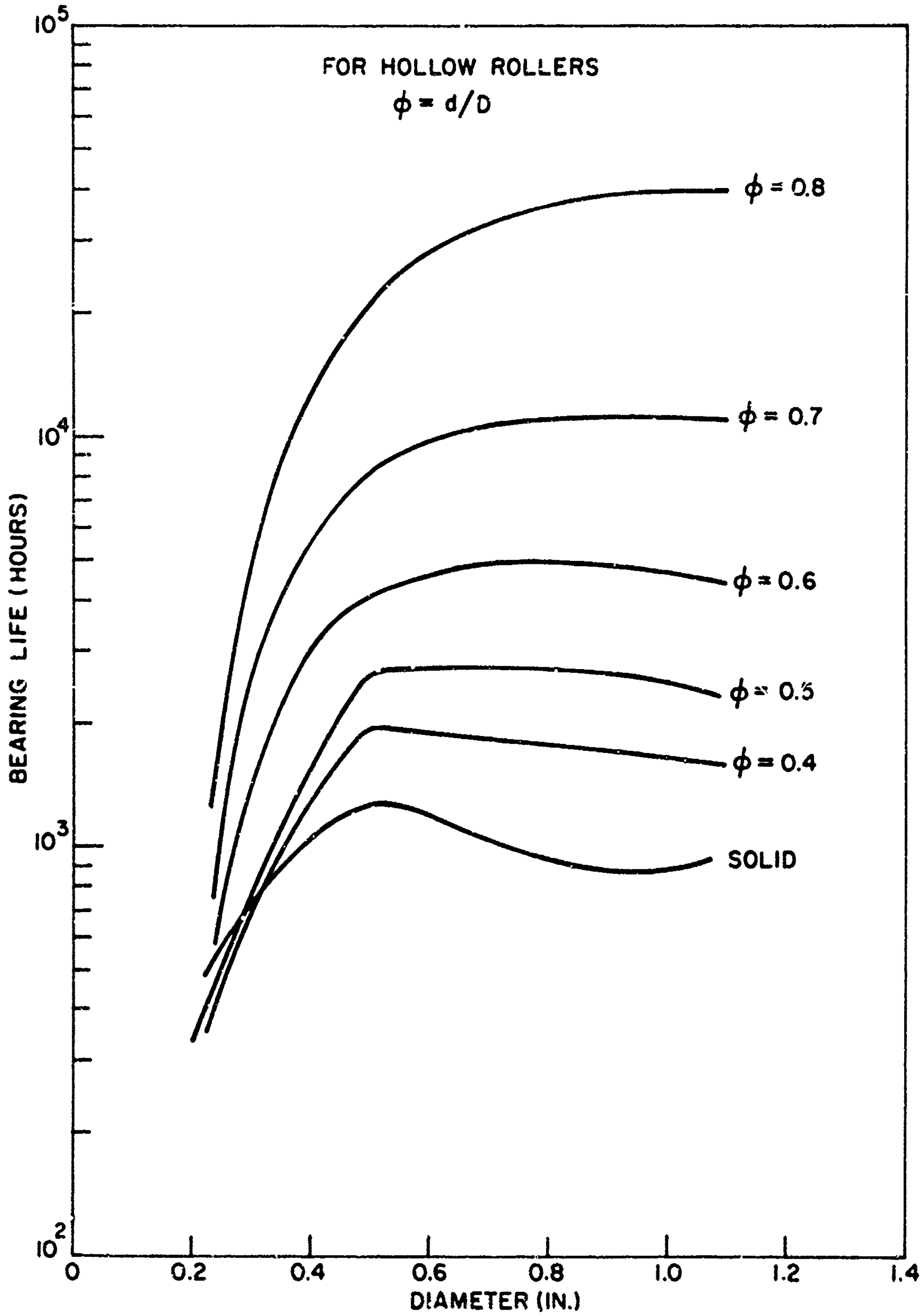

Figure 5. Bearing Life vs. Roller Diam. (Hollow Rollers)

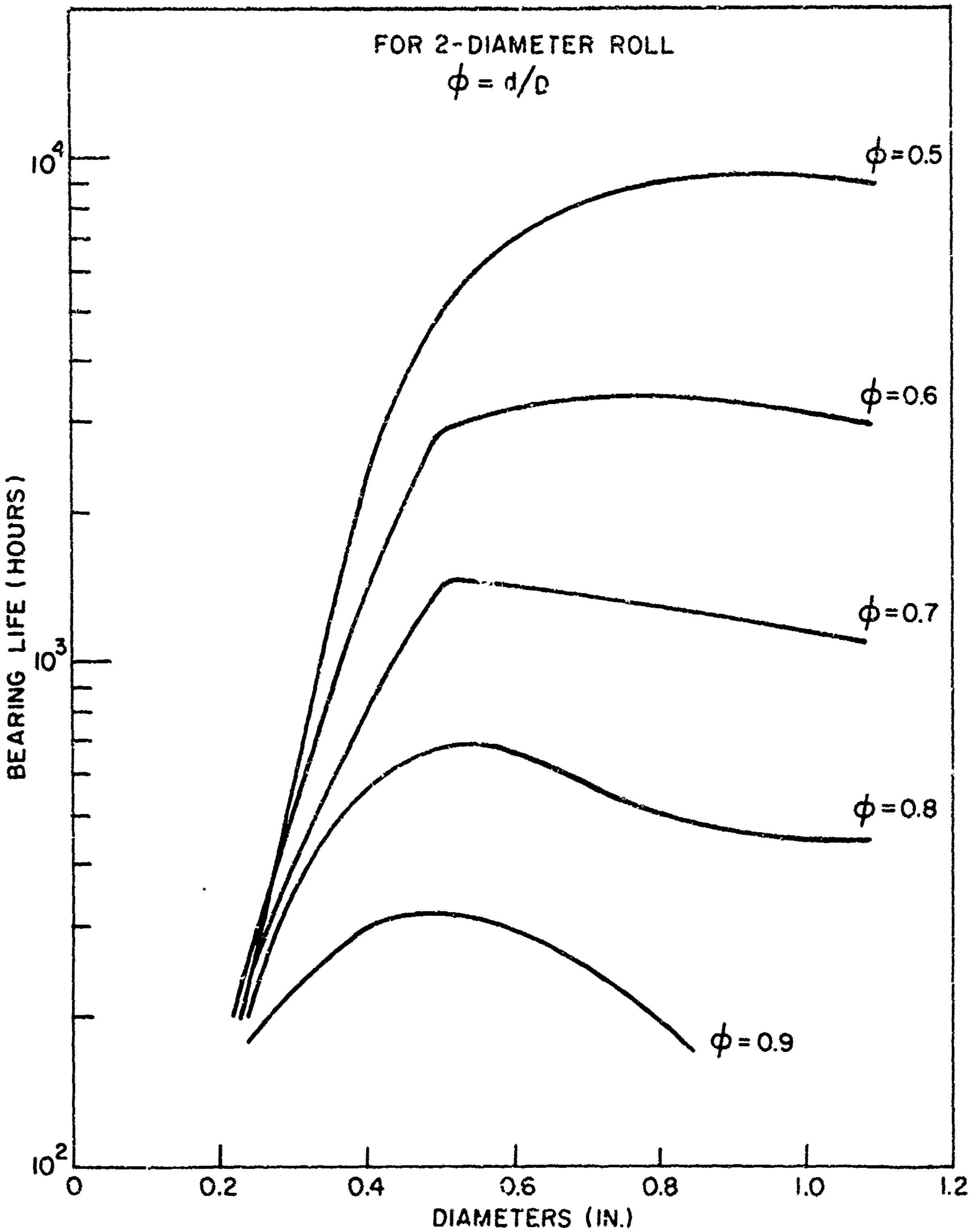

Figure 6. Bearing Life vs. Roller Diam. (Dual Diam. Rollers)

are of interest, (e) the requirement for 0.01 inches maximum radial deformation under 2,000 lbs. load indicates that hollow rollers over 0.7 hollowness are not recommended. The parametric life study also shows that L-10 fatigue life can be a limiting factor at 4.0 x 10^6 DN operation.

3. CAGE-SLIP AND HORSEPOWER LOSS STUDY

The most promising configurations resulting from the parametric study were used in a full EHD computer analysis (Reference 1) containing the latest available elastohydrodynamic (EHD) technology (Reference 4). The majority of the computer runs were made with MIL-L-7808 oil at 250°F oil inlet temperature. One check run each for a single diameter and a dual diameter roller configuration were made with Polyphenyl Ether 5P4E lubricant at 500°F oil inlet temperature. The actual run data is summarized in Table III, which also contains a summary of results including percentage cage slip and horsepower dissipation. More detailed information is summarized in Table IV. L-10 life, roller load, film thickness, and specific film thickness data as well as sliding speeds at both the outer and inner races are given for the maximum loaded roller.

The primary problem encountered in high speed mainshaft roller bearings is cage slip. This is the phenomena which results in high sliding velocities between the rollers and the inner race contacts. Severe glazing and micro-pitting results in bearing failure. The full EHD computer analysis gives detailed information regarding slip conditions. Figure 7 shows the percentage cage slip as a function of radial load for various operating conditions. An inner race land riding cage with hollow rollers has considerable slip and is used as a reference point in Figure 7. Seven hundred pounds radial load are required for non-slip or synchronous running of the cage. The outer race land riding hollow roller design has considerably higher slip than any of the other configurations and only one check run is plotted on Figure 7. The beneficial effects of having the frictional torque and the cage land contact acting as a driving torque indicates that an inner land riding cage

Table III

SCHEDULE OF COMPUTER RUNS

Run No.	Symbol	Brg. Type 1. Hollow-Inner 2. Hollow-Outer 3. 2 Dia.-Inner	Load Lbs	Speed DN $\times 10^{-6}$	Lube 7808 @ 250°F 5P4E @ 500°F	% Oil in Brg Cavity	Results			Cage RPM
							% Cage Slip	H.P.	L-10 Life Hours (Fatigue)	
1	△	1	666	4.0	7808	.6	11.53	52.8	6,108	
2	△	1	666	4.0	7808	.15	SYN	28.4	3,030	13,224
3	△	1	333	4.0	7808	.15	21.66	22.5	25,562	10,364
4	▽	2	333	4.0	7808	.15	64.97	9.6	953,167	
5	△	1	333	3.0	7808	.15	19.85	13.9	131,307	
6	△	1	333	2.0	7808	.15	9.02	6.6	487,022	
7	△	1	333	1.0	7808	.15	SYN	1.82	2.29×10^6	
8	▲	1	333	4.0	5P4E	.15	17.14	17.5	17,751	10,961
9	□	3	333	4.0	7808	.15	4.58	21.4	9,630	8,390
10	■	3	333	4.0	5P4E	.15	SYN	17.2	7,505	8,792
11	□	3	100	4.0	7808	.15	25.96	16.0	142,522	6,510
12	□	3	333	[illegible]	7808	.15	SYN	5.2	44,301	

Table IV

SUMMARY OF COMPUTER RESULTS

Run No.	Symbol	Speed $DN\times10^{-6}$	Load Lbs	% Cage Slip	MAXIMUM LOADED ROLLER: OUTER Roll LD Lbs	OUTER EHD Film $h\times10^6$	OUTER Λ	OUTER Slide in./sec	Inner Roll LD Lbs	Inner EHD Film $h\times10^6$	Inner Λ	Inner Slide in./sec	No. of Loaded Rollers
1	△	4.0	666	11.53	336	13.08	1.46	0.7	138	13.91	1.55	1079.	9
2	△	4.0	666	SYN	378	13.05	1.46	0.5	190	14.20	1.59	2.9	9
3	△	4.0	333	21.66	219	13.66	1.53	0	72	15.05	1.68	2028.	9
4	▽	4.0	333	64.97	101	11.35	1.27	0	71	14.29	1.60	6086.	9
5	△	3.0	333	19.85	185	13.02	1.46	1.73	99	13.63	1.52	1393.	5
6	△	2.0	333	9.02	159	12.12	1.36	2.5	110	12.19	1.36	420	5
7	△	1.0	333	SYN	132	9.04	1.01	2.4	117	8.63	0.97	3.2	5
8	▲	4.0	333	17.14	238	2.79	0.31	0	74	2.94	0.33	1606.	9
9	□	4.0	333	4.58	266	8.74	0.98	0.1	139	12.87	1.44	412.	5
10	■	4.0	333	SYN	280	2.09	0.23	0	141	2.23	0.25	0.05	3
11	□	4.0	100	25.96	131	8.85	0.99	0	59	14.57	1.63	2335.	3
12	□	2.0	333	SYN	248	6.68	0.75	0.5	213	11.02	1.23	2.0	3

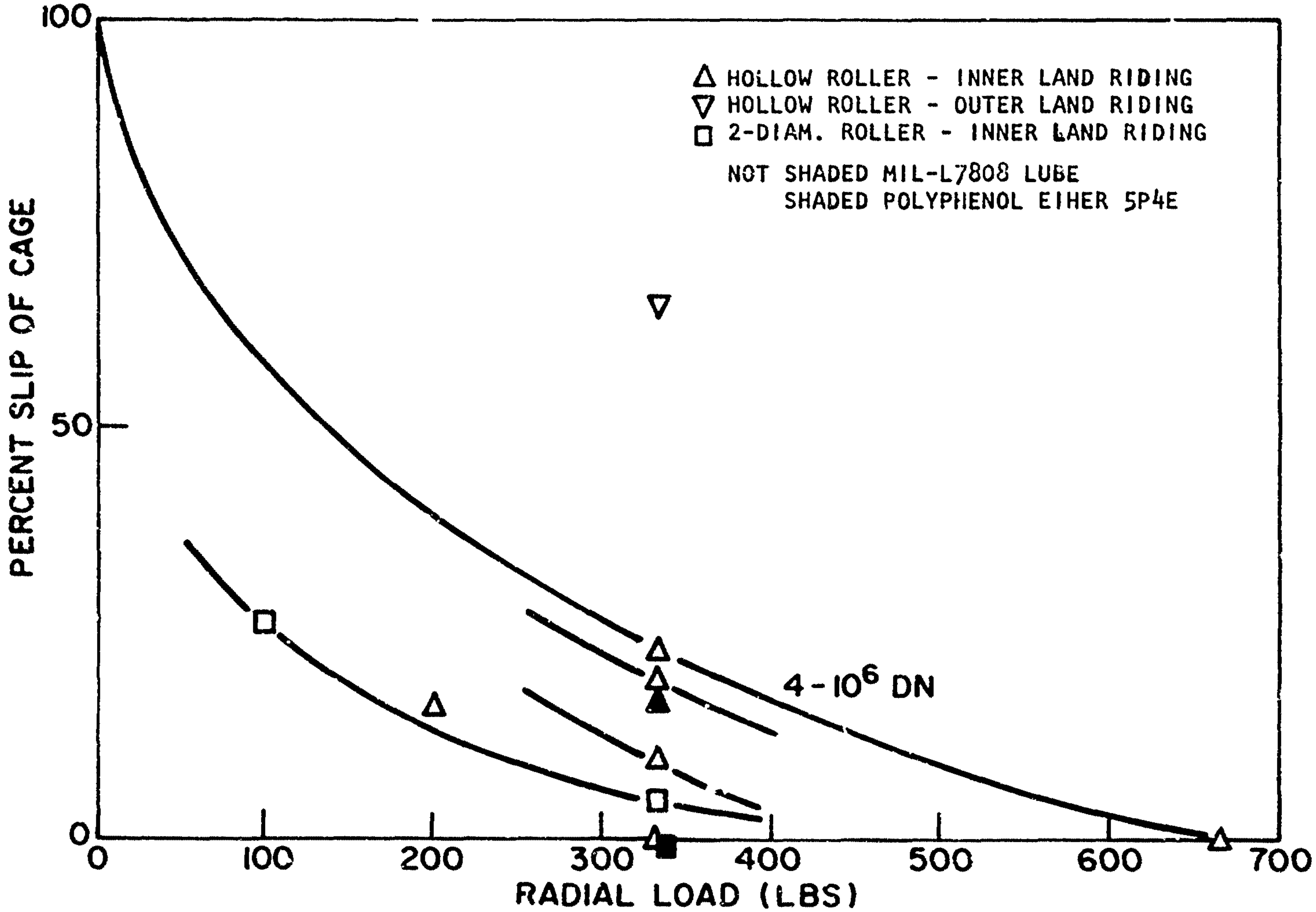

Figure 7. Cage Slip Percent vs. Radial Load

configuration should be considered. For this reason all dual diameter roller computer runs were made with an inner land riding cage configuration. The dual diameter roller bearing has significantly less cage slip as shown on Figure 7. Another way to represent sliding or cage slip is to show the reduction in cage rpm as a function of radial load. This is given in Figure 8. It is immediately apparent that the hollow roller inner-land-riding cage speed or a single diameter roller bearing concept cage speed is considerably higher than the corresponding cage speed for the dual diameter roller concept. As evident in Figure 8, a much lower load is required to prevent sliding or cage slip in the dual diameter roller concept.

An object of the present study is to minimize heat generation in the bearing. An indication of heat generation is the computed horsepower loss of the bearing. As shown on Figure 9, the horsepower losses for both the inner land riding cage configurations (single diameter roller and dual diameter roller) are essentially the same. Horsepower losses are expected to be somewhat lower with the use of Polyphenyl Ether 5P4E lubricant as compared to MIL-L-7808 oil. The oil viscosity of the 5P4E at 500°F is less than that of the 7808 at 250°F. Viscous drag losses predominate in the bearing at 4.0×10^6 DN. Therefore, lower oil viscosity (at synchronous cage speed) will result in less power loss.

4. SERIES HYBRID BEARING

The series hybrid bearing concept, Figure 1d, consists of an oil film bearing between the inner race of the roller bearing and the shaft. The concept is one of speed sharing or speed reduction. The rotative speed of the roller bearing inner race is determined by the frictional torque of the oil film journal bearing matching the frictional torque of the roller bearing. The advantage of speed sharing is the fact that reduction speed on the inner race of the roller bearing results in a lower operating DN speed regime.

A three lobe oil film hydrodynamic bearing was considered for this application. Satisfactory bearing stability (absence of half-frequency

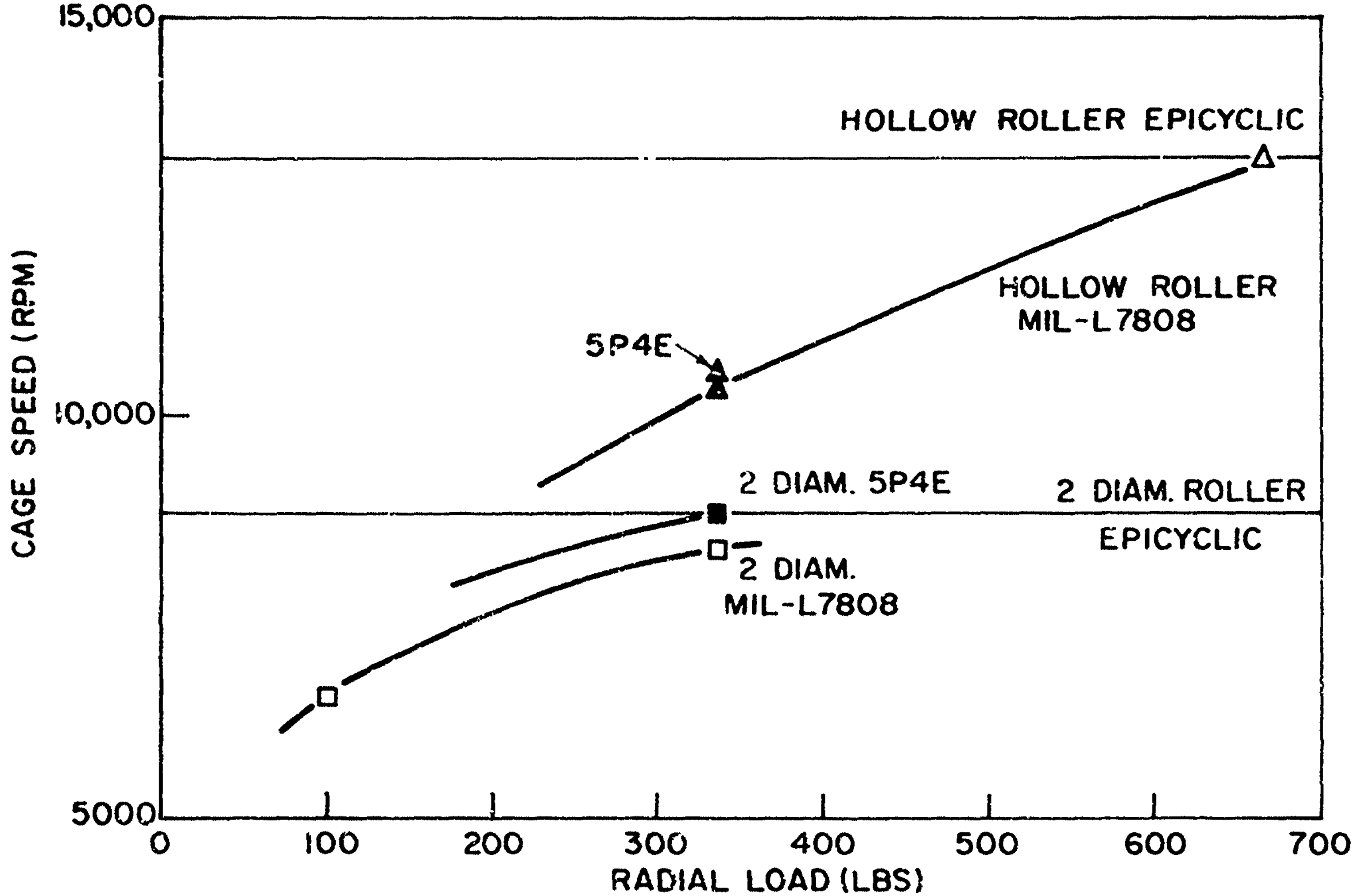

Figure 8. Cage Speed in RPM vs. Radial Load

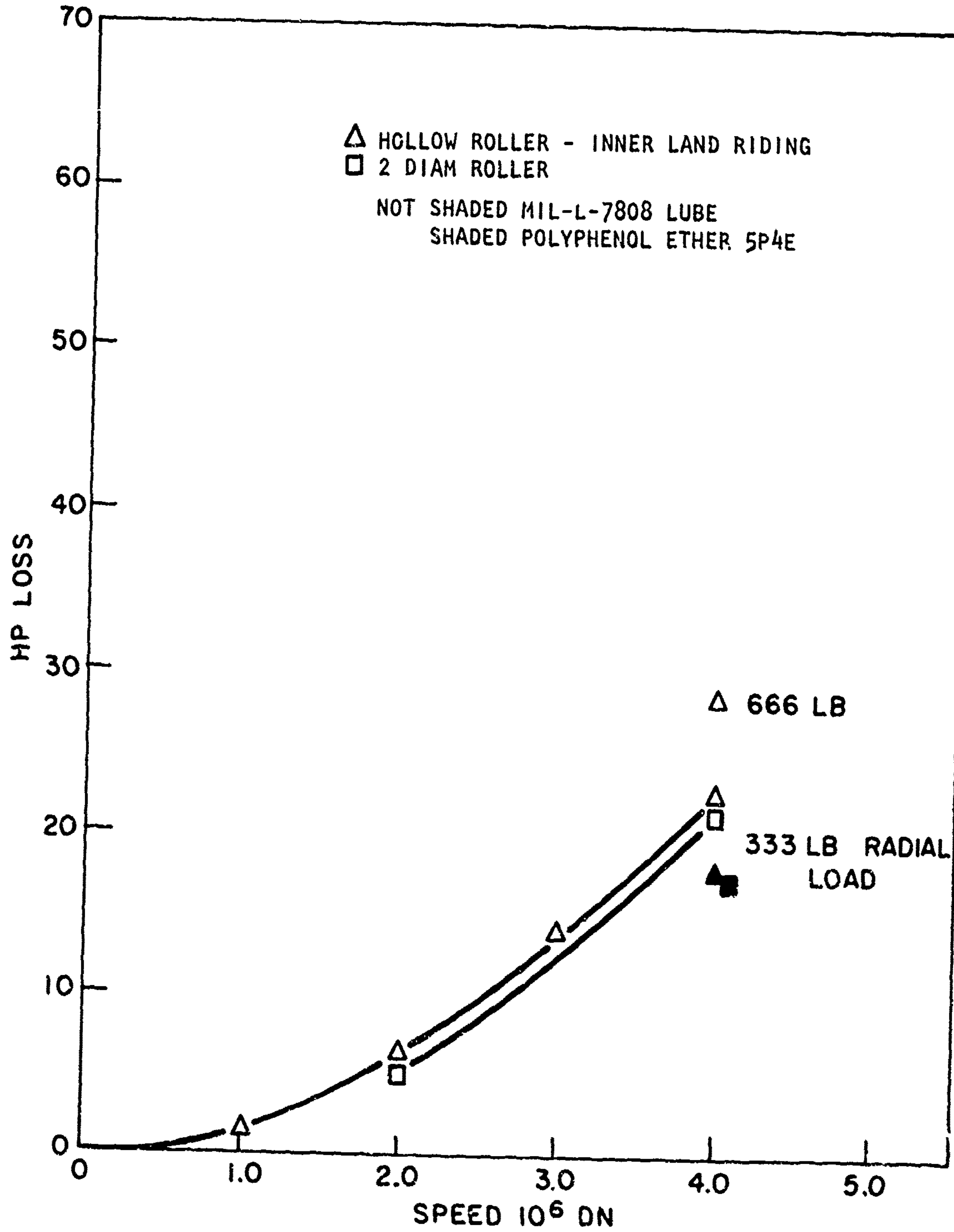

Figure 9. Horsepower Loss vs. Speed

whirl) can be obtained with this type of bearing. Good inherent stability was shown to exist under a shaft weight of 35 lbs. (representing an anticipated test rig shaft). This stability decreases as shaft weight increases, however, satisfactory stability for the bearing under study could be obtained up to 200 lbs. shaft weight. Minimum oil films on the order 0.001 inch can be anticipated under light 200 lb. loadings. The oil films would reduce to 0.0004 inches under the maximum 2,000 lbs. applied external load. The frictional torque of a three-lobe journal bearing was computed. The roller bearing inner race, Figure 1d, when supported on an oil film journal bearing only, would be completely free to move axially with respect to the shaft. Thus locating oil film bearings would be required to maintain the position of the roller bearing inner race. Locating thrust loads would be small. One approach is to use a conical type bearing (Reference 5). A pair of thrust bearings operating against the face of the roller bearing inner race were envisioned as a series of step pad thrust surfaces. The frictional torque of such surfaces amounted to approximately 15 or 20% of the overall journal bearing friction. This amount was added to the oil film bearing system torques.

The operation of the journal bearing would be in the turbulent regime and factors for the computation of turbulent friction are usually applied to laminar friction estimates. This approach was used in arriving at the total journal bearing friction curve. The friction loss vs. speed ratio for MIL-L-7808 oil at 250° is shown in Figure 10. The solid lines indicate the friction torque expressed in inch pounds of the oil film journal and thrust bearing surfaces is a function of the ratio of the roller bearing inner race speed to shaft speed. The dashed curve represents the frictional torque of the inner land riding cage hollow roller bearing configuration. The point of intersection of these two frictional torque curves defines the operating speed of the roller bearing inner race. It is seen in Figure 10 that the present bearing system would result in a speed ratio of 0.84. Recent work by NASA (Reference 5) with a series hybrid concept using a ball thrust bearing and an oil

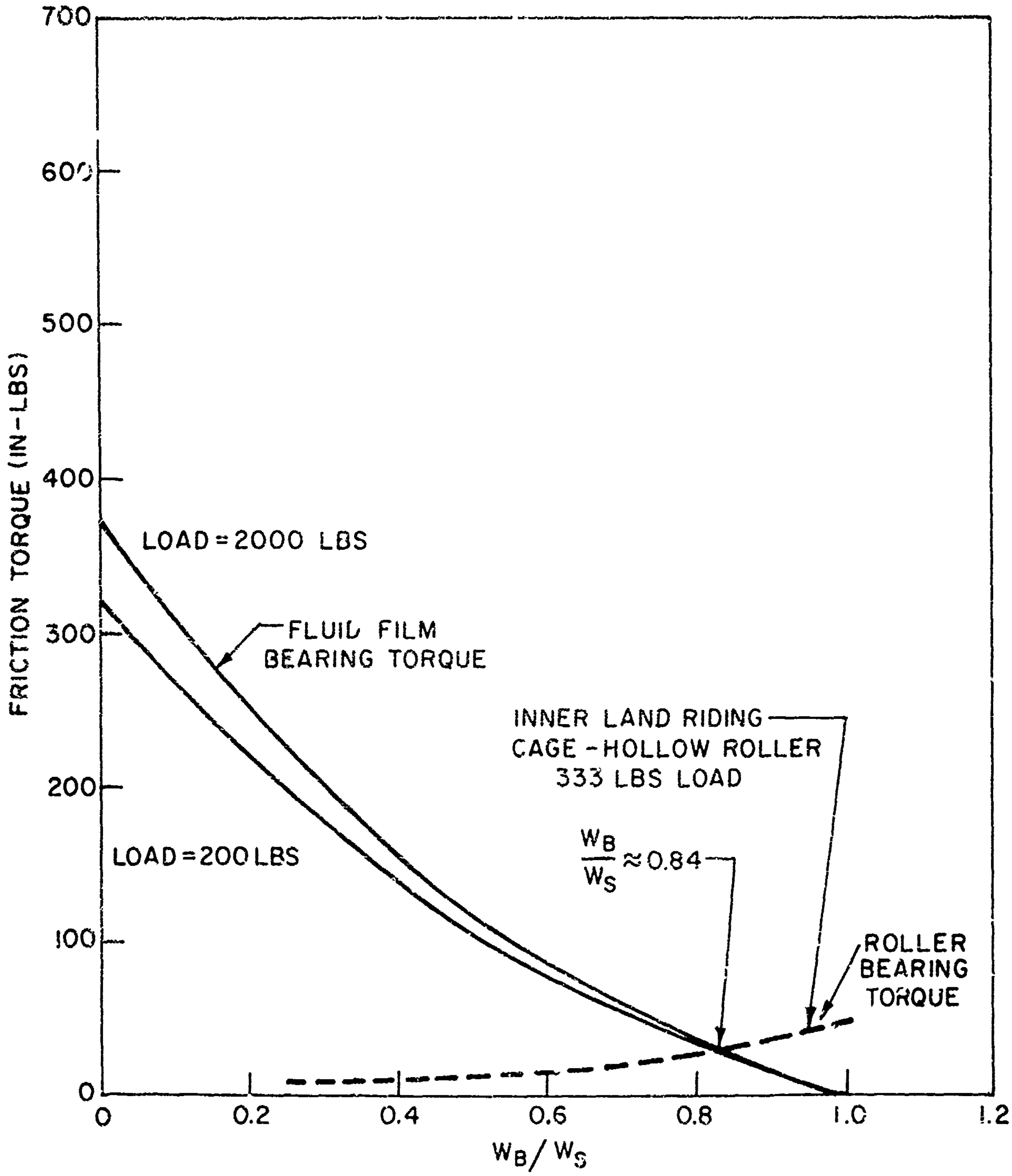

Figure 10. Friction Loss vs. Speed Ratio, MIL-L-7808 Oil

film thrust bearing surface resulted in a speed sharing ratio of approximately 0.66 at best. The analysis is highly dependent upon accurate calculation of frictional torques. The frictional torques even in the turbulent regime of the fluid bearing has been fairly well established and correlated with experimental results and can be considered realistic. High speed roller bearing torque needs to be carefully verified to determine the anticipated speed sharing ratio. It is possible to add frictional torque to the roller bearing concepts by increasing the amount of oil forced through the bearing. Thus, it is possible by raising the frictional torque of the roller bearing to obtain a more favorable speed sharing ratio as could be seen by raising the curve on Figure 10. However, any reductions in roller bearing torque would result in reduction in the anticipated speed sharing ratio.

5. SELECTION OF DUAL DIAMETER ROLLER BEARING

The dual diameter roller bearing concept, Figure 2, with an inner land riding cage was recommended for the thorough design analysis, fabrication and prototype testing. Selection of the dual diameter roller bearing concept was based upon the lower cage speeds obtained which result in significantly less cage slip.

The series hybrid bearing concept is interesting but was not recommended for further study under the present program. Operation of the series hybrid bearing design is highly dependent upon accurate determination of roller bearing friction torque. The horsepower losses of both conventional and dual diameter roller bearing concepts, Figure 9, are shown to be essentially the same. Therefore the selection of a roller bearing configuration for further development at this time does not affect future consideration of development of the series hybrid bearing concept.

SECTION III

LUBRICANT SELECTION

A summary of full scale bearing test results of 8 candidate high temperature (600°F) lubricants is given in Table V, which was taken from Reference 6. All of the lubricants in this study were operated with an inerting blanket of nitrogen gas. Another recent study (References 7 and 8) considered five candidate high temperature lubricants. In this case Table VI, all of the lubricants were again protected by an inert nitrogen blanketing gas with the exception of Polyphenyl Ether 5P4E. The Polyphenyl Ether was operated in an oxygen atmosphere. The only advanced lubricant showing reasonable success without special inert oxidation protection is the 5P4E Polyphenyl Ether. Figure 11 is a reproduction of a report of bearing fatigue life experiments with Polyphenyl Ether (Reference 8). Indications are that Polyphenyl Ether is an acceptable high temperature lubricant up to 600°F but that the failure mode may be one of moderate glazing and micropitting of the races and rolling elements. This is attributed to thinner EHD lubricant films in the operating race and roller contacts. The various bearing configurations were analyzed with 5P4E Polyphenyl Ether at 500°F to determine the operating specific film thicknesses in the roller race contacts.

The properties of MIL-L-7808 and Polyphenyl Ether lubricants are discussed in the elastohydrodynamic lubrication preliminary design manual (Reference 4). Additional data (Reference 9) regarding high pressure viscometer experiments with Polyphenyl Ether 5P4E were also used for estimating properties of this lubricant at 500°F. Lubricant data as a function of operating temperature is given in Table VII for the MIL-L-7808 and 5P4E lubricants. This data as a function of temperature is consistent with the extrapolation routines of Reference 4.

Table V

SUMMARY OF TEST RESULTS

Performance	Fluid (s)	Measured h/σ @ 600°F	Typical Bearing Condition
Excellent	1. Super Refined Mineral Oil Plus 10% High Molecular Weight Resin.	3.6-4.0	Good.
Good	2. Perflorinated Polyether.	3-4(Initially) <1.8 (Long-Term)	Minor Glazing And Micropitting.
	3. Modified Fluorsilicone.	<1.8	
Acceptable	4. Synthetic Hydrocarbon Plus 10% High Molecular Weight Resin.	<1.8	Moderate Glazing And Micropitting
	5. Modified Polyphenyl Ether.	<1.8	
Unacceptable	6. Super Refined Mineral Oil Without High Molecular Weight Resin.	2.6-3.6 (Initially) <1.8 (Long-Term)	
	7. Synthetic Hydrocarbon Without High Molecular Weight Resin.	3.5-4.0	Heavy Glazing And Pitting.
	8. Highly Hindered Ester.	<1.8	

Table VI

PROPERTIES OF TEST LUBRICANTS

Lubricant designation	Base Stock	Additive content	Flash point, °F	Fire point, °F	Kinematic viscosity, cs, at- 100°F	210°F	500°F	Specific heat at 500°F, Btu/(lb.)(°F)	Density at 500°F lb./ft.^{3}
NA-XL-10	Super-refined naphthenic mineral oil	(a)	445	495	79	8.4	1.1	0.660	45.7
NA-XL-13	Synthetic paraffinic oil	None	530	580	314	32	[b]2.9	-	-
NA-XL-16	Polyester-hindered type	(c)	480	540	27.6	5.2	[b]1.0	-	-
NA-XL-20	Fluorocarbon	None	-	-	335	29	2.1	.317	94
NA-XL-22	5P4E polyphenyl ether	None	550	660	363	13.1	1.2	.496	63.1
NA-XL-23	5P4E polyphenyl ether	(d)	550	660	363	13.1	1.2	.496	63.1
NA-XL-24	Synthetic paraffinic oil	(e)	530	580	314	32	[b]2.9	-	-

[a]Oxidation inhibitor, extreme pressure additive, and antifoam agent.

[b]Extrapolated.

[c]Oxidation inhibitor and dispersant.

[d]Oxidation inhibitor.

[e]Antiwear additive.

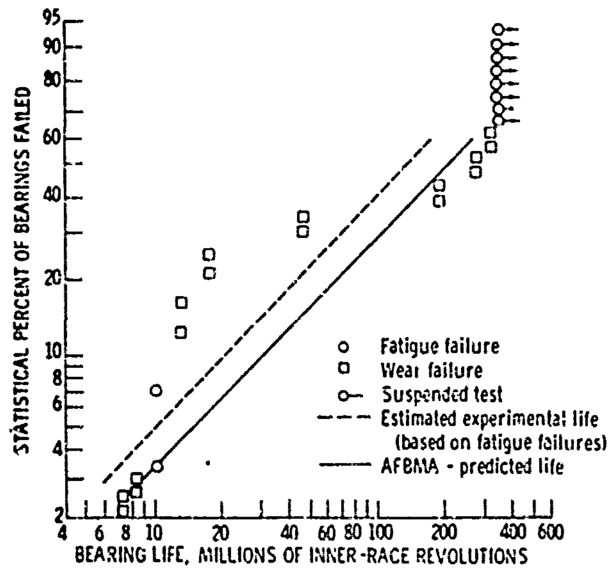

Figure 11. Bearing Life with 5P4E Lubricant

Rolling-element fatigue life of 120-mm bore angular-contact ball bearings run with polyphenyl ether lubricant. Material, AISI M-50 steel; thrust load, 4365 lb; speed, 12,000 rpm; temperature, 600°F air environment; [failure index, 2 out of 26.]

Table VII

LUBRICANT PROPERTIES USED IN THE ANALYSIS

MIL-L-7808 LUBRICANT PROPERTIES

Temperature (°F)	Viscosity (lb-sec/in^2)	Alpha (in^2/lb)	Beta (°F)	Gama (in^2-°F/lb.)	Therm.Cond. (BTU/°F-HR-FT)	Spec. Heat (BTU/lb.-°F)	Wt. Dens. (lb./in^3)
.15000+03	.11000-05	.88400-04	.49130+04	.63000-01	.09050+00	.48400+00	.33100-01
.20000+03	.45000-06	.81000-04	.49130+04	.63000-01	.08700-01	.51200+00	.32300-01
.25000+03	.30500-06	.76200-04	.49130+04	.63000-01	.83000-01	.53100+00	.31600-01
.30000+03	.21500-06	.72800-04	.49130+04	.63000-01	.79400-01	.55000+00	.30800-01
.35000+03	.16000-06	.70600-04	.49130+04	.63000-01	.75600-01	.56800+00	.30100-01
.40000+03	.12000-06	.69000-04	.49130+04	.63000-01	.72000-01	.58800+00	.29400-01

Polyphenyl Ether LUBRICANT PROPERTIES (5P4E)

Temperature (°F)	Viscosity (lb/sec/in^2)	Alpha (in^2/lb)	Beta (°F)	Gama (in^2-°F/lb.)	Therm.Cond. (BTU/°F-HR-FT)	Spec. Heat (BTU/lb-°F)	Wt. Dens. (lb./in^3)
.30000+03	.80000-06	.66000-04	.65040+04	.18300+00	.77300-01	.46200+00	.40700-01
.35000+03	.44000-06	.54000-04	.65040+04	.18300+00	.77100-01	.47800+00	.40400-01
.40000+03	.26000-06	.43000-04	.65040+04	.18300+00	.76900-01	.49200+00	.40100-01
.45000+03	.16000-06	.33000-04	.65040+04	.18300+00	.76700-01	.51100+00	.39800-01
.50000+03	.10000-06	.26000-04	.65040+04	.18300+00	.76600-01	.52700+00	.39500-01
.55000+3	.65000-07	.19000-04	.65040+04	.18300+00	.76400-01	.54400+00	.39200-01

SECTION IV

DUAL DIAMETER BEARING ANALYSIS AND DESIGN

1. DESIGN CONSIDERATIONS

The dual diameter roller bearing concept was selected as a result of the preliminary configuration study. Selection was based upon the lower cage speeds obtained which will result in significantly less cage slip. The orbital cage speed of the dual diameter roller bearing with a diameter ratio of 0.5 will result in a 1/3 reduction of cage speed as seen by Figure 4. A major roll diameter of 0.5 inches was selected as an optimum based on Figure 6. The resulting estimated bearing life (under the duty cycle of Table II) would be 5,000 hours L-10 life shown on Figure 6. This is well in excess of the design goal of 1,000 hours.

The primary problem encountered in high speed mainshaft roller bearings is cage slip. This is a phenomena which results in high sliding velocities between rollers and inner race contacts. Severe glazing and micropitting results in bearing failure. The minimum radial load to prevent skid or cage slip in the dual diameter roller bearing is 333 lbs. as shown on Figures 7 and 8. This minimum radial load was used in the design and performance evaluation calculations. Heavier radial loads will result in reduced bearing fatigue life, but do not endanger the bearing from a skid or cage slip standpoint and are of relatively minor interest. It is essential to assure that cage slip will not occur under operating conditions. A complete systems analysis (Reference 1) incorporating the latest available elastohydrodynamic lubrication technology (Reference 4) and including fluid drag forces and thermal effects were selected as the best approach to achieve a practical design.

2. INNER RACE STRESSES

A study of the effect of inner race thickness and total interference fit between the inner race and shaft (with the hollow test shaft) to determine race circumferential, hoop or tangential tension stresses was conducted using standard ring formulas. Race radial thickness over 0.25 inches has little effect upon reducing circumferential tangential stresses. Race thicknesses less than 0.250 inches radial thickness can result in unacceptably high stresses. Therefore the inner race thickness should meet or exceed 0.25 inches.

High shaft speeds (up to 28,600 rpm) will create significant circumferential, hoop or tangential stresses in the inner race. Figure 12 shows a magnitude of this maximum tangential stress as a function of shaft speed expressed both in rpm and DN values for the 140 mm bore bearing. Approximately 50,000 psi tangential stress can be anticipated at 4.0×10^6 DN with the 0.25 inch thick race of the prototype bearing design.

Approximate physical properties of M-50 fully hardened steel are given in Table VIII. The material is brittle at room temperature and care must be exercised to prevent over-stressing. The material does become more ductile as temperature increases. The effect of stresses due to speed, Figure 12, and stresses due to interference fit are essentially additive. Approximately 0.012 inches diametral interference fit would be required at room temperature to assure a working interference fit of 0.001 at 4.0×10^6 DN operation. This heavy interference fit would result in almost 60,000 psi tangential ring stresses initially. It was decided to compromise with a lesser interference fit at room temperature (0.0063 inches) and allow the inner race to become loose with respect to the shaft at approximately 3.0×10^6 DN. Key slots in the inner race allow the race to be axially clamped and prevent relative rotation of the race and shaft. The loose fit between inner race and shaft at speeds over 3.0×10^6 DN will keep the inner race tangential stresses to less than 60,000 psi.

High tensile ring stresses may have a detrimental effect on inner race rolling contact fatigue. Thermal gradients may also cause the interference

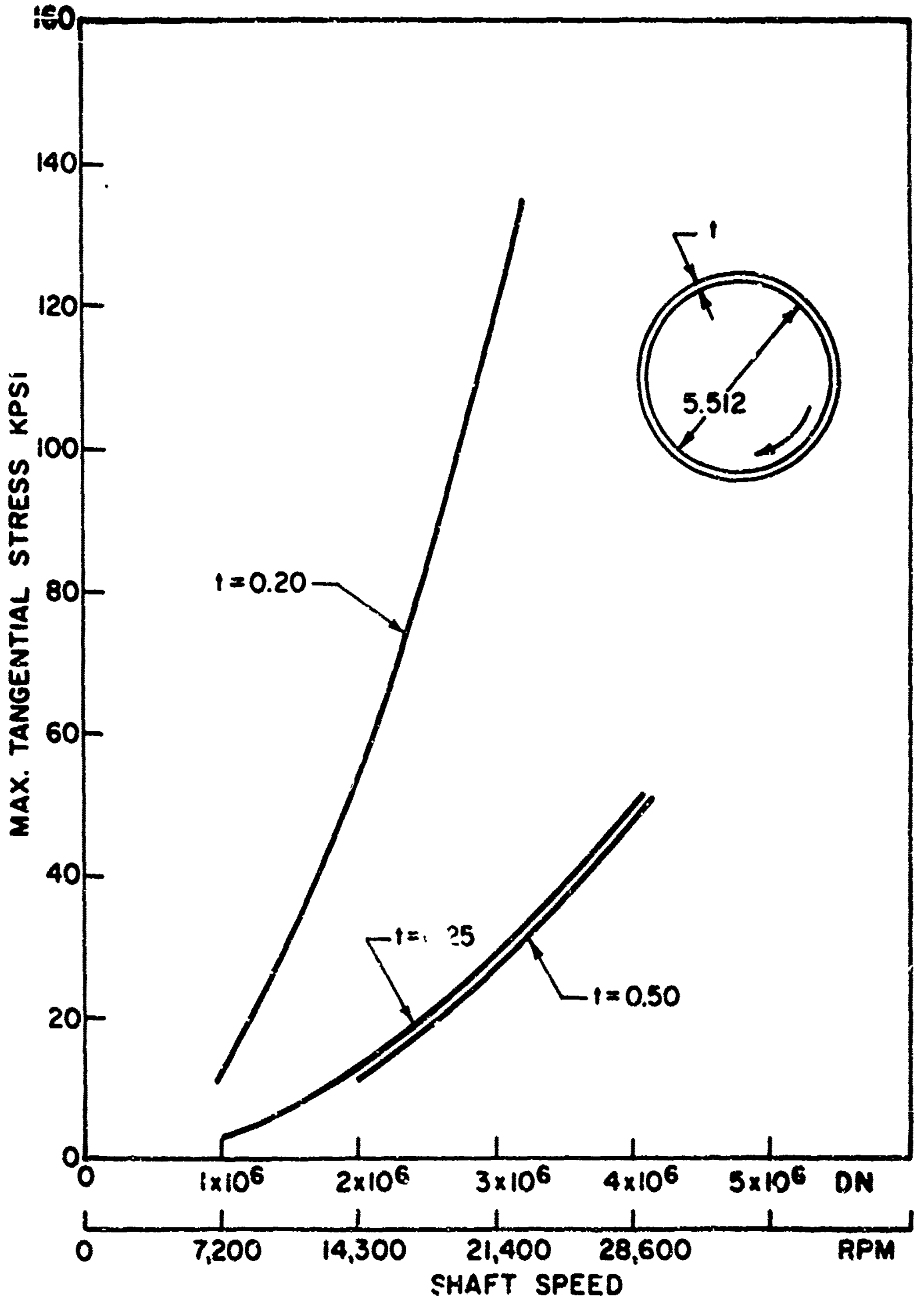

Figure 12. Inner Race Maximum Tangential Stress vs. Shaft Speed

TABLE VIII

PROPERTIES OF M-50 HARDENED TO RC-60
Per VASCO Technical Bulletin

Property	Room Temp.	800°F
Tensile ULT. (psi)	411,500	345,000
Tensile Yield (psi)	388,000	262,500
Elongation (1.5" gauge) (%)	2	6
Red. of Area (%)	2	17

fit to increase (depending upon the amount of under inner race cooling). Therefore every effort was made to limit inner race tangential stresses at maxim ...d and 500°F operation. A partially hollow or compliant inner race ...sign Figure 13 was selected to provide access for the under and through inner race lubrication scheme. The beam bending compliancy may also provide relief from thermal lockup or thermal preloading at high temperature and high speed operation.

An existing FIRL finite element computer program was used to evaluate the tangential ring stresses in the actual inner race design at 4.0×10^6 and 3.5×10^6 DN. Figure 13 illustrates the inner race model and the location of various tangential stresses. The stress values of Figure 13 are in good agreement with the approximate solutions used to obtain the values in Figure 12. It is readily apparent that stresses on the order of 57,000 psi will occur in the inner race at 4.0×10^6 DN. Stress level will drop to approximately 44,000 psi maximum at 3.5×10^6 DN (25,000 rpm). A third case was analyzed where circumferential line loads were applied in the vicinity of the roller inner race contacts to simulate stress conditions under 500 lb. external radial load. It can be seen from Table IX that the stress values range between a high of 43,000 psi and a low of 29,000 psi. The only available data to date for M-50 steel at 500°F in reverse bending fatigue (Reference 10) indicates a life which is asymptotic at 60,000 psi bending stresses beyond 10^8 cycles. The fluctuation of inner race bending stresses are all unidirectional and remain tensile as shown in Table IX and do not exceed a maximum value of 43,000 psi. The inner race compliant section calculates to have adequate reverse bending fatigue properties.

3. LUBRICATION

The method of lubrication for the dual diameter roller bearing is illustrated in Figure 14. Jet oil is introduced to an undercut in the test shaft as shown. Oil then passes through the shaft to the undercut portion of the inner race which acts as an oil reservoir. Centrifugal force resulting from shaft rotation then provides pressure to force a flow of oil through orifice holes in the inner race. This oil is then

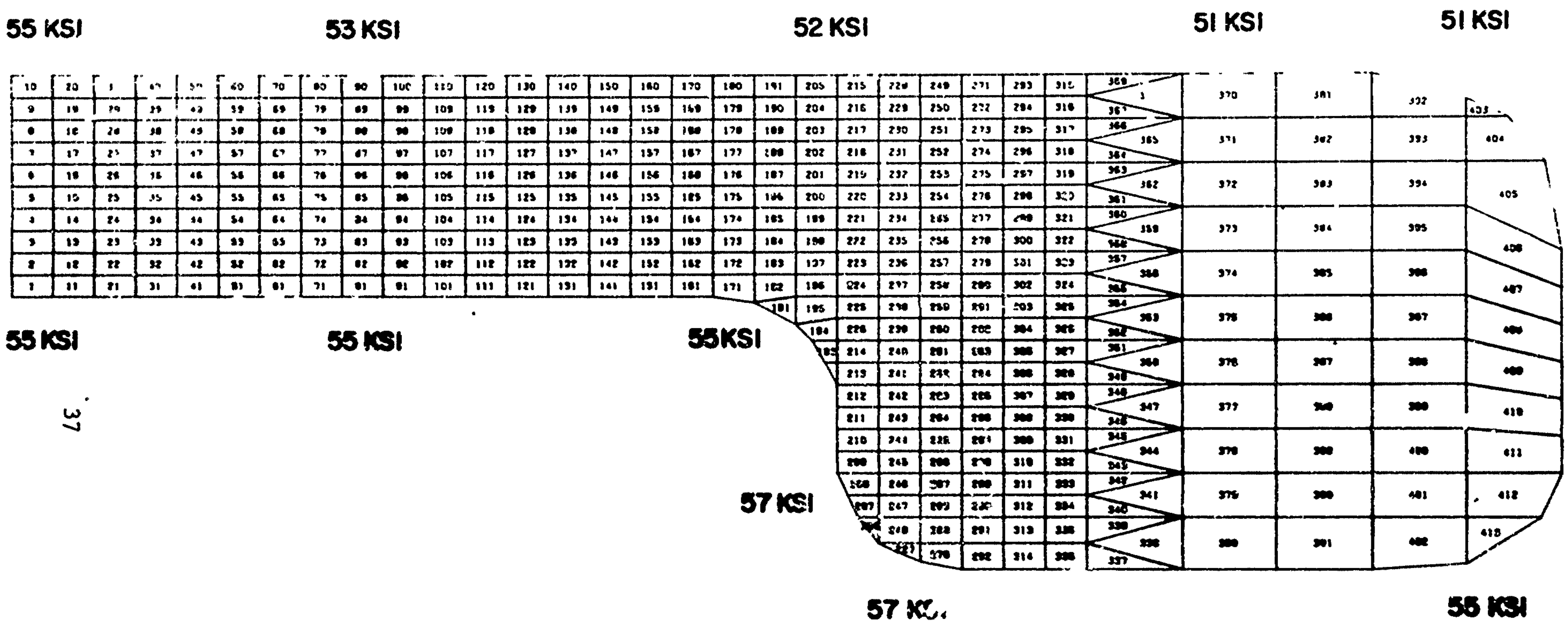

Figure 13. Finite Element Analysis of Inner Race Tangential Stresses at 4.0 x 10^6 DN

TABLE IX

INNER RACE TANGENTIAL STRESS (KSI)

Loading/Element No.	1	10	81	90	171	208	215	270	370	402	392
4.0×10^6 DN	55	55	55	53	55	57	52	57	51	55	51
3.5×10^6 DN	42	41	42	41	41	43	40	44	39	43	39
3.5×10^6 DN 500 lbs. Radial Load	37	23	36	33	37	40	36	41	38	43	39

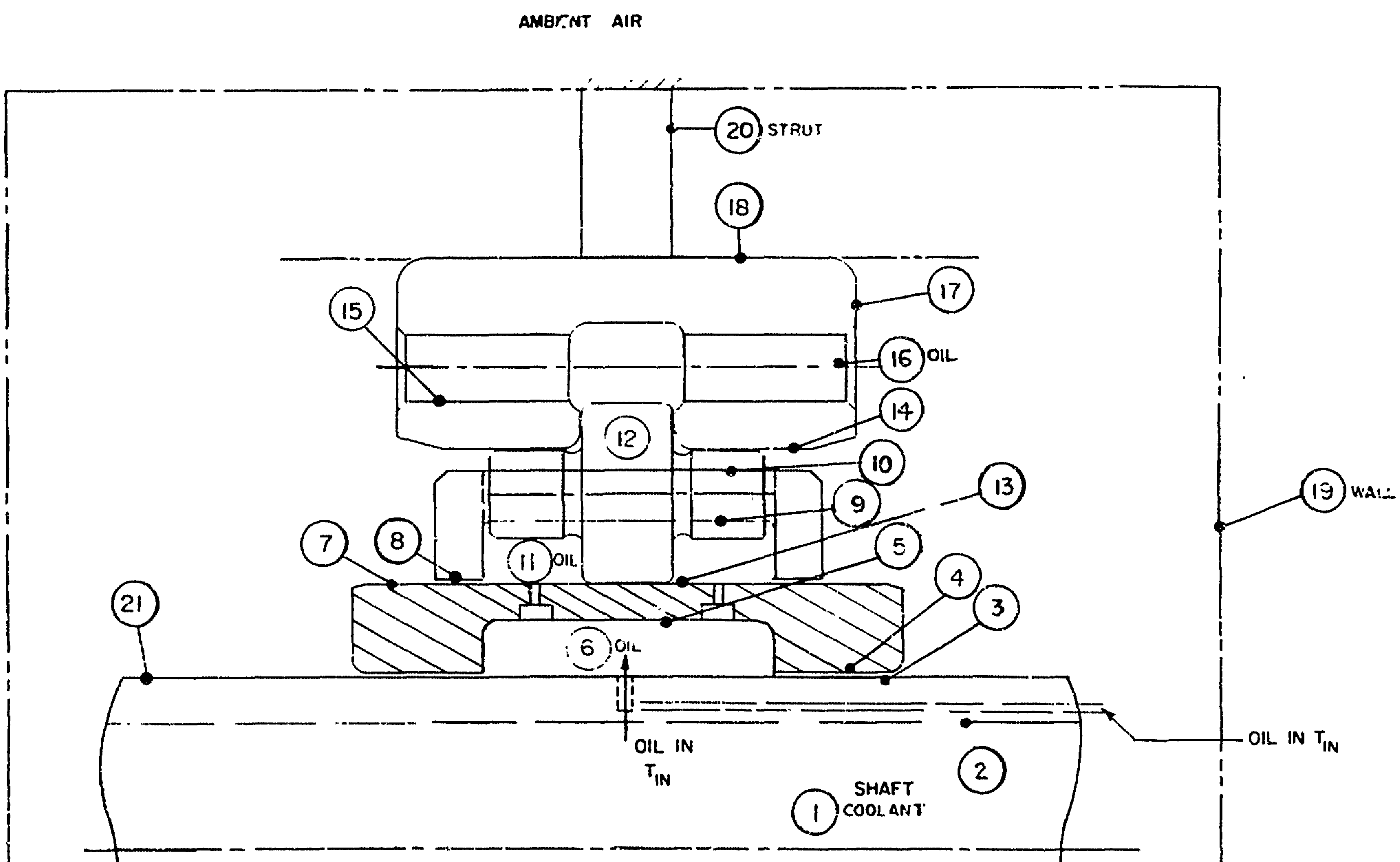

Figure 14. Thermal Nodes and Methods of Lubrication

introduced to the underside of the cage and is further circulated throughout the bearing by the pumping action of the rollers. Auxiliary jet oil lubrication into the sides or faces of the bearing can also be provided as necessary to obtain satisfactory cooling.

Three computer analysis runs were executed using three different flow rates (6.1, 12.0 and 18.0 lbs./min.) of 5P4E at 500°F oil inlet temperature. The minimum load to prevent skid of 333 lbs. and the top design shaft speed of 28,560 rpm (4.0 x 10^6 DN) were used. A complete thermal analysis was included in the solutions. A summary of the effects of oil flow upon bearing performance is given in Table X and shown graphically in Figure 15. Examination of Figure 15 shows no clear maxima or minima characteristics. It is evident that increased oil flow rate results in reduced outlet temperature and increased bearing horsepower loss. The outlet oil temperature shows some indication of leveling out below 6 lbs. per minute, but at unacceptably high values in excess of 700°F. Increasing the oil flow from 6 to 12 lbs. per minute drops the outlet oil temperature by 51.8°F. Increasing the oil flow from 12-18 lbs. per minute drops the outlet oil temperature by only 22.3°F.

An oil flow rate of 12 lbs./min. was selected as the design point. This flow can be obtained with 6 orifices of 0.028 inches diameter. The calculated oil outlet temperature of 4.0 x 10^6 DN is 598.5°F which is consistent with the program goal of 600°F operation. Table XI gives the resulting oil flow rates for 5P4E at 500°F oil inlet and MIL-L-7808 at 250°F oil inlet as a function of shaft speed.

4. PERFORMANCE ANALYSIS

Eight computer solutions were executed at various shaft speeds with 5P4E and MIL-L-7808 oil lubricant under a constant bearing radial load of 333 pounds. A summary of these computer runs and performance results are contained in Table XII. Initial fit-up conditions are 0.0063 inches shrink fit between bearing inner race and the shaft and 0.011 inches initial (machined or ground) diametral clearance. All of the solutions summarized in Table XII included a full thermal analysis consisting of 21 thermal modes described in Figure 14. Description of the node locations and the temperature

TABLE X

EFFECT OF OIL FLOW RATE ON BEARING PERFORMANCE

	Run 2P	3P	4P
Flow (lbs/min)	6.1	12.0	18.0
HP (loss)	21.7	23.53	25.4
Temp. Out of Brg. (°F)	650.3	598.5	576.2
Sump. Temp. (°F)	608.1	561.8	544.4

Shaft Speed 28,560 RPM (4.0×10^6 DN)
Lubricant: 5P4E @500°F oil inlet
Radial Load: 333 lbs

TABLE XI

OIL FLOW RATE VS. SPEED (DN)

		Oil Flow Rate lbs/min			
Lubricant	Inlet Temp. °F	4.0×10^6 DN	3.0×10^6 DN	2.0×10^6 DN	1.0×10^6 DN
Polyphenyl Ether 5P4E	500	12.0	9.03	6.05	3.0
MIL-L-7808	250	8.98	6.82	4.60	2.33

Six 0.028" Diam. Orificies in Inner Race

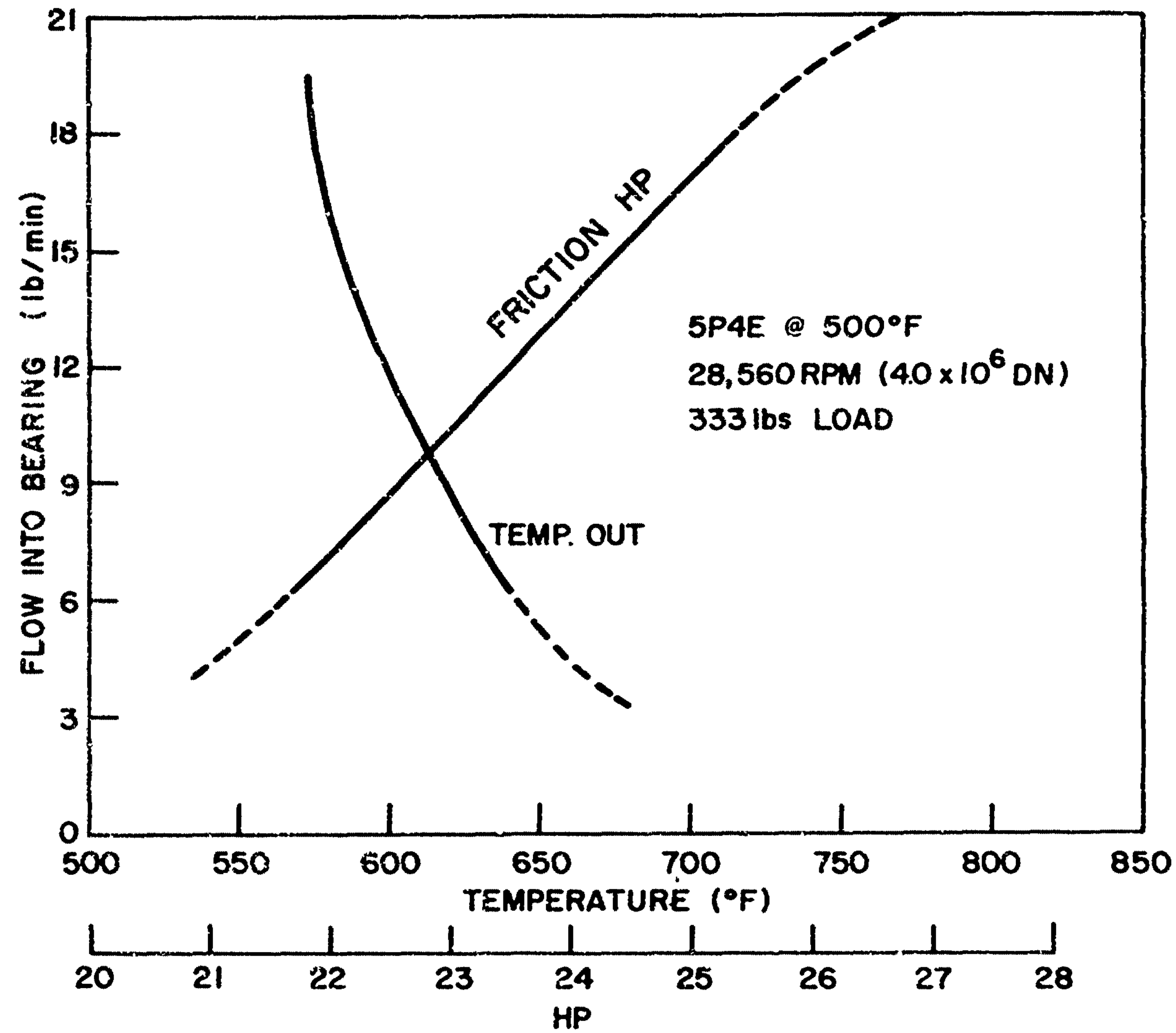

Figure 15. Effect of Oil Flow Rate Upon Outlet Temperature and Bearing Power Loss

TABLE XII

SUMMARY OF PERFORMANCE ANALYSIS COMPUTER RUNS

Run No.	5P	6P	7P	8P	9P	10P	11P	12P
Speed DN	4×10^6	3×10^6	2×10^6	1×10^6	4×10^6	3×10^6	2×10^6	1×10^6
Lube Type	5P4E	5P4E	5P4E	5P4E	7808	7808	7808	7808
Lube Flow Rate (lb/min.)	12.0	9.03	6.05	3.0	8.984	6.819	4.6	2.327
L_{10} Life (Hrs.)	7,236	22,496	63,329	1.7×10^6	8,036	23,962	71,756	2.1×10^6
Total Hp.	22.6	10.8	4.0	0.9	26.6	14.4	5.9	1.2
Operating Clear (Mils)	3.3[(1)]	6.6	7.0	7.3	1.6[(1)]	6.2	6.3	6.3
Cage Operating Clear (Mils) (Diametral)	32.	32.	32.0	32.0	32.0	34.0	33.0	32.0
No. Loaded Rollers	3	3	3	3	5	3	3	3
Radial Deflect (Mils)	2.0	3.7	3.9	3.9	1.1	3.4	3.5	3.5

(1) Inner Race loose on Shaft

profiles for the 8 performance runs are summarized in Table XIII.

The temperatures when using the Polyphenyl Ether 5P4E lubricant are acceptable at all speeds. The average oil temperature within the bearing (node 11) at 4.0×10^6 DN operation of 631.9°F is acceptable for short duration test runs. Operating temperatures with MIL-L-7808 oil are not acceptable and auxiliary side jet lubrication was required during the initial checkout test runs with this lubricant.

The predicted frictional horsepower losses are shown in Figure 16 as a function of the speed parameter DN. Horsepower losses are also summarized in Table XII. A total loss of 22.6 horsepower was predicted at 4.0×10^6 DN using Polyphenyl Ether 5P4E at 500°F oil inlet temperatures.

Radial displacements are summarized in Table XII and include one half of the operating internal clearance in the bearing. The specifications require that the total radial displacement not exceed 0.010 inches under 2000 lbs. radial load. An additional elastic deflection between rollers and raceways of 0.0006 inches should be added to the values in Table XII to adjust for the difference between the 333 lb. analysis load and the 2000 lb. specification load. All total displacement values are well below (less than half) maximum allowable values. The largest radial displacements occur at the lowest shaft speeds. The effects of shaft speed and thermal effects in the bearing tend to decrease diametral clearance. A summary of the fluid film forces and roller contact forces acting on the cage are given in Table XIV. It is evident from the table that the driving torque resulting from the loaded rollers contacting the cage pockets is not sufficient to prevent serious cage slip at 4.0×10^6 DN operation. The fluid film drag on the inner surface and inner race to cage land is necessary to drive the cage at speed and prevent cage slip. An outer riding cage with resultant fluid drag torques at the outer race land contacts would result in significant cage slip at 4.0×10^6 DN. Roller to cage web contact forces of 10.3 pounds are predicted at the maximum DN operation.

TABLE XIII

SUMMARY OF TEMPERATURE PROFILES FOR DUAL DIAMETER ROLLER BEARING

No.	Location								
	DN	$4x10^6$	$3x10^6$	$2x10^6$	$1x10^6$	$4x10^6$	$3x10^6$	$2x10^6$	$1x10^6$
	Lube	5P4E	5P4E	5P4E	5P4E	7808	7808	7808	7808
	Run	5P	6P	7P	8P	9P	10P	11P	12P
1.	Inner Shaft Coolant	660.8	601.4	545.5	476.5	514.2	470.5	379.5	280.9
2.	Inner Shaft Surface	556.6	540.7	514.4	488.4	346.6	347.1	307.5	263.7
3.	Outer Shaft Surface at Bearing	535.6	535.2	512.3	488.9	314.4	337.9	303.4	263.1
4.	Inner Race at Shaft	613.3	558.4	521.8	491.6	453.8	374.0	320.6	267.1
5.	Under-cut Surface of Inner Race	615.8	564.0	524.1	492.2	456.3	382.4	324.5	268.0
6.	Under Race Coolant	529.5	517.4	503.1	485.5	297.8	289.0	274.6	253.9
7.	Inner Race Beyond Roller Contact	628.1	571.3	526.8	492.8	469.3	391.5	328.6	268.8
8.	Cage at the Land	665.6	600.8	542.4	498.9	549.7	462.2	369.1	282.0
9.	Cage Inner Surface	674.2	604.0	543.5	499.4	554.6	465.3	370.4	282.4
10.	Cage Outer Surface	672.6	603.0	543.1	499.4	552.0	464.1	369.9	282.4
11.	Internal Lubricant to Bearing	631.9	576.6	529.3	494.5	465.9	404.8	338.9	272.7
12.	Rollers	673.4	601.8	543.3	498.5	557.9	464.6	370.8	282.3
13.	Inner Race at Rollers	627.1	570.1	526.1	492.6	465.5	388.8	327.2	268.5
14.	Inner Surface of Outer Race	623.5	570.7	525.7	492.3	446.4	389.7	329.3	269.1
15.	Inner Cooled Surface Outer Race	621.6	569.7	525.3	492.1	444.2	388.3	328.6	268.9
16.	Outer Race Lubricant	620.0	568.9	525.0	491.9	442.3	387.1	328.0	268.8
17.	Outer Cooled Surface Outer Race	618.5	568.0	524.6	491.8	440.4	386.0	327.5	268.6
18.	Bearing Outer Diameter	603.8	560.2	521.3	490.3	422.8	374.8	322.0	267.3
19.	Chamber Wall (Inner Side)	548.5	515.0	484.7	459.2	359.4	325.6	287.5	246.8
20.	Loading Bolt (Strut) Root	491.3	458.6	429.2	405.7	354.1	317.1	276.0	233.0
21.	Shaft (External to Bearing)	574.7	545.4	515.6	490.1	371.5	345.9	306.1	263.4
	Sump Oil Temperature	581.8	547.4	516.2	490.0	385.0	348.5	307.3	263.3
	EHD Contact Temperature	584.9	548.6	519.8	500.7	377.7	347.0	303.8	267.4
	Δt Rise (Input - No. 11)	131.9	76.6	29.3	- 5.5	215.9	154.8	88.9	22.7

5P4E Input Temperature 500°F
7808 Input Temperature 250°F

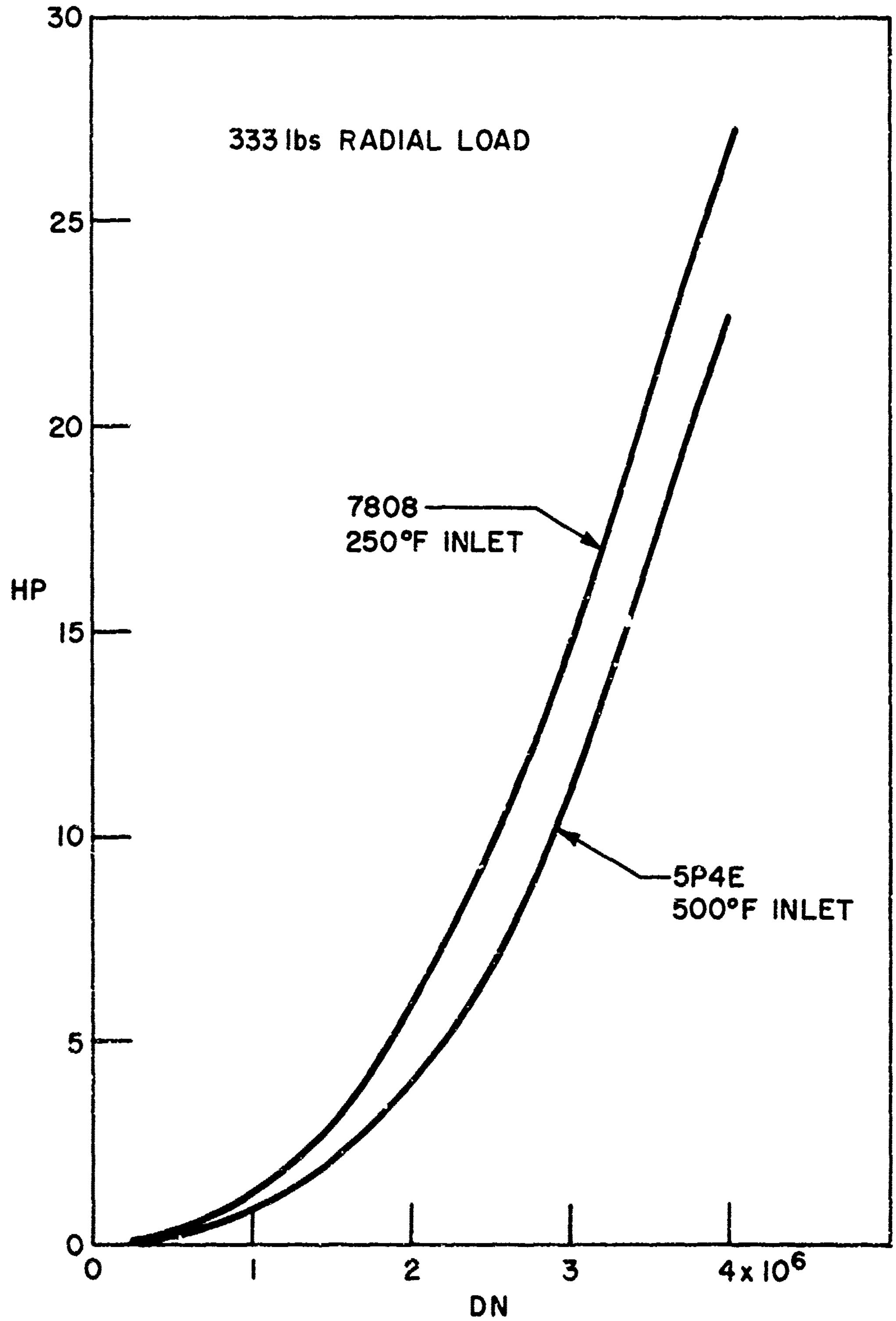

Figure 16. Dual Diameter Roller Bearing
Frictional Horsepower Losses

TABLE XIV

SUMMARY OF CAGE ANALYSIS

Speed(DN)	$4x10^6$	$3x10^6$	$2x10^6$	$1x10^6$	$4x10^6$	$3x10^6$	$2x10^6$	$1x10^6$
Lube	5P4E	5P4E	5P4E	5P4E	7808	7808	7808	7808
Run No.	5P	6P	7P	8P	9P	10P	11P	12P
Cage Clearance (Operating)(Mils)	32.	32.	32.	32.	32.	34.	33.	32.
% Cage Slip from Synchronous	.0006	.0005	.0004	.001	0.31	.05	.09	.12
Cage Torque (in-lb)								
From Driving Rollers	48.7	29.7	16.3	6.3	49.9	32.2	18.2	6.8
At the Land Contact	14.5	10.5	6.3	2.4	19.8	13.7	8.4	3.3
On Inner Cage Surface	38.6	23.8	11.6	3.3	35.4	21.6	10.8	3.1
On Outer Cage Surface	4.5	2.8	1.36	.14	4.1	2.5	.59	.4
On Cage Sides	.51	.33	.10	.04	.32	.23	.14	.06
Cage Driving Force (lbs) on Max Loaded Roller	10.3	9.6	4.1	4.1	7.4(2)	9.7	7.1	3.9
Cage Drag Force (lbs) on Unloaded Roller	1.7	1.1	.65	.36	1.97	1.45	.93	.39

(1) + Indicates Driving Torque
- Indicates Drag Torque

(2) Has 5 rollers in contact
All others have three.

5. EHD PARAMETERS

The outer race to roller contact EHD conditions for unloaded rollers are summarized in Table XV. The outer race to roller conditions for the maximum loaded roller in each case are summarized in Table XVI. The inner race contact EHD conditions for the maximum loaded roller are summarized in Table XVII.

Thin elastohydrodynamic (EHD) oil films (less than 3.0×10^{-6} inches) are predicted with Polyphenyl Ether 5P4E lubricant at 500°F oil inlet temperature for the bearing. The calculated oil inlet temperature at the entrance to the EHD contacts are given in the appropriate tables. The thin EHD films result in low (approximately 0.25) specific film values. Specific film thickness is the ratio of the actual oil film thickness to the root mean square of the contacting surface finishes. Operation at 600°F or higher temperatures with 5P4E lubricant can be expected to result in surface oriented damage or distress prior to any evidence of classical sub-surface oriented fatigue damage.

Somewhat thicker EHD films are predicted with MIL-L-7808 oil applied to the bearing at 250°F. The specific films are approximately 1.0 which is still in the surface related distress region of operation.

The sliding contribution to the total traction values between roller and race contacts is predominant for both contacts of the maximum loaded rollers (Tables XVI and XVII). The rolling contribution to the total traction is significant at the outer race contact of the unloaded rollers, Table XV. All of the rolling contacts are in the low slip (sliding velocities less than 1.0 inches per second) region, with the exception of 1.0×10^6 DN operation with 5P4E lubricant.

6. DESIGN DRAWINGS

The five drawings (Figures 17-21) completely describe the final design of the dual diameter roller bearing.

TABLE XV

TRACTION VALUES - OUTER RACE CONTACT - UNLOADED ROLLERS

Oil	DN	% Cage Slip	Rolling Entrainment: Velocity (in/sec)	Sliding Velocity (in/sec)	P_{oj} lbs	Coefficient of Traction	Sliding Tract.	Rolling Tract.	Total Tract.	Oil Film Thick.	EHD Contact Temp.	Traction Ratio Roll/Slide	Specific Film
5P4E	4×10^6	.00065	3112	0.0112	139	$.7\times10^{-5}$	.00097	-1.512	1.513	1.41×10^{-6}	585°F	1.0	.249
5P4E	3×10^6	.0005	2332	0.187	78	0.03	2.34	-1.42	.920	1.7×10^{-6}	549°F	1.54	.306
5P4E	2×10^6	.00038	1555	0.622	35	0.037	1.295	-0.80	.495	1.9×10^{-6}	520°F	1.62	.337
5P4E	1×10^6	.0005	762	15.56	8.7	0.034	.296	-0.04	.256	1.7×10^{-6}	501°F	.156	.299
MIL-L 7808	4×10^6	.035	3109	.995	139	0.013	1.807	-0.083	1.724	6.2×10^{-6}	378°F	.048	1.09
7808	3×10^6	.055	2329	2.70	78	0.017	1.326	-0.10	1.226	6.4×10^{-6}	347°F	.082	1.13
7808	2×10^6	.09	1545	9.32	35	0.024	0.84	-0.12	.72	6.7×10^{-6}	304°F	.167	1.19
7808	1×10^6	.116	762	15.5	8.7	0.036	0.31	-0.074	.236	6.2×10^{-6}	267°F	.313	1.09

TABLE XVI

TRACTION VALUES - OUTER RACE CONTACT - MAXIMUM LOADED ROLLERS

Oil	DN	% Cage Slip	Rolling Entrain-ment Velocity (in/sec)	Sliding Velocity (in/sec)	P_{oj} lbs.	Trac-tion Coeff.	Sliding Tract.	Rolling Tract.	Total Tract.	Oil Film Thick.	EHD Contact Temp.	Ratio Roll/ T_{oj}	Spec. Film
5P4E	$4x10^6$	.00065	3112	-0.007	294	0.02	-5.88	- .219	-6.099	$1.28x10^{-6}$	585°F	.036	.226
5P4E	$3x10^6$	.0005	2334	-0.0097	266	0.02	-5.32	- .50	-5.82	$1.47x10^{-6}$	549°F	.086	.260
5P4E	$2x10^6$	.00038	1556	-0.0053	226	0.016	-3.54	- .08	-3.62	$1.49x10^{-6}$	520°F	.022	.264
5P4E	$1x10^6$	.0005	778	- .0032	201	0.012	-2.41	- .14	-2.55	$1.13x10^{-6}$	501°F	.055	.200
MIL-L 7808	$4x10^6$	.035	3110	- .261	269	0.015	-4.04	-0.13	-4.17	$5.7x10^{-6}$	378°F	.031	1.0
7808	$3x10^6$	.055	2333	- .90	260	0.022	-5.72	-0.07	-5.79	$5.5x10^{-6}$	347°F	.012	.97
7808	$2x10^6$	.09	1556	-1.21	218	0.019	-4.14	-0.16	-4.30	$5.3x10^{-6}$	304°F	.037	.94
7808	$1x10^6$	.116	778	- .78	191	0.012	-2.29	-0.09	-2.38	$4.2x10^{-6}$	267°F	.038	1.09

TABLE XVII

TRACTION VALUES - INNER RACE CONTACT - MAXIMUM LOADED ROLLERS

Oil	DN	% Cage Slip	Rolling Entrainment Velocity (in/sec)	Sliding Velocity (in/sec)	P_{ij} lbs	Traction Coeff.	Sliding Tract.	Rolling Tract.	Total Tract.	Oil Film Thick.	EHD Contact Temp.	Ratio Roll/ σ_j	Spec. Film
5P4E	$4x10^6$	.00065	6224	.05	155	0.028	4.340	-0.145	4.195	$2x10^{-6}$	585°F	0.033	.355
5P4E	$3x10^6$	.0005	4668	.013	188	0.021	3.948	-0.194	3.754	$2.5x10^{-6}$	549°F	0.052	.449
5P4E	$2x10^6$	.00038	3112	.0065	191	0.013	2.480	-0.110	2.37	$3.0x10^{-6}$	520°F	0.046	.532
5P4E	$1x10^6$	.0005	1556	.0047	193	0.0086	1.659	-0.059	1.60	$2.2x10^{-6}$	501°F	0.036	.396
MIL-L 7808	$4x10^6$	.035	6220	2.60	131	0.0258	3.379	-0.160	3.219	$9.6x10^{-6}$	378°F	0.049	1.70
7808	$3x10^6$	.055	4666	1.91	182	0.022	4.004	-0.087	3.917	$9.3x10^{-6}$	347°F	0.022	1.64
7808	$2x10^6$	.09	3112	1.65	183	0.016	2.928	-0.116	2.812	$9.4x10^{-6}$	304°F	0.041	1.67
7808	$1x10^6$	.116	1556	1.06	182	0.0087	1.58	-0.09	1.49	$7.8x10^{-6}$	267°F	0.06	1.38

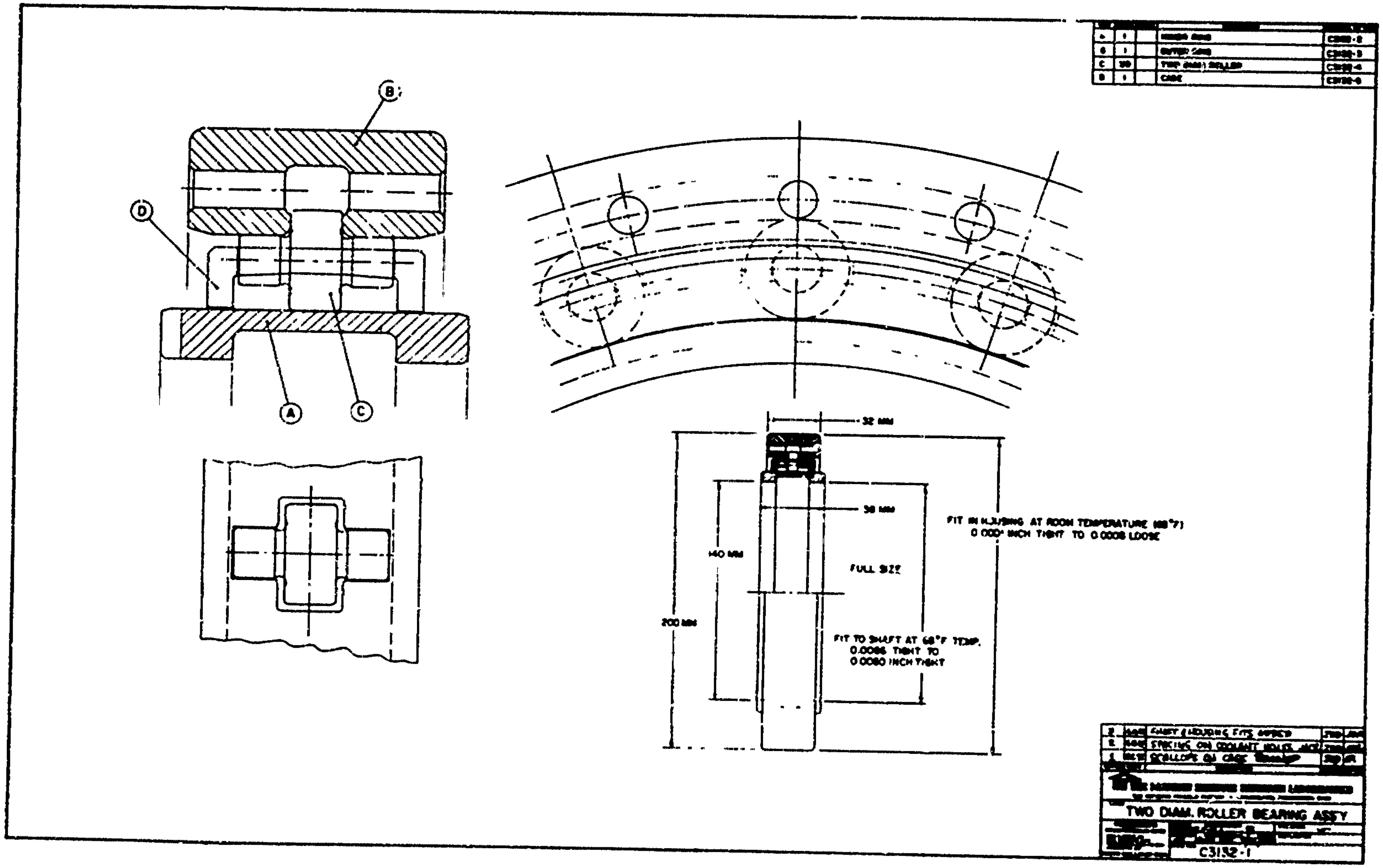

Figure 17. Two Diameter Roller Bearing Assembly

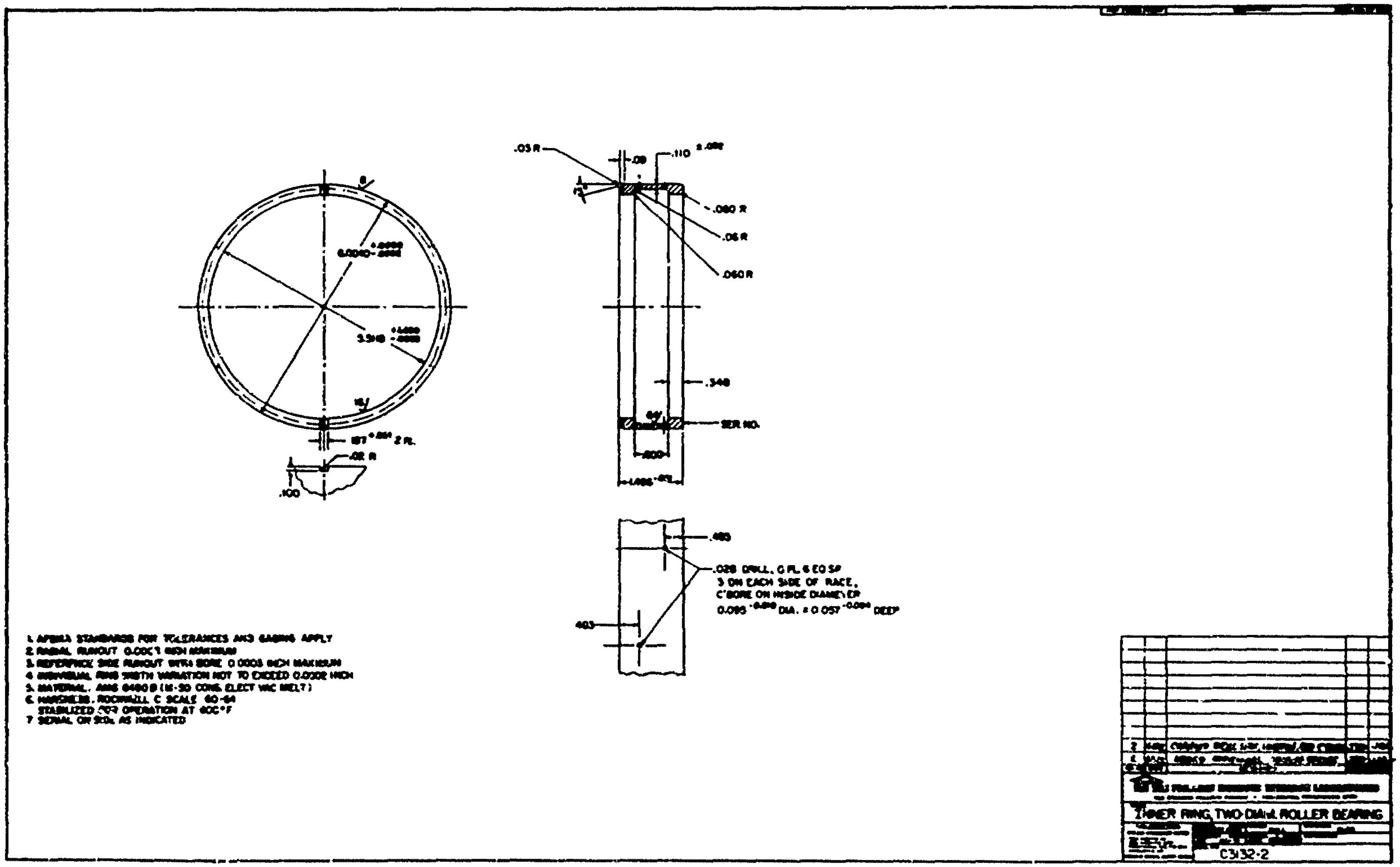

Figure 18. Inner Ring, Two Diameter Roller Bearing

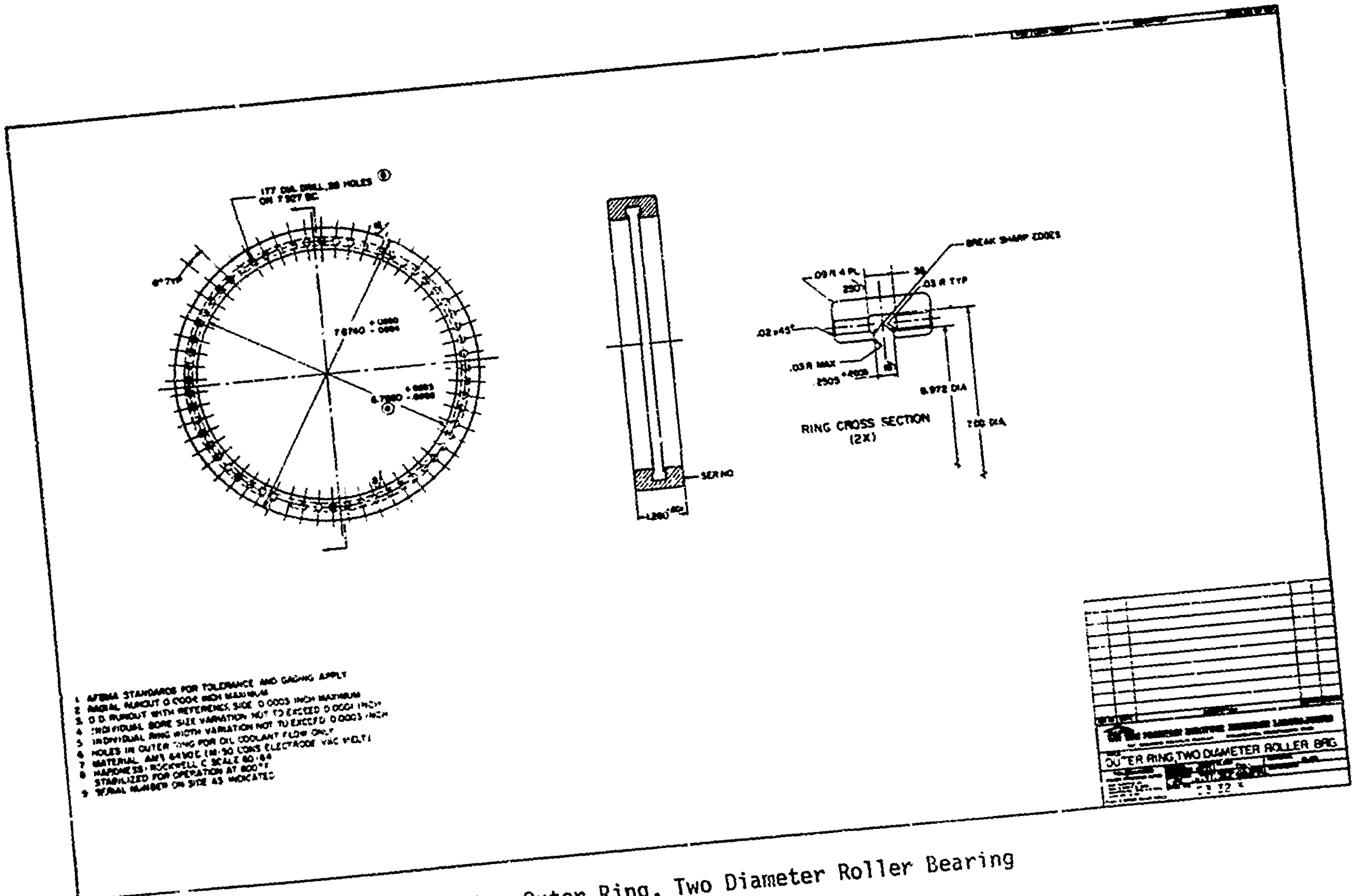

Figure 19. Outer Ring, Two Diameter Roller Bearing

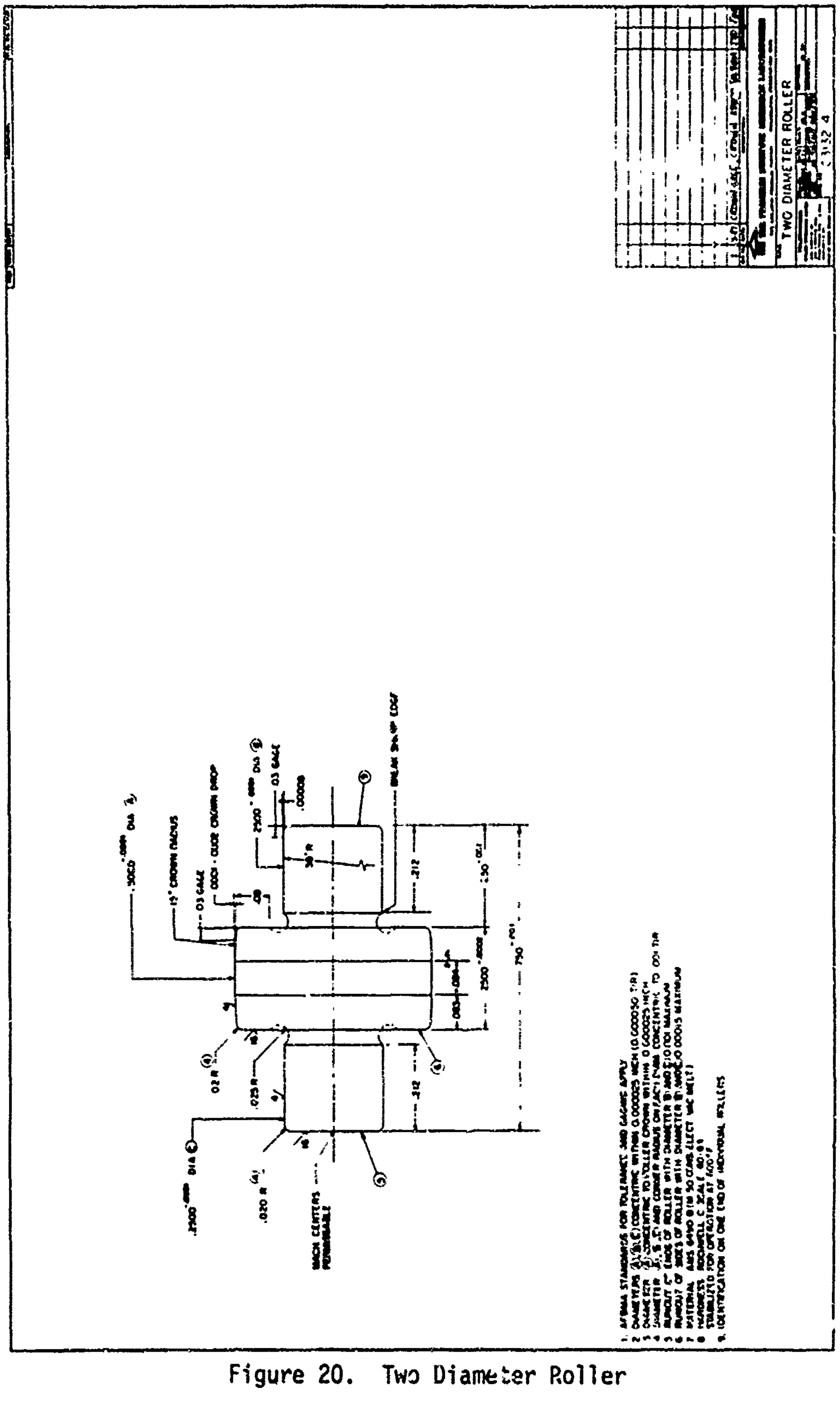

Figure 20. Two Diameter Roller

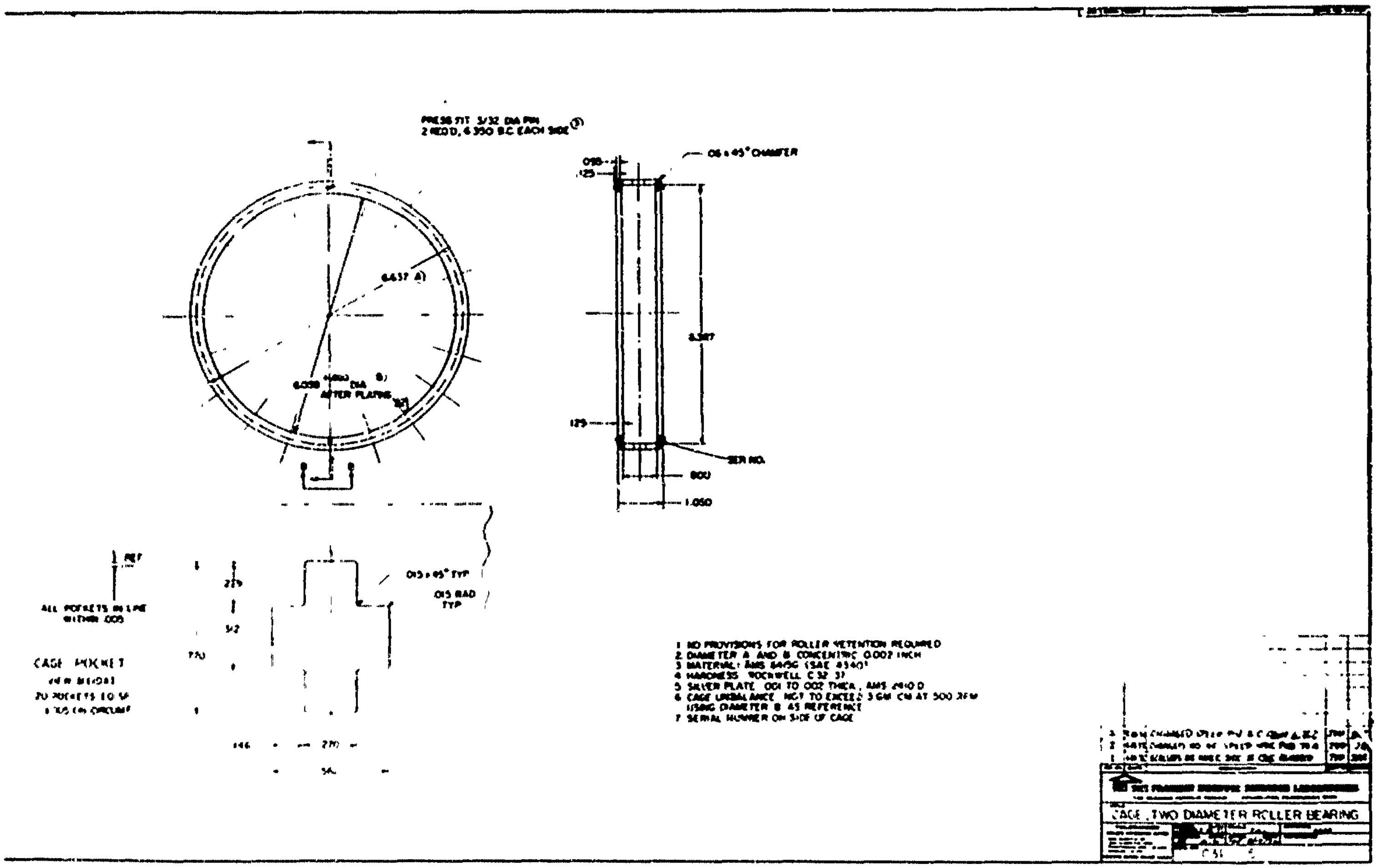

Figure 21. Cage, Two Diameter Roller Bearing

SECTION V

DUAL DIAMETER BEARING FABRICATION

Six prototype test bearings Figure 22 were fabricated to the design drawings (Figures 17-21) by the Bower Bearing Div., Federal-Mogul Corporation, Detroit, Mich. A summary of the six prototype bearing dimensional sizes and variations are given in Table XVIII.

The inner race roller path circularity and contour for test bearing No. 3 are shown in Figures 23 and 24 and are representative of all of the bearings. The circularity and raceway contour of the outer race roller path are shown in Figures 25 and 26 for test bearing No. 3.

The roller design for the dual diameter roller, Figure 20, is not an easy shape to produce. However, the test bearing rollers were centerless ground and crowns were maintained within drawing limits on all three roller portions, as shown by the typical roller traces, Figure 27.

All material specifications, silver plating, balance, etc., are given in the design drawings, Figures 17-21. All prototype bearings met or exceeded the design drawing requirements.

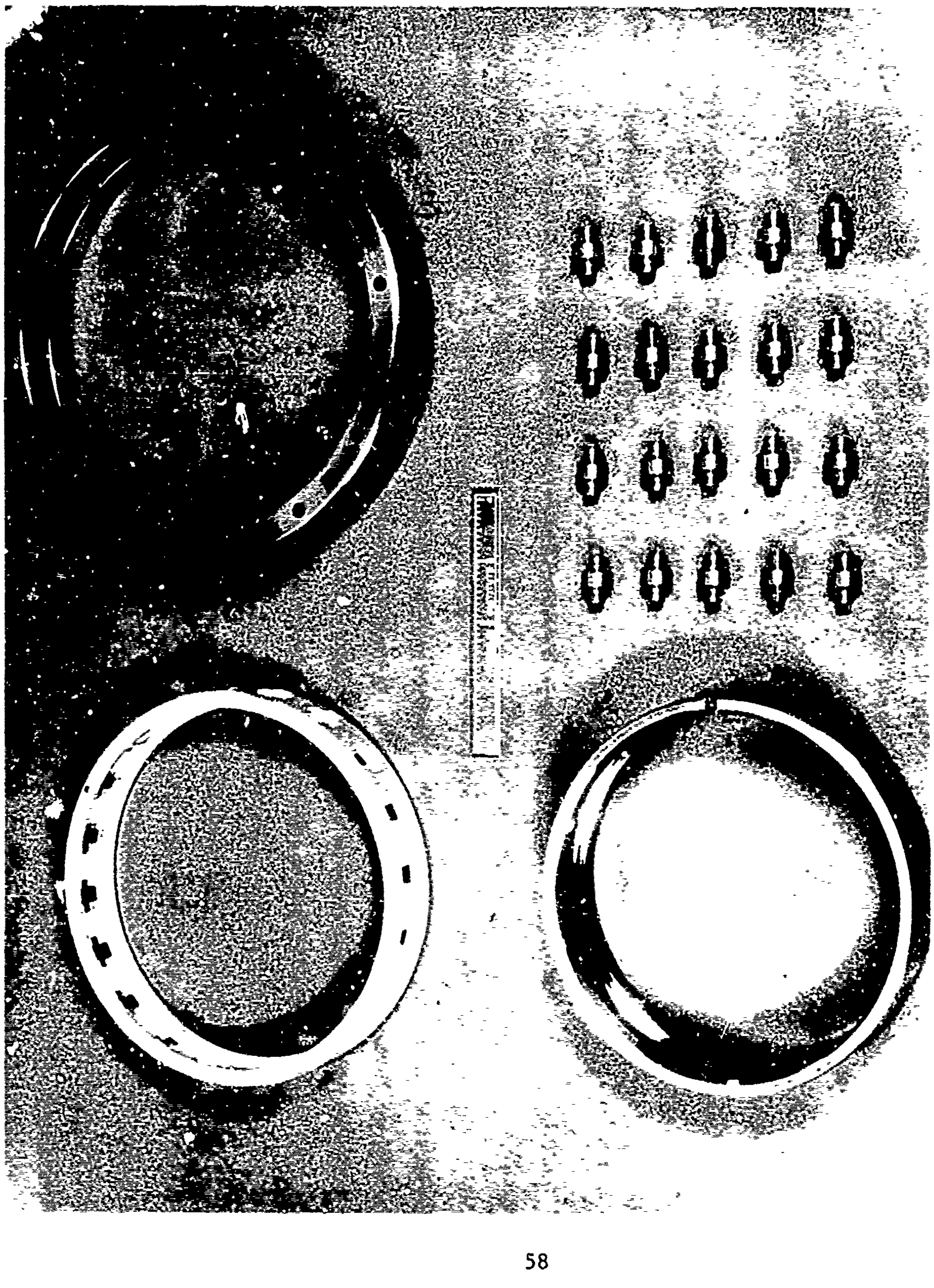

Figure 22. Dual Diameter Roller Brg. Ass'y.

Table XVIII

Serial Number	A1	B2	C3	D4	E5	F6
Inner Races - C3132-2						
O.D. Size	6.00384	6.00385	6.00395	6.00396	6.00385	6.00390
Taper	0.000020	0.00040	0.000070	0.000070	0.000020	0.000038
Out-of-Round	0.000050	0.000050	0.000050	0.000050	0.000050	0.000050
Bore Land	5.51160	5.51160	5.51165	5.51170	5.51165	5.51165
Bore Land	5.57160	5.51165	5.57165	5.51170	5.51165	5.51165
Out-of-Round	0.000050	0.00015	0.00015	0.00015	0.00015	0.00015
Concentric	0.00010	0.00025	0.00015	0.00013	0.00012	0.00010
Width	1.4955	1.4951	1.4955	1.4955	1.4954	1.4954
O.D. Surface Finish	2AA	2-1/2/3AA	2/2-1/2AA	1-1/2/2AA	1-1/2/2AA	2AA
Outer Races - C3132-2						
O.D. Size	7.8739	7.8736	7.8738	7.8736	7.8739	7.8738
Taper	6.001	0.0001	0.0001	0.0001	0.0001	0.0001
Out-of-Round	0.0001	0.001	0.0001	0.0001	0.0001	0.0001
I.D. Track	6.76416	6.76414	6.76416	6.76420	6.76416	6.76412
Out-of-Round	0.00015	0.00015	0.00015	0.00015	0.00015	0.0001
Taper	0.000050	0.000050	0.000050	0.000050	0.000050	0.000050
Concentric	0.00010	0.000050	0.00015	0.00015	0.00010	0.0010
Flange Opening	0.2508	0.2508	0.2512	0.2508	0.2508	0.2511
Parallel Face to Wall	0.00015	.0001	0.00015	0.00015	0.00015	0.00015
Parallel Wall to Wall	0.0001	0.0001	0.0001	0.0001	0.00015	0.0001
I.D. Surface Finish	5AA	4AA	5AA	5AA	3-1/2/4AA	4/5AA
Flange Surface Ion	2AA	2-1/2/3AA	2/2-1/2AA	1-1/2/2AA	1-1/2/2AA	2AA
Cage - C3132-5						
O.D. Size (A)	6.6436/6.6442	6.6428/6.6434	6.6423/6.6438	6.6426/6.6430	6.6427/6.6433	6.64221/6.6428
O.D. Size (B)	6.6434/6.6444	6.6427/6.6432	6.6424/6.6436	6.6427/6.6432	6.6424/6.6433	6.6423/6.6424
O.D. Out-of-Round	.0006/.001	.0006/.0005	.0013/.0012	.0004/.0005	.0006/.0005	.0003/.0001
I.D. Size (A)	6.0404/6.0415	6.0408/6.0412	6.0408/6.0414	6.0410/6.0417	6.0408/6.0412	6.0412/6.0422
I.D. Size (B)	6.0408/6.0412	6.0408/6.0412	6:0404/6.0412	6.0409/6.0413	6.0405/6.0412	6.0412/6.042
Concentric ID/OD	.001 TIR	.001 TIR	.001 TIR	.0012 TIR	.0012 TIR	.0008 TIR
Squareness	.001 TIR	.001 TIR	.0011 TIR	.001 TIR	.00105 TIR	.0008 TIR
Width	1.057	1.0572	1.0565	1.055	1.055	1.055
Cage Balance GM/cm @ 500 rpm	0.2-0.3	0.3-0.2	0.4-0.3	0.2-0.2	0.5-0.3	0.5-0.1
Pkt. Flg. from Side	-.0004	-.0004	-.0004	-	-	-
Rollers - C3132-4						
Large O.D.	.5000/.49995					
Out-of-Round	.000050 max.					
Width	.2500/.2501					
Width Sq. w 5 OD	.00010 max.					
Wall to .2500	.00010 max.					
Small OD	.249975/.249925					
Out-of-Round	.000050 max.					
Length	.2500/.24901					
Face Sq. w .25 OD	.0012 max.					
Overall Length	.7500/.7490					
3 Dia's Concentric	0.000050 TIR					
Finish Dia's	3 RMS					
Finish End	5 RMS					
ASSEMBLED DIAM CLEARANCE	0.0103	0.0103	0.0102	0.0102	0.0103	0.0102

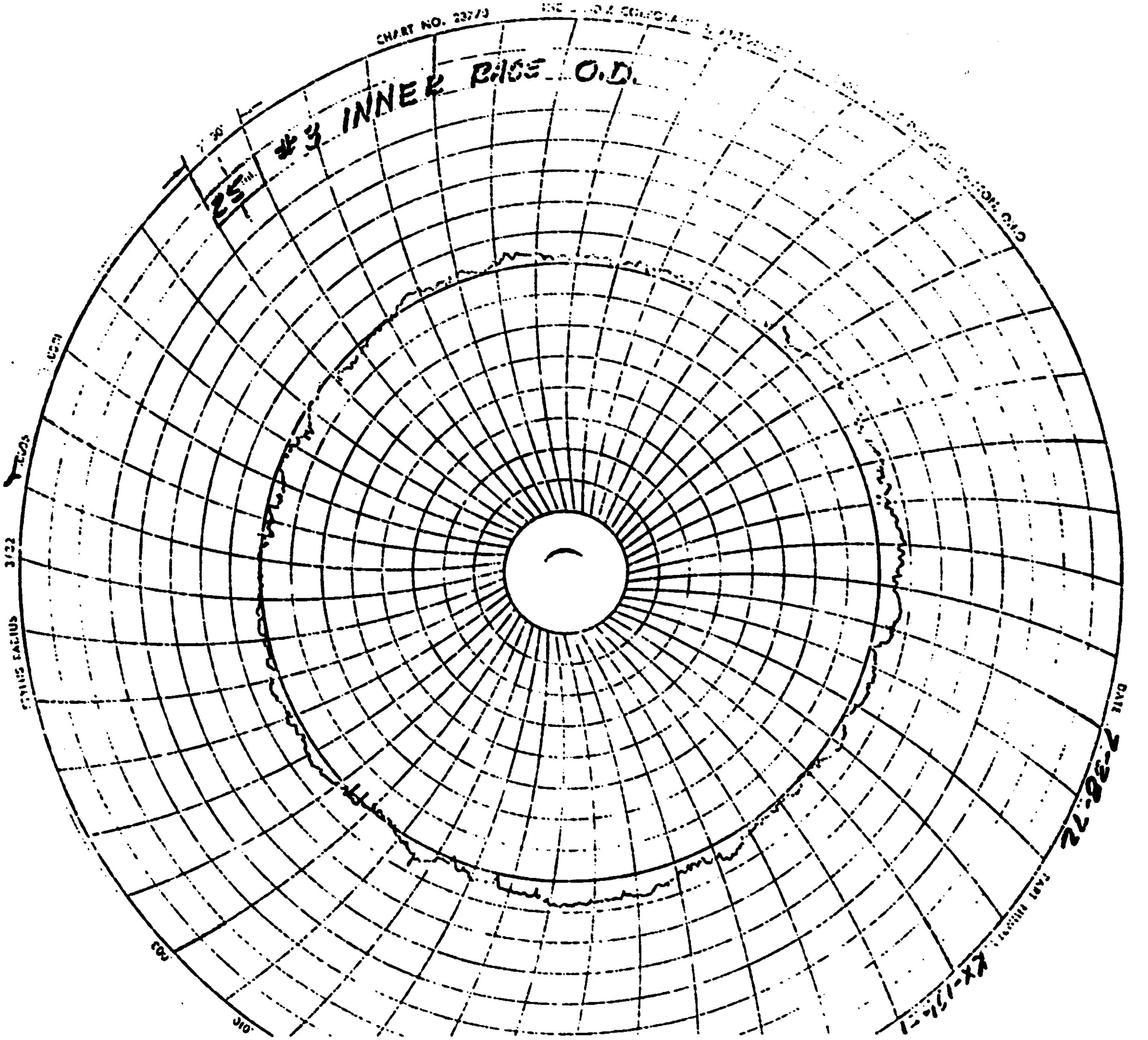

Figure 23. Bearing No. C3 Inner Race Circularity

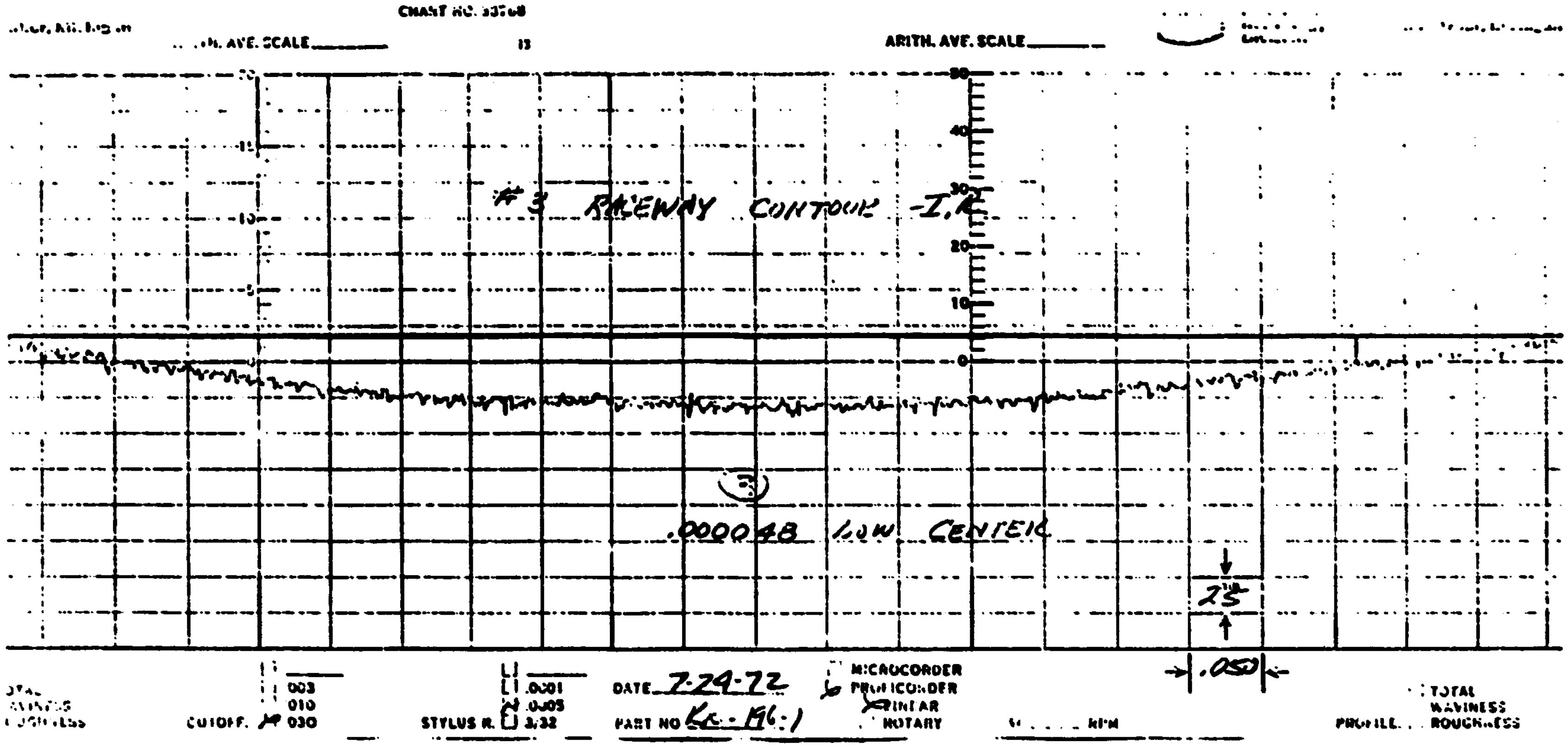

Figure 24. Bearing No. C3 Inner Raceway Contour

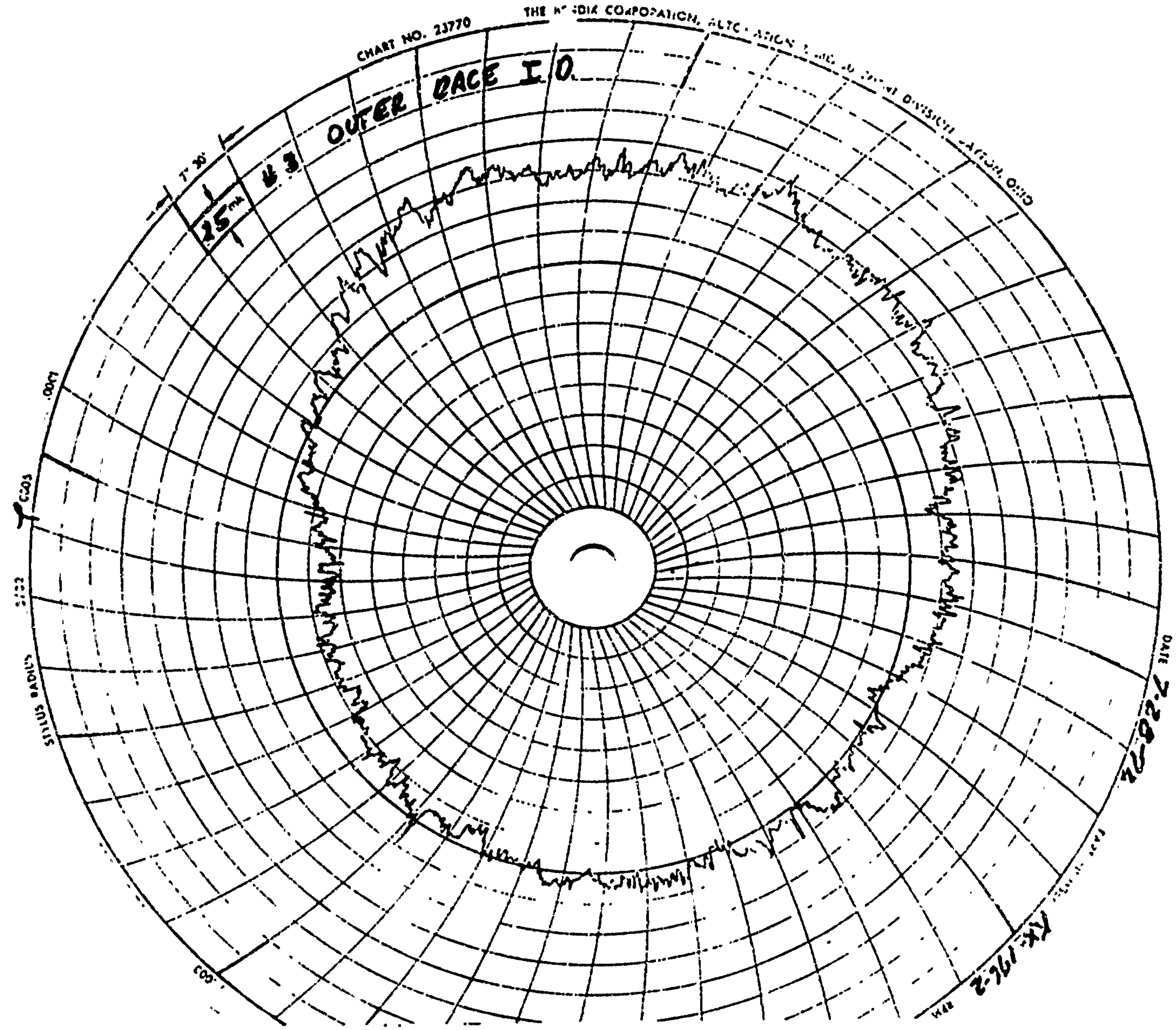

Figure 25. Bearing No. C3 Outer Race Circularity

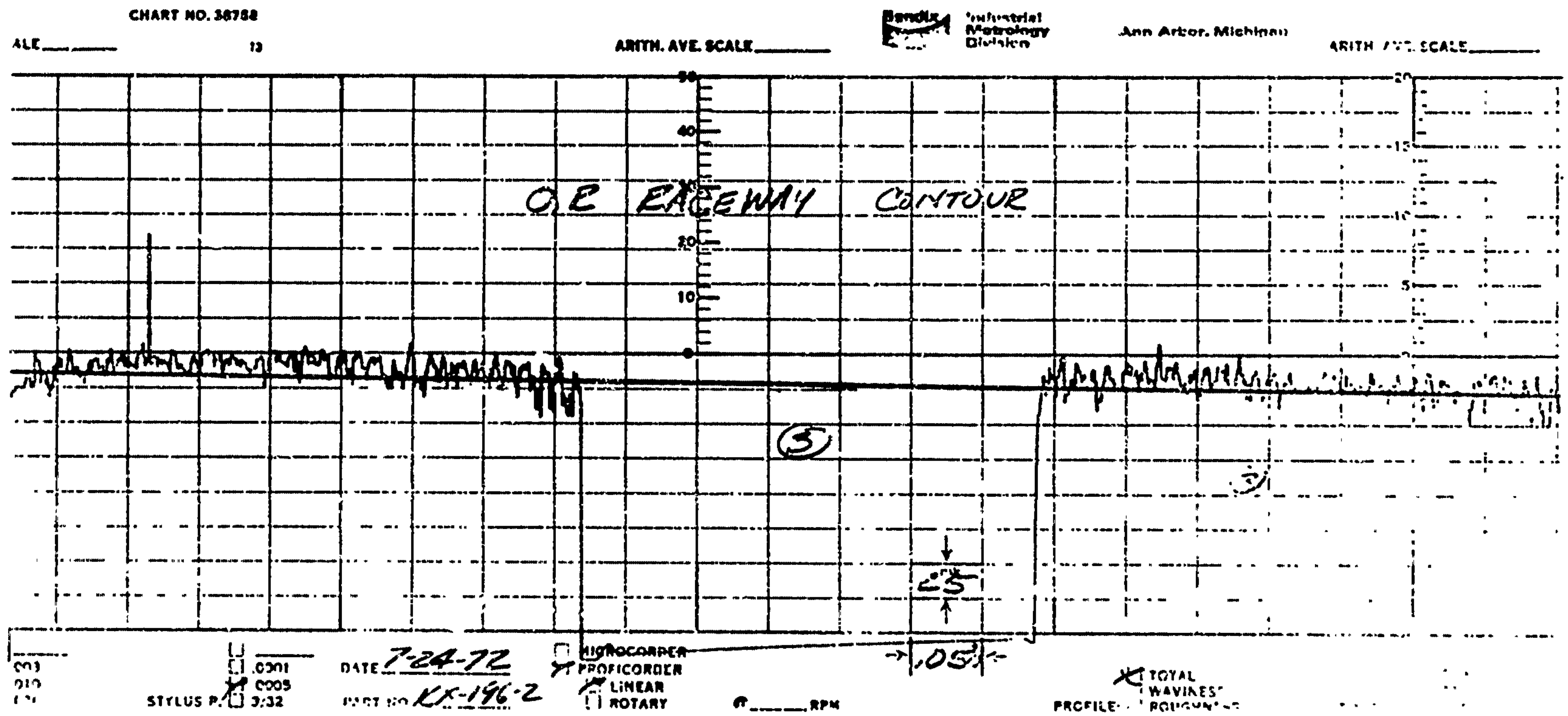

Figure 26. Bearing No. C3 Outer Raceway Contour

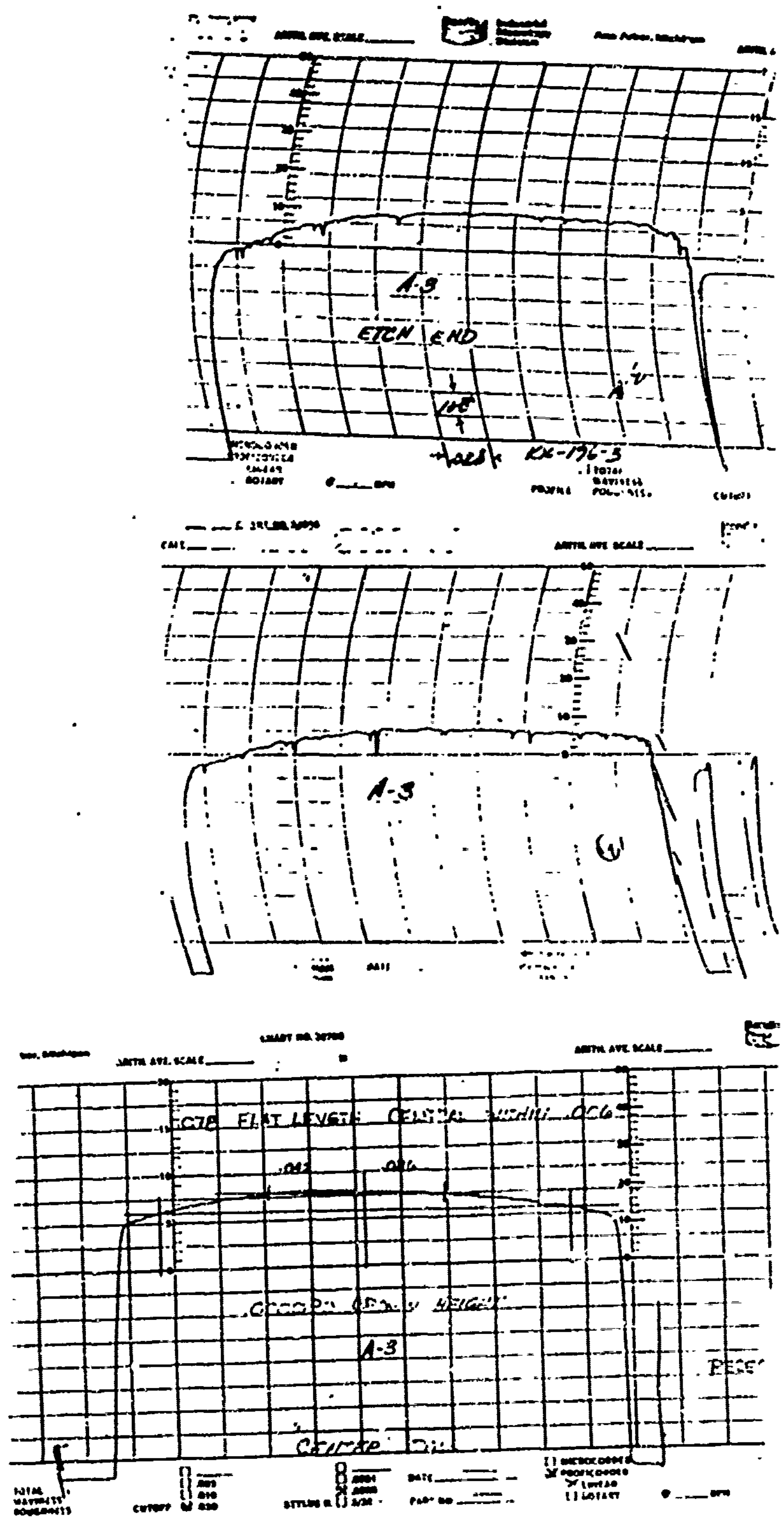

Figure 27. Typical Dual Diameter Roller Crown Profile Traces

SECTION VI

DUAL DIAMETER BEARING TESTS

1. TEST RIG

The dual diameter bearing testing was performed at Midwest Aero Industries, Div. Pure Carbon Co., St. Mary's, Pa., on an existing 250 hp drive test stand with an eddy current clutch and speed increaser gear box. The test rig is shown in Figures 28 and 29. A cross-sectional drawing of the rig is given in Figure 30. The numbered locations correspond to the thermocouple temperature readings of the actual test data. All of the original test log sheets are contained in the Appendix.

The test rig consists of a short hollow shaft supported by two 75 mm bore slave roller bearings. The dual diameter roller bearing, 140 mm bore, is supported midway between the two slave bearings. Radial load is applied by pulling upward on the test bearing housing through a large ring as shown on Figure 30. Oil to the dual diameter bearing is introduced through three orifices, location No. 1, and jeted to a scoop on the test shaft. The oil then travels to the recess under the dual diameter bearing, up through the bearing, out into the rig cavity, and exits the drain through points 2 and 4. The test shaft is driven by a splined quill shaft between the rig and the speed increaser gear box. The area for the quill shaft drive is shown with the cover removed in Figure 28. The entire test head shown in Figure 30 and a transition cone covering the quill drive shaft are cantilevered from the speed increaser gear box, as can be seen in Figures 28 and 29.

Two prototype dual diameter roller bearings were tested under the current contract. The first bearing was operated with MIL-L-7808 oil at approximately 250°F inlet temperature to gain a feel for the power losses and general operation of the bearing with a known lubricant. The first test bearing was then operated with Polyphenyl Ether 5P4E lubricant at approximately

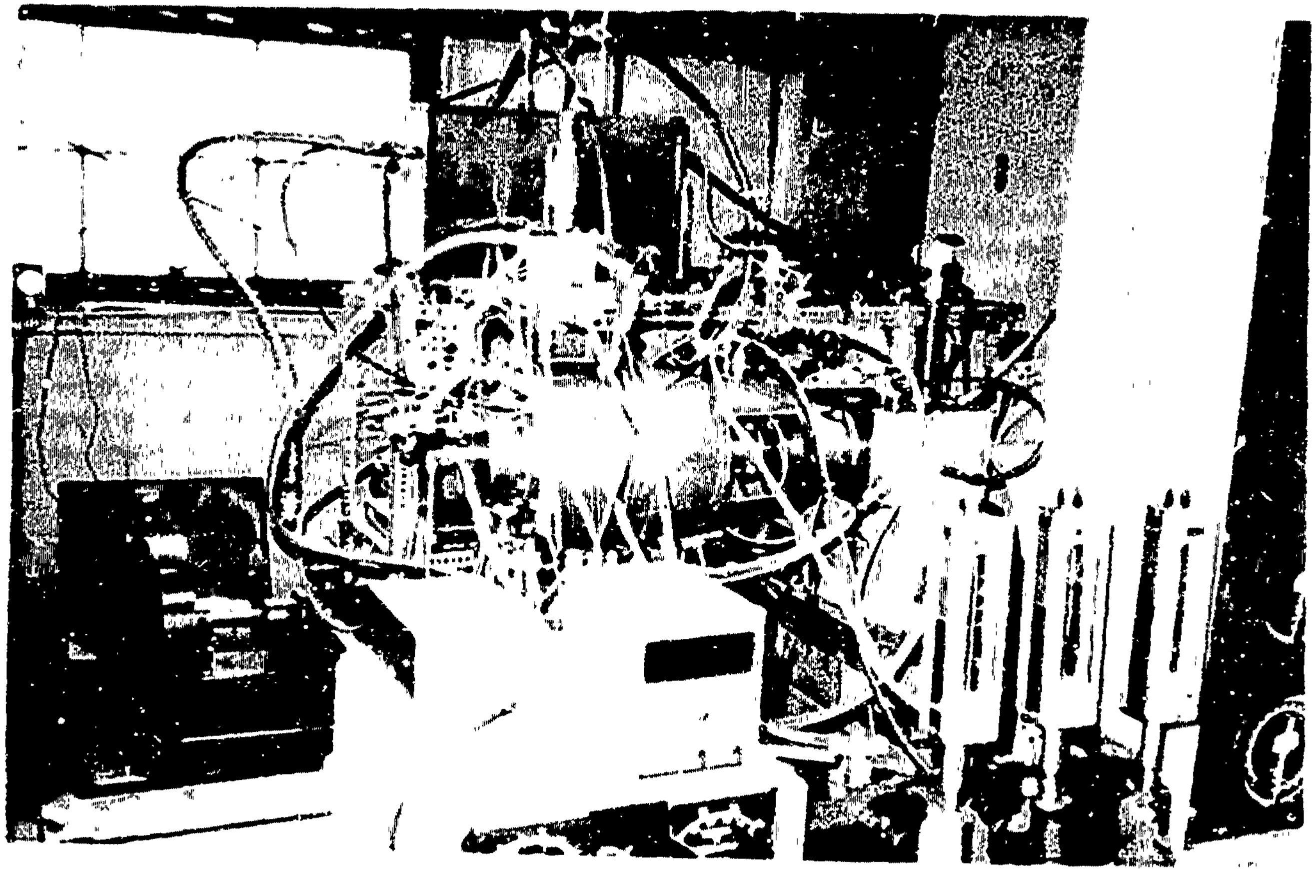

Figure 28. Dual Diameter Roller Bearing Test Stand

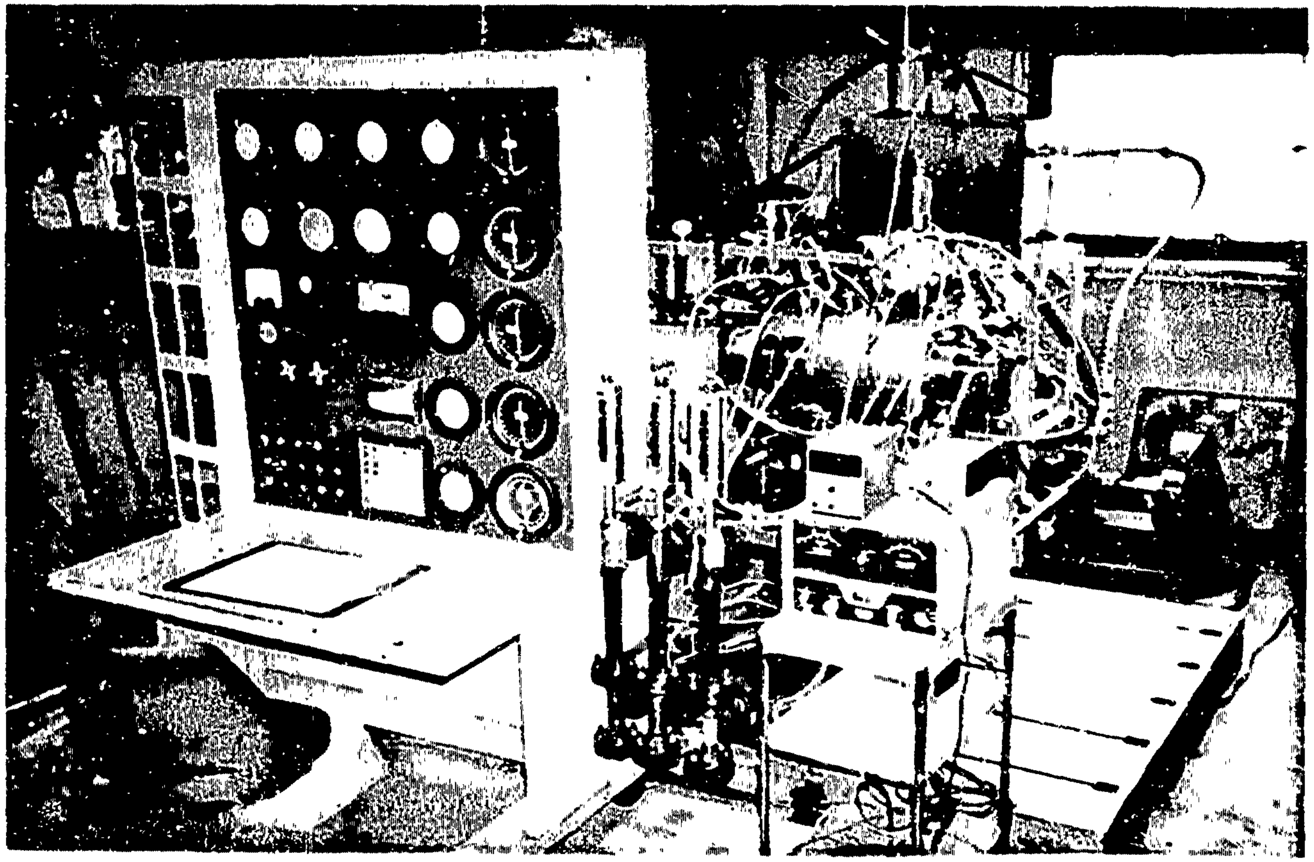

Figure 29. Dual Diameter Roller Bearing Instrumentation

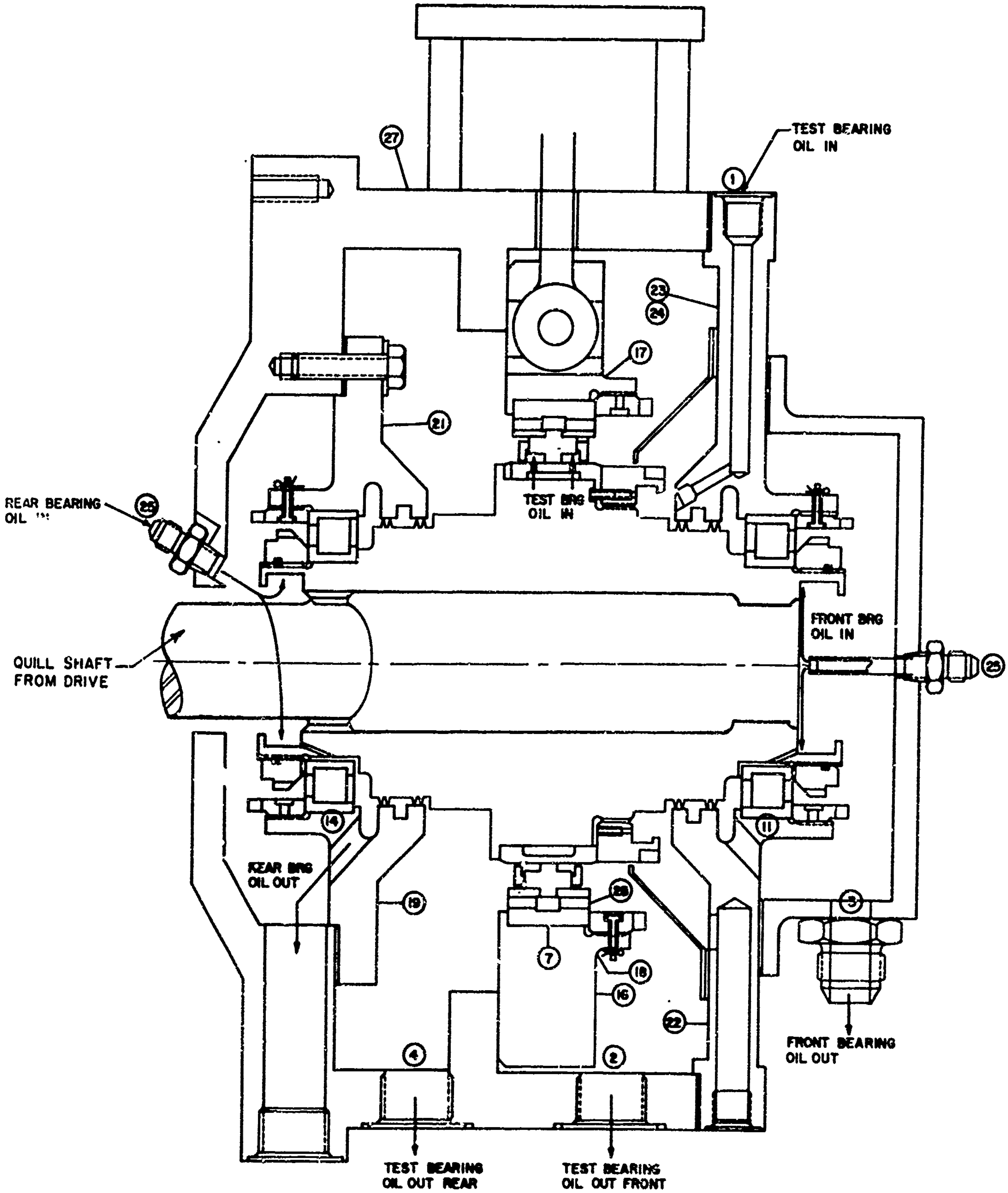

Figure 30. Cross Section of Dual Diameter Bearing Test

500°F oil inlet temperatures up to and including 3.25 x 10^6 DN operation. The second test bearing was operated with Polyphenyl Ether 5P4E lubricant at approximately 500°F oil inlet temperature and successfully completed 30 minutes of continuous operation at 3.5 x 10^6 DN (25,000 rpm) with stabilized temperatures. The second test bearing was then subjected to a series of rapid acceleration/deceleration tests and removed for visual inspection.

2. MIL-L-7808, TEST BEARING A1

A data summary sheet for the operation of the first test bearing s/n No. A1 is shown in Table XIX. The bearing outer race and front and rear drain oil temperature increases as a function of bearing speed for the testing shown in Figure 31.

Twenty-five minutes of successful operation at 3.50 x 10^6 DN was obtained (see runs 49 and 50). The bearing was removed from the test cell and visually inspected. The inner race, rollers and outer race showed some discoloration due to operating at 300°F average outer race temperatures. The rolling surfaces looked to be in excellent condition with only the normal amount of burnishing to be expected after completion of 13 hours and 40 minutes accumulated running time.

The cage was found to be badly worn on the inner land riding diameters over approximately a 35 degree arc on both lands. The worn areas had penetrated the silver plating and significantly deformed the steel. The worn areas were directly under one of the cage pins used for cage speed instrumentation. It appeared that the cage had excessive mass unbalance in operation which led to the localized wearing on the inner land surfaces. The s/n No. A1 cage was not reused. The inner race, outer race and roller complement however were in excellent condition and were reused for the second set of tests.

3. 5P4E, TEST BEARING A1

s/n No. A1 bearing with the s/n No. B2 cage was assembled in the test rig for the high temperature Polyphenyl Ether test. A data summary sheet

Table XIX

DATA SUMMARY SHEET FIRST TEST BEARING - MIL-L-7808 OIL

PURE CARBON CO—DATA SUMMARY SHEET

TEST OF — Dual Diameter Roller Bearing in MIL-L-7808 Oil S/N 1

CUSTOMER — A.F.A.P.L. PROJ. NO. — B1001

DATE — 12-12-72 TEST DATE — Oct 72

Reading No	DN	Load lbs	Oil Flow lb/min	Oil Temp °F	O.R. Temp Avg °F	O.R. ΔT Over Oil °F	Oil Out Frnt °F	ΔT °F	Oil Out Rear °F	ΔT °F	Vib 1/Rev Horz Mils	Vib 1/Rev Vert Mils
9	0.5	471	5.3	248	219	-29	227	-21	207	-41	0.6	0.8
11	0.5	954	5.3	246	221	-25	230	-16	210	-36	0.5	0.75
15	0.75	477	5.3	250	23[illegible]	-18	235	-15	215	-35	0.25	0.15
19	0.75	477	8.5	245	23[illegible]	-8	240	-5	232	-13	0.25	0.15
21	1.00	477	8.5	246	242	-4	240	-[illegible]	239	-7	0.14	0.08
23	1.25	477	8.5	248	249	1	242	[illegible]	242	-6	0.21	0.07
25	1.50	477	8.5	250	260	10	247	-1	249	-2	0.50	0.05
31	1.75	453	8.5	241	263	22	247	6	248	7	0.60	0.09
33	2.00	482	8.7	240	271	31	251	11	252	12	0.40	0.06
35	2.25	482	8.6	245	283	28	260	15	261	16	0.50	0.07
38	2.50	482	8.5	248	297	49	270	22	276	28	0.30	0.40
39	2.50	459	9.0	248	293	45	270	22	275	27	—	—
41	2.75	447	8.9	249	302	53	275	26	280	31	0.70	0.05
46	2.50	500	9.4	250	281	31	271	21	273	23	1.00	0.20
47	3.00	458	9.9	246	301	55	285	39	294	48	0.95	0.55
48	3.25	474	9.6	255	320	65	300	45	319	64	0.70	0.25
49	3.50	471	9.6	262	336	74	310	48	317	55	0.50	1.00
51	3.50	462	8.6	265	340	75	315	50	32[illegible]	64		

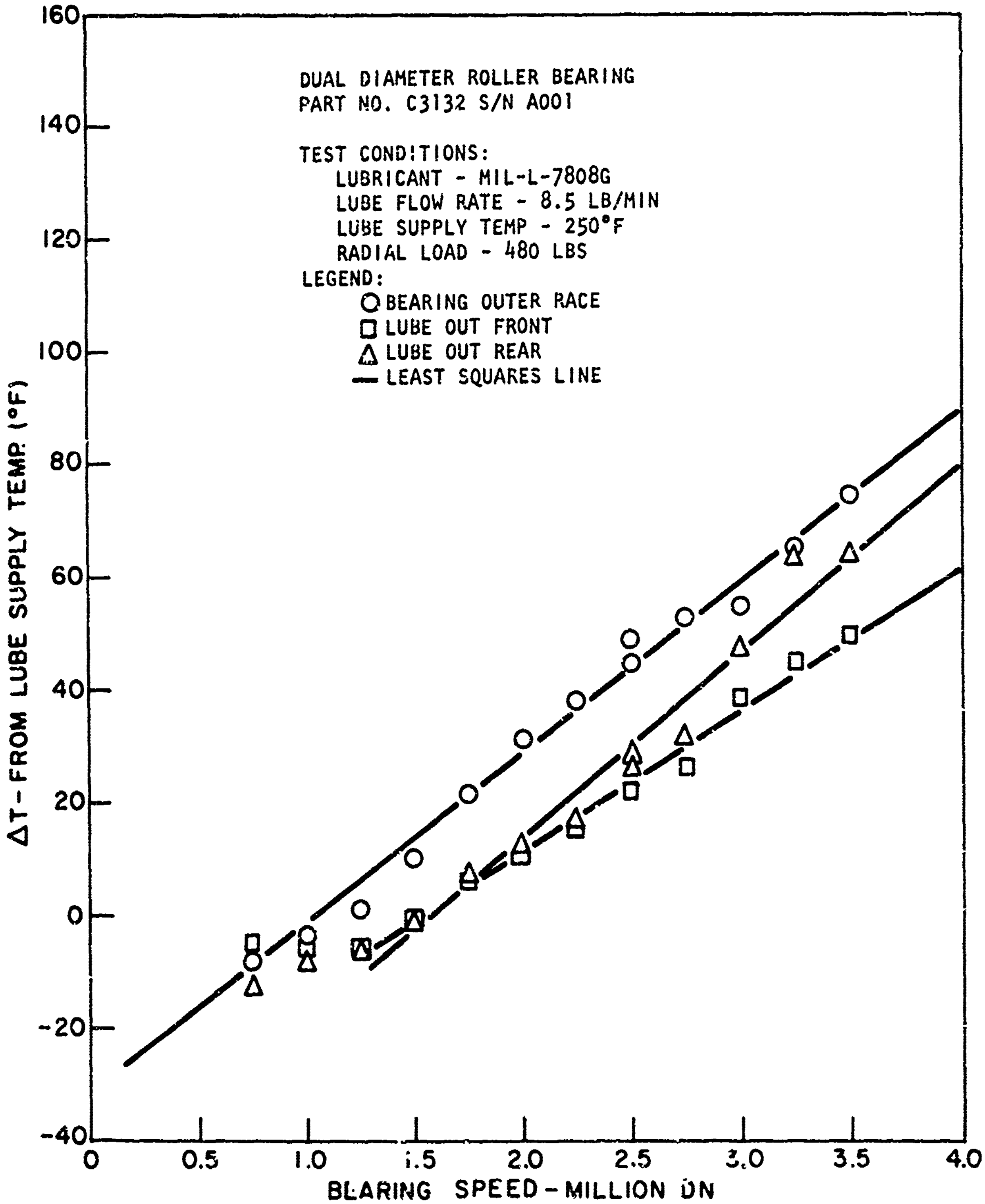

Figure 31. Test Bearing No. 1, ΔT vs. Speed, MIL-L-7808 G

is given in Table XX. The temperature differentials in the bearing for the outer race and drain temperatures are shown on Figure 32. The bearing was initially operated up to and including 3.0×10^6 DN operation. At this point the Polyphenyl Ether lubricant was being pumped back through the quill shaft Figure 30, to the gear box and mixing with MIL-L-7808 oil in the gear box system. The rig was shut down and lube system changed so that the gear box as well as the test head would operate on 5P4E lubricant and would avoid the loss of excessive amounts of the test oil. Testing was then resumed and resulted in the second set of curves as shown on Figure 32.

Successful operation of the test bearing was accomplished up to and including 3.25×10^6 DN operation. After approximately 10 minutes operation at 3.50×10^6 DN operation (run No. 86), the bearing failed abruptly as evidenced by a seizure and a dead stop of the test shaft. The failed test bearing was then removed for visual examination. The inner race had separated and formed into two circumferential halves approximately in the center of the race. The rings had also snapped open at a location corresponding to one of the key slots as shown in Figure 33. A considerable amount of debris was trapped between the inner race cavity and the shaft. Figure 34 is a photograph of the rollers, cage and outer race assembly still in the outer race loading ring. The rollers all had a flat surface on the major diameter which presumably was caused when the rollers locked up and braked the inner race to a complete halt. Several of the rollers are shown on Figure 35. All of the rollers had at least one of the small diameters separated from the body of the roller as shown in Figure 35 and in several cases both minor diameters had been separated. Subsequent metallurgical examination of the fractured surfaces supports the fact that the small diameters were twisted or torqued out of the major diameter. They were not reversed bending fatigue failures. Complete seizure of the inner race creating sufficient friction to grind flat from the rollers (as shown in Figure 35) would create tremendous torques on the minor roller diameters. The outer race is shown in Figure 36 and the cage is shown in Figure 37. The cage suffered serious distortion as would be anticipated.

Table XX

DATA SUMMARY SHEET FIRST TEST BEARING - POLYPHENYL ETHER 5P4E

PURE CARBON CO—DATA SUMMARY SHEET

TEST OF – Dual Diameter Roller Bearing in Poly Phenyl Ether 5P4E @ 500°F S/N1

CUSTOMER – F/RL

PROJ. NO. – B1001

DATE – 12-18-72

TEST DATE – 11-6-72

Reading No	DN	Load lbs	Oil Flow lb/min	Oil Temp °F	O.R. Temp. Avg °F	O.R. ΔT overall °F	Oil Out FRT °F	ΔT °F	Oil Out REAR °F	ΔT	Vib H/Rev Horiz Mils	Vib H/Rev Vert Mils
61	0.5	491	9.9	495	407	-38	490	45	475	-30	.25	.55
64	1.0	453	10.6	450	422	-28	505	55	490	40	.15	.06
67	1.5	471	10.4	480	458	-22	535	65	535	55	.17	.10
70	2.0	451	10.4	485	476	-9	555	70	555	70	.30	.25
73	2.5	459	9.9	480	488	+8	560	80	555	75	.40	.15
75	2.75	471	8.5	480	492	+12	555	75	540	40	—	—
77	3.00	488	9.3	485	503	+18	565	80	535	50	.26	.13
80	1.0	471	9.2	490	408	-82	480	-10	470	-20	—	—
82	2.0	465	9.5	470	424	-46	490	+20	455	+15	—	—
84	3.0	459	9.8	448	477	+29	525	+77	500	52	.24	.20
85	1.325	471	10.0	462	503	+41	550	+88	530	+65	1.90	.40
86	3.50	459	10.2	470	520	+50	570	+100	550	+80	2.10	1.10
100	0.5			250	211	-39	270	20	250	0		

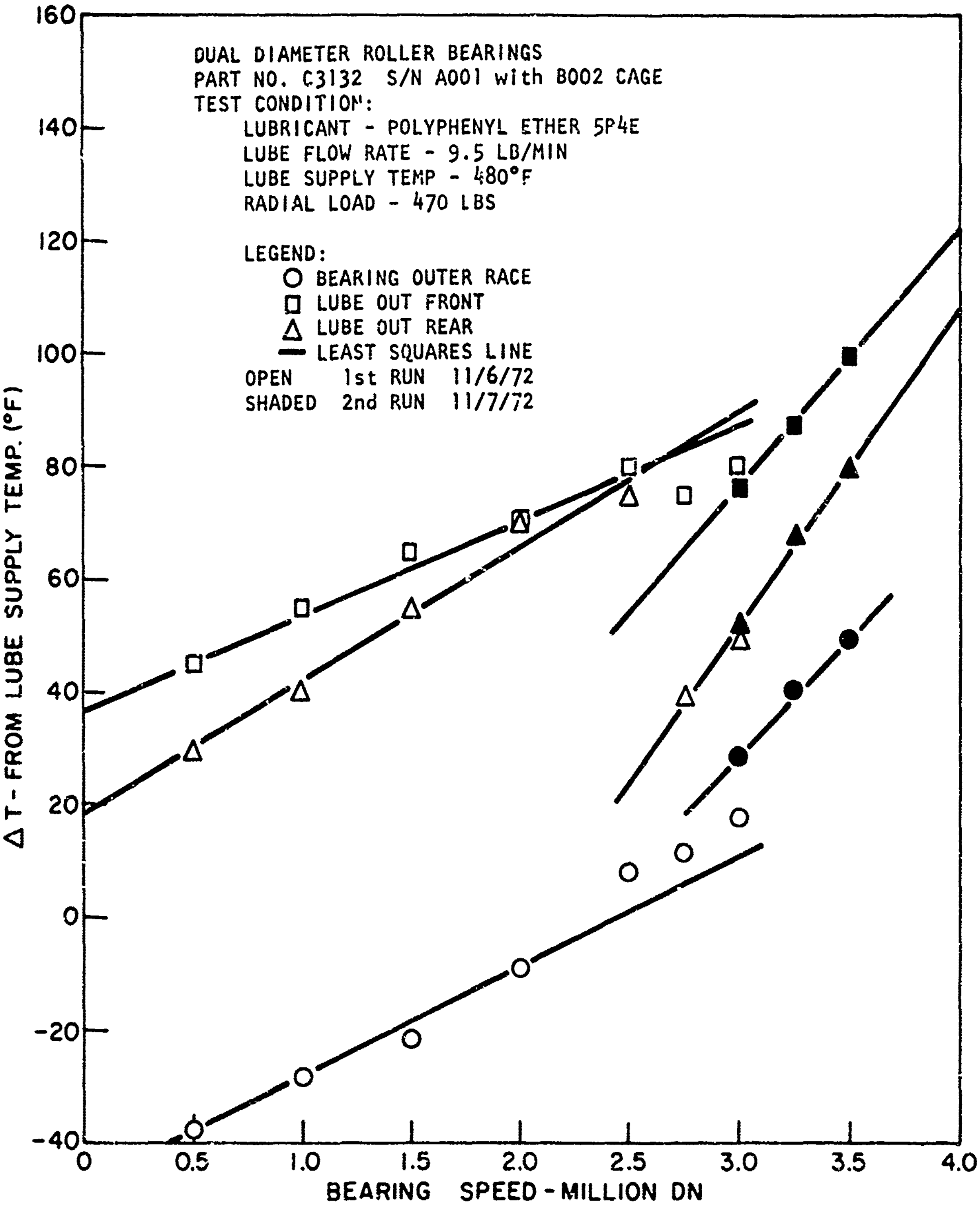

Figure 32. Test Bearing No. 1, ΔT vs. Speed, Polyphenyl Ether, 5P4E

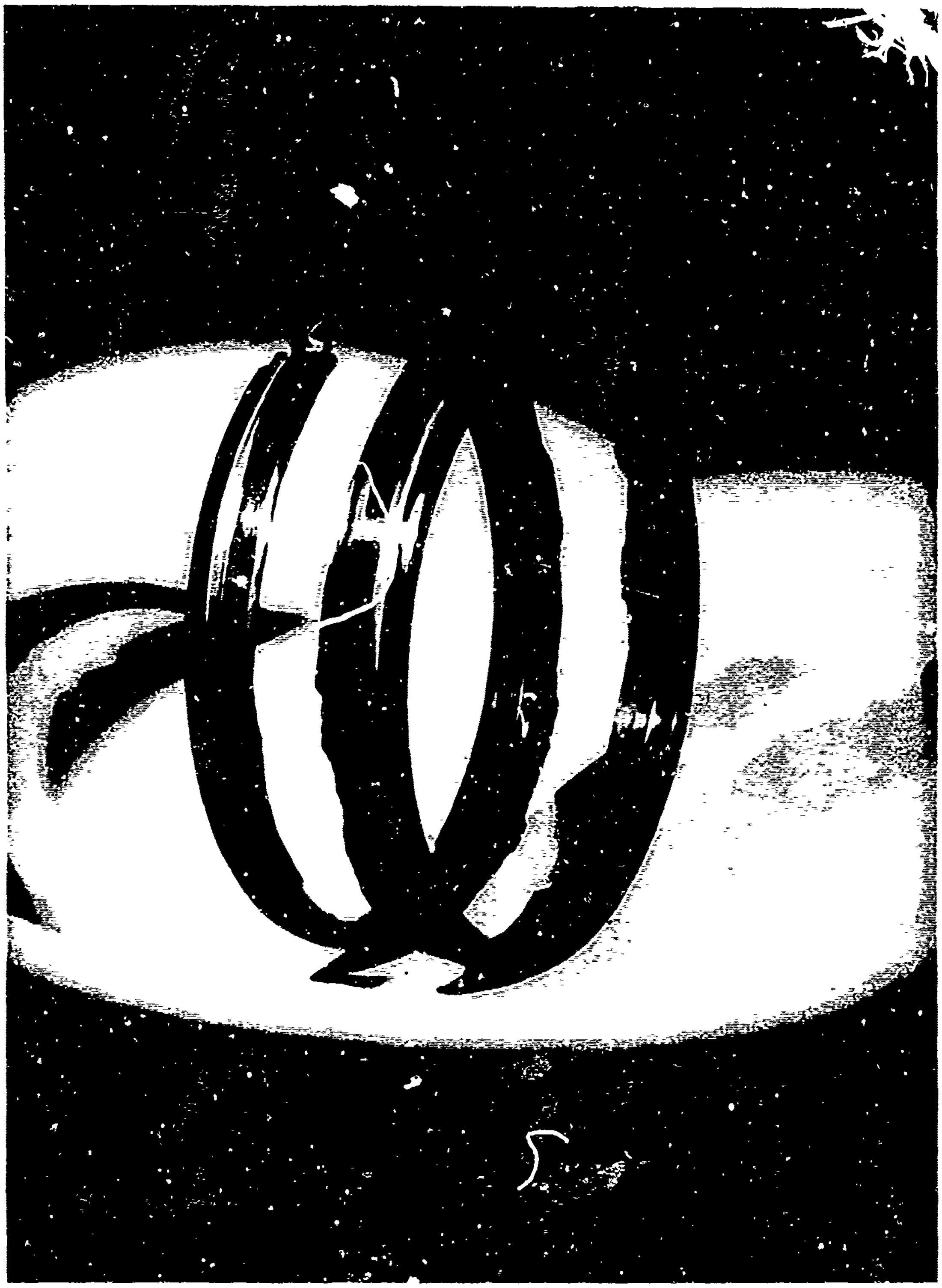

Figure 33. Test Bearing No. 1,
Inner Race Failure

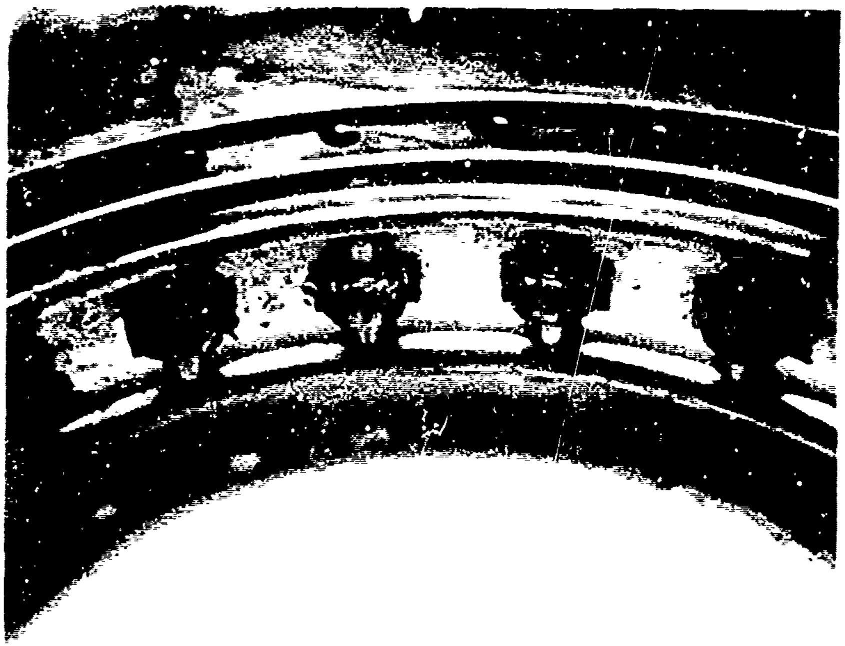

Figure 34. Test Bearing No. 1 Outer Race
Cage Roller Assembly Failure

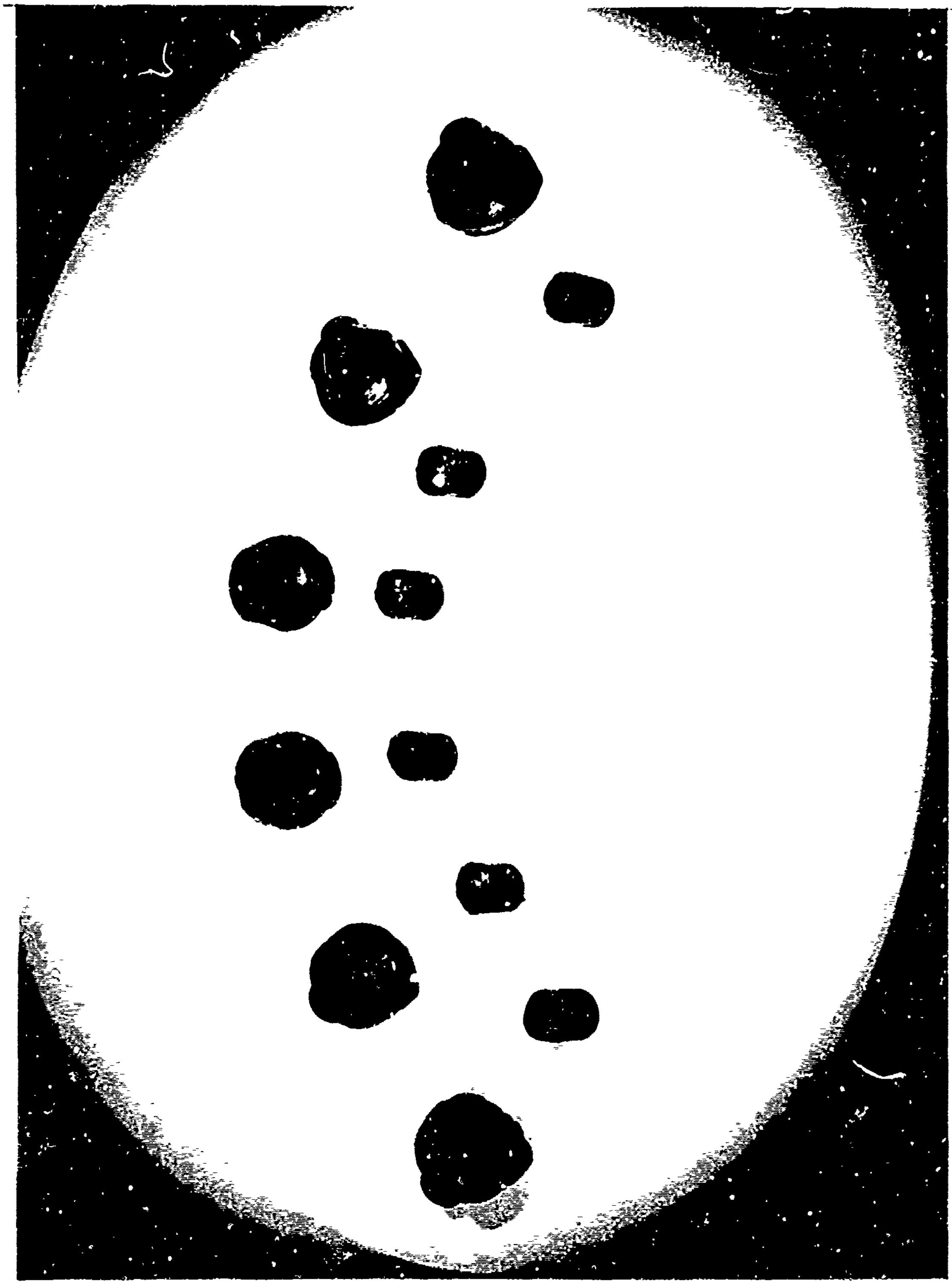

Figure 35. Failed Rollers

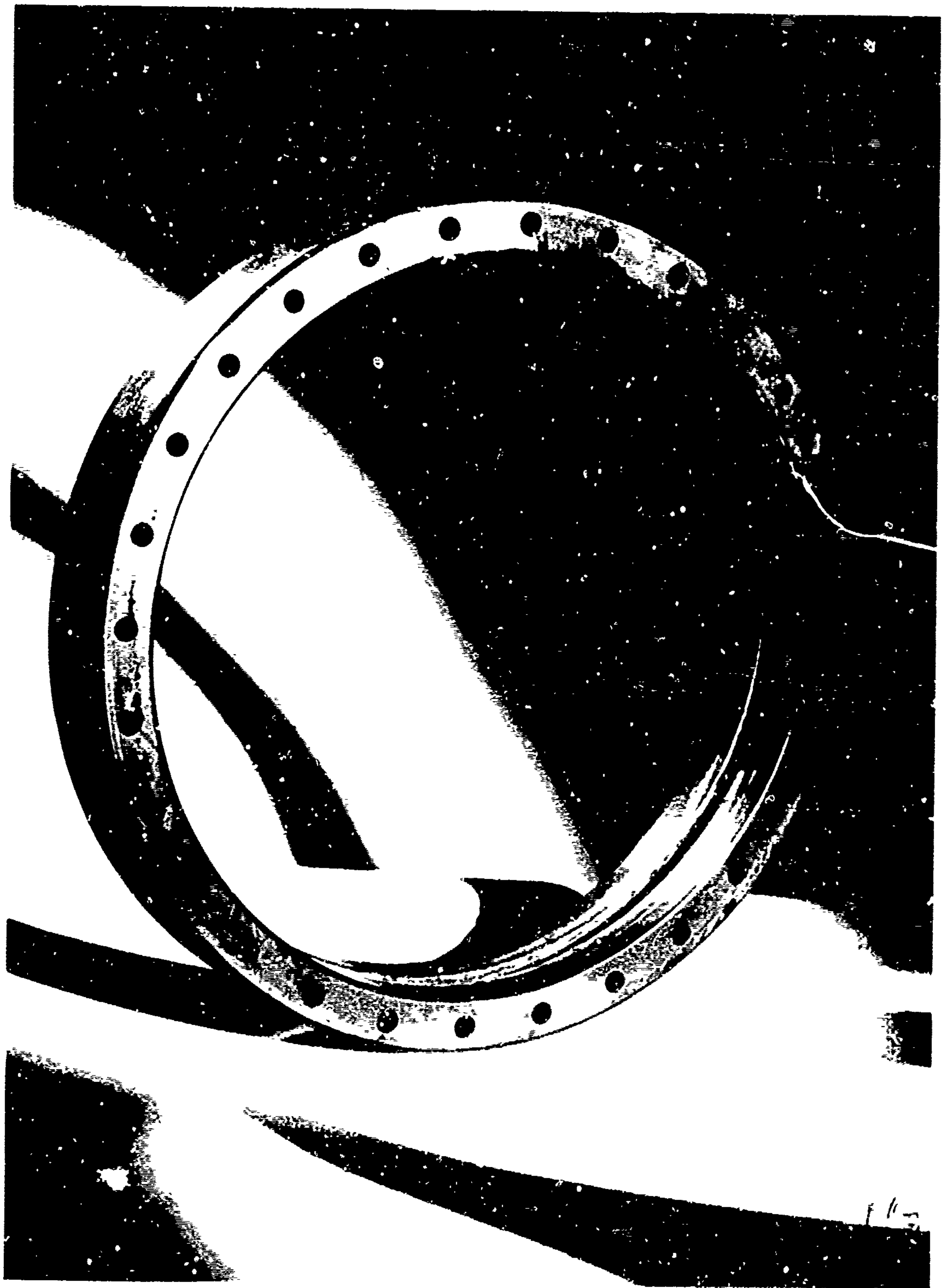

Figure 36. Test Bearing No. 1 Outer Ring Failure

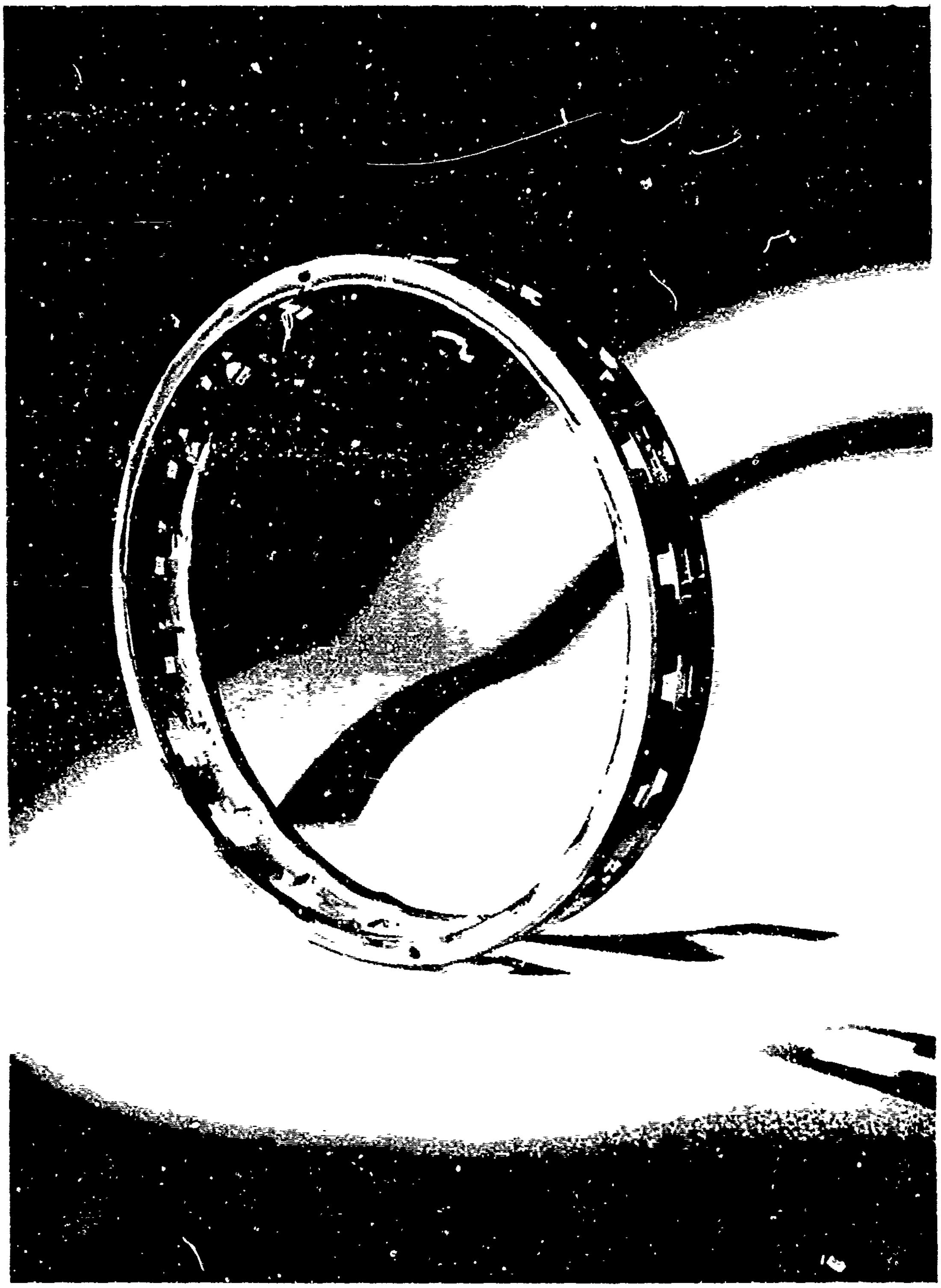

Figure 37. Test Bearing No. 1 Cage Failure

The test bearing A1 accumulated a total of 24 hours operation at various speeds of which 10 hours and 20 minutes were with the Polyphenyl Ether lubricant at high temperature. The failure of the inner race, Figure 33, can be explained by two possible failure modes, the first being thermal lockup of the bearing where the growth of the inner race both thermally and due to centrifugal forces exceeds the growth rate of the outer race resulting in internal diametral preload. Roller bearings are exceptionally stiff and small amounts of diametral preload (on the order of 0.0002 inches or more) can result in very high roller loadings. Greatly increased roller loadings at the inner race contact (see Figure 17) would then undoubtedly fail in reverse bending fatigue. The second possible failure mode is that sufficient clearance did remain in the bearing and that failure of the inner race was due entirely to reverse bending fatigue. The finite element analysis of the inner ring as shown on Figure 13 and summarized in Table IX did not indicate that excessive stress variation would be anticipated at 3.5×10^6 DN operation. Therefore, thermal lockup was suspected. The fact that the bearing did operate for approximately 10 minutes at the higher speed level, however, is not indicative of thermal lockup. Thermal lockup occurs very rapidly after an increase of speed.

The concern over thermal lockup was resolved by additional thermal analysis of the test bearing operating conditions. The initial thermal gradients in the bearing for design purposes did not include any effects of external energy being introduced into the system because of dissipation in the slave bearing. Table XXI shows the results of the thermal analysis with external energy introduced at node 21 on the shaft surface external to the test bearing. Also the effect of insulation around the outer diameter or outer surface of the test head was introduced into this analysis. The results of the improved thermal analysis for the actual load, speed and lubricant supply conditions of the test agree closely with the observed temperatures of Table XX. The outer race temperature per analysis (node 18), was 527.86°F as compared to average observed outer race temperatures of 520°F. The total ΔT to the oil by analysis in Table XXI was (node 11)

TABLE XXI

Thermal Analysis of First Test Bearing Conditions with 5P4E

THE CONVERGED TEMPERATURE DISTRIBUTION (DEG F.) IS AS FOLLOWS:

1	INNER SHAFT COOLANT	=	695.616692
2	INNER SHAFT SURFACE	=	545.986656
3	OUTER SHAFT SURFACE AT BEARING	=	522.194206
4	INNER RACE AT SHAFT	=	540.528114
5	UNDER-CUT SURFACE OF INNER RACE	=	544.477898
6	UNDER RACE COOLANT	=	500.870083
7	INNER RACE BEYOND ROLLER CONTACT	=	550.633530
8	CAGE AT THE LAND	=	576.609593
9	CAGE INNER SURFACE	=	582.211388
10	CAGE OUTER SURFACE	=	581.600281
11	INTERNAL LUBRICANT TO BEARING	=	555.119461
12	ROLLERS	=	586.775314
13	INNER RACE AT ROLLERS	=	550.068855
14	INNER SURFACE OF OUTER RACE	=	547.625595
15	INNER COOLED SURFACE OUTER RACE	=	546.366028
16	OUTER RACE LUBRICANT	=	545.315437
17	OUTER COOLED SURFACE OUTER RACE	=	544.274139
18	BEARING OUTER DIAMETER	=	527.860451
19	CHAMBER WALL (INNER SIDE)	=	513.459312
20	LOADING BOLT (STRUT) ROOT	=	474.929092
21	SHAFT (EXTERNAL TO BEARING)	=	575.953255
	BULK TEMPERATURE RISE OF LUBRICANT	=	41.275596
	AVERAGE BULK OIL TEMPERATURE	=	528.370239

555° less oil inlet temperature of 470° resulting in an 85° ΔT to the oil. This compares very favorably to the 90° average of the oil out front and oil out rear of Table XX. The calculated internal diametral clearance in the bearing under the thermal gradients shown in Table XXI is 0.0051 inches. This number includes all thermal and centrifugal growths. A number of variations in the assumptions of the thermal analysis such as percentage air oil mixture, etc. were tried and found to have little effect on the thermal gradients in the bearing. Therefore the conclusion was reached that the bearing did not fail due to thermal lockup but rather failed due to reverse bending fatigue of the undercut inner race. The finite element analysis summarized in Table IX would indicate that the stress variations with roller loading should not have exceeded the long term life value in reverse bending fatigue. However, the test bearing at the point of failure had experienced 39.7×10^6 cycles of stress or roller load variations between rollers and inner races with both MIL-L-7808 and the 5P4E lubricant. The values were essentially equal with each type of oil. The decision was made to proceed with testing of the second bearing on the assumption that thermal lockup was not the failure mode and to limit the bearing load to no more than 500 pounds so as not to significantly increase the danger of failure due to reverse bending fatigue.

4. 5P4E, TEST BEARING C3

The second test bearing, Serial No. C3, was assembled in the rig for high temperature testing with 5P4E lubricant. A summary data sheet of the test is given in Table XXII and the ΔT's as a function of speed are plotted in Figure 38. This bearing achieved 30 minutes of temperature stabilized operation at 3.5×10^6 DN (25,000 rpm) under a 471 lb. radial load. The only variation in test conditions over the first test bearing was the addition of an auxiliary jet towards the rear of the bearing at the inner race and cage land contact. This auxiliary jet supplied approximately 2 lbs. per minute oil flow of the total reported in the test log.

The test bearing was then subjected to four rapid acceleration and deceleration tests between 1.5×10^6 DN and 3.5×10^6 DN in 15 seconds each.

TABLE XXII

DATA SUMMARY SHEET, SECOND TEST BEARING POLYPHENYL ETHER 5P4E

PURE CARBON CO—DATA SUMMARY SHEET

TEST OF — Dual Diameter Roller Brg. 4N3 w Polyphenyl Ether 5P4E @ 500°F | CUSTOMER — FIGL | PROJ. NO. — 81801 | DATE — 12-23-72 | TEST DATE — 12-21-72

Reading No	DN	Load lbs	Oil Flow lb/min	Oil Temp °F	OR Temp Avg °F	ΔT over oil °F	Oil out FRT	ΔT	Oil CKT Rear	ΔT		Y.b ... Mils
104	0.5	476	[illegible]	355	308	−47	366	+11	300	−55		
106	1.0	453	[illegible]	400	372	−28	420	+20	405	+5		
112	1.5	453	13.0	(1) 420	397	−23	460	+40	450	+30		
114	2.0	453	13.1	455	444	−11	490	+35	480	+25		
116	2.5	453	13.0	455	466	+11	500	+45	490	+35		
119	0.5	459	13.4	330	291	−39	345	+15	280	−50		
125	3.0	488	9.3	460	500	+40	515	+55	490	+30		
126	3.0	477	15.6	445	463	+18	470	+25	455	+10		
127	3.25	471	17.9	475	501	+25	530	+55	515	+40		
128	3.43	471	16.8	495	525	+30	550	+55	540	+45		
129	3.45	471	11.3	510	539	+29	565	+55	555	+45		
130	3.43	471	21.4	515	542	+27	570	+55	565	+50		
131	3.43	471	21.4	530	545	+25	575	+55	570	+50		
132	1.60	471	21.4	500	493	−7	540	+40	535	+35		
133	.63	471	23.3	430	439	+9	450	+20	470	+40		

(1) Possibly 10°F Low

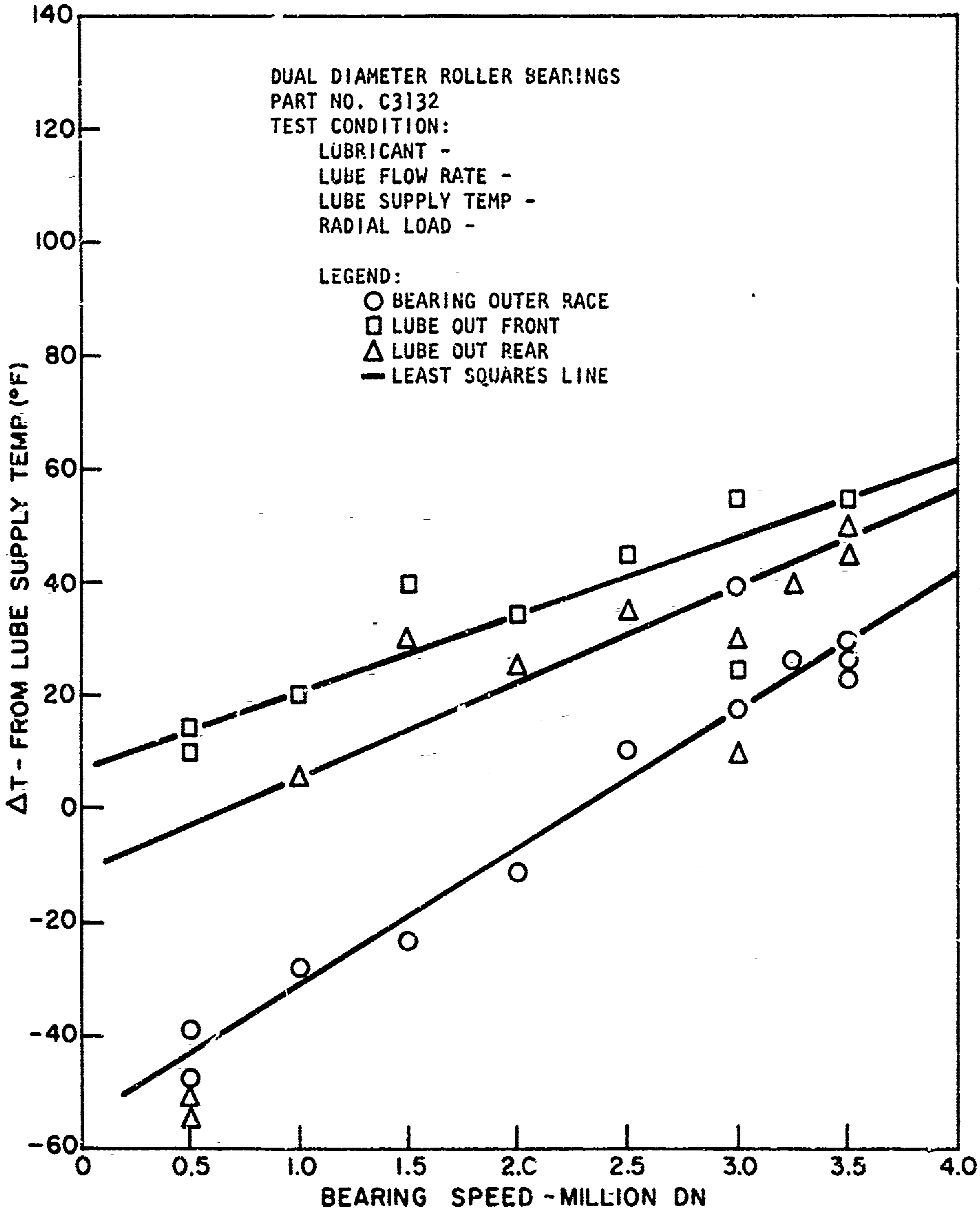

Figure 38. Test Bearing No. 2 ΔT vs. Speed, Polyphenyl Ether, 5P4E

The second test bearing is shown in Figure 39. All of the race and roller operating surfaces were in excellent condition. The cage was in good condition and showed even burnished wear areas in the cage roller to pocket contacting surfaces. With the exception of the riding land, the cage was in excellent condition. The silver plate was not worn through at any position and very little discoloration was noticed. The cage inner land riding surfaces however were discolored over a 90° arc indicating insufficient lubricant to the cage lands. The inner race shows a uniformly burnished area in the center of the race where the rollers contacted. Distress is noted in the cage land riding areas on the inner race. The outer race was in excellent condition. There was some indication in the discoloration due to temperature that the rear of the bearing was cooler than the front face of the bearing. This can be attributed to the auxiliary oil jet directed at the rear face of the bearing.

The Polyphenyl Ether 5P4E lubricant used in the test was supplied by the Aero Propulsion Laboratory, Wright-Patterson Air Force Base. Some of the fluid was new fluid and some of the fluid furnished was reconstituted fluid. It was noted that when new 5P4E fluid was added to the oil sump, that foaming of the oil occurred for a period of 10 to 20 minutes and then subsided. This foaming did not occur when reconstituted 5P4E fluid was added to the sump. The foaming action did not seem to have any effect upon bearing operation.

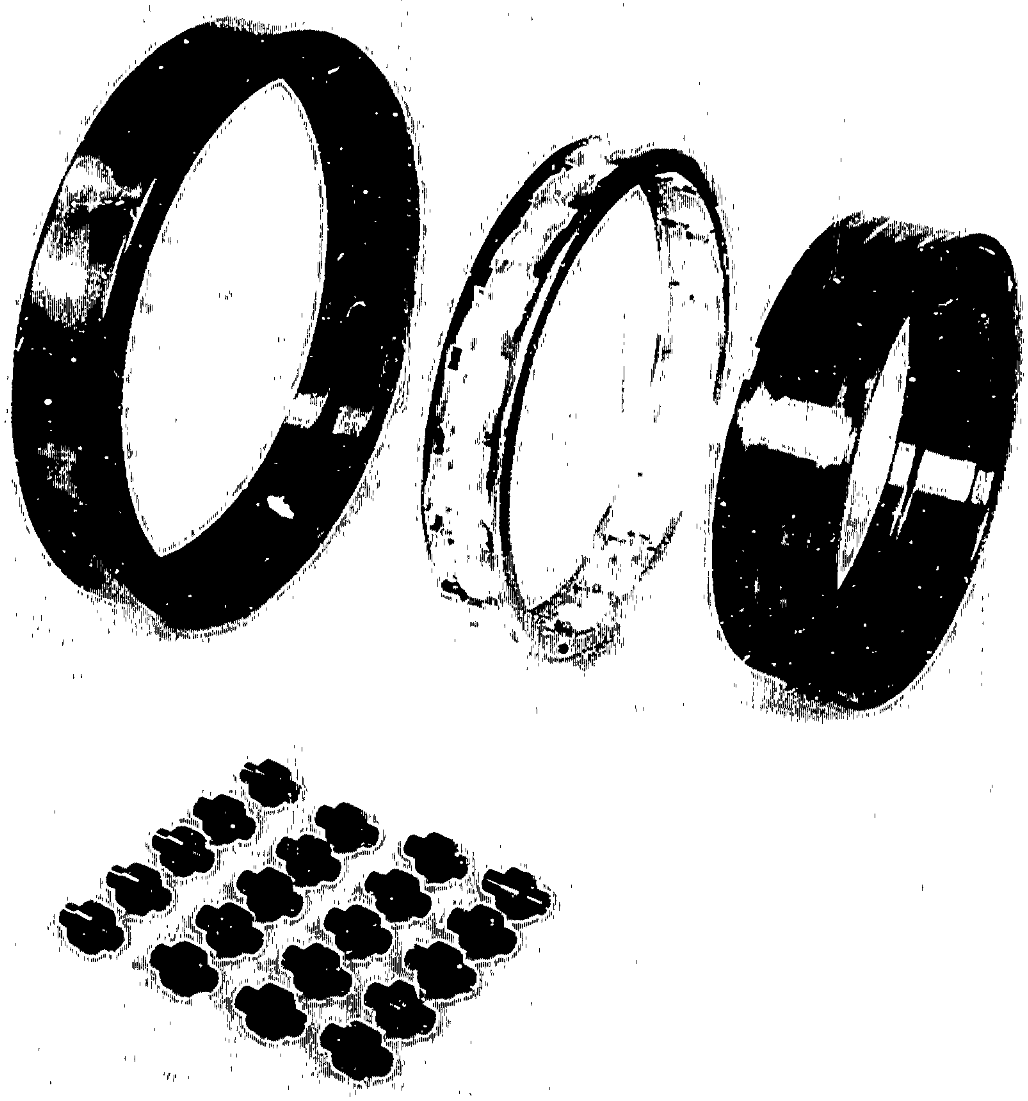

Figure 39. Second Dual Diameter Test Bearing

FIG 39

SECTION VII

CONCLUSIONS

The second dual diameter roller bearing successfully operated for 30 minutes of stabilized temperature operation at a shaft speed of 25,000 rpm. This is 3.5×10^6 DN operation of a 140 mm bore bearing. External radial load was 471 lbs. and the lubricant was 5P4E Polyphenyl Ether at approximately 500°F oil inlet temperature.

The failure of the first test bearing was attributed to reverse bending fatigue of the M-50 steel inner race at high speed and 600°F operating temperatures. The calculated stress levels were below known allowable stress levels for long term operation. This suggests that additional carefully controlled reverse bending fatigue data is required for M-50 bearing steels for elevated temperature operation. Any future tests of the dual diameter should use a solid inner race, eliminating the undercut.

The lubrication method of introducing the oil to a cavity in the inner race and through orifices directly into the bearing intering was generally successful, however distress and wear was observed at the cage inner land riding surface.

The successful operation of the second test bearing establishes the validity of the design approach. A complete systems analysis using existing state-of-the-art elastohydrodynamic technology, fluid mechanics, theory and thermal analysis techniques, can be used to design a completely new bearing concept and enable initial prototype testing to be successful at speeds and temperatures beyond the realm of current experience.

APPENDIX I

TEST LOGS

TEST LOG SHEET—

MIDWEST AERO INDUSTRIES CORP.

TECHNICIAN		PROJ NO. 81001	SHEET A
WITNESS		CUSTOMER FIRL	PAGE 1
WITNESS	TEST OF — Dual Dia. Roller Brg. S/N 1 in 7808 oil	P.O. NO. 19046	DATE 10-12-72
WITNESS	PURPOSE — To 3.5 Million DN OPERATION	TEST CELL 250 hp	

TECH INIT	No.	CLOCK TIME	Clutch Speed	Rig Speed	Load Pres.	Load Test Brg	Oil Flow T-B	Conv. Oil Flow T-B	Oil Flow F-O	Conv. Oil Flow F-R	Oil Flow R-R	Conv. Oil Flow R-R	Test Rig Pump Disch.	Supp. Oil Pump Disch.	Supp. Oil Pillow Out	Test Brg Oil In	Front Brg Oil In	Rear Brg Oil In	G/B Oil In	Remarks	Time on Test Brg. Hrs	Time on Test Brg. Min
	NO.	HR-MIN	RPM	RPM	PSI	lbs	lb/min	lb/min	lb/min	lb/min	lb/min	lb/min	PSI	PSI	PSI	PSI	PSI	PSI	PSI		Hrs	Min
			Test Rig was Assembled with Following Bearings																			
			Test Bearing P/N Franklin Institute P/N C3132 S/N A2																			
			Front Bearing P/N MAIC P/N FRT 100824 S/N																			
			Rear Bearing P/N MAIC P/N FRT 100824 S/N																			
			Support Oil Tank was filled with approx. 25 gallons of Humble 3389 Lubricant																			
		0900																				
			Start oil pumps and check for oil leaks – Turn on heaters and preheat oil																			
	1	1100	0	0	0	0	7.0	7.5	5.0	53	2.0	2.1	—	65	65	2.5	43	46	—			
		1150	Start Drive & Set Approx 0.5 Million DN																			
	2	1200	600	4204	36	384	5.0	5.3	5.0	53	2.0	21	-	67	66	3.0	41	27	—	Oil Flowing From Rear Seal Dr.		
		1210	Oil Leakage from Rear Drain Stopped on coast down at approx 1000 rpm – Shutdown																		0	20
		1215	Start Drive To calibrate Tachometer and check out system																			
	3	1335	550	3858	36	394	5.0	53	5.0	53	1.5	1.6	—	67	65	2.0	41	30		Oil from rear seal drain	0	40
	4	1350	895	3920	36	394	5.0	5.3	5.0	53	1.5	1.6	—	67	65	1.5	40	23		" " " " "	0	55
	5	1405	1020	7196	36	391	5.0	53	50	53	1.5	1.6	—	67	65	1.5	40	29		" " " " "	1	10
		1410	When oil flow to rear bearing is shut off oil from rear drain stops – Shutdown																		1	15
			Rear oil jet removed & inspected – Partially plugged by loose piece of hose																			
			The 3000 watt heater installed between flowmeter and oil in to Test bearing																			
10-29-72																						
		0900	Start pumps and Turn on heaters To preheat oil & rig																			
	6	1045	0	0	42	465	5.0	5.3	4.0	43	4.0	43	—	80	77	2.5	33	33	—			
		1100	Start Drive & Set 0.5 Million DN																			
	7	1110	520	3643	425	471	5.0	5.3	40	43	3.0	3.2	—	80	78	2.5	33	10	—		1	25
	8	1120	520	3643	425	471	5.0	5.3	[illegible]	43	3.0	3.2	—	80	77	2.5	33	10	—		1	35
	9	1130	520	3643	425	471	5.0	53	40	43	3.0	3.2	—	80	77	2.5	33	10	—		1	45
		1135	Increase load pressure To 85 PSI																		1	50
	10	1145	520	3643	890	960	5.0	5.3	40	43	3.0	32	—	93	91	3.0	28	12.5	—		2	—

NOTES:

TEST LOG SHEET–

TECHNICIAN	
WITNESS	
WITNESS	
WITNESS	

MIDWEST AERO INDUSTRIES CORP.

TEST OF — Dual Rig Roller Brg. SW 1 in 7808 Oil
PURPOSE — 3.5 Million DN Operation

PROJ. NO. B1001
CUSTOMER FIRL
P. O. NO. 19046
TEST CELL 250 hp

SHEET A OF C
PAGE 2 OF
DATE 10-24-72

TECH INIT.	Point	CLOCK TIME	Clutch Speed	Rig Speed	Load Pres.	Load Test Brg	Oil Flow T-B	Corr. Oil Flow T-B	Oil Flow F-B	Corr. Oil Flow F-B	Oil Flow R-B	Corr. Oil Flow R-B	Test Rig Pump Disch	G/B Pump Disch.	G/B Pump After Filter	Test Brg Oil In	F-B Oil IN	R-B Oil IN	G/B Oil IN		Time on Test Hrs	Time on Test Min
	NO.	HR-MIN	RPM	RPM	PSI	lbs	lb/min	lb/min	lb/min	lb/min	lb/min	lb/min	PSI	PSI	PSI	PSI	PSI	PSI	PSI		Hrs	Min
	11	1155	520	3643	82.5	954	5.0	5.3	4.0	4.3	3.0	3.2	—	93	91	3.3	28	12.5	—		2	10
		1205	Set 0.75 Million DN and reduce load pressure																		2	20
	12	1215	760	5325	41.5	459	5.0	5.3	4.0	4.3	3.0	3.2	—	78	76	2.5	29	12.5	—		2	30
	13	1250	765	5360	41.0	453	5.0	5.3	4.0	4.3	3.0	3.2	—	78	75	2.5	30.	13.0	—		3	5
	14	1310	765	5360	41.5	459														3KW Heater Cutting Out	3	25
	15	1340	765	5360	42.5	471	5.0	5.3	4.0	4.3	3.0	3.2	—	81	78	2.5	30	12.5	—		3	55
	16	1520	765	5360	38.0	418	8.0	8.5	3.0	3.2	3.0	3.2	—	71	61	19.5	17	15.5	—	Heater still Cutting Out	5	35
	17	1530	765	5360	42.0	465	8.5	9.1	3.5	3.7	3.0	3.2	—	80	77	15.5	19.5	12.5	—		5	45
	18	1545	765	5360	43.0	477	8.0	8.5	3.5	3.7	3.0	3.2	—	82	80	13.5	18.5	12.5	—		6	—
	19	1555	765	5360	43.0	477	8.0	8.5	3.5	3.7	3.0	3.2	—	82	80	12.5	18.5	12.5	—		6	10
		1600	Set 1.0 Million DN																		6	15
	20	1615	1020	7146	43.0	477	8.0	8.5	3.5	3.7	3.0	3.2	—	82	80	13.5	18.5	12.5	—		6	30
	21	1625	1020	7146	43.0	477	8.0	8.5	3.5	3.7	3.0	3.2	—	82	80	13.5	18.5	12.5	—		6	40
		1635	Set 1.25 Million DN																		6	50
	22	1645	1270	8898	43.0	477	8.0	8.5	3.5	3.7	3.0	3.2		83	81	13.5	18.0	16.5	—		7	—
	23	1655	1270	8898	43.0	477	8.0	8.5	3.5	3.7	3.0	3.2		83	81	13.5	18.0	16.5	—		7	10
		1705	Set 1.50 Million DN																		7	20
	24	1710	1525	10684	42.5	471	8.0	8.5	3.5	3.7	3.0	3.2		82	80	13.5	17.5	16.5	—		7	25
	25	1720	1525	10684	43.0	477	8.0	8.5	3.5	3.7	3.0	3.2		82	80	13.5	17.5	16.5	—		7	35
		1725	Accel. to 1.75 Million DN — No Problems																		7	40
		1730	Shutdown End of Shift																		7	45
10-25-72																						
		0930	Start Pumps and turn on heaters to preheat oil & rig																			
		1000	Temperatures Stabilized But Power Demand To High To Start																			
		1300	Start Drive and Set 0.5 Million DN																			
	26	1320	515	3608	41.5	459	8.0	8.5	3.0	3.2	3.0	3.2		80	78	13.5	14.5	14.5			8	05
		1335	Accel to 1.0 Million DN																		8	20
	27	1345	1010	7076	41.5	459	8.0	8.5	3.1	3.3	3.0	3.2		80	77	14.0	15.0	15.0			8	30
		1400	Set 1.5 Million DN																		8	45

NOTES:

TEST LOG SHEET—

MIDWEST AERO INDUSTRIES CORP.

TECHNICIAN
WITNESS
WITNESS
WITNESS

TEST OF — Axial Diameter Roller Brg S/N 1 G/D Dr. 7808
PURPOSE —

PROJ. NO. B1001
CUSTOMER FIRL
P.O. NO. 19046
TEST CELL 250 hp

SHEET A of C
PAGE 3 of
DATE 10-25-72

TECH INIT.	Hours NO	CLOCK TIME HR-MIN	Clutch Speed RPM	Rig Speed RPM	Load Pres. PSI	Load Test Brg lbs	Oil Flow T-B lb/min	Corr. Oil Flow T-B lb/min	Oil Flow F-B lb/min	Corr. Oil Flow F-B lb/min	Oil Flow R-B lb/min	Corr. Oil Flow R-G lb/min	Test Rig Pump Disch PSI	G/B Pump Disch PSI	Test Brg Oil Inlet PSI	Test Brg Oil TH PSI	F-B Oil IN PSI	R-G Oil IN PSI	G/B Oil IN PSI					Spin Pot setting	Time on Test Hr	Time on Test Min
	28	1910	1530	18719	40.5	447	8.0	8.5	3.1	3.3	3.0	3.2	~~44~~	78	75	14.6	15.0	14.8	—						8	55
		1923	Set	1.75	Million ON																				9	08
	29	1930	1980	12411	43.0	451	8.1	8.6	2.1	3.3	3.0	3.2	—	77	75	14.9	14.5	14.5	—	OIL LEAK FROM G/B Joint					9	15
	30	1940	1785	12506	41.0	453	8.0	8.5	3.1	3.3	3.0	3.2	—	78	76	14.5	14.5	14.5	—						9	25
	31	1950	1785	12506	41.0	453	8.0	8.5	3.0	3.2	3.0	3.2	—	78	76	14.5	14.0	14.0	—						9	35
		1500	Set	2.0	Million ON																				9	45
	32	1505	2040	19292	43.5	482	8.2	8.7	3.1	3.3	3.0	3.2	—	83	81	15.0	14.5	14.5	—						9	50
	33	1510	2040	19293	43.5	482	8.2	8.7	3.0	3.2	3.0	3.2	—	83	81	15.0	14.5	14.5	—						10	00
		1515	Set	2.35	Million ON																				10	05
	34	1520	2300	16114	43.5	482	8.1	8.6	3.1	3.3	3.1	3.3	—	83	81	15.0	14.5	14.5	—						10	10
	35	1525	2300	16114	43.5	482	8.1	8.6	3.0	3.2	3.0	3.2	—	83	81	14.5	14.0	14.0	—						10	15
		1530	Set	2.50	Million ON																				10	20
	36	1535	2550	17865	43.5	482	8.0	8.5	3.1	3.3	3.1	3.3	—	83	81	14.0	14.0	14.0	—						10	25
	37	1540	2550	17865	43.5	482	8.0	8.5	3.1	3.3	3.1	3.3	—	83	81	14.0	14.0	14.0	—						10	30
	38	1547	2550	17865	43.5	482	8.0	8.5	3.1	3.3	3.1	3.3	—	83	81	14.0	14.0	13.5	—						10	37
		1550	Increased	Oil	Flow to above bearings																				10	40
	39	1555	2550	17865	41.5	459	8.4	9.0		4.5	4.3	4.6	—	80	77	16.0	40.0	40.0	—						10	45
		1559	Set	2.75	Million ON																				10	49
	40	1605	2800	19617	40.5	447	8.3	8.9	4.1	4.4	4.2	4.5		80	77	15.0	38.0	38.0	—						10	55
	41	1610	2800	19617	40.5	447	8.3	8.9	4.1	4.4	4.2	4.5		78	75	15.0	38.0	38.0	—						11	00
		1615	Shutdown - Noise from G/B and oil leak from G/B insert																						11	05

10-26-72

Removed inspection cover from transition case - Rig + G/B turned free - G/B output bearing looked good.
Pulled G/B drain line and found some small metal chips. Checked oil filter - both contained
about 1/2 cc of dirt including metal chips - some magnetic some not. Cleaned housings and installed
new 5 micron filters. Tightened bolts on G/B insert and applied RTV around flange. Added
pressure gage in G/B oil line, T/C to measure G/B oil out and flow [illegible]

1440	Start Pumps and heater			
1520	Start Drive & Set 0.5 Million ON			0-72

NOTES:

TEST LOG SHEET-	TECHNICIAN	MIDWEST AERO INDUSTRIES CORP.	PROJ NO. B1001	SHEET A OF C
	WITNESS		CUSTOMER FIRL	PAGE 4 OF
	WITNESS	TEST OF — Dual Diameter Roller Brg SN 1 [illegible]	P.O. NO. 19096	DATE 10-26-72
	WITNESS	PURPOSE —	TEST CELL 250 hp	

TECH INIT	Reading	CLOCK TIME	Clutch Speed	Rig Speed	Load Pres.	Load Test Brg	Oil Flow T-B	Corr. Oil Flow T-B	Oil Flow F-B	Corr Oil Flow F-B	Oil Flow R-B	Corr. Oil Flow R-B	Test Rig Pump Disch	G/B Pump Disch	G/B Pump After Filter	Test Brg Oil IN	F-B Oil IN	R-B Oil IN	G/B Oil IN		Speed per Setting	Time Test	Time Brg
	NO.	HR-MIN	RPM	RPM	PSI	lbs	lb/min	lb/min	lb/min	lb/min	lb/min	lb/min	PSI	PSI	PSI	PSI	PSI	PSI	PSI			Hr	Min
	42	1545	515	3603	445	494	8.8	9.4	3.0	3.2	3.0	3.2	~~84~~	84	82	13.5	12.0	13.0	—		0-32	11	30
		1607	Set	1.0 Million	ON																	11	52
	43	1610	1010	7076	43	477	8.8	9.4	3.2	3.4	3.0	3.2		83	80	13.0	13.6	13.5	—		0-32	11	55
		1615	Set	1.5 Million	ON																	12	00
	44	1625	1530	10719	525	471	8.8	9.4	3.0	3.2	2.9	3.1		82	80	13.0	13.5	13.3	—	Clicking Noise from G/B	1-	12	10
		1630	Set	2.0 Million	ON																	12	15
	45	1640	2040	14292	470	465	8.8	9.4	3.0	3.2	3.0	3.2		81	79	13.0	14.3	13.8	—		2-03	12	25
		1645	Set	2.5 Million	ON																	12	30
	46	1655	2560	17935	450	500	8.8	9.4	3.1	3.3	3.0	3.2		86	84	13.0	15.5	14.3	11.5		2-47	12	40
		1700	Set	3.0 Million	ON																	12	55
	47	1705	3060	21438	440	488	9.3	9.9	3.1	3.3	3.0	3.2		83	80	15.5	15.0	13.2	19.5		2-82	12	50
		1710	Set	3.25 Million	ON																	12	55
	48	1715	3310	23190	425	474	9.0	9.6	3.3	3.5	4.3	4.6		82	80	14.9	15.0	38.0	17.0		2-44	13	00
		1720	Set	3.50 Million	ON																	13	05
	49	1730	3480	24350	425	471	9.0	9.6	3.2	3.4	4.0	4.3		81	80	14.3	16.0	38.0	16.0		3-0	13	15
	50	1740	3480	24380	41.8	462	8.1	8.6	3.2	3.4	4.1	4.4		82	80	12.6	16.0	37.8	15.2			13	25
		1745	Set	1.0 Million	ON - For Cool Down																	13	30
		1750	Set	0.5 Million	ON - " " "																	13	35
		1755	Shutdown - End of Shift																			13	40

10-27-72 thru 11-2-72: Disassembled Test Rig and inspected all parts. The following major items were noted:

Test Bearing - Heavy wear on cage and on [illegible] side of bearing - [illegible] [illegible] Shaft [illegible] land - [illegible] [illegible] [illegible] [illegible] cage speed was [illegible] [illegible] [illegible] wear [illegible] and [illegible] [illegible] three pins.

Support Bearings - Both bearings had about .0005 to .001 wear on ends of rollers.

Outer [illegible] retaining nut was [illegible] but [illegible] [illegible] [illegible] [illegible] [illegible]

Gearbox [illegible] [illegible] [illegible] retaining nut [illegible] loose and [illegible] [illegible] [illegible] the [illegible] [illegible]. Probable cause of gearbox noise.

Front bearing felt a little rough and was replaced with a new bearing.

Rebuilt test rig with same parts as used during initial run except the roller [illegible] was replaced with the one from bearing SN 2.

NOTES:

TEST LOG SHEET–

TECHNICIAN
WITNESS
WITNESS
WITNESS

MIDWEST AERO INDUSTRIES CORP.

TEST OF — Dual Piece Roller Brg S/N 1 Mod in 5P4E
PURPOSE — 3.5 Million DN Operation

PROJ NO. 61001
CUSTOMER FIRL
P.O. NO. 19046
TEST CELL 250 hp

SHEET 4 OF 6
PAGE 5 OF
DATE 11-3-72

TECH INIT.	Run No	CLOCK TIME	Clutch Speed	Rig Speed	Load Pres.	Load Test Brg	Oil Flow T-B	Corr. Oil Flow T-B	Oil Flow F-B	Corr. Oil Flow F-B	Oil Flow R-B	Corr. Oil Flow R-B	Test Rig Pump Disch	G/B Pump Disch	G/B Pump After Filter	Test Brg Oil In	F-B Oil In	R-B Oil In	G/B Oil In						Test Bearing Running Time	
	NO	HR-MIN	RPM	RPM	PSI	lbs	lb/min	lb/min	lb/min	lb/min	lb/min	lb/min	PSI	PSI	PSI	PSI	PSI	PSI	PSI						Hrs	Min.
			Added Separated oil system for high temperature oil to test bearing and rig support bearings																							
			Added 5 gallons of 5P4E from container no 1 to high temperature system - Installed 5 micron Bendix Filter																							
		1200	Preheating oil in tank to 250°F																							
		1300	Started Pump - Pump seized in about 30 sec - Shutdown and inspected pump - Bearing failure																							
			Removed [illegible] pump and replaced with Viking pump																							
11-4-72																										
		0830	Preheating oil to check ~~for~~ for leaks - Added 2 gallons of 5P4E oil from container no 2																							
		1000	Oil Temp reached 400°F start cool down to insulate lines and tank																							
		1500	Heating oil to 350°F - Noticed oil flow to test bearing low - opened tank fill pipe and foam came pouring out - cooled down to 200°F and foam went away - oil flow back to normal																							
		1520	Start Drive and set 0.5 Million DN - add 2 gallons of 5P4E oil from container no 2																							
	51	1525	515	3608	75	~~400~~	10.0	[illegible]	4.0	4.9	4.0	4.9	113	68	62	45	42	26							13	45
		1533	Oil foaming at site gage and out fill pipe - Oil Temp 270°F																						13	53
			No oil flow thru Test Bearing jet at 8 o'clock position (line cold)																						14	00
	52	1540	515	3608	32	406	12.8	15.0	5.0	5.9	4.3	5.0		70	62	79	43	43							14	15
	53	1555	515	3608																					14	30
	54	1610	515	3608	39	429	130	151	50	58	3.5	9.1	69	75	72	69	49	28							14	45
	55	1625	515	3608	42	465	130	151	58	69	5.8	6.8	69	80	75	40	575	80.5							14	50
		1630	Turn off heaters - Temp gage at 450°F																						15	00
		1640	Turn off drive - Set tank heater for 200°F and leave pump run on high temp system																							
		1800	High Temp System Running @ 80 PSI and 200°F																							
		2200	" " " " " " " "																							
11-5-72		0700	Removed Oil Manifold to test bearing oil jets and back pressured - 8 o/c jet still not working																							
		1330	High Temp System Running @ 30 PSI and 200°F																							
		1830	" " " " " " " "																							

NOTES:

TEST LOG SHEET–

TECHNICIAN
WITNESS
WITNESS [illegible]
WITNESS [illegible]

MIDWEST AERO INDUSTRIES CORP.

TEST OF — 2801 Drive Roller Brg 3/4:1 Red in SP4E
PURPOSE — 3.5 Million on operation

PROJ NO. 01001
CUSTOMER FIRL
P.O. NO. 19046
TEST CELL 250 hp

SHEET 6 of 6
PAGE 6 of [illegible]
DATE 11-6-72

TECH INIT.	Reading NO.	CLOCK TIME	Clutch Speed	Rig Speed	Load Pres.	Load Test Brg	Oil Flow T-B	Corr. Oil Flow F-A	Oil Flow F-B	Corr. Oil Flow F-B	Oil Flow R-B	Corr. Oil Flow R-B	Test Rig Pump Disch	G/B Pump Disch	G/B Pump After Filter	Test Brg Oil In	F-B Oil IN	R-B Oil IN	G/B Oil IN					Time
	NO.	Hr-Min	RPM	RPM	PSI	lbs	lb/min	lb/min	lb/min	lb/min	lb/min	lb/min	PSI	PSI	PSI	PSI	PSI	PSI	PSI					Hr : Min
		1015	Start Drive Set 0.5 Million ON																					
	56	1025	510	3573	40.5	497	10.1	11.9	—	—	2.5	2.9	56	80	77	45	38	8	60				C-30	15 : [illegible]
	57	1050	505	3534	40.5	497	10.0	11.7	—	—	3.0	3.5	49	77	73	40	31	14.5	65					15 : [illegible]
	58	1100	505	3530	40.5	497	11.0	12.8	4.0	4.7	3.5	4.1	60	78	75	48	15	18	49					15 : [illegible]
	59	1130	505	3530	34.5	435	9.0	10.4	4.0	4.6	3.8	4.4	52	75	72	29	28.5	27	47					15 : 45
	60	1140	505	3530	40.5	497	8.5	9.9	4.0	4.6	3.5	4.1	49	76	72	27	26.5	25	48					16 : 15
	61	1155	505	3538	40.0	491	8.5	9.9	3.9	4.5	3.8	4.4	53	76	73	27	26.0	27	48					16 : 25
		1201	Set 0.75 Million ON																					16 : [illegible]
		1205	Set 1.00 Million ON																				0-41	[illegible] : 45
	62	1215	1020	7196	42.0	465	8.5	9.9	4.1	4.8	3.8	4.4	59	80	76	30.0	32.5	30.0	51				[illegible]	[illegible]
	63	1230	1024	7196	44.5	459	9.0	10.4	4.5	5.2	3.5	4.5	58	80	77	32.5	32.5	26.5	50					17 : [illegible]
	64	1245	1020	7196	41.0	453	9.1	10.6	4.2	4.9	3.9	4.5	55	75	75	34.0	28.5	26.5	50					17 : 15
		1300	Set 1.50 Million ON																					17 : [illegible]
	65	1315																					1-47	17 : 45
	66	1330	1520	10649	42.5	471	9.2	10.7	4.0	4.6	3.7	4.3	56	80	76	28.0	28.5	27.0	50					18 : [illegible]
	67	1345	1520	10649	42.5	471	9.0	10.4	3.9	4.5	3.7	4.3	56	80	77	28.0	25.5	27.5	50					18 : 15
		1350	Set 2.00 Million ON																					18 : [illegible]
	68	1400	2010	14293	42.5	471	9.0	10.4	3.9	4.5	3.9	4.5	56	80	77	22.5	30.0	32.0	50				1-53	18 : [illegible]
	69	1415	2010	14192	[illegible]	465	9.0	10.4	3.9	4.5	3.9	4.5	56	80	77	26.0	28.5	30.5	49					18 : 45
	70	1425	2010	14192	41.5	459	9.0	10.4	3.8	4.4	3.8	4.4	56	79	76	26.0	27.5	31.0	48					19 : [illegible]
		1430	Set 2.50 Million ON																					19 : 10
	71	1445	2570	17795	41.5	459	8.5	9.9	3.8	4.4	3.8	4.4	53	80	77	26.5	28.0	30.5	48				2-	19 : 15
	72	1455	2570	17795	41.5	459	8.5	9.9	3.9	4.5	3.9	4.5	59	80	77	26.5	29.0	31.5	48					19 : 30
	73	1503	2590	17795	41.5	459	8.5	9.9	3.9	4.5	3.9	4.5	59	80	77	25.5	28.5	30.5	48					19 : 40
		1508	Set 2.75 Million ON																					19 : 45
		1515	add 1 Gallon S SP4E Oil from container No 2																				2-58	19 : 53
	74	1525	2810	19687	42.5	471	9.0	9.3	3.9	4.5	3.9	4.5	52	82	80	24.5	27.5	29.0	50.0					[illegible]
	75	1540	2810	19687	42.5	471	7.5	8.7	3.5	4.1	3.0	3.5	50	82	80	23.0	25.0	22.0	50.0					20 : 10
		1550	add 1/2 Gallon SP4E Oil from container No 3																					[illegible]
		1555	Set 3.0 Million ON																					[illegible]
																							2-74	[illegible]

NOTES:

TEST LOG SHEET–	TECHNICIAN	MIDWEST AERO INDUSTRIES CORP.	PROJ NO. 81051	SHEET A OF C
	WITNESS		CUSTOMER FIRL	PAGE 7 OF
	WITNESS JJ Ramsey	TEST OF — Full Size Roller Brg S/N 1 Mod 10	P.O. NO. 19046	DATE 11-6-72
	WITNESS F.D. Defazio	PURPOSE — 3.5 Million DN OPERATION SP4E	TEST CELL 250 hp	

TECH INIT.	Run No.	CLOCK TIME	Clutch Speed	Rig Speed	Load Pres.	Load Test Brg	Oil Flow T-B	Corr. Oil Flow T-B	Oil Flow F-B	Corr. Oil Flow F-B	Oil Flow R-B	Corr. Oil Flow R-B	Test Rig Pump Disch	G/B Pump Disch	G/B Pump After Filter	Test Brg Oil In	F-B Oil In	R-B Oil In	GB Oil In			Time	
	NO.	HR-MIN	RPM	RPM	PSI	lbs	lb/min	lb/min	lb/min	lb/min	lb/min	lb/min	PSI	PSI	PSI	PSI	PSI	PSI	PSI			Hr	
	76	1605	3060	21438	435	482	8.5	9.9	3.8	4.4	3.8	4.4	51	83	82	245	255	28.0	43			20	55
	77	1615	3060	21438	440	488	8.0	9.3	3.8	4.4	3.8	4.4	50	85	82	21.5	235	275	43	Added 1½ Gal from No. 3		21	00
		1635	Set 1.0 Million DN – Losing Oil too rapidly – Pumping from Rig into Transition Case and into Gearbox oil system.																			21	20
		1640	Set 1.0 Million DN –																			21	25
	78	1642			430	476	9.5	11.0	3.8	4.4	4.0	46	58	85	83	390	260	324	43			21	27
		1645	Set 0.5 Million DN																			21	30
		1650	Shutdown Drive – Let Oil System Circulate at 200°F																			21	25
11-7-72																							
		~~1410~~	Start Change oil system to leave Rig & Gearbox both on SP4E system –																				
		1600	Add 2 Gallons Oil from Container No. 3 and 2 gallons from container no 4																				
		1610	Start Drive & Set 0.5 Million DN																			21	35
		1625	Test Brg Oil to 300°F Sleeve Brg 260°F F/B 185°F																		0-30	21	50
		1640	Set 1.0 ~~DN~~ Million DN																		0-42	22	05
	79	1655	1010	7076	355	388	7.8	9.0	3.9	4.6	3.7	4.3	76	65	62	74	25	20	10			22	20
	80	1715	1010	7076	485	471	7.9	9.2	4.0	4.[illegible]	4.2	4.9	72	81	78	70	27	31	13			22	40
		1725	Set 2.0 Million DN																		1-48	22	75
	81	1730	2090	14292	42.5	471	8.1	9.4	3.8	4.4	3.9	4.6	70	80	77	67	24	25	16.5			22	55
	82	1740	2090	14292	420	485	8.2	9.5	3.9	4.6	3.8	4.4	71	80	77	685	30	23	13.0			23	05
		1795	Set 3.0 Million DN – Checked Test Brg Oil dn – Has been reading 5°F High																			23	10
	83	1800	3060	21438	415	459	8.2	9.5	4.1	4.8	4.2	4.9	72	79	76	70	30.5	310	25.0			23	25
	84	1810	3060	21438	415	459	8.4	9.8	3.9	4.6	4.2	4.9	76	79	76	73	260	340	240			23	35
		1815	Set 3.25 Million DN																			23	40
	85	1825	3315	23225	425	471	8.6	10.0	4.1	4.8	4.1	4.8	78	80	76	755	325	335	25.5			23	50
		1830	Set 3.50 Million DN																			23	55
	86	1835	3530	24731	41.5	459	8.8	10.2	4.0	4.7	4.2	4.9	82	81	77	790	290	350	105/110			24	00
		1840	Rig vs G/B Torque – Stripped Clutch – Shut Off Drive Motor – Turn Off Heaters																			24	05
			Rig Disassembled – Test Bearing Failure – There were fatigued through [illegible] in inner race																				
			Shoe Cage and out of test rig [illegible]																				

NOTES:

TEST LOG SHEET–

TECHNICIAN
WITNESS
WITNESS
WITNESS

PURE CARBON CO.
ST. MARYS, PA.

TEST OF =
PURPOSE =

PROJ NO.
CUSTOMER
P.O. NO.
TEST CELL

SHEET A OF C
PAGE 8 OF
DATE 11-15-72

TQ HP IN ON	Run No.	Clock Time	Clutch Speed	Inp Speed	Load Pres.	T-B Radial Load	T-B Oil Flow	Comb TB Oil Flow	F-B Oil Flow	Comb F-B Oil Flow	R-B Oil Flow	Comb R-B Oil Flow	T-A Pump Disch	G/B Pump Disch	G/B Pump After Filter	T-B Oil In	F-B Oil In	R-B Oil In	G/B Oil In	Clutch Wink In					Time Ck Running	
	No.	hr-min	RPM	RPM	PSI	lb	#/hr	#/hr	#/hr	#/hr	#/hr	#/hr	PSI	PSI	PSI	PSI	PSI	PSI	PSI	PSI					Hr	Min
			Added 3 Gallon Oil from Container No 4 to make Flowmeter calibration check																						0	0
11-15-72																										
		0990	Start Drive - Accel to 0.5 Million ON - Start Heating Oil to 200°F																							
495	100	0995	535	3574	33	359	12		4.5		4.5		42	60	56	6.5	35	35	15	—					0	15
		1000	Clutch Seized! - Water Not Turned On - Pressure Switch did not work																						0	20
11-15-72		Thru 12-20-72																								
		Removed failed [illegible] Clutch and Installed Louis Allis Clutch																								
12-20-72		Checked Safety Switches and set to proper levels																								
		Started Pumps and checked for oil leaks - set heaters for 200°F and let run over night																								
12-21-72																										
		0940	Start G/B Pump & increase Pump - T&B static readings																	—						..
	101	0940	6	0	41.5	494	11.5	13.4	5.5	64	4.5	5.2	61	83	83	51.5	28.5	21.5	29.5							
		0947	Set 0.5 Million ON																					18	0	20
050	102	1000	510	3573	40.0	942	11.0	12.8	4.6	53	4.9	5.1	58	75	75	500	375	28.0	23.0						0	35
"	103	1032	510	3573	41.0	441	5.5	11.1	5.3	62	4.9	5.7	72	75	72	36.0	34.2	36.4	24.5						1	05
		1045	2KW Heaters in Tank Not Working Thermostat Burnt Out																							
050	104	1100	510	3573	41.0	476	11.5	13.4	5.0	58	4.8	5.6	69	81	78	60.0	32.0	43.0	19.5						1	35
		1105	Set 1.0 Million ON																					1-11	1	40
1.00	105	1120	1020	7146	40.0	491	11.5	13.4	4.3	50	4.7	5.5	65	77	7[illegible]	58.0	30.0	40.0	16.5						1	55
1.00	106	1140	1020	7146	41.0	453	11.4	13.3	4.3	5.0	4.7	5.5	62	78	75	56.0	28.5	38.5	15.5					1-5:	2	15
		1150	Set 1.5 Million ON																						2	25
		1155	Shut down A C [illegible] clicking noise from G/B - Removed side panel from transition case and couldn't																						2	30
			see anything wrong - quill shaft was free but shaft binds up slightly when turned turn by hand																							
	107	1255	0		41.5	459	11.5	13.4	51	6.0	3.1	3.6	54	76	75	45.0	25.0	25.0	0							
	108	1325	0		41.5	459																				
		1335	Start Drive & set 0.5 Million ON																						2	30
0.50	109	1345	510	3573	41.0	453	11.0	12.8	5.0	56	4.8	5.6	57	77	74	52.0	44.0	45.0	15.0						2	40
		1350	Set 1.0 Million ON																						2	45
1.00	110	1355	1020	7146	41.0	453	11.0	12.8	5.2	6.0	4.9	5.7	61	78	75	55.0	46.0	48.0	11.0						2	50
		1400	Set 1.5 Million ON																						2	55

NOTES:

TEST LOG SHEET–

PURE CARBON CO.
ST. MARYS, PA.

TECHNICIAN
WITNESS
WITNESS
WITNESS
TEST OF —
PURPOSE —

PROJ NO.
CUSTOMER
P. O. NO.
TEST CELL

SHEET A OF —
FILE 2 OF
DATE 12-21-72.

TECH UNIT DN	No.	CLOCK TIME	Cmbr Speed	Rig Speed	T-B Bear Press	T-B Radial Load	T-B Oil Flow	Corr T-B Oil Flow	T-B Oil Flow	Corr P-B Oil Flow	P-B Oil Flow	Corr SB Oil Flow	T-B Pump Disch	S/B Pump Disch	G/M Pump & After Filter	T-B Oil In	P-B Oil In	R-B Oil In	G/M Oil In	Clean Water In					Time on Bearing
	NO.	HR-MIN	RPM	RPM	PSI	lb	lb/min	lb/min	lb/min	lb/min	lb/min	lb/min	PSI	PSI	PSI	PSI	PSI	PSI	PSI	PSI					HRS : MIN
1.5	111	1910	1530	10719	41.0	453	11.2	13.0	5.2	6.0	4.9	5.7	61	77	74	55	45	46	12.0	—					3:05
"	112	1920	1530	10719	41.0	453	11.2	13.0	5.8	6.0	4.9	5.7	60	77	74	54.5	44.5	45.5	11.0	—					3:15
		1925	Set 2.0 Million DN																					2-44	3:20
2.0	113	1435	2040	14292	41.0	453	11.2	13.0	5.8	6.0	4.9	5.7	69	77	74	58.0	46	46.5	14.0						3:30
"	114	1445	2040	14292	41.0	453	11.3	13.1	5.2	6.0	5.0	5.8	64	77	74	60.0	48	48	13.0						3:40
		1450	Set 2.5 Million DN																					3-0	3:45
2.50	115	1500	2550	17865	41.0	453	11.2	13.0	5.3	6.1	5.0	5.8	66	77	74	60.0	48	46.5	23.0					3	3:55
"	116	1510	2550	17865	41.0	453	11.2	13.0	5.3	6.1	5.0	5.8	66	77	74	60.0	46	45.5	21.0						4:05
		1520	Shutdown Unable To Obtain Any Higher Speed – Leave high Temp pump circulate																						
		Changed Speed Setting Potentiometer from 1000 to [illegible]																							
12-22-71																									
		0905	Start Drive and Set 0.5 Million DN																					0-20	4:05
0.5	117	0915	515	3608	40.5	447	16.28		4.2	49	3.9	4.5	62	69	65	43.0	15.4	17.5	11.0						4:15
"	118	0930	515	3605	36.0	399	16.23		3.7	43	3.3	3.8	46	67	64	34.5	11.5	15.2	10.0						4:30
"	119	0945	515	3608	41.5	459	11.5	13.4	4.5	52	4.5	5.2	57	77	75	47.0	34.0	37.0	25.0						4:45
		0950	Set 1.0 Million DN																					0-92	4:50
1.00	120	1000	1030	7146	42.5	447	11.5	13.4	4.8	56	4.6	5.3	61	75	72	48.5	41.5	40.0	18.0						5:00
		1010	Set 1.5 Million DN																					1-62	5:10
2.0		1015	Set 2.0 Million DN																					2-32	5:15
2.00	121	1025	2040	14292	41.5	459	12.0	13.9	4.5	5.2	4.0	4.6	60	79	76	50.0	38.0	35.5	18.0						5:25
		1035	Set 3.5 Million DN – Can Not Get Any High Speed – Shut Down																						
		1040	Shut down – Install 200 mesh screen in Tach Feed Back Circuit of Clutch – Cleaned Out Rear Oil Jet																						
		1155	Start Drive – 1.0 0.5 Million DN																					0-30	
0.5	122	1215			42.5	471	14.0	16.3	11.2	4.9	3.9	4.5	70	91	77	62.5	22.5	26.0	25.5						
		1235	Set 1.5 Million DN																					1-0	
1.5	123	1245	1530	10719	42.5	471	9.5	11.0	5.0	5.8	5.0	5.8	69	81	78	63.5	40.0	47.0	17.0						
		1250	Set 2.5 Million DN																					2-15	
2.5	124	1305	2560	17935	44.5	494	8.5	9.9	5.0	5.8	5.0	5.8	66	81	78	60.0	37.0	44.5	24.5						
		1315	Set 3.0 Million DN																					2-40	
3.00	125	1320	3060	21438	44.0	488	8.0	9.3	4.8	5.6	4.8	5.6	71	81	78	66.0	33.0	43.0	26.0						

NOTES: ? T.B Thermometer stuck on readings 117 & 118

Reading 119 Oil Jet To Rear of Test Bearing Plugged

TEST LOG SHEET–

TECHNICIAN
WITNESS
WITNESS
WITNESS

PURE CARBON CO.
ST. MARYS, PA.

TEST OF —
PURPOSE —

PROJ. NO.
CUSTOMER
P. O. NO.
TEST CELL

SHEET A OF C
PAGE 10 OF
DATE 12-22-77

[illegible] AN	Run No.	CLOCK TIME	Shaft Speed	Air Speed	T-B [illegible]	T-B [illegible]	T-B oil flow	[illegible] T-B oil flow	F-B oil flow	[illegible] F-B oil flow	A-B oil flow	[illegible] A-B oil flow	T-B fuel [illegible]	G/B fuel [illegible]	G/B [illegible]	T-B oil in	F-B oil in	A-B oil in	G/B oil in	[illegible] in	Time of operation
	HP	HR-MIN	RPM	RPM	PSI	10	flow	flow	flow	flow	flow	flow	PSI	PSI	PSI	PSI	PSI	PSI	PSI	PSI	[illegible]
		1330	Shut down oil flow to tail bearing down to 3.5 Million — Add 2 gallons of oil from container No 4																		
—	—	1415	Start Drive and set 0.5 Million DN																		
		1425	Set 1.0 Million DN																		0-7
		1430	Set 1.5 Million DN																		0.51
		1432	Set 2.0 Million DN																		1-03
		1435	Set 2.5 Million DN																		1-50
		1440	Set 3.0 " DN																		1-97
2.00	126	1445	3960	21488	420	477	13.5	15.6	5.1	5.9	5.0	5.8	83	81	78	97.0	56.0	42.0	27.0	—	2-10
		1450	Set 3.25 Million DN																		
236	127	1452	3380	23260	42.5	471	15.5	17.9	6.0	7.0	5.0	5.8	99	81	78	91.0	57.0	42.0	35.0		
		1455	Set 3.50 Million DN																		
243	128	1500	3500	24581	42.5	471	14.5	16.8	5.8	6.9	5.1	5.9	91	81	78	84.0	52.0	40.0	26.0	--	
243	129	1510	3500	24521	42.5	471	14.6	16.8	5.8	6.7	5.0	5.8	90	81	78	82.0	50.0	36.0	22.0		
243	130	1515	3500	24521	42.5	471	18.5	21.4	4.9	5.7	5.0	5.8	62	81	78	50.0	42.0	36.0	20.0		
243	131	1520	3500	24521	42.5	471	18.5	21.4	4.9	5.7	5.0	5.8	62	81	78	50.0	42.0	36.0	20.0		
		1525	Rapid Accel to 1.5 Million DN																		
			Made 4 Rapid Accel – Decel – See below																		
		1530	Set 1.5 Million DN																		
1.6	132	1535	1630	11410	42.5	471	18.5	21.4	5.0	5.8	5.0	5.8	69	81	78	52.0	42.5	37.0	20.0		
		1540	Set 1.0 Million DN — Turn off oil heater																		
.68	133	1545	690	4484	42.5	471	20.0	23.3	5.2	6.0	5.0	5.8	70	81	78	55.0	44.0	35.0	18.0		
		1555	Shutdown																		

NOTES: * Reduced Controller for Max Speed

1525 Rapid Accel 1.5 Million DN to 3.5 Million DN in 15 sec
" Decel 3.5 " " to 1.5 " " " 15 sec

RUNS 100–133 OIL JET DIRECTED AT RETAINER OF TEST BRG ~2 #/MIN OF T/B OIL FLOW TO IT

TEST LOG SHEET— TEMP °F

TECHNICIAN
WITNESS
WITNESS
WITNESS

MIDWEST AERO INDUSTRIES CORP.

TEST OF —
PURPOSE —

PROJ. NO.
CUSTOMER
P.O. NO.
TEST CELL

SHEET [illegible] OF [illegible]
PAGE 1 OF
DATE 10-17-72

TECH INIT	NO.	CLOCK TIME HR-MIN	1 OIL IN	2 T/B OIL OUT	3 F-B OIL	4	5	6 T-B RACE 9 O'CLOCK	7 T-B RACE 6 O'CLOCK	8 T-B RACE 3 O'CLOCK	9 T-B RACE 12 O'CLOCK	10 F-B RACE 3 O'CLOCK	11 F-B RACE 6 O'CLOCK	12 F-B RACE 10 O'CLOCK	13 R-B RACE 3 O'CLOCK	14 R-B RACE 6 O'CLOCK	15 R-B RACE 10 O'CLOCK	16 T-B HSG WALL	17 T-B HSG WALL 12 O'CLOCK	18 T-B HSG WALL 6 O'CLOCK	19 R-B HSG WALL 6 O'CLOCK	20 G/B OIL IN	21 A-B HSG WALL 12 O'CLOCK	22 F-B HSG WALL 6 O'CLOCK	23 F-B HSG WALL 10 O'CLOCK	24 F-B HSG WALL 12 O'CLOCK
	1	1150	180	150	175	135	120	125	—	130	120	155	170	160	130	155	130	155	120	150	160	[illegible]	120	170	135	140
		1159	Start Drive — Initial Rotation																							
	2	1200	185	180	185	170	172	175		175	172	185	170	188	175	177	175	180	170	180	170	185	160	175	160	185
		1210	Shutdown																							
		1300																								
		1315	Start																							
	3	1335	192	190	191	180	186	190	—	190	188	197	200	198	185	190	188	190	135	190	150	200	175	155	175	175
	4	1350	196	200	200	190	195	199	—	[illegible]	186	201	201	202	198	200	200	200	152	200	190	205	185	190	[illegible]	[illegible]
	5	1405	200	201	202	200	201	202	—	204	202	209	210	210	208	210	210	208	200	206	205	201	192	195	192	185
	10-24-72		New Day																							
	6	1045	285	180	145	140	145	150	—	150	148	175	170	140	140	135	150	160	150	160	145	140	155	210	165	175
		11.00	Set Point No I A1 0.5[illegible]° ON																							
	7	11.10	245	225	150	200	210	215	—	215	210	165	160	165	155	155	155	220	205	220	165	135	160	205	150	190
	8	1120	248	226	150	205	215	220	—	220	216	169	165	168	[illegible]	155	158	225	210	222	159	135	165	215	185	199
	9	1130	248	227	150	207	218	220	—	221	218	169	165	169	159	155	160	226	211	222	160	135	169	210	190	199
	10	1145	235	220		200	210	213	—	214	210	170	165	170	160	155	160	220				140				
	11	1155	246	230	160	210	220	232	—	222	220	175	170	175	161	160	165	227	215	225	165	140	170	210	193	201
	12	1215	[illegible]	210	152	206	209	210	—	211	210	165	161	165	161	160	163	215	208	213	160	[illegible]	[illegible]	[illegible]	[illegible]	[illegible]
	13	1250	249	230	165	210	221	225	—	225	221	175	171	175	171	170	172	227	218	225	170	150	175	202	185	155
	14	1310	249	230	170	216	226	230	—	230	227															
	15	1350	250	235	160	215	230	234	—	233	230	170	163	171	170	168	170	236	[illegible]	232	170	135	180	210	155	201
	16	1520	250	243	199	232	236	240	—	240	237	205	201	205	198	196	199	245	235	245	195	190	200	230	210	215
	17	1530	258	245	202	235	239	243	—	244	240	209	204	210	201	200	202	250	240	248	200	194	205	235	220	220
	18	1545	247	240	194	232	237	240	—	240	236	201	200	201	197	192	[illegible]	243	232	240	195	175	201	205	215	215
	19	1555	245	240	193	232	235	239	—	239	236	201	198	200	194	192	[illegible]	241	232	240	192	175	200	225	215	215
	20	1615	245	240	195	237	240	241	—	241	240	203	201	202	200	200	201	243	237	242	198	179	205	227	219	219
	21	1625	246	240	196	239	240	242	—	243	241	205	202	204	203	201	204	245	239	244	199	179	206	226	220	220
	22	1645	247	241	203	242	246	250	—	249	249	211	210	211	210	210	210	250	243	249	204	179	210	235	225	229
	23	1655	248	242	204	242	247	250	—	250	249	210	210	211	210	210	211	252	244	[illegible]	205	183	211	235	[illegible]	230

NOTES:

TEST LOG SHEET–

MIDWEST AERO INDUSTRIES CORP.

[illegible] • P.O. Box [illegible] • Oak Ridge Station • Royal Oak, Michigan [illegible]

TECHNICIAN
WITNESS
WITNESS
WITNESS

TEST OF —
PURPOSE —

PROJ. NO.
CUSTOMER
P.O. NO.
TEST CELL

SHEET 6 OF 6
PAGE [illegible] OF
DATE 6-24-72

TECH INIT	NO.	CLOCK TIME HR-MIN	OIL IN T-B	T-B OIL OUT FRT	F-B OIL OUT	T-B OIL OUT REAR	T-B RACE 2%	T-B RACE 4%	T-1 [illegible] 6%	T-B RACE 8%	T-B RACE 10%	F-B RACE 2%	F-B RACE 6%	F-B RACE 10%	F-B RACE 2%	R-B RACE 6%	R-B RACE 10%	T-B HSG [illegible]	T-B HSG WALL 12%	T-B HSG WALL 6%	R-B HSG [illegible] 6%	C/A OIL IN	R-B HSG [illegible] 12%	F-B [illegible] 6%	F-B [illegible] 12%	F-B [illegible] 12%
			1	2	3	4	5	6	7	8	9	10	11	12	13	14	15	16	17	18	19	20	21	22	23	24
1.5	24	1710	250	248	212	247	255	259	—	259	255	229	226	220	220	226	231	265	251	252	212	180	216	243	[illegible]	[illegible]
	25	1920	250	240	222	249	260	260	—	260	260	221	215	220	221	221	222	257	254	255	212	181	218	[illegible]	225	237
	New	Day	10-25-72						[illegible]																	
[illegible]	26	1320	240	230	188	210	220	225		225	220	200	192	199	182	180	183	230	218	226	181	175	182	225	204	203
1.0	27	1345	239	236	195	230	235	238	200	236	233	200	198	200	198	195	199	236	230	235	195	173	200	220	210	210
1.5	28	1410	242	240	211	251	249	252	212	252	251	218	219	213	214	218	220	250	244	250	210	180	215	237	[illegible]	[illegible]
	29	1430	245	244	247	245	263	264	229	262	265	232	243	228	231	230	231	258	255	255	222	175	225	245	240	[illegible]
1.5	30	1440	243	249	220	250	265	269	230	271	265	229	226	229	233	232	235	259	256	255	222	175	239	[illegible]	240	232
	31	1450	241	247	217	248	261	265	230	265	262	225	222	225	230	230	231	256	255	256	220	172	235	[illegible]	[illegible]	[illegible]
[illegible]	32	1505	239	250	231	250	265	270	251	270	270	231	230	232	205	245	240	240	240	257	231	174	232	[illegible]	[illegible]	[illegible]
	33	1510	240	252	232	257	270	271	232	272	271	231	230	231	240	240	242	260	260	250	231	174	232	[illegible]	[illegible]	[illegible]
[illegible]	34	1520	241	257	231	258	280	280	240	281	281	244	242	242	258	250	261	271	270	269	241	175	242	[illegible]	[illegible]	[illegible]
	35	1525	245	260	233	261	281	283	241	283	285	248	243	245	266	266	270	272	271	270	243	174	243	254	[illegible]	[illegible]
	36	1535	247	267	236	270	280	281	240	291	291	[illegible]	253	255	292	292	258	280	275	270	250	176	266	260	[illegible]	[illegible]
[illegible]	37	1540	248	270	240	275	242	246	253	257	257	259	255	260	287	290	250	[illegible]	260	280	261	180	265	265	[illegible]	[illegible]
	38	1545	244	270	241	276	253	255	257	299	[illegible]	260	255	260	250	250	252	243	260	280	262	180	265	[illegible]	[illegible]	[illegible]
	39	1555	249	270	180	275	250	252	257	[illegible]	261	245	240	246	264	265	262	270	273	225	257	175	256	[illegible]	[illegible]	[illegible]
[illegible]	40	1603	245	275	245	288	300	303	24	303	301	250	253	251	245	247	250	240	267	253	[illegible]	151	262	220	265	241
	41	1608	245	275	235	280	300	302	322	302	302	250	250	251	240	240	242	250	255	275	260	158	265	210	220	[illegible]
	New	Day	10-26-72																							
	42	1545	240	230	290	211	217	219	190	220	218	200	198	200	198	185	187	221	212	220	186	179	187	225	206	205
	43	1610	218	239	201	230	225	226	192	229	222	210	207	210	200	200	201	230	221	210	150	170	190	[illegible]	[illegible]	[illegible]
	44	1625	252	260	225	250	240	242	203	246	245	225	227	228	222	[illegible]	227	245	235	240	245	142	211	233	[illegible]	[illegible]
	45	1640	250	260	[illegible]	260	255	256	215	252	257	276	276	237	245	245	245	258	251	257	[illegible]	150	[illegible]	[illegible]	[illegible]	[illegible]
	46	1655	250	271	250	273	280	281	240	283	290	261	261	260	240	241	285	272	270	270	[illegible]	154	[illegible]	[illegible]	[illegible]	[illegible]
	47	1705	246	255	271	260	258	301	250	303	301	289	260	290	323	325	322	290	240	281	241	158	[illegible]	[illegible]	[illegible]	[illegible]
	[illegible]	[illegible]	255	300	260	[illegible]	319	320	275	320	320	305	305	304	322	322	326	302	300	300	297	245	249	[illegible]	241	236
	[illegible]	1730	262	310	300	317	315	335	322	332	334	324	321	324	321	325	325	308	311	301	265	210	295	255	261	275
	[illegible]	[illegible]																								

NOTES:

TEST LOG SHEET–

TECHNICIAN	
WITNESS	
WITNESS	
WITNESS	

MIDWEST AERO INDUSTRIES CORP.

TEST OF —

PURPOSE —

PROJ. NO.	
CUSTOMER	
P. O. NO.	
TEST CELL	
SHEET	[illegible] OF [illegible]
PAGE	[illegible] OF
DATE	[illegible]

TECH INIT		CLOCK TIME	OIL IN T-B	OIL OUT ECT T-B	F-B OIL OUT	T-B REAR OIL OUT	T-B RACE 2%	T-B RACE 4%	T-B RACE 6%	T-B RACE 8%	T-B RACE 10%	F-B RACE 2%	F-B RACE 6%	F-B RACE 10%	R-B RACE 2%	R-B RACE 6%	R-B RACE 10%	T-B HSG [illegible]	T-B HSG WALL 12%	T-B HSG WALL 6%	F-B HSG WALL 6%	G/B OIL IN	F-B HSG WALL 12%	[illegible]	[illegible]	[illegible]
	NO.	HR-MIN	1	2	3	4	5	6	7	8	9	10	11	12	13	14	15	16	17	18	19	20	21	22	23	24
	98	1240	265	315	300	325	340	340	267	340	341	321	324	324	324	325	325	310	315	307	264	300	265	250	252	[illegible]

NOTES:

TEST LOG SHEET–

TECHNICIAN	
WITNESS	
WITNESS	
WITNESS	

MIDWEST AERO INDUSTRIES CORP.

TEST OF —	
PURPOSE —	
PROJ. NO.	
CUSTOMER	
P. O. NO.	
TEST CELL	
SHEET	6 of
PAGE	4 of
DATE	11-4-72

TECH INIT.	NO	CLOCK TIME HR-MIN	1	2	3	4	5	6	7	8	9	10	11	12	13	14	15	16	17	18	19	20	21	22	23	24
	51	1525	235	250	250	240	210	210	216	Rev.	205	230	235	230	218	219	215	219	OPEN	212	205	90	190	215	150	165
	52	1540	280	300	310	290	250	255	257	"	252	275	280	278	270	271	270	260	"	255	255	105	245	260	210	225
	53	1555	350	350	350	335	300	295	300	[illegible]	295	310	310	310	290	290	290	305		300	295	125	295	310	280	
	54	1610	395	410	385	390	355	250	348	343	348	340	335	335	330	330	333	350	—	350	340	150	335	350	345	335
	55	1625	445	475	455	460	400	395	400	395	390	400	403	385	390	390	390	405		400	375	232	375	405	365	36
		1630	Turn Off Heater (oil [illegible] up to 460°F) Cool Off for Shut down																							

NOTES:

R.N.

TEST LOG SHEET–TEMP °F

TECHNICIAN
WITNESS
WITNESS
WITNESS

MIDWEST AERO INDUSTRIES CORP.

TEST OF —
PURPOSE —

PROJ NO.
CUSTOMER
P. O. NO.
TEST CELL

SHEET [illegible]
PAGE 1 OF
DATE 11-6-72

TACH INST. ON	NO.	CLOCK TIME HR-MIN	OIL IN T-B 1	T-B OIL OUT FRT 2	F-B OIL OUT 3	T-B OIL OUT REAR 4	T-B RACE 2% 5	T-B RACE 4% 6	T-B RACE 6% 7	T-B RACE 8% 8	T-B RACE 10% 9	F-B RACE 2% 10	F-B RACE 6% 11	F-B RACE 10% 12
0.5	56	1025	240	245	249	225	205	205	210	205	200	235	235	235
	57	1053	265	315	300	305	265	265	270	265	260	225	275	275
	58	1100	320	300	340	310	310	320	320	320	315	310	315	315
	59	1130	450	480	430	460	385	385	400	385	385	345	385	380
	60	1140	445	455	430	470	400	400	410	400	395	345	390	380
	61	1155	445	[illegible]	[illegible]	415	410	410	410	405	420	355	390	350
	62	1215	445	500	440	440	415	420	425	420	415	400	395	358
	63	1230	450	505	440	450	425	425	425	420	415	400	400	355
	64	1245	450	505	445	450	425	425	425	420	415	405	400	400
	65	1315	470	530	490	445	450	450	465	450	460	470	425	425
	66	1330	475	545	485	535	455	460	460	455	450	425	430	420
	67	1345	455	545	455	535	460	460	460	455	455	425	420	420
	68	1400	465	515	450	530	465	460	460	455	455	435	430	430
	69	1415	450	550	460	550	475	475	475	470	465	440	435	430
	70	1425	465	530	495	550	480	480	480	470	420	440	435	435
	71	1445	495	560	515	565	500	500	495	490	450	460	455	455
	72	1453	460	560	515	555	495	450	450	485	455	460	440	460
	73	1503	480	560	520	555	495	490	490	485	482	465	460	460
	74	1525	480	555	530	525	500	485	465	460	460	470	465	470
	75	1540	460	555	535	520	520	495	460	485	460	470	465	465
	76	1605	480	560	525	535	505	500	500	450	455	480	425	475
	~~72~~	[illegible]	[illegible]	[illegible]	[illegible]	505	525	[illegible]	520	520	[illegible]	[illegible]	[illegible]	[illegible]
	77	1615	485	565	530	535	510	525	500	500	500	480	460	480
	78	1640	440	525	475	500	445	445	440	440	440	430	425	425
	Rec'd	~	ROA	11-7-72										
	79	1655	440	410	370	420	365	375	375	365	355	320	340	335
	80	1715	450	450	440	420	410	410	445	445	400	365	365	365
	81	1730	445	440	430	450	420	420	420	415	440	350	385	385
	82	1810	400	490	440	485	430	425	428	420	440	380	382	382
	83	1800	485	570	485	490	475	470	465	460	465	440	440	440

NO.	R-B RACE 2% 13	R-B RACE (LINER) 6% 14	R-B RACE 10% 15	T-B HSG WALL 6% 16	T-B HSG WALL 12% 17	T-B HSG WALL 6% 18	R-B HSG WALL 6% 19	G/B OIL IN 20	R-B HSG WALL 12% 21	F-B HSG WALL 6% 22	F-B HSG WALL 10% 23	F-B HSG WALL 12% 24
56	195	200	200	210	[illegible]	205	180	108	195	210	180	195
57	245	250	240	270	—	270	235	205	255	[illegible]	[illegible]	[illegible]
58	280	280	280	330	—	325	275	140	260	335	[illegible]	[illegible]
59	365	370	365	403	—	385	[illegible]	150	330	[illegible]	360	[illegible]
60	370	375	370	405	—	400	[illegible]	155	[illegible]	[illegible]	370	[illegible]
61	375	375	370	410	—	405	365	160	350	[illegible]	[illegible]	[illegible]
62	385	385	385	425	—	420	325	175	360	410	[illegible]	325
63	385	390	385	425	—	420	375	175	365	[illegible]	[illegible]	[illegible]
64	385	390	385	425	—	420	375	150	365	[illegible]	[illegible]	[illegible]
65	420	425	425	460	—	455	400	135	365	[illegible]	[illegible]	[illegible]
66	405	410	405	460	—	455	360	150	365	[illegible]	[illegible]	[illegible]
67	410	410	410	460	—	440	375	150	355	[illegible]	[illegible]	[illegible]
68	425	430	425	460	—	455	410	[illegible]	440	[illegible]	[illegible]	[illegible]
69	430	430	430	425	—	420	415	205	475	[illegible]	[illegible]	[illegible]
70	430	430	430	425	—	465	440	210	[illegible]	[illegible]	[illegible]	[illegible]
71	430	450	400	450	—	455	430	215	[illegible]	[illegible]	[illegible]	[illegible]
72	455	455	455	450	—	400	435	225	[illegible]	[illegible]	[illegible]	[illegible]
73	455	460	460	485	—	48[illegible]	435	230	440	462	455	450
74	465	465	450	485	—	480	452	235	455	460	[illegible]	[illegible]
75	460	460	445	[illegible]	—	[illegible]	445	235	[illegible]	[illegible]	[illegible]	[illegible]
76	500	510	450	450	—	485	470	240	420	425	470	[illegible]
~~72~~	[illegible]	[illegible]	[illegible]	[illegible]	[illegible]	[illegible]						
77	460	480	465	500	—	495	465	245	465	472	470	465
78	420	405	410	430	—	440	410	242	[illegible]	420	[illegible]	[illegible]
Rec'd												
79	340	305	345	375	—	370	335	275	300	[illegible]	[illegible]	[illegible]
80	345	345	[illegible]	415	—	410	330	220	[illegible]	[illegible]	[illegible]	[illegible]
81	380	375	375	420	—	420	360	220	365	[illegible]	375	360
82	380	379	382	433	—	420	365	245	370	375	350	[illegible]
83	445	445	448	460	—	455	435	240	420	445	[illegible]	[illegible]

NOTES:

TEST LOG SHEET– Temp °F

TECHNICIAN
WITNESS
WITNESS
WITNESS

MIDWEST AERO INDUSTRIES CORP.

TEST OF —
PURPOSE —

PROJ NO.
CUSTOMER
P. O. NO.
TEST CELL

SHEET 6 OF 6
PAGE 6 OF
DATE 11-7-72

TECH INIT		CLOCK TIME	OIL IN T-B	T-A OIL OUT FRT	F-A OIL OUT	T-B OIL OUT REAR	T-A RACE 2%	T-A RACE 4%	T-B RACE 6%	T-A RACE 8%	T-A RACE 10%	F-A RACE 2%
	NO	HR-MIN	1	2	3	4	5	6	7	8	9	10
	94	1818	444	535	495	500	460	450	477	475	475	455
	95	1821	462	553	510	520	525	525	520	520	520	470
	96	1431	470	520	525	530	525	520	520	515	515	495

	F-A RACE 6%	F-A RACE 10%	R-B RACE 2%	R-A RACE 6%	R-B RACE 10%	T-A HSG WALL 6%	T-A HSG WALL 12%	T-B HSG WALL 6%	R-A HSG WALL 6%	G/A OIL IN	R-B HSG WALL 12%	F-A HSG WALL 6%	F-B HSG WALL 10%	F-B HSG WALL 12%
NO	11	12	13	14	15	16	17	18	19	20	21	22	23	24
94	450	450	455	455	460	470	—	465	435	350	440	450	450	460
95	470	470	460	472	460	455	—	460	463	260	465	470	[illegible]	[illegible]
96	485	495	520	500	510	510	—	523	470	260	450	455	455	475

NOTES:

TEST LOG SHEET — TEMP °F

TECHNICIAN
WITNESS
WITNESS
WITNESS

PURE CARBON CO.
ST. MARYS, PA.

TEST OF —
PURPOSE —

PROJ NO.
CUSTOMER
P. O. NO.
TEST CELL

SHEET [illegible] OF [illegible]
PAGE
DATE 11-16-72

TECH INIT	READING NO.	CLOCK TIME HR-MIN	T-B OIL IN (1)	T-B OIL OUT FR (2)	F-B OIL OUT (3)	T-B OIL OUT REAR (4)	T-B RACE 2% (5)	T-B RACE 4% (6)	T-B RACE 6% (7)	T-B RACE 8% (8)	T-B RACE 10% (9)	F-B RACE 2% (10)	F-B RACE 6% (11)	F-B RACE 10% (12)	R-B RACE 2% (13)	R-B RACE 6% (14)	R-B RACE 10% (15)	T-B HSG WALL 6% (16)	T-B HSG WALL 12% (17)	T-B HSG WALL 6% (18)	R-B HSG WALL 6% (19)	G/B OIL IN (20)	R-B HSG WALL 12% (21)	F-B HSG WALL 6% (22)	F-B HSG WALL 10% (23)	F-B HSG WALL 12% (24)
	100	0945	280	270	250	250	210	215	212	210	210	225	225	225	215	—	200	218	205	212	208	195	110	220	200	202
12-11-72																										
U	101	0940	210	218	192	195	172	178	170	170	165	155	153	199	177	N/C	175	125	120	122	180	185	123	180	172	[illegible]
0.5	102	1000	159	205	208	200	165	200	197	197	155	210	215	213	200	"	189	185	150	185	150	155	[illegible]	170	150	175
↓	103	1030	335	320	260	260	270	276	272	270	270	270	270	270	235	"	230	280	260	270	230	185	—	290	250	240
↓	104	1100	355	366	325	350	305	315	310	305	305	305	315	305	272	"	270	320	300	310	270	245	[illegible]	[illegible]	[illegible]	[illegible]
1.0	105	1120	330	329	340	385	345	350	350	345	345	325	325	325	302	"	300	308	370	338	300	305	[illegible]	[illegible]	[illegible]	[illegible]
↓	106	1140	[illegible]	[illegible]	358	405	370	378	372	370	370	378	345	345	329	"	315	378	360	375	320	220	—	365	[illegible]	[illegible]
O	107	1255	425	460	400	450	310	385	350	350	310	365	380	370	315	"	310	385	305	385	330	—		330	340	310
55	108	1325	470	460	370	495	390	410	380	385	345	395	401	395	340	"	335	410	330	405	350	295	330	410	370	335
5.[illegible]	109	1345	428	430	358	420	362	370	365	365	360	348	342	342	325	"	310	370	355	510	315	222	360	365	372	320
1.0	110	1355	408	410	380	420	370	325	325	325	325	350	350	350	330	"	323	350	365	325	322	220	320	325	[illegible]	325
1.5	111	1410	412	418	355	437	330	310	350	358	350	365	360	360	345	"	335	345	380	350	345	[illegible]	[illegible]	[illegible]	[illegible]	322
"	112	1420	420	460	415	750	355	400	358	355	352	320	365	320	353	"	345	400	355	355	360	242	315	[illegible]	[illegible]	[illegible]
2.0	113	1435	400	470	435	470	430	425	425	422	422	400	400	400	382	"	375	425	415	425	350	238	320	402	393	[illegible]
"	114	1445	455	450	450	480	448	450	445	445	440	445	415	415	400	"	350	455	430	440	342	248	350	420	420	[illegible]
2.5	115	1500	470	510	410	450	420	420	420	468	420	440	443	445	425	"	425	465	460	460	415	330	400	[illegible]	[illegible]	[illegible]
"	116	1510	455	520	420	458	465	420	465	465	407	445	445	445	440	"	470	465	460	458	420	325	420	440	[illegible]	[illegible]
[illegible]	12-12-72																									
[illegible]	117	0715	330	260	210	200	210	220	212	211	213	225	225	225	205	"	185	225	210	205	190	150	185	230	[illegible]	[illegible]
	118	0930	320	325	280	275	270	290	225	210	270	275	275	274	240	"	225	[illegible]	260	270	270	212	220	232	[illegible]	[illegible]
	119	0940	330	345	270	250	250	300	290	285	240	270	260	250	160	"	245	300	280	215	230	245	240	150	[illegible]	[illegible]
	120	1115	375	318	330	335	345	335	335	335	322	322	322	340	250	"	275	345	320	310	285	215	270	255	[illegible]	250
	121	1135	410	400	370	435	355	400	400	358	355	335	370	375	355	"	[illegible]	[illegible]	[illegible]	[illegible]	365	250	310	[illegible]	[illegible]	[illegible]
5	122	1215	330	315	260	330	305	310	310	310	305	295	255	255	275	"	265	310	300	310	275	230	265	255	275	260
	123	1235	400	420	350	400	375	385	340	340	375	340	340	340	320	"	305	385	365	355	325	260	320	[illegible]	[illegible]	[illegible]
	124	1305	455	470	395	445	450	455	455	452	450	425	425	425	415	"	355	450	440	440	390	270	400	430	420	405
	125	1330	460	515	470	460	505	500	475	455	505	455	458	455	475	"	455	455	450	405	405	361	450	425	420	450
	126	1445	445	470	400	455	465	465	465	455	465	465	445	465	450	"	380	466	460	455	440	320	445	450	420	445
	127	1442	470	510	515	515	500	520	505	485	505	520	520	505	520	"	470	505	455	450	475	363	450	452	[illegible]	[illegible]

NOTES:

TEST LOG SHEET–	TECHNICIAN	PURE CARBON CO. ST. MARYS, PA.	PROJ NO.	SHEET 4 OF
	WITNESS		CUSTOMER	PAGE OF
	WITNESS	TEST OF —	P.O. NO.	DATE 12-22-72
	WITNESS	PURPOSE —	TEST CELL	

F-CH AMPS DW		CLOCK TIME	T-8 OIL IN	T-8 OIL OUT EXT	F-8 OIL OUT	T-8 OIL OUT RAMP	T-8 RAGS 2%	T-8 RAGS 4%	F-8 RAGS 6%	T-8 RAGS 8%	T-8 RAGS 10%	F-8 RAGS 2%	F-8 RAGS 6%	F-8 RAGS 10%	R-8 RAGS 2%	R-8 RAGS 6%	R-8 RAGS 10%	T-8 NEG WALL 6%	T-8 NEG WALL 12%	T-8 NEG WALL 6%	R-8 NEG WALL 6%	G/B OIL IN	R-8 NEG WALL 12%	F-8 NEG WALL 6%	F-8 NEG WALL 12%	F-8 POS WALL 12%
	NO.	HR-MIN	1	2	3	4	5	6	7	8	9	10	11	12	13	14	15	16	17	18	19	20	21	22	23	24
3.5	DE	1500	495	530	510	500	525	525	525	523	520	520	510	520	520	[illegible]	490	540	525	515	495	350	510	500	505	495
3.5	DE	1510	520	525	530	555	535	530	545	530	535	[illegible]	545	535	545	"	505	530	525	525	520	375	525	515	515	525
3.5	130	1515	515	570	535	565	540	545	540	542	545	535	530	535	540	"	465	535	530	530	520	365	530	520	520	510
3.5	131	1520	520	575	540	570	540	545	545	545	550	535	530	535	545	"	400	540	530	530	525	365	520	520	520	510
	132	1535	500	540	500	535	455	455	490	480	493	480	470	475	460	"	300	450	465	450	460	350	465	420	465	455
	133	1545	430	450	430	430	445	435	440	440	435	420	415	415	415	—	—	420	440	415	410	325	420	395	425	400

NOTES: READING FOR 133 FROM #5 THRU #10 COULD HAVE BEEN 50°F LOWER.

TEST LOG SHEET--

TECHNICIAN	
WITNESS	
WITNESS	
WITNESS	

MIDWEST AERO INDUSTRIES CORP.

TEST OF — Dual Bearing Rolls Brg 3/4 in 2808
PURPOSE —

PROJ NO.	B1001
CUSTOMER	FIRL
P.O. NO.	19046
TEST CELL	270 hp

SHEET 6 OF 6
PAGE 1 OF
DATE 10-12-72

TECH HRS D11	NO	CLOCK TIME HR-MIN	Vibration @ 3600 MILS	Vibration @ W/B 1/REV MILS	Vibration Wyro @ Rig 1/REV MILS	VEL IN/SEC	CPM	Vibration @ 3600 CPM MILS	Vibration @ G/B 1/REV MILS	Vibration VERT @ Rig 1/REV MILS	VEL IN/SEC	CPM	Cage Speed	Corr. Cage Speed RPM	Slave Brg Oil 25 °F	G/B Oil Out 26 °F	Rig Housing Skin 27 °F	T-B Oil Out 28 °F	CAGE SPEED RASER COUNT BOW	CAGE SPEED CAL 1/2 SEC (RPM) HKN	AVG
	1	1100											0								
	2	1200																			
	3	1335	0.7	—	0.35	—	—	0.9	—	1.1	—	—	—								
	4	1350	0.7	—	0.3	—	—	0.9	—	0.15	—	—									
	5	1405	0.6	—	0.15			0.9	—	0.15	—	—									
10-24-72																					
	6	1045	—	—	—	—	—	—	—	—	—	—	—								
	7	1110	0.6	—	—	—	—	0.8	—	—	—	—	38/49								
	8	1120	0.6	—	—	—	—	0.8	—	—	—	—	34/48								
	9	1130	0.6	—	—	—	—	0.8	—	—	—	—	38/54								
	10	1145	0.5	—	—	—	—	0.75	—	—	—	—	37/50								
	11	1155	0.5	—	—	—	—	0.75	—	—	—	—	33/47								
	12	1215											50/63								
	13	1250	0.60		0.30			0.60		0.19			53/59								
	14	1310																			
	15	1340	0.60		0.25			0.30		0.15											
	16	1520																			
	17	1530																			
	18	1545											49/62								
	19	1555											48/62								
	20	1615	0.60		0.17			0.60		0.08			72/85								
	21	1625											59/72								
	22	1645	0.60		0.21			0.25		0.07			78/104								
	23	1655	0.										78/100								
	24	1710	0.50		0.50			0.60		0.05			89/125								
	25	1720											87/126								
10-25-72																					
0.5	26	1320											73/95						1125	1222	1169
1.0	27	1345											73/86						2335	2415	2401
1.5	28	1410	0.4		0.1			0.5		0.09			83/102						2630	2749	2706

NOTES:

TEST LOG SHEET–						TECHNICIAN			MIDWEST AERO INDUSTRIES CORP.						PROJ. NO. B1001			SHEET C OF C	
						WITNESS									CUSTOMER FIRL			PAGE 2 OF	
						WITNESS			TEST OF — Prol Dan. Follow Brg SINT in 7000 cell						P.O. NO. 19046			DATE 10-25-72	
						WITNESS			PURPOSE —						TEST CELL 250 hp				

Test Time Hrs	No.	Clock Time	Vibration Horiz @ 360° mils	Vibration Horiz @ 46 mils	Vibration Horiz @ mils	Vel in/sec	Vel cpm	Vibration Vert @ 360 mils	Vibration Vert @ 46 mils	Vibration Vert mils	Vel in/sec	Vel cpm	Cage Speed revs/sec	Cage Speed RPM	Shaft Brg Oil In 25 °F	G/B Oil Out 26 °F	Rig Housing Skin 27 °F	T-A Oil Out 38 °F	Accel. Failure Ind. mv	Accel. Failure Ind. mv				Cage Speed Based on Count (RPM) LOW	HIGH	AVG
1.75	29	1430																								
"	30	1440																								
"	31	1450	0.5		0.6			0.6		0.09			505/175											3543	3579	3561
2.00	32	1505											193/17													
"	33	1515	0.7		0.4			0.4		0.06			121/158											4559	4653	4522
2.25	34	1520											143/163													
"	35	1525	0.5		0.5			0.5		0.09														4754	[illegible]	4505
2.50	36	1535											135/174													
"	37	1540																								
"	38	1547	0.3		0.8			0.5		0.40														4873	5055	4764
"	39	1555											145/182													
2.75	40	1605											137/180											4733	4951	4842
"	41	1610	0.2		0.7			0.5		0.05																
10-26-72															176	155										
0.50	42	1595	1.5		1.5			0.5		0.5					~~[illegible]~~	~~[illegible]~~			.06	.01						
1.00	43	1610	0.8	0.13	0.25			0.6	0.2	0.10					~~[illegible]~~	~~[illegible]~~			.20	.02						
1.50	44	1625	0.8	1.00	0.45			0.6	0.3	0.17					191	160			.30	.04						
2.00	45	1640	0.3	0.20	0.70	0.3	2500	0.3	0.2	0.20	0.3	6400			191	165			.45	.07						
2.50	46	1655	0.3	0.10	1.00	1.0	13000	0.1	0.1	0.20	0.6	36,000	161/152		191	175			.80	.24						
3.00	47	1705	0.20	0.15	0.95	0.9	22000	0.4	0.2	0.50	0.5	40,000	190/250		195	172			.88	.20						
3.25	48	1715	0.15	0.15	0.70	0.9	22000	0.15	0.15	0.25	0.6	45000	190/266		200	190			.70	.95						
3.50	49	1730	0.20	0.20	0.50	0.55	24000	0.15	0.15	1.00	0.5	24000	200/355		210	—			.65	.30						
3.80	50	1750													201	—										
11-4-72																										
	51	1524	—	—	—	—	—	—	—	—	—	—	—		255	95	170	275								
	52	1540	—	—	—	—	—	—	—	—	—	—	—		290	100	200	320								
	53	1555	—	—	—	—	—	—	—	—	—	—	—		335	180	260	370								
	54	1610	—	—	—	—	—	—	—	—	—	—	—		340	110	310	415								
	55	1625	—	—	—	—	—	—	—	—	—	—	—		410	115	315	505								

NOTES:

TEST LOG SHEET–

TECHNICIAN
WITNESS
WITNESS
WITNESS

MIDWEST AERO INDUSTRIES CORP.

TEST OF —
PURPOSE —

PROJ NO.
CUSTOMER
P.O. NO.
TEST CELL

SHEET C OF C
PAGE 3 OF
DATE 11-6-72

TECH INIT	Reading NO.	CLOCK TIME HR-MIN	Vibration Horz. @ 3600 rpm mils	Vibration Horz. @ ... Brg mils	Vibration Horz. @ Rig Brg mils	Vel in/sec	Vel CPM	Vibration Vert @ 3600 rpm mils	Vibration Vert @ ... Brg mils	Vibration Vert @ Rig Brg mils	Vel in/sec	Vel CPM	Cage speed cps	Corr. Cage Speed RPM	Slave Brg Oil In 25 °F	G/B Oil Out 26 °F	Rig Housing Skin 27 °F	T-B Oil Out 28 °F	Oil Out HSK 39	Accel Vert	Accel Horiz
	56	1025	0.25	0.01	0.25	0.03	36000	0.55	0.08	0.55	0.09	[illegible]	51/55		210	95	165	250		.04	.01
	57	1050											59/56		270	205	200	255		.04	.01
	58	1100											31/40		245	130	240	420		.04	.01
	59	1130											23/28		415	140	315	435		.04	.01
	60	1140											22/27		420	145	330	495		.04	.01
	61	1155											21/25		445	155	346	490			
	62	1215											40/45		415	165	358	500			
	63	1230													515	167	362	525			
	64	1245	0.15	0.20	0.15	0.11	[illegible]	0.10	0.30	0.06	0.08	[illegible]	35/46		425	130	366	575		.16	.05
		1315	0.10	0.90	0.17	0.15	[illegible]	0.20	0.60	0.10	0.09	30,000	52/57		440	150	380	420		.22	.05
	66	1330	...	...	—	—	—	—					53/51		425	190	365	460		.24	
	67	1345		—	—	—	—	—					50/56		430	195	355	460		.25	.05
	68	1400											37/66		435	192	405	[illegible]			
	69	1415	0.25	0.30	0.30	0.18	[illegible]	0.20	0.30	0.25	0.23	39,000	41/65		445	195	415	470		.20	.05
	70	1425	—	—	—		—						51/65		451	200	440	470		.26	.05
	71	1445	0.25	0.15	0.40	0.35	26000	0.25	0.10	0.15	0.25	35000	5/11		450	210	445	495		.26	.05
	72	1455	-	—	—	—	—						3/10		420	215	415	475		.26	.05
	73	1503													430	220	495	485			
	74	1525		—	—	—	—						—		435	225	450	475		.29	.05
	75	1540											—		430	230	455	490		.27	
	76	1605	0.25	0.28	0.26	0.26	32,000	0.20	0.10	0.13	0.23	63,000	—		437	236	455	495		.35	.05
	77	1615											24/49		410	240	460	462		.30	.05
	78	1632											51/54		411	235	411	422		.16	.01
		[illegible]	[illegible]	11-7-72																	
	79	1655													360	270	310	345		.15	.01
	80	1715											51/60		360	180	325	420	140	.16	.01
	81	1730											41/92		355	205	363	420	145	.24	.05
	82	1740											63/63		360	210	365	422	140	.24	.05
	83	1800											19/155		355	255	420	460	135	.35	.09

NOTES:

TEST LOG SHEET–	TECHNICIAN WITNESS WITNESS WITNESS	MIDWEST AERO INDUSTRIES CORP. TEST OF — PURPOSE —	PROJ NO. CUSTOMER P.O. NO. TEST CELL	SHEET 6 OF 6 PAGE 4 OF DATE 11-7-72

TECH INIT	Reading	CLOCK TIME	Vibration 3 Brg	6/8	Main Brg	Vel				Vibration Vert			Cage Speed	Conv Cage Speed	Slave Brg Oil In	6/8 Oil Out	Rig Housing Skin	7-8 Oil Out	Water Out H.E.X.						Accel Lat	Accel Vert
	NO.	HR-MIN													25	26	27	28	29						mv	mv
	84	1810	.25	.23	.24	.25	3900	.20	.11	.20	.25	4000	54/60		440	[illegible]	430	445	130						.35	.56
	85	1825	.25	.20	1.9	1.7	2300	.25	.25	.90	.90	23000	38/120		445	250	460	495	120						.37	.08
	86	1835			2.1					1.1			151/151		415	280	475	500	120						.56	.11

NOTES:

TEST LOG SHEET–

TECHNICIAN	
WITNESS	
WITNESS	
WITNESS	

PURE CARBON CO.
ST. MARYS, PA.

TEST OF —
PURPOSE —

PROJ. NO.	
CUSTOMER	
P.O. NO.	
TEST CELL	

SHEET C of C
PAGE 5 of [illegible]
DATE 11-16-72

Temp. DN	No.	Clock Time	Vibration–Horz @ 3600 cpm	Vibration–Horz G/B 1/Rev	Vibration–Horz Rig 1/Rev	Horz Vel	Horz Vel	Vibration–Vert @ 3600 cpm	Vibration–Vert G/B 1/Rev	Vibration–Vert Rig 1/Rev	Vert Vel	Vert Vel	Accel Horz	Accel Vert	Slave Brg Oil In °F	G/B Oil Out °F	Rig Housing Skin °F	T-B Oil Out °F	B-Fb Water Out °F	T-B Oil In °F	Vol Lever Outer Min °F
	NO	HR-MIN	mils	mils	mils	in/sec	cpm	mils	mils	mils		cpm			25	26	27	28	29	30	31
	100	0945	—	—	—	—	—	—	—	—	—	—			—	—	—	—	—	—	—
12-2	-72																				
0	101	0540													110	130	160	175	58	204	170
0.5	102	1000	1.6	.03	1.6	.22	22,000	.26	.15	.26	.05	30,000	.08	.05	105	140	170	152	90	155	179
	103	1030													225	155	225	205	115	390	250
	104	1100													260	178	253	121	123	345	262
1.5	105	1120	1.8	.90	.22	.21	13,000	.25	.25	.13	.06	11,500			[illegible]	[illegible]	[illegible]	365	[illegible]	[illegible]	315
	106	1140													300	215	310	340	116	340	330
0	107	1235													335	—	290	400	—	420	330
0	108	1315													330	262	335	405	115	465	355
0.5	109	1345											.01	.05	325	190	335	375	96	317	332
1.0	110	1355											.01	.15	305	190	340	340	90	365	332
1.5	111	1410	1.3	1.8	.16	.22	24,000	.20	20	.09	.20	~~10,500~~	.01	.21	310	155	350	395	55	403	340
	112	1430											~~[illegible]~~	~~[illegible]~~	325	180	330	405	85	410	345
2.0	113	1435	1.3	1.8	.90	.25	25,000	.15	0.6	.16	.10	36,000	.02	26	345	235	370	425	50	[illegible]	350
"	114	1445													360	250	350	440	90	442	350
2.5	115	1500	1.7	0.6	.64	.52	20,000	.19	0.11	.23	.30	39,000	.02	.40	340	290	420	465	85	460	415
	116	1510													350	365	430	455	125	430	430
	12-6	D	27	.13	.22	.22									180	148	165	225	155	265	140
0.5	117	0912													225	155	265	250	185	330	235
"	118	0930																			
"	119	0945											.01	.05	240	188	235	205	215	325	263
1.0	120	1000						.12		.11	.18	32,000	.01	.11	265	188	260	345	85	350	255
3.0	121	1035						.11	0.6	.15	.09	36,000	.02	.29	300	240	350	400	95	400	355
	122	1215									~~[illegible]~~	~~[illegible]~~			250	150	260	315	90	325	270
	123	1255						.16	1.7	<.05	.15	3000	.01	.20	253	[illegible]	255	350	55	405	300
	124	1300						.20	.13	.23			.02	.36	375	280	384	440	105	445	400
	125	1310						.60	.32	.95	1.1	19,000	—	.66	350	305	440	465	110	455	390
	126	1445						.15	.30	.55	0.9	22,000	—	.36	380	[illegible]	405	450	55	460	465
	127	1455											—	.75	425	370	450	450	105	465	465

NOTES:

TEST LOG SHEET–	TECHNICIAN	PURE CARBON CO. ST. MARYS, PA.	PROJ NO.	SHEET C OF C
	WITNESS		CUSTOMER	PAGE C OF
	WITNESS	TEST OF —	P.O. NO.	DATE 12-22-72
	WITNESS	PURPOSE —	TEST CELL	

TECH. INIT.	Reading NO	CLOCK TIME hr-min	Q mils	VIBRATION HORZ w/o filter mils	w/ filter mils	VEL	VEL cpm	Q mils	VIBRATION VERT w/o filter mils	w/ filter mils	VEL	VEL cpm	ACCEL	ACCEL	°F 25	°F 26	°F 27	°F 28	°F 29	°F 30	°F 31
	125	1500						0.9	—	.55	0.8	4000	—	1.00	440	355	485	508	120	480	490
	128	1510											—	1.10	455	330	500	520	125	500	495
	130	1517						0.3	(1)	.18	0.6	7800	—	1.10	465	355	505	520	130	500	510
	131	1520											—	1.05	470	350	520	535	110	510	510
	132	1535						0.2	1.6	.10	0.17	2500	—	.37	470	370	450	450	125	485	420
	133	1545													365	315	435	395	115	385	415

NOTES: @ 1512 Test Pump Discharge Drop to 160 PSI readjusted Bypass flow
(1) Unfiltered Disp. 4 mils @ < 500 cpm

APPENDIX II

GAS TURBINE ENGINE MAINSHAFT ROLLER BEARING - SYSTEM ANALYSIS

By

J. H. Rumbarger, Principal Engineer, Member ASME
E. G. Filetti, Senior Staff Engineer, Member ASME
D. Gubernick Student, Drexel University, Coop Employee, FIRL

The Franklin Institute Research Laboratories
Philadelphia, Pennsylvania

Submitted to
Lubrication Division of ASME
For Publication (without presentation) in
Journal of Lubrication Technology

August 1972.

ABSTRACT

An interdiciplinary systems analysis is presented for high-speed gas turbine engine mainshaft roller bearings which will enable the designer to meet the demands for ever higher rotative speeds and operating temperatures. The latest elastohydrodynamic experimental traction data is included. Analytical results cite a need for better definition of the rolling friction portion of the total traction. A fluid mechanics model for the detailed analysis of fluid drags is developed based upon a turbulent vortex-dominated flow and includes the effect of lubricant flow through the bearing. Typical cage equilibrium solutions show evidence of possible unstable operation. A complete thermal analysis including dynamic and thermal effects upon bearing dimensions and resulting clearances is also included. Heat transfer coefficients are given in detail. Shaft power loss and cage slip predictions as a function of load, speed, and lubricant supply correlate well with available experimental data.

LIST OF FIGURES

Fig. No.		Page
1	Surface Velocities and Relative Rotational Speeds of Raceways and Rollers Including Slip at Each Contact as a Result of Cage Slip	38
2	Forces and Moments Acting on a Loaded Roller	39
3	Forces and Moments Acting on an Unloaded Roller . . .	40
4	Solution Techniques Flow Chart	41
5	Roller Clearance Distribution in Cage	42
6	Mathematical Model of Horizontal and Vertical Relative Velocity Distributions in Roller-Shoulder Contact	43
7	Roller Bearing Cage Speed Correlation	44
8	Influence of Oil/Air Ratio on Each Solution	45
9	Influence of Oil/Air Ratio on Each Solution	46

LIST OF TABLES

Table No.		Page
1	Dimensional Models	47
2	Description of Thermal Analysis by Nodes	48
3	Typical Thermal Analysis	49
4	Typical EHD Film Thickness and Traction Values	50

INTRODUCTION

The use of elastohydrodynamic lubrication theory for rolling bearing analysis was first suggested by Dowson and Higginson[1]. The first use of digital computers for the analysis of high speed roller bearing performance was by Harris[2]. The Harris paper presented an analytical method to predict skidding in high-speed roller bearings. The influence of the amount of lubricant supply on cage and roller motion in high speed roller bearings was experimentally described and analytically discussed by Boness[3]. A refinement was introduced by Poplawski[4] with the solution of all of the loaded rollers under the varying load pattern resulting from external radial load. He also introduced a fluid "churning" loss and cage pilot surface friction formulations.

All of the previous analytical work used the Dowson-Higginson[1] isothermal elastohydrodynamic (EHD), formulation. A recent comprehensive review of EHD theory and experimental data by McGrew, et al[5] resulted in selection and recommendation of the latest and most applicable EHD formulations. This preliminary EHD design manual[5] also presents computer subroutines for the calculation of oil film thickness including thermal effects developed by Cheng[6] and EHD traction subroutines fitted to available disk machine experimental data.

The present paper presents a system analysis of a high-speed roller bearing under radial loading as commonly used on gas turbine engine mainshafts. Oil film thickness, traction, and hydrodynamic pressure forces acting in an elastohydrodynamic roller-race contact are computed according to the latest available techniques[5]. A complete fluid mechanics model is developed in order to more accurately predict the fluid drag losses acting upon roller, race, and cage moving surfaces. Turbulent vortex-dominated flow theory is used to calculate boundary layer stresses. Finally, a complete thermal analysis is described.

Combining the resulting thermal deformations with deformations of the bearing components due to centrifugal growth completely defines changes in critical bearing operating parameters at each step of the iterative solution process. The thickness of an EHD oil film is determined by the temperature and viscosity at the inlet to the contact. This inlet oil temperature is very sensitive to the temperature gradients which exist within the bearing. Oil viscosity changes and dimensional changes throughout the bearing as a function of temperatures are included. The thermal solution as expected is dependent upon lubricant flow rate, method of application (under inner race, thorough bearing, etc.) and external heat paths.

LOAD AND SPEED EQUILIBRIUM

Elastohydrodynamic Pressure Forces and Tractions

The surface velocities and relative rotational speeds of rollers and raceways are shown in Fig. 1 and follow the nomenclature of Harris[2]. Sliding velocities, V_{ij} and V_{oj} are defined as positive when the surface velocity of the race is greater than the surface velocity of the roller and is equal to their difference. The rolling or entrainment velocities U_{ij} and U_{oj} are always positive and defined as the average of raceway and roller surface velocities. The sliding velocities and entrainment velocities are made dimensionless by introduction of the fluid entrance viscosity, η_e, reduced modulus of elasticity, E', and equivalent cylinder radius, R, for each contact as suggested by Dowson[1].

Forces and moments acting on a loaded roller are shown in Fig. 2 and those acting on an unloaded roller are shown in Fig. 3. The effect of cage orbital speed, ω_c, is to create a dynamic body force on the roller acting radially outwards. Figs. 2 and 3 use D'Alembert's principle[7] to represent the summation of this roller body forces as an inertia force CF* acting through the center mass of the rollers.

$$CF^* = \frac{1}{2} M_r E \omega_c^2 \tag{1}$$

Thus Figs. 2 and 3 are free body diagrams of the roller in static and dynamic steady state equilibrium with all static and dynamic forces shown.

Fluid pressure forces Q_{ij} and Q_{oj} tending to translate the roller relative to the raceways are described by Dowson, etal[1] and approximated by Harris[2] for synthetic lubricants as:

$$\left.\begin{aligned} \bar{Q}_{ij} &= 18.4\ (1-\gamma)\ G^{-0.3}\ \bar{U}_{ij}^{\ 0.7} \\ \bar{Q}_{oj} &= 18.4\ (1+\gamma)\ G^{-0.3}\ \bar{U}_{oj}^{\ 0.7} \end{aligned}\right\} \qquad (2)$$

Traction forces T_{ij} and T_{oj} consist of fluid frictional drag forces as described by elastohydrodynamic lubrication theory. They consist of rolling and sliding friction forces. Using the Harris[2] approximation for Q_{ij} and Q_{oj} they are expressed as:

$$\left.\begin{aligned} T_{ij} &= -9.2G^{-03}\bar{U}_{ij}^{\ 0.7}\ \ell_{ij}E'R_i + \frac{|V_{ij}|}{V_{ij}}\ f(T_e)_i\ P_{ij} \\ T_{oj} &= -9.2G^{-0.3}\ \bar{U}_{oj}^{\ 0.7}\ell_{oj}\ E'R_o + \frac{|V_{oj}|}{V_{oj}}\ f(Te)_o P_{oj} \end{aligned}\right\} \qquad (3)$$

The coefficient of traction, f, for the sliding portion has been obtained by experiment from disk machines. This coefficient has been curve fitted to existing data by McGrew, etal[5] as a function of three dimensionless parameters G_1, G_2, G_3 and is represented symbolically as:

$$f(Te) = F\left(G_1,\ G_2,\ G_3,\ 30°C\right) - 0.001\ (Te-86°F) \qquad (4)$$

where Te is the temperature, °F, at the entrance to the EHD contact. The three dimensionless parameters (given in the nomenclature) express shear rate effects, thermal heating effects, and pressure viscosity effects, respectively. Graphs and computer subroutines for the traction coefficient, f , are given in reference, [5] and are not repeated in this paper.

It should be noted that this representation of experimentally obtained traction data is extrapolated for both high and low sliding velocities to make the data useful over a wide range for the analysis of bearing systems. At small values of G_1 all curves of, f, have a 45° slope. This corresponds to the fact that at small sliding speeds the frictional coefficient varies linearly with sliding speed.

P_{oj} and P_{ij} are raceway normal forces transmitted to the roller by the external bearing load. F_{add} is a force resulting from contact between the roller and the guiding shoulders of the raceway. M_{rj} is a symbolic representation of all of the fluid resisting moments acting on the roller. F_{cj} is loading due to the cage. A loaded roller, Fig. 2, which drives the cage results in a positive value of F_{cj} as shown. An unloaded roller is driven by the cage as shown in Fig. 3. A retarding torque is always present as a result of rubbing coulomb friction between the roller and cage pocket.

Load Roller Equilibrium

Summation of forces in the horizontal and vertical directions, Fig. 2, for the loaded roller must equal zero for steady state translating equilibrium.

$$Q_{ij} + T_{ij} - Q_{oj} - T_{oj} - F_{cj} \pm F_{add} = 0 \tag{5}$$

$$P_{ij} + CF^{*} - \mu F_{cj} - P_{oj} = 0 \tag{6}$$

Summation of moments about the roller axis of rotation, Fig. 2, must equal zero for steady state rotary motion equilibrium: (The term F_{add} resulting from roller end contact with the guiding shoulder is described later by Eq. (36).

$$T_{ij}\frac{d}{2} + T_{oj}\frac{d}{2} - \mu Fc_j\frac{d}{2} - M_{rj} \neq 0 \stackrel{\sim}{=} I_{rj}\frac{\partial \omega r_j}{\partial t} \tag{7}$$

The equations of equilibrium for the unloaded roller are similar and can easily be derived from Fig. 3. (Also Ref. [2]).

EHD Oil Film Thickness

The average oil film thickness in the Hertzian zone is computed according to the Dowson, etal[1] isothermal theory for line contact and modified with the Cheng[6] thermal correction factor, ϕ_T.[5] The film thickness is determined by the lubricant velocity, η_e, at the inlet.

$$h = \frac{1.6\ G^{0.6}\ \bar{U}^{\ 0.7} R\ \phi_T}{\bar{W}^{\ 0.13}} \tag{8}$$

Roller Load Distribution

The summation of all inner race loadings, P_{ij}, equals the applied external radial load, F_x. For simplicity,the solution will be given in a single degree of freedom, along X. Then:

$$F_x - \sum_{j=1}^{z} P_{ij} \cos \phi_j \neq 0 = \varepsilon LD \tag{9}$$

where

$$\cos \phi_j = \frac{2\ j\ \pi}{Z} \tag{10}$$

Cage Equilibrium

Steady state rotation of the cage requires that the summation of all fluid film forces and roller to cage forces acting on the cage be in equilibrium. The sum of the moments of all of the fluid film forces acting on the cage surfaces and taken about the center of bearing rotation will be represented symbolically by M_c and will be considered to be a drag or retarding moment when expressed in the positive sense. An inner land riding cage will develop a driving torque in the land, which helps to drive the cage. An outer land riding cage develops a drag torque in the lands. An unloaded roller by definition has a negative cage force F_c, Fig. 3. A loaded roller has either a psotive driving cage force, F_c, or a negative drag force, per Eq. (5) and Fig. 2.

$$\frac{E}{2} \sum_{j=1}^{z} (F_{cj}) - M_c \neq 0 \tilde{=} I_c \ \frac{\partial \omega_c}{\partial t} \tag{11}$$

Method of Solution

A flow chart of the method of solution is given in Fig. 4. The solution consists of six nested single degree of freedom iterative loops. Two convergence schemes are used. Load distribution solutions are solved using classical Newton-Raphson matrix inversion techniques[8] Roller speed and cage speed solutions use a modified time step solution because of the multiple valued traction function.

Equations (7) and (11) are written as inequalities where the right hand side is the product of the polar moment of inertia and the first time derivative of the rotational speed. The desired steady state solution will occur when the right hand side vanishes. The magnitude and sign of the right hand side is used to compute the increment of cage or roller speed. Roller inertias are small, and extremely small time steps would be required for solution. A modified time step in the form of cage or roller speed steps proportional to the right hand side (or moment unbalance) are used for the solution. Initial step size is determined by experience to minimize computer execution time. Changes in speed regiems (DN values) and change of lubricant usually requ' es an adjustment in step size.

Determination of Loaded Rollers

The radial displacement, $\delta\phi_j$, at any location angle, ϕ_j, is:

$$\delta\phi_j = X\cos\phi_j - \frac{Pd}{2} + x'_\phi \qquad (12)$$

where x'_ϕ is a constant deviation from a true circular profile. A plus value of x'_ϕ means a radially outward deviation of the inner race or a radial inward deviation of the outer race at location ϕ, or the algebraic sum of deviations of both races from a true circular profile. An elliptical out-of-round race or any race shape in general[9] can be described by specifying values of x' for every location angle, ϕ_j.

A quantity, δ_{TOTAL}, is defined as the total deflection requirement for an unloaded roller assuming that it is initially in dry line contact (no EHL film, no roller load, no bearing clearance) with both inner and outer races.

$$\delta_{TOTAL} = {}_u\delta o - {}_u h_o - {}_u h_1 - {}_u\delta ROT + {}_u\delta CF \quad (13)$$

where:
$$ {}_u\delta_o = \left(\frac{CF^*}{K_o}\right)^{9/10} \quad (14)$$

$$K_o = 11.4 \times 10^6 \, \ell_o^{\,8/9} \quad (15)$$

${}_u\delta_o$ is the elastic compression or approach of the roll centerline towards a distant point in the outer race using the Palmgren[8] approximation.

${}_u h_o$ is the EHD film thickness at the outer race contact per Eq. (8).

${}_u h_1$ is the EHD film thickness at the inner race contact per Eq. (8) with a load of P_{ij}/ℓ_{ij} = 1.0 lbs./inch.

${}_u\delta_{ROT}$ is the increase in diameter of the unloaded roller caused by rotation, ω_{rj}, about its own axis. (See Table 1).

${}_u\delta_{CF}$ is the compression of a hollow roller as a ring due to the inertia force CF^*[10].

$${}_u\delta_{CF} = \frac{CF^* r^3}{EI}\left(\frac{0.4674}{2\pi}\right) \quad (16)$$

r = the mean radius of the hollow roller (in.)

I = area moment of Inertia of the ring section ($in.^4$)

Determination of a loaded roller is then made by:

$$\left.\begin{array}{lll} \delta_{\phi_j} \leq \delta_{TOTAL} & P_{ij} = 0 & \text{UNLOADED} \\ \delta_{\phi_j} > \delta_{TOTAL} & P_{ij} > 0 & \text{LOADED} \end{array}\right\} \qquad (17)$$

Eq. (17) states that if the total radial displacement, $\delta\phi_j$, is greater than the radial displacement value, δ_{TOTAL} of an unloaded roller; then the roller is loaded. If $\delta\phi_j > \delta_{TOTAL}$ then P_{ij}/ℓ_{ij} must equal or exceed 1.0 lb/inch. This test is made at each roller location as shown by iteration loop 4, Fig. 4, for the radial load solution.

Solution of a Loaded Roller

The solution of a loaded roller according to Eq. (5), (6), and (7) is accomplished by means of two nested iterations #5-Inner Race Roll Load, P_{ij} and #6-Roll Speed, ω_{rj}, as shown in Fig. 4.

The inner loop #6 to determine roll speed ω_{rj} (by means of Eq. (7)) is solved using the modified time step technique described above. This solution requires a known value of the inner race load, P_{ij}.

The inner race loading, P_{ij}, of a loaded roller is determined by using Newton-Raphson iteration (loop 5 of Fig. 4) and assuming an initial value of P_{ij} an then calculating corrections to it. An initial value can be closely determined from the external radial load and using Stribeck's constant for the maximum roller load.

The cage to roller contact force F_{cj} is solved directly from Eq. (5) for a given value of ω_{rj}. Roller speed is determined by iteratively solving Eq. (7) with a modified time step or incremental values of ω_{rj}. The solution of Eq. (7) is very sensitive to small changes to torques about the roll axis.

The μFcj term of Eq. (6) is neglected in the solution. The coulcmb coefficient of friction μ is usually less than 0.1. The traction coefficient in the EHD contact, $f(T_e)$, is always less than 0.1 and usually less than .01. Thus the F_{cj} term is always less than 1% and usually less than 0.1% of P_{oj}.

The relationship of radial displacement, x, of the inner ring upon a loaded roller is:

$$\delta_{oj} + \delta_{ij} - h_{oj} - h_{ij} + \delta_{CF_j} + \delta_{r_j} - \delta_{rot_j} - X\cos\phi_j + \frac{Pd}{2} - X'_\phi \neq 0 = \varepsilon_j \quad (18)$$

Where δ_{CF_j} and δ_{r_j} refer to a hollow roller and are omitted from Eq. (18) when solving solid rollers. δ_{r_j} is the ring compression of a hollow roller per Timoshenko[11] as:

$$\delta_{r_j} = \frac{C_{rj}}{\ell_{ij}} \cdot P_{ij} \quad (19)$$

$$C_{rj} = \frac{r^2}{tEe} \left\{ \frac{\Pi}{4} - \frac{2}{\Pi} \left(1 - \frac{e^2}{r^2}\right) + 2\frac{e}{R} \left[\frac{2}{\Pi}\left(1 - \frac{e}{r}\right) - \frac{\Pi}{8}\right] + \frac{\Pi}{4} \frac{\alpha E e}{[\text{illegible}]} \right\} \quad (20)$$

Subsequent values of P_{ij} are then:

$$\left(P_{ij}\right)_{p+1} = \left(P_{ij}\right)_p - \left(\delta\varepsilon_j / \delta P_{ij}\right)_p \quad (21)$$

Solution of Eq. (18) using corrected values of P_{ij} from Eq. (21) is rapid and no convergence difficulties have been encountered.

The load carried by each loaded roller is determined by the Radial load solution loop No. 4 of Fig. 4. Eq. (9) is solved by Newton-Raphson iteration using the radial displacement, x of Eq. (18) as the variable. An initial value of x is computed using an assumption for the value of P_{ij}, Eqs. (6, 15, and 16), assuming pure rolling (no slip) for the maximum loaded roller speed,and cage speeed. Subsequent values of x are:

$$(X)_{p+1} = (X)_{p} - \left\{ \frac{\partial \varepsilon LD}{\partial X} \right\}_{p} \quad (22)$$

Solution of Eq. (9) using the corrected values of x is rapid and no convergence difficulties have been encountered.

FLUID MECHANICS MODEL

Flow models for the (usually) turbulent flow field are briefly discussed, and then applied to calculation of fluid drags acting on roller and cage surfaces. The influence of the mixed component lubricant-air fluid field is treated with respect to definition of wall shear stresses explicit in the calculation of fluid drags. Lastly, the consequences of the fluid drags acting on roller and cage surfaces are described in relation to their influence on bearing behavior.

At least one previous investigator, Poplawski[4], has included the effects of fluid drags in an analytical model of roller bearing performance. This model lumped the effects of fluid drags into a "churning loss" and suggested the use of an effective air-oil density to improve the analytical description. The Poplawski[4] model demonstrated significantly better correlation with existing experimental data than did the original Harris[2] model. The present work examines in more detail the influence of fluid drag torques acting on individual surfaces, and accounts for the driving influence of such torques on certain cage and roller surfaces as well as the retarding influences of such torques. Both the energy dissipation and the convective heat transfer within the bearings are closely associated with the viscous fluid behavior of the lubricant. The techniques employed in this analysis use a combination of empirical and theoretical treatments to define these effects.

From the standpoint of the dynamic solution of the interacting rollers, races, and cage, the most important factor is calculation of the friction drags on the element surfaces. In general, this effect is described by an equation of the form:

$$T = \tau_w A r \tag{23}$$

where T is the drag torque acting over the element surface,

A is the surface area,

r is the reference radius from the center of rotation,

τ_w is the wall shear stress

The description of the wall shear stress is a function of the fluid properties, the motion of the surface with respect to the fluid body, and the proximity of other surfaces influenced by the same fluid. Regarding the last mentioned, close clearances between rotating members of the bearing have especially strong influences.

Fritz[12] has investigated the wall shear stress phenomenon in journal bearings with vortex turbulent flow. Examination of typical roller-cage clearance to roller radius ratios, and Reynolds and Taylor numbers representative of 1×10^6 DN and higher bearing operation clearly place such fluid flows in the turbulent-vortex regime as defined by Fritz[12] and illustrated for a typical case in his Fig. 3. For surface finishes and bearing dimensions typical of 1×10^6 DN and higher roller bearings, the flows representative of cage surfaces appears to be in the couette turbulence regime.

Wall shear stress for a surface rotating in a viscous fluid is defined by the relation[13]:

$$\tau_w = f(1/2\ \rho\ U^2) \qquad (24)$$

where U = mass average velocity of fluid

ρ = fluid density

f = friction factor

For this correlation, $U = \frac{r\omega}{2}$

The applicable friction factors from Fritz[12], and curve fitted for computer analysis' are:

$$f/f_L = 1.3 \left(\frac{N_{Ta}}{41}\right)^{0.539474} \qquad (25)$$

for the vortex-turbulent correlation and

$$f/f_L = 3.0 \left(\frac{N_{Re}}{2500}\right)^{0.85596} \qquad (26)$$

for the couette turbulent correlation.

Here,

$$N_{Re} = \frac{r\omega C}{\nu} \qquad \text{is the Reynolds number} \qquad (27)$$

$$N_{Ta} = \frac{r\omega C}{\nu}\sqrt{\frac{C}{r}} \qquad \text{is the Taylor number} \qquad (28)$$

and

$$f_L = \frac{16}{N_{Re}} \qquad \text{is the laminar friction factor} \qquad (29)$$

Should calculation yield a Reynolds number less than 2500, or a Taylor number less than 41, a circumstance virtually impossible in high speed roller bearings, the appropriate friction factor then can be taken as the laminar friction factor f_L.

In addition to the fluid drag acting on the cylindrical surfaces, the roller ends or cage sides provide an additional source of drag. Per Refs. [13] and [14] for a rotating disk wetted on both sides, the total moment resulting from fluid drag about the disk centerline is given by:

$$M_T = \frac{1}{2}\rho\,\omega^2\,r^5\,C_n \qquad (30)$$

$$\text{where} \quad C_n = \begin{cases} 3.87/(N_{Re})^{1/2} & \text{for laminar flow, } N_{Re} < 300{,}000 \\ 0.196/(N_{Re})^{1/5} & \text{for turbulent flow, } N_{Re} > 300{,}000 \end{cases} \qquad (31)$$

$$\text{where here} \quad N_{Re} = \left[\frac{r^2\omega}{\nu}\right] \qquad (32)$$

For hollow rollers and for the cage, account must be taken of the areas pertinent to the calculations by modifying the radius factor of the disk equation to the form:

$$r^5 = r_{out}^3 \left(r_{out}^2 - r_{in}^2\right) \tag{33}$$

where

r_{out} is the outer radius

r_{in} is the inside radius

This is at least true to a good approximation in the case of the roller, since examination of the integral from which a closed form solution of (30) is derived shows that approximately 75% of the total moment contribution comes from the area defined by the outer 50% of the roller radius. In the case of the cage, the "disk" torque acting on the cage side surfaces is less justifiable on theoretical grounds, but the calculated effect has been shown to be small with respect to the cylindrical surface contribution in this instance.

Basic to the above calculations is the realization that high-speed roller bearings never are completely flooded with lubricant, and seldom are more than 15 to 20% full of oil within the bearing for very high speed operation. Indeed, an excess of oil within the bearing has been conclusively shown by Boness to produce adverse effects on bearing operation[3]. Motion of the many moving parts within the bearing, in particular the pumping action of the rollers, will tend to induce an air oil mixture within the bearing. Hueristically, it can be argued that for pure viscosity effects in a turbulent regime, this phenomenon will have little tendency to change the fluid behavior from that of a flooded bearing, since in general such effects are confined to relatively thin boundary layers adjacent to the surfaces. Further, the turbulent mechanisms of momentum and energy transfer depends on physical displacement of fluid particles. However, the density or inertia effects of the air oil mixture can be drastically influenced by comparison to that of a flooded bearing. Hence, it becomes necessary to modify the density of the fluid mixture, choosing a volumetric basis for the calculation:

$$\rho_{av} = (\rho_{oil} \times \text{oil volume} + \rho_{air} \times \text{air volume})/\text{Total Volume}$$

$$\cong \rho_{oil} \times \frac{\text{oil volume}}{\text{Total volume}}, \text{ defined as } \rho_{oil} \times \text{DECFUL} = \text{DENS} \qquad (34)$$

The apparent density of the fluid is taken as this in roller drag calculations. Recognizing that the land regions and the cage surface on the close clearance land side will be somewhat restrictive to free flow of oil out such regions, the oil density in this region is taken as:

$$\rho_{HIGH} = \frac{\rho_{oil} \times \text{DECFUL}}{0.4 + 0.6\ \text{DECFUL}} \qquad (35)$$

The fluid density in other regions is taken as:

$$\rho_{LOW} = \frac{\rho_{oil} \times \text{DECFUL}^2}{0.4 + 0.6\ \text{DECFUL}} \qquad (36)$$

These relations derive from flow continuity considerations, assuming 40% of the total flow will be on average confined within the higher density region. While admittedly arbitrary, these assumptions have led to excellent correlation with existing empirical data.

Roller Fluid Drag Torque

Consider the drag torque acting on the cylindrical roller surface, as computed from equations (23) through (29), T_{rcyl}. In this case, careful consideration must be given to the calculation of the characteristic radial clearance required in the calculation. From the close clearance region between the rollers and the cage, and the interrace cage geometry, it is possible to define a characteristic clearance between the rollers and the surrounding elements. Figure 5 illustrates the geometry. This clearance is defined by:

$$C = C_{CH} = \frac{1}{2\pi} \int_{\text{Circumference}} C(\theta)d\theta \qquad (37)$$

Five distinct zones must be considered in the calculation on each semi-cylindrical half of the roller. Rollers are assumed to be in contact with either the leading cage pocket surface (driving roller) or the lagging cage pocket surface (driven roller). Generally, rollers carrying load are driving rollers and unloaded rollers are always cage-driven. Comparing the two roller surfaces, therefore, the only zone not symmetric with respect to the radial ray through the roller center is Zone III, where the entire diametral pocket clearance is taken as 10% of the roller radius. Calculation of the clearance is then straightforward, given dimensions of the cage, rollers, and races.

Similarly, the drag torque acting on the roller ends, T_{rend}, is computed directed from Equations (30) through (33). For all roller calculations, the appropriate density is computed from Equation (34).

While not totally fluid mechanical in origin, the sensitive nature of the roller equilibrium solution requires consideration of the influence of the contact between the roller and the guiding shoulders of the cage in the torque equilibrium solution. Computer results show this effect to contribute generally 5 to 10% of total roller drag moment. Further, for a roller guided on the outer race shoulder, this moment can either drive or retard the roller, depending on the distribution of relative local velocities between roller and shoulder. The calculation requires the assumption of a coulomb coefficient of friction between the roller and shoulders, generally taken as 0.05 to 0.08 for a well lubricated contact. While strictly an integral over the contact area, the moment can be closely approximated by dividing the contact area into a number of horizontal and vertical strips or lamina as shown in Figure 6 for a roller guided on the outer race. A similar situation exists for a roller guided on the inner race, but the appropriate relative kinematics must be used. Further, for the inner race guided roller, the local race speed always exceeds the local roller speed, and hence always produces a net driving · ·que on the roller. The moment contribution, T_{add}, of the contact tc ·e roller moment is then given by

$$T_{add} = \mu_c \frac{F_{jG}}{A_G} \left\{ \sum_{N=1}^{N} \frac{|V_{Ri} - V_{Hji}|}{(V_{Ri} - V_{Hji})} A_{Hji} \, r_{Hji} - 2 \sum_{l=1}^{S/2} A_{Vjk} \, r_{Vjk} \right\} \tag{38}$$

The second term always produces a retarding moment, while the sign of the first term, at least for an outer race guided roller, is dependent on the velocity distribution over the contact region.

The resultant vertical force is self-equilibrating, since the velocity distribution is asymmetric with respect to the radial ray through the roller center. However, the horizontal resultant can be either positive or negative, and contributes to the contact force between the roller and the cage, as evidenced in Equation (5). This resultant force is given by

$$F_{add} = \frac{\mu_c F_{jG}}{A_G} \sum_{i=1}^{N} \frac{|V_{Ri} - V_{Hji}|}{(V_{Ri} - V_{Hji})} A_{Hji} \tag{39}$$

Note that these quantities are functions of velocity, and must be determined at each roller iteration. Since F_{jG} is constant in any given problem, the derivatives of F_{add} and T_{add} are not involved in any of the Newton-Raphson iterations.

The contact force between the roller ends and the guiding race shoulder, F_{jG} acts in the direction of the roller axis. Such a force can arise from a variety of sources. Among these are differential pressure acting across the bearing, cage angular misalignments, roller skewing due to gyroscopic moments, and unbalances in the various rotating members which give rise to dynamic forces between the roller and the guiding shoulder.

In this formulation of the problem, the contact force was assumed to arise from differential pressure resulting from crossflow of lubricant through and out of the bearing. This axial crossflow was assumed to be superimposed on the swirling turbulent flow pattern existing in the annular spaces between the rollers, cage, and races. In traversing the distance across the bearing, the resistance to flow in the roller axis direction, and hence the differential pressure across the bearing, will depend not only on the axial flow, but also on the flow in the tangential direction. We assume the same turbulent flow mechanism to be operating in both the axial and tangential directions. This leads, after some manipulation, to a differential pressure relation

$$\delta_p = \frac{f\rho \, \ell_p \, E\omega_c \, L\overline{V}}{16 \, A_x} \tag{40}$$

where

ℓ_p is the peripheral length of a typical crossflow passage

E is the bearing pitch diameter

$\overline{V}$ is a "length of peripheral surface averaged" circumferential velocity

ω_c is the cage angular speed

L is the bearing length

A_x is the area of a typical crossflow passage

Calculation of the friction factor uses the Blasius relation[13]

$$f = 0.3164/(\sqrt[4]{N_{Re}}) \tag{41}$$

where here

$$N_{Re} = \frac{4\overline{V} \, A_x}{\ell_p \, \nu} \tag{42}$$

It is assumed that this differential pressure acts uniformly on the cage side and the roller disk area exposed to the crossflow. Defining this area as Ap, finally,

$$F_{jG} = \delta p \; A_p \tag{43}$$

which is the force appropriate to Equations (38) and (39).

The total fluid drag moment, M_{rj} acting on the roller in Equation (7) is then calculated as:

$$M_{rj} = T_{rcyl} + T_{rend} \pm T_{add} \tag{44}$$

Note, while the first two terms are always positive in this formulation, the algebraic sigh of T_{add} is determined by the relative velocity distribution, as discussed above.

Cage Fluid Drag Torque

The fluid drag torque acting on the cage is composed of the fluid torques acting on the inner and outer cage surfaces, the cage sides, and the cage land surface. Its influence in the equilibrium solution for the cage is indicated in Equation (11) by the quantity M_c.

Calculation of the four component drag torques proceeds directly from Equations (23) through (29) for the inner and outer cage surfaces and for lands, and from Equations (30) through (33) for the cage sides. The appropriate radii and clearances for these calculations are the local cage surface radii and clearances between adjacent surfaces. Fluid densities in the various regions are computed from Equation (35) and (36). Dimensional changes with speed and thermal effects resulting from dissipation are insignificant in these calculations, except in the case of close land clearances.

The total drag moment acting on the cage is then computed from

$$M_c = T_{cout} - T_{cin} + T_{cside} \pm T_{cland} \tag{45}$$

Note that since the total drag moment positive sense is in the direction of retarding cage motion, the outer surface and side torque terms are always positive. The inner surface drag torque always acts to increase cage speed and is hence always negative. The sign of the land surface torque is positive for an outer land riding cage and negative for an inner land riding cage.

Influence of Fluid Drag Torques on Solution

Figure 7 compares the predictions of three analytical models with samples of previously published test data of roller bearing cage slip as a function of applied radial load. The present model demonstrates almost exact correlation with this data across the load range for which data is available. Close correlation is shown by the Poplawski[4] model, which uses a simplified fluid drag correlation. The Harris[2] model matches closely the trend of the test data, but differs significantly in the magnitude of slip predicted across the load range. In addition to the correlation shown for an outer land riding cage, the present model has also accurately predicted the experimentally measured* cage slip of an inner land riding cage bearing.

Power dissipations predicted by the model closely match available rig data.** Shaft horsepower dissipation is computed by summing all torques acting on the inner race. The prediction and distribution of these dissipative losses is essential for accurate determination of thermal gradients and operating temperatures. Predictions for two conventional roller bearings analyzed for comparison are summarized below. Operation was approximately 2.0×10^6 DN.

Bearing	Experimental Power Dissipation, Hp	Computer Power Dissipation, Hp
130 MM Bore	5.80	6.94
115 MM Bore	4.25	3.89

*Data courtesy of Boeing Co., Vertol Division, Philadelphia, Pa.

**Data courtesy of Midwest Aero Industries, Div. Pure Carbon Co., St. Marys, Pa.

Both bearings were operated at near synchronous condition. This calculation is extremely sensitive to the amount of lubricant within the bearing, estimated at between 10 to 15% by volume by the test agency. The 100 MM bearing was analyzed for 15% oil-to-air ratio within the bearing, and the 115 MM bearing was analyzed for a 10% oil-to-air ratio. It will be noted that the results bracket the experimental data, being high for the higher oil/air ratio and low for the lower oil/air ratio. A repeat of this analysis taking both bearings at about a 13% oil/air ratio would yield results matching the experimental data.

The foregoing illustrates generally the sensitivity of the solution to fluid drag influences. As further illustration, consider Figure 8 which compares two cage error curves as functions of cage speed for all other conditions the same. For this relatively low speed application, a difference of 10% in oil/air ratio produced a 2% difference in cage slip.

The shape of the cage error curve, of Figure 8, provides a possible further insight into the bi-stable operation of bearings noted by some investigators. Dr. Ehrich [15] noted this phenomenon, and hypothesized its origin as systematic changes in bearing clearances coupled with dynamic phenomenon of shaft rotation. The cage error vs speed curve always has the same characteristic shape, for which three solutions are possible when slip occurs. One root is always close to synchronous, where the steep slope of the error-speed curve requires successive predictions at small slip valves to obtain a solutions. Other solutions are possible if the error curve changes sign at less than synchronous speed (two possible additional solutions), or if the error curve is tangent to the abscissa of one point. Since the magnitudes of the errors are strong functions of speed and load, and to a lesser extent of oil/air ratio, it is possible that for some combination of these variables the bearing operation may oscillate between two closely spaced roots. This might occur as thermally induced dimensional changes in internal diametral and close land clearances change the operating conditions of the bearing. Such operation has been demonstrated using the present model with thermal and dynamic effects considered. One computer run found about 3% slip on the first iteration (without thermal gradients), but sought the synchronous solution when the results of thermal gradients resulting from the first iteration were reflected in the second. While not conclusive at this time, this subject bears extensive further investigation, with comparison to actual test data as it becomes available.

DIMENSIONAL MODEL

The model accounts for changes which occur during bearing operation as a result of dynamic (centrifugal effects) and thermal deformations. The effects considered to be most significant are:

- Changes in bearing internal diametral clearance (IDC) with dynamic and thermal deformations and with shrink fit between the inner race and the shaft.
- Changes in bearing internal diametral clearance (IDC) due to changes in roller (especially hollow rollers) diameter with dynamic and thermal growth.
- Changes in close clearance guiding cage/race lands with thermal and dynamic deformations, and for an inner land riding cage, changes in the clearance with shrink fit between shaft and inner race.

The use of simple closed form expressions to predict the dynamic and thermal dimensional changes occurring in bearing members is desirable, since this greatly simplifies the system analysis. Predictions of such deformations, on the other hand, must be more than order of magnitude accurate to realistically describe the influence of such operation dependent variables on bearing performance. In the process of model selection, estimates of deformations from available closed form solutions were compared to the results of more sophisticated analyses, using finite element computer solutions of typical bearing element geometries.

Dynamic Deformations

The dynamic deformation models selected for the races, rollers, and cage are given in Table 1 and are obtained from standard theory of elasticity sources.[16 and 17] Comparison of finite element solutions for a 0.50 "diameter hollow roller with a 0.25" diameter hole showed closest agreement with the generalized plane strain solution. At roller speeds of 150,000 RPM and higher, a ± 4% bulging and contraction of the outer surface near the roller edges was calculated in the finite element solution. This cannot be predicted by any of the closed form solutions, however, since it is common practice to crown rollers, this variation is not considered significant. For a solid roller, little comparative difference was noted for any of the closed form deformation relations, and hence a plane stress relation was used for simplicity.

Both the inner and outer surface deformations of the inner race, are significant. The deformation of the inner surface contributes to change in the shrink fit between the race and the shaft, and deformation of the outer surface influences both the bearing IDC and the land clearance of an inner land riding cage. The closed form dynamic deformation relation best describing the behavior of both race surfaces was found to be the plane strain relation. These relations generally predict deformation within 5% of the finite element results even at extreme speed, providing race undercuts or other irregularities such as guiding shoulders are small.

The shaft outer surface deformation is also significant in that it contributes to change in shrink fit. While not checked against a finite element model, the shaft conforms to the basic assumptions of the plane strain relation.

The deformations of the cage land surfaces are significant in the determination of clearances required in the calculation of cage land fluid viscous drag. Agreement of closed form predictions with the results of finite element modeling were within 15 to 20% for this deformation for all closed form solutions. However, the calculation of the fluid viscous drag has been determined to be insensitive to this variation, changing only about 2% at maximum speed. This larger deviation is the result of the inability of the closed form solutions to account for the difference in cage surface and land diameters or to account for bending deformations resulting from the additional mass of the land protrusions. Over the relatively narrow land width, the land surface deformation is fortunately quite uniform, as predicted by finite element analysis. The closed form solution best matching the finite element results, within the limitations discussed, was the plane stress formation.

Shrink fit (Δ) between the inner race and shaft acts to decrease the bearing internal diametral clearance (IDC), as compared to the IDC of an unmounted assembled bearing. Also, for an inner land riding cage bearing, the shrink fit decreases the close land clearance. An extensive treatment of this subject is contained in references [18].

Thermal Deformations

The model used for calculations [16] of thermal deformations assumes an axisymmetric temperature distribution, uniform end deformations and cylindrical geometry. The radial deformation of the i^{th} bearing surface, having inner radius, r_I, and outer radius, r_o, is given by:

$$\delta T_i = \frac{2\alpha r_i}{\left(r_o^2 - r_I^2\right)} \int_{r_I}^{r_o} T_r \, dr = \frac{2\alpha r_i}{\left(r_o^2 - r_I^2\right)} \left\{ (T_{out} - T_{ref}) \left[\frac{r_o^2}{2} - \frac{\left(r_o^2 - r_I^2\right)}{4 \ln \left(\frac{r_o}{r_I}\right)} \right] + (T_{in} - T_{ref}) \left[\frac{(r_o^2 - r^2)}{4 \ln \left(\frac{r_o}{r_I}\right)} - \frac{r_I^2}{2} \right] \right\} \quad (46)$$

The above relations are known to be quite accurate within the governing assumptions. No attempt has been made to date to confirm in detail their accuracy for this application. Comparison of thermal growth predictions to the limited empirical data available to the authors shows reasonable agreement of the magnitude of these deformations.

When applying the above to prediction of the thermal growth of the outer race, it must be noted that no radial constraint is included in the formulation. This is typical of the test environment of roller bearings where loading is accomplished through an external yoke, but growth of the outer race is otherwise unconstrained. Other application of this type of analysis must consider any radial constraint appropriate to the application, particularly because of the possibility of bearing thermal lock-up.

From the above, it follows that when the surface temperatures of all bearing elements are known, the thermal deformations of the bearing members are completely defined.

THERMAL ANALYSIS

Problem Formulation

The temperature field within the bearing must be known in order to compute thermal deformations. With the basic assumption of axisymmetric temperature distribution, the techniques of performing such an analysis are well known. Harris [19] has applied heat transfer techniques to the determination of bearing temperature distributions. The technique presented here will basically follow this presentation, with additional emphasis on the calculation and distribution of power dissipation within the bearing and on calculation of convective conductances or heat transfer coefficients appropriate to the calculation.

All three modes of heat transfer, conduction, convection, and radiation can operate between bearing members and between the bearing and its environment. Conduction is a linear phenomenon. Convection is basically non-linear in that the convective conductance is strongly velocity and temperature dependent. However, in the iterative solution technique used, Fig. 4, velocity is fixed at each step of the iteration. Temperature dependence is mainly reflected in fluid property changes. Since the iterative scheme employs the updated temperatures from the previous temperature iteration solution in the convective conductance calculations for the current temperature solution, the convective mode formulation is linear at each temperature iteration. Radiation heat transfer depends on differences of forth powers of surface temperatures, and is hence always non-linear. The forms of the conductive, convective, and radiation heat transfer equations respectively are:

$$H_{cond_{ij}} = \begin{cases} \dfrac{2\pi k l_s}{\ln\left(\dfrac{r_o}{r_I}\right)} \Delta T_{ij}; & \text{hollow cylindrical body of length } l_s\text{, in radial direction} \\ kA_T \dfrac{\Delta T_{ij}}{\Delta L}\ ; & \text{axial direction, through area } A_T \text{ over distance } \Delta L \end{cases} \tag{47}$$

$$H_{conv_{ij}} = h_k A_{s_k} \Delta T_{ij} \tag{48}$$

$$H_{rad_{ij}} = \frac{\sigma\left[(T_i + 460)^4 - (T_j + 460)^4\right]}{\dfrac{(1-\xi_m)}{\xi_m A_{s_m}} + \dfrac{1}{\bar{F}_{m,n} A_{s_m}} + \dfrac{(1-\xi_n)}{\xi_n A_{s_n}}} \tag{49}$$

where

σ = Boltzmann radiation constant

ξ_m and ξ_n are the emissivities associated with the m^{th} and n^{th} surfaces, respectively.

$\bar{F}_{m,n}$ = view factor of n^{th} surface seen from m^{th} surface

These equations are basic, and are derived in any standard heat transfer text, such as reference [20].

The radiation mode of heat transfer becomes significant only for temperature differences of the order of 100°F and higher. For normal bearing operation, such conditions do not exist within the bearing. However, heat transfer by this mode can be significant between the bearing and its environment, and must be included.

Formulation of the heat transfer problem requires discretizing the bearing elements into a set of nodes, and writing a Kirchkoff energy balance at each node. The power dissipation occurring within the bearing acts as the driving potential, and must be computed and distributed among the nodes. Fig. 9 defines the nodal pattern used in this analysis. In this model, provisions are made for coolant flow through the outer race and through the shaft, and for lubricant to be flowing both through the bearing and under the inner race. Any of these flows except the flow through the bearing may be set to zero. The coolant through the outer race, and the lubricant flows under the race and through the bearing are assumed to mix external to the bearing, and to wash the inner surface of the chamber, the shaft, and the exterior of the bearing. The environment external to the bearing assumes the assembly to be enclosed in a test chamber, and to be loaded through an external yoke extending through the chamber. The governing equations are then of the form, for nodes i = 1 to 21,

$$\sum_{j=1}^{21} H_{ij} + \sum_{k=1}^{N_i} Q_k = \varepsilon_i \tag{50}$$

Here H_{ij} is the energy transfer between nodes i and j, and the Q_k are the dissipations, external energy inputs, energy transfer to coolant or lubricant flows, or losses from a typical node i. N_i is the total number of Q_k at node i. Table 2 illustrates the flow of energy between all nodes, and defines the Q_k quantities at each node. The explicit forms of the equations defined generally by (50) are derivable directly from Table 2. Note that all energy fluxes other than losses are assumed to enter each node. The temperature differences of equations (47), (48) and (49) may thus be uniformly taken at $(T_j - T_i)$ at each node i.

The energy balances of equations (50) are equated to the error functions ε_i, where ε_i approaches zero for the steady state equilibrium set of temperatures. At each temperature iteration, Fig. 4, in the bearing solution, this non-linear set of equations is solved by Newton-Raphson iteration techniques. As an initial guess of the temperature field to start the iterative process, setting all temperatures equal to the previous value of bearing oil temperature, T_{11}, has been found to produce rapid convergence. To implement the Newton-Raphson solution scheme, the set of equations (50), with the H_{ij} quantities expressed in terms of equations (47), (48), and (49) must be rewritten in the form

$$\sum_{j=1}^{21}\left(A_{ij}T_j + A^*_{ij}T_j{}^4\right) + \sum_{k=1}^{N_i'} Q_k + \sum_{k=1}^{(N_i-N_i')} B_k = c_i \tag{51}$$

Here the A_{ij} are thermal admittances for terms originating from convection and conduction, and A^*_{ij} are thermal admittances for terms originating from radiation. N_i' is the total number of quantities, Q_k at node i not explicitly containing temperature, and B_k are constants originating from such sources as products of lubricant mass flow rates, specific heats, and inlet temperatures. The non-linear set of equations (51) for i = 1 to 21 is then directly solvable for the temperature field using the Newton-Raphson solution technique.

Power Dissipation

As previously stated, the driving potentials which result in thermal deformations are the power dissipations occurring within the bearing. These arise from fluid boundary layer and coulomb friction phenomenon. The distribution of the component dissipations is shown in Table 2. The total power expended within the bearing must appear at the shaft surface, since this is the driven member, and is easily calculated as the sum of all roller to inner race tractions and the sum of the fluid drags acting on the inner race and shaft surfaces (including land torques for an inner land riding cage). Shaft power loss is an important design factor and one that until now could only be estimated emperically based upon test experience.

Power dissipations at specific nodes, shown in Table 2, are also easily calculated. Roller to race contact dissipation is the product of the EHD traction and the sliding velocity in the contact. Fluid drag moments are a ribed by the fluid mechanics model.

Ext l energy input such as energy dissipations by slave bearings supporting the shaft in test apparatus, other supporting bearings in an engine, energy input from turbine gasses, etc., must be calculated separately and introduced as heat sources or sinks at the appropriate nodes of Table 2.

Heat Transfer Coefficients

Correct values of the heat transfer coefficients, or more properly the convective conductances, used in the thermal analysis are essential to obtaining a representative solution. While standard techniques of determining these quantities can be used for non-rotating surfaces, the shaft, cage, and roller surfaces pose a special problem. Bjorklund[21] has investigated the problem for the case of concentric rotating cylinders. The techniques and correlations of this source will be used here.

For two concentric rotating cylinders, with the annular space between them containing a viscous fluid, the critical Taylor number for both is given by

$$N_{Ta_{cr_\eta}} = \left[\frac{48.7\left(2 + \frac{C}{r_5}\right)}{(1-\eta)\left[1-\eta\left(1+\frac{C}{r_5}\right)\right]\left[0.0571\left(\frac{1+\eta}{1-\eta} - 0.625\frac{C}{r_5}\right) + \frac{.00056}{\frac{1+\eta}{1-\eta} - 0.625\frac{C}{r_5}}\right]} \right] \qquad (52)$$

where

$$\eta = \frac{\omega_c}{\Omega} \quad \text{Speed ratio} \qquad (53)$$

C = radial clearance between inner race and inner cage surfaces or between inner race surface and cage land surface for an inner land riding cage.

The Taylor number for this condition is given by

$$N_{Ta} = \sqrt{\frac{C}{R}}\,(R\omega c/\beta) \tag{54}$$

where

β = kinematic viscosity of fluid

R = radius of inner rotating member

$\omega = \begin{cases} \Omega \text{ for inner race to cage condition,} \\ \omega_c \text{ for outer race to cage condition} \end{cases}$

The Nusselt number for pure conductance through the fluid is given by

$$N_{Nu_{cond}} = \left(\frac{C}{R}\right) \Big/ \ln\left(1 + \frac{C}{R}\right) \tag{55}$$

and the ratio of the local Nusselt number to the conduction Nusselt number is given by

$$\frac{N_{Nu}}{N_{Nu_{cond}}} = 1.1\left[\frac{N_{Ta} - \left(N_{Ta_{cr_\eta}} - N_{Ta_{cr_{\eta=0}}}\right)\left(1 - 3.5\frac{C}{r_5}\right)}{41.1 + \left(N_{Ta_{cr_\eta}} - N_{Ta_{cr_{\eta=0}}}\right)\left(3.5\frac{C}{r_5}\right)}\right]^{1/2} \tag{56}$$

Finally, the convective conductance is given by

$$h = \frac{k_f}{C} N_{Nu} \tag{57}$$

where k_f = thermal conductivity of the fluid.

For the inner cylinder rotating only,

$$\frac{N_{Nu}}{N_{Nu_{cond}}} = 0.175\, N_{Ta}^{1/2} \tag{58}$$

applies as an alternate to equation (53).

Here the appropriate C is the radial clearance between the outer race and cage outer surface or cage lands for an outer land riding cage. Equations (52) through (58) can be used directly to obtain the appropriate coefficients for the race and cage cylindrical surfaces. Over the vertical cage surfaces, an average of the coefficients of the bounding cylindrical surfaces is recommended. These relations also define the coefficient values on the roller surfaces, using equation (58) and the average roller clearance defined by equation (37). In all of the above calculations, the fluid density used for the calculation of the kinematic viscosity should be computed as discussed in equations (34-36). The variation of fluid properties with temperature must also be considered, updating the fluid properties at each step of the iterative solution.

Coefficients for the outer bearing surfaces and the chamber inner and outer surfaces are computed from a correlation suggested by Jakob[22] for natural convection of fluids in contact with horizontal cylinders

$$h = 0.525 \frac{k_f}{D_r} \left(\frac{D_r^3 \gamma g \Delta t}{\beta^2} \cdot \frac{\beta}{\alpha_d} \right)^{0.25} \qquad (59)$$

where

D_r = diameter of cylinder

γ = coefficient of volumetric expansion

g = gravitational acceleration

α_d = thermal diffusivity

Δt = absolute value of temperature difference between surface and bulk fluid temperature

For condition inside the chamber, the fluid properties appropriate to the calculation are those of the lubricant, since the bearing outer surface, the shaft, and the inner chamber wall are assumed to be washed with the mixed oil. The temperature difference should be taken between the surface temperature in question and the mixed lubricant temperature, which is computed from

$$T_{ave} = \frac{\dot{m}_6 \, c_{p_6} T_6 + \dot{m}_{11} \, c_{p_{11}} T_{11} + \dot{m}_{16} \, c_{p_{16}} T_{16}}{(\dot{m}_6 \, c_{p_6} + \dot{m}_{11} \, c_{p_{11}} + \dot{m}_{16} \, c_{p_{16}})} \tag{60}$$

where

$\dot{m}_i$ is the mass flow rate of the i^{th} lubricant

c_{p_i} is the specific heat of the i^{th} lubricant at Temperature T_i

For the outer chamber surface, the appropriate fluid properties are those of air, and the temperature difference is taken between the chamber wall and the external ambient. For external circulation of air over the chamber, forced convection relations must be used, for which standard formulations can be obtained from Kays[23].

The shaft surface coefficients can be obtained from equations (52) through (58), using equation (58) rather than equation (56), if care is taken to use mass averaged fluid properties. The resulting prediction will be higher than the actual coefficient value. The clearance required here is the difference between shaft and chamber radii. This result should be checked against the prediction of equation (59), which provides a lower bound on the coefficient value, and engineering judgement used to choose the proper valve of the coefficient.

The heat transfer coefficient for the external surface of the loading yoke depends on the geometry of the member. Generally, this can be treated as a fin heated at the root, and standard correlations applied, such as those of reference [20].

Sample Thermal Analysis Results

The results of the thermal analysis of a conventional inner land riding roller bearing operating at 2×10^6 DN are summarized in Table 3. The guiding shoulders for the rollers were on the outer race. Two cases are compared, for conditions with and without under race cooling. This analysis was accomplished using specified operating values of IDC and land clearances, and hence the results are quite comparable for cage slips and power dissipations. The original conditions necessary to achieve the specified operating conditions were computed from the results of the thermal analysis and considering dynamic influences, and are summarized in Table 3 along with results pertinent to the thermal analysis.

The results shown in Table 3 are consistent, showing generally lower temperatures for the case with additional cooling, and a higher oil temperature rise for the reduced cooling case. Also, with under race cooling the temperature difference from the inner to the outer race is 13.7°F, as compared to a temperature difference of 34.7°F for the case of no under race cooling. These results are in general agreement with measured values for comparable bearing operating conditions.

DISCUSSION OF APPLICATION OF EXPERIMENTAL TRACTION DATA AND ROLLER KINEMATICS

Typical traction values for several roller bearings from 65mm bore to 140mm bore and for shaft speeds from 1.0×10^6 DN through 4.0×10^6 DN with MIL-L-7808 oil are presented in Table 4, for unloaded and the maximum loaded roller contacts. All tabulated values were computed with the full EHD, fluid mechanics, dimensional, and thermal models described in this paper.

A roller always rotates near a pure rolling condition (low sliding velocity) at the outer race contact of a roller bearing with inner race or shaft rotation. Sliding velocities from near zero to 3 in/sec are typical as shown in Tables 4a and 4b for outer-race contact.

An unloaded roller, Table 4a, rotates about its own axis at an angular speed slightly less than the angular speed required for pure rolling at the outer race contact. Positive sliding (outer race relative surface velocity is greater than the roller surface velocity) always occurs and is in the range of near zero to 3 in/sec. The rolling portion of the total traction value is significant and cannot be ignored. Indeed the rolling portion can even predominate as shown by the ratio of rolling traction to total traction in Table 4a.

A loaded roller which produces a cage driving force rotates about its own axis at an angular speed slightly greater than the angular speed required for pure rolling at the outer race contact. Negative sliding occurs and is in the range of near zero to -3 in/sec as shown in Table 4b. The maximum loaded roller and most of the loaded rollers in the bearing have negative sliding at the outer race. Occasionally a lightly loaded roller or rollers near the entry and exit from the radial load zone will have positive sliding at the outer race contact. Such rollers result in a net drag on the cage similar to completely unloaded rollers. In all cases the rolling portion of the total traction is significant and cannot be ignored.

A loaded roller always has positive sliding at the inner race contact. Typical values are shown in Table 4c. A bearing operating at essentially epicyclic cage speed (no cage slip) has very low values of sliding velocity (< 3 in/sec) at the inner race contact and the rolling portion of the total traction is significant. A bearing operating with measureable cage slip can develop high values of positive sliding velocity at the inner race contact as shown in Table 4c. In these cases the sliding portion of the traction reaches a ceiling value and again the rolling portion of the total traction value is significant and cannot be ignored.

A high speed roller bearing with elastohydrodynamic oil films cannot operate under a pure rolling condition. An examination of the traction formulation of Eq. (3) shows that for zero sliding vehocities the traction at both inner and outer races would be negative and no equilibrium solution can occur as shown in Fig. 2. Some cage slip (however small) must occur.

RECOMMENDATIONS

1. Experimental data defining the rolling portion of the total traction force in an EHD contact is needed. The accuracy and usefulness of a complete systems analysis of a high speed roller bearing is very dependent upon good rolling friction data.

Archard and Crook[1] have stated that for loads which develop essentially parallel surfaces in the Hertzian contact and at speeds of sliding above a few centimeters per second, the sliding component of traction predominates and the rolling component can be ignored. This assumption has been generally accepted and has led to an emphasis upon obtaining twin disk traction data only for sliding conditions by current researchers.

Typical twin disk machines (with equal size disks) measure only the sliding contribution to the total traction in an EHD contact. Because of disk symmetry the data is also symmetric about zero sliding speeds, i.e., the traction value vanishes at zero sliding and reversal of the relative sliding direction reverses the direction of the traction. The rolling portion of the total traction is very small compared to maximum traction values. The instrumentation of existing traction machines is not designed to measure small magnitudes of rolling traction, indeed the contribution of rolling traction is calibrated-out along with disk support bearing friction. Symmetry of test machine geometry leads to symmetry of results. Special attention to non-symmetrical bench rig design and instrumentation is required.

2. Cage dynamics need to be explored and better defined both experimentally and analytically. Bi-stable [15] operation is shown to be possible by the present analysis.

ACKNOWLEDGEMENT

The authors express their thanks to The Franklin Institute Research Laboratories for sponsoring development of the computer program and preparation of this paper.

FIGURES

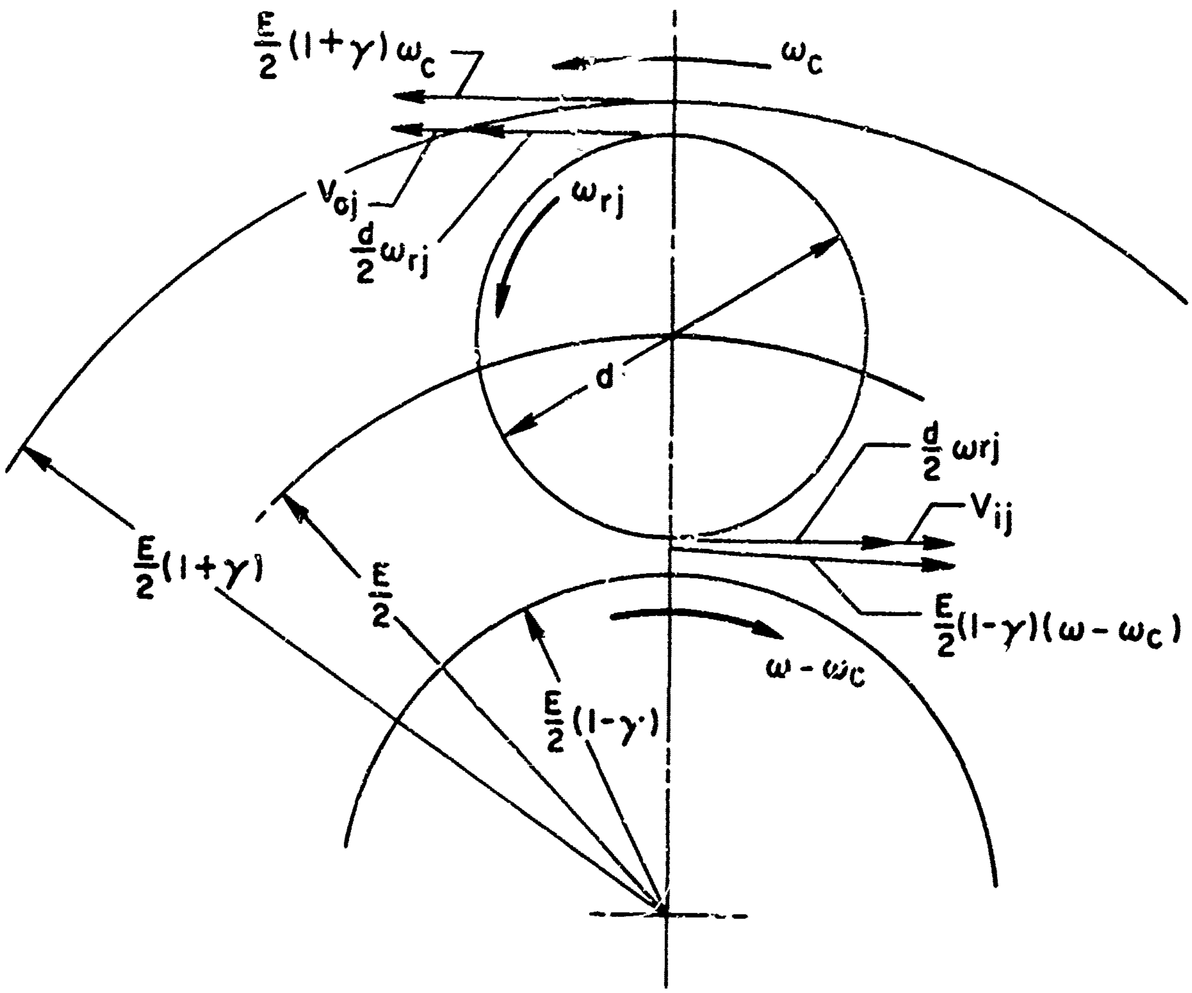

Figure 1. Surface Velocities and Relative Rotational Speeds of Raceways and Rollers Including Slip at Each Contact as a Result of Cage Slip

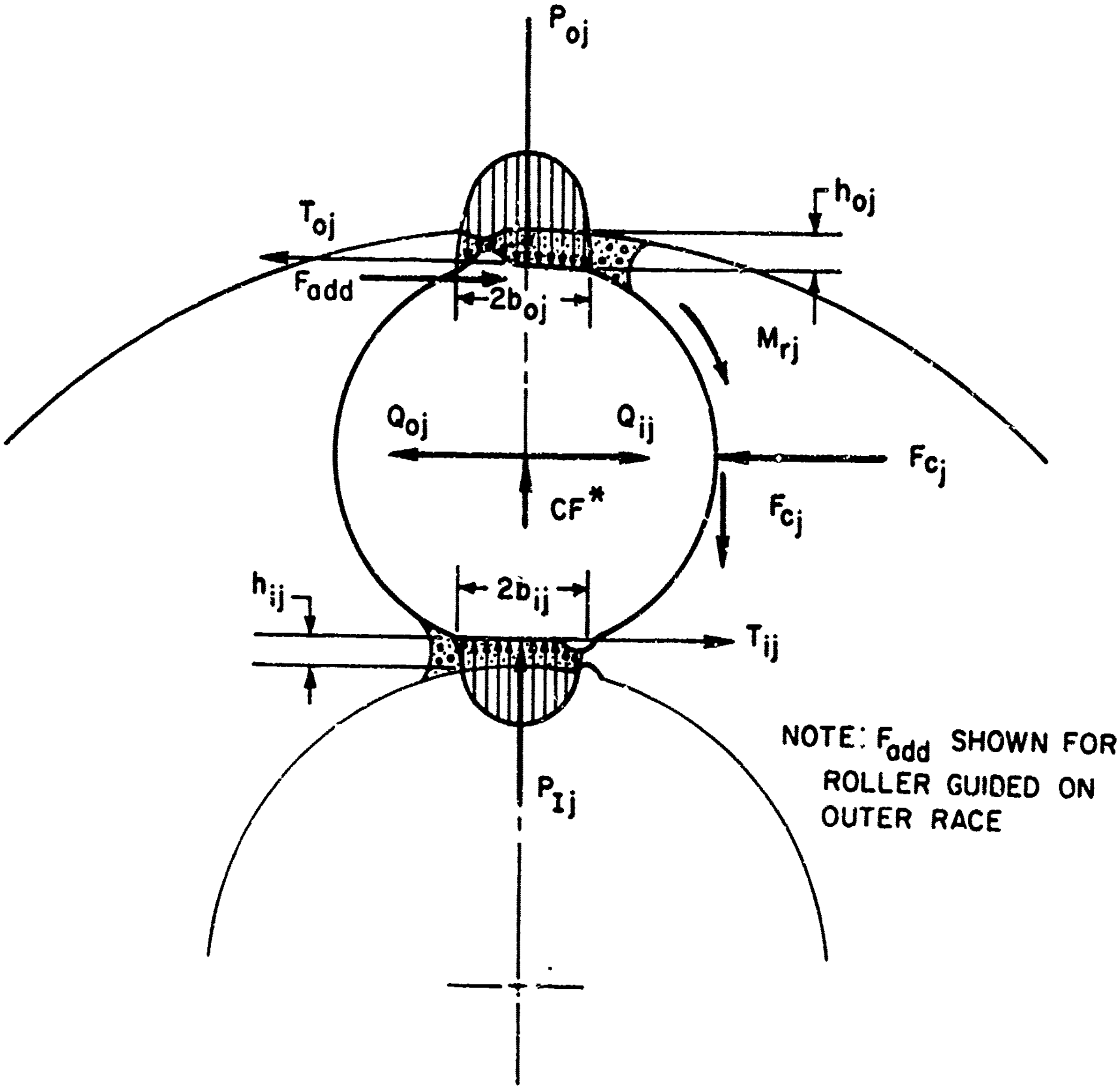

Figure 2. Forces and Moments Acting on a Loaded Roller

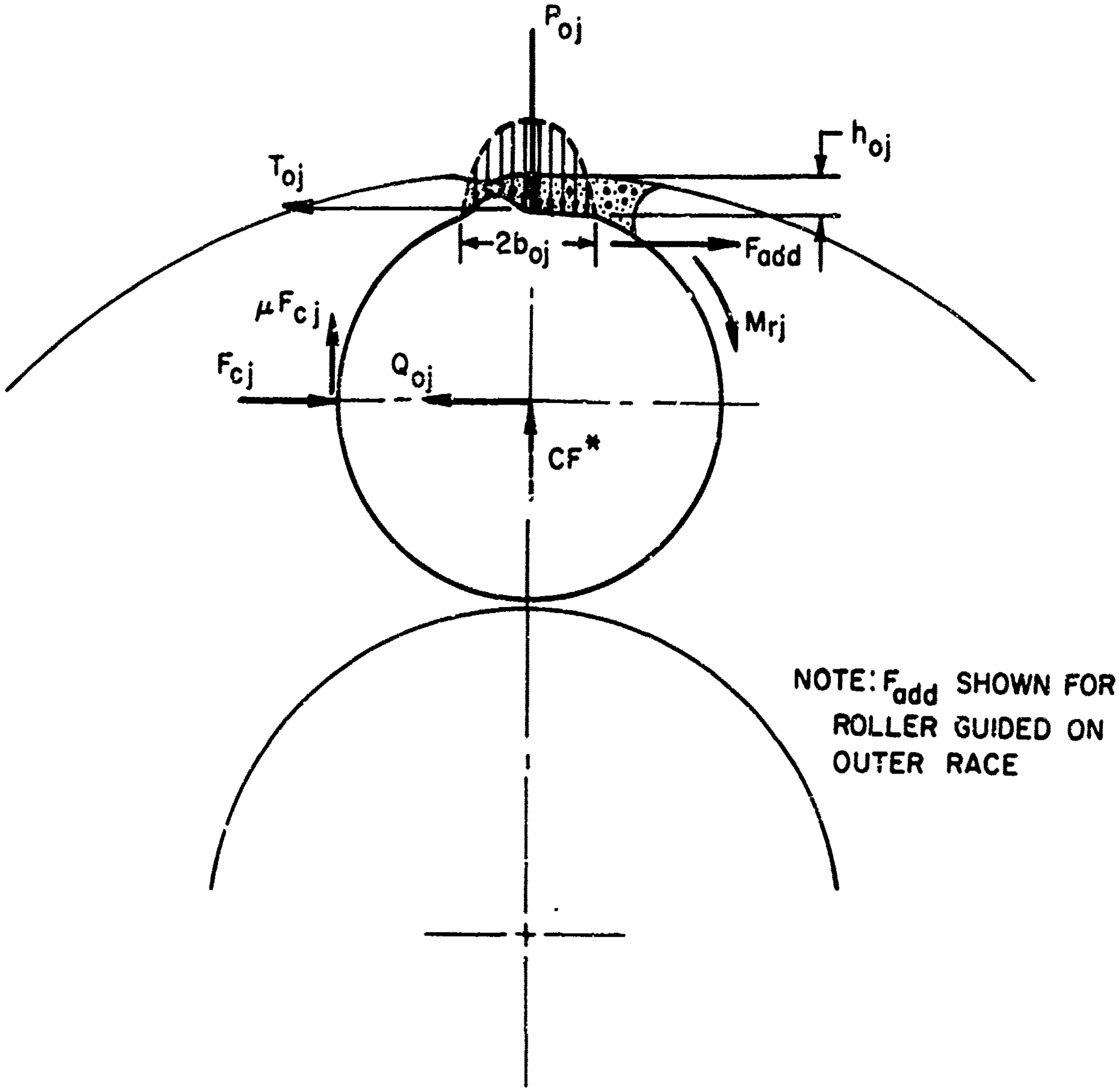

Figure 3. Forces and Moments Acting on an Unloaded Roller

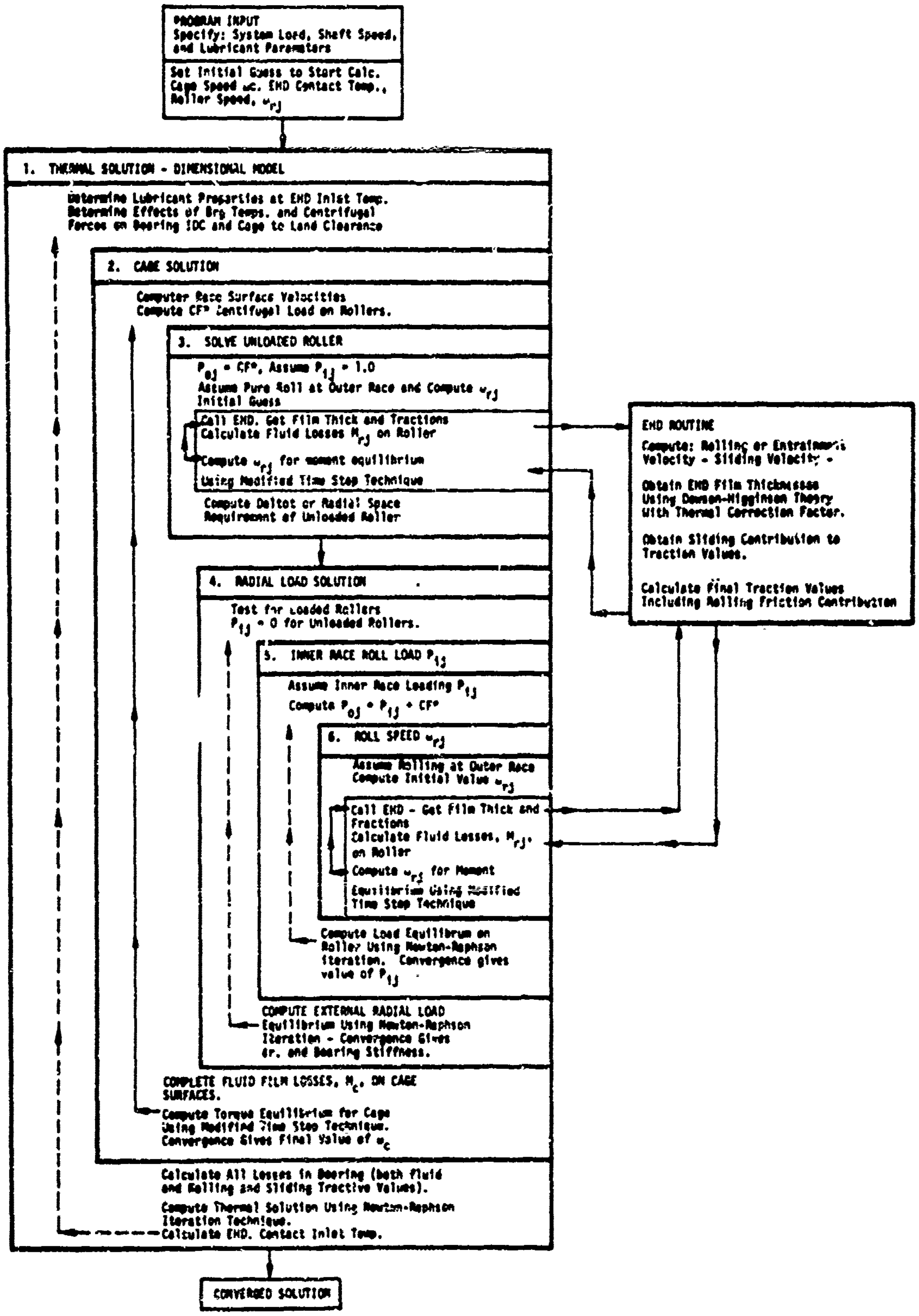

Figure 4. Solution Techniques Flow Chart

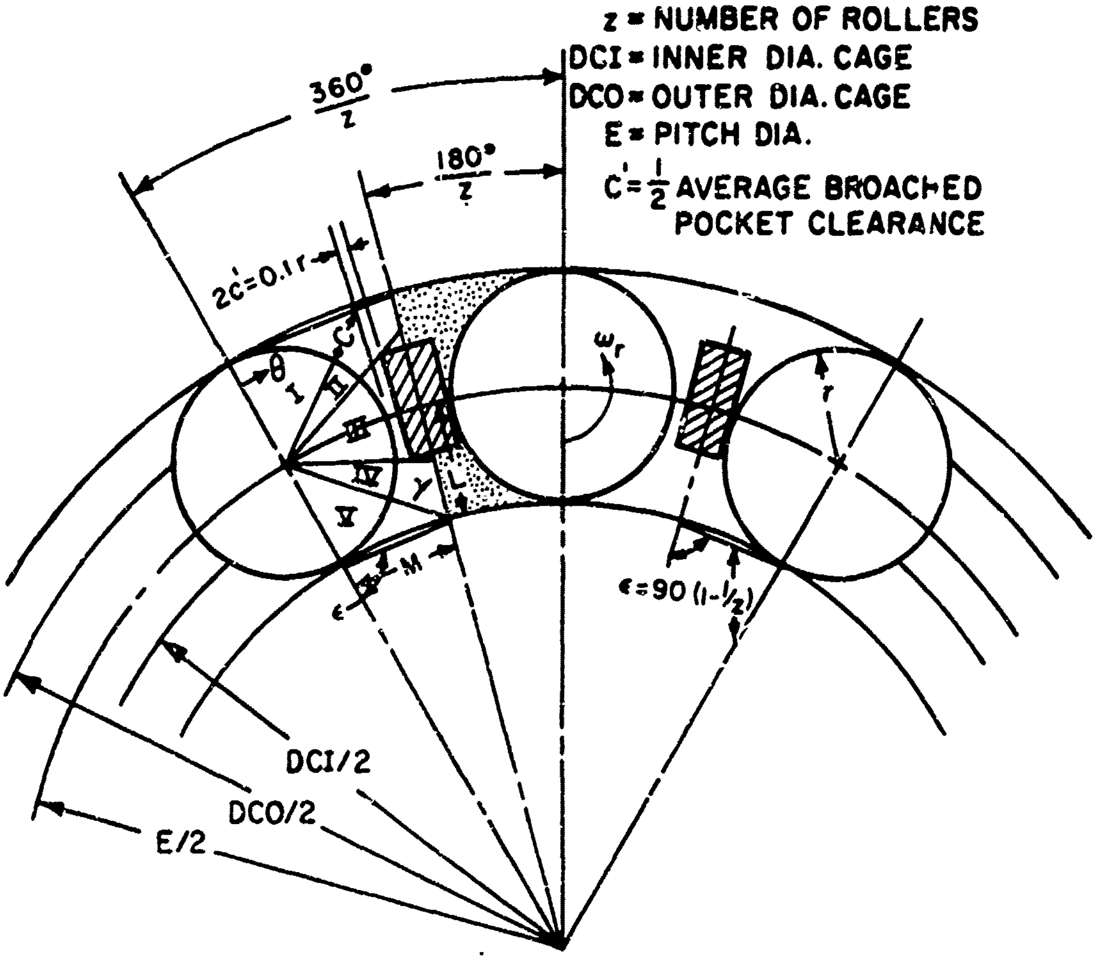

Figure 5. Roller Clearance Distribution in Cage

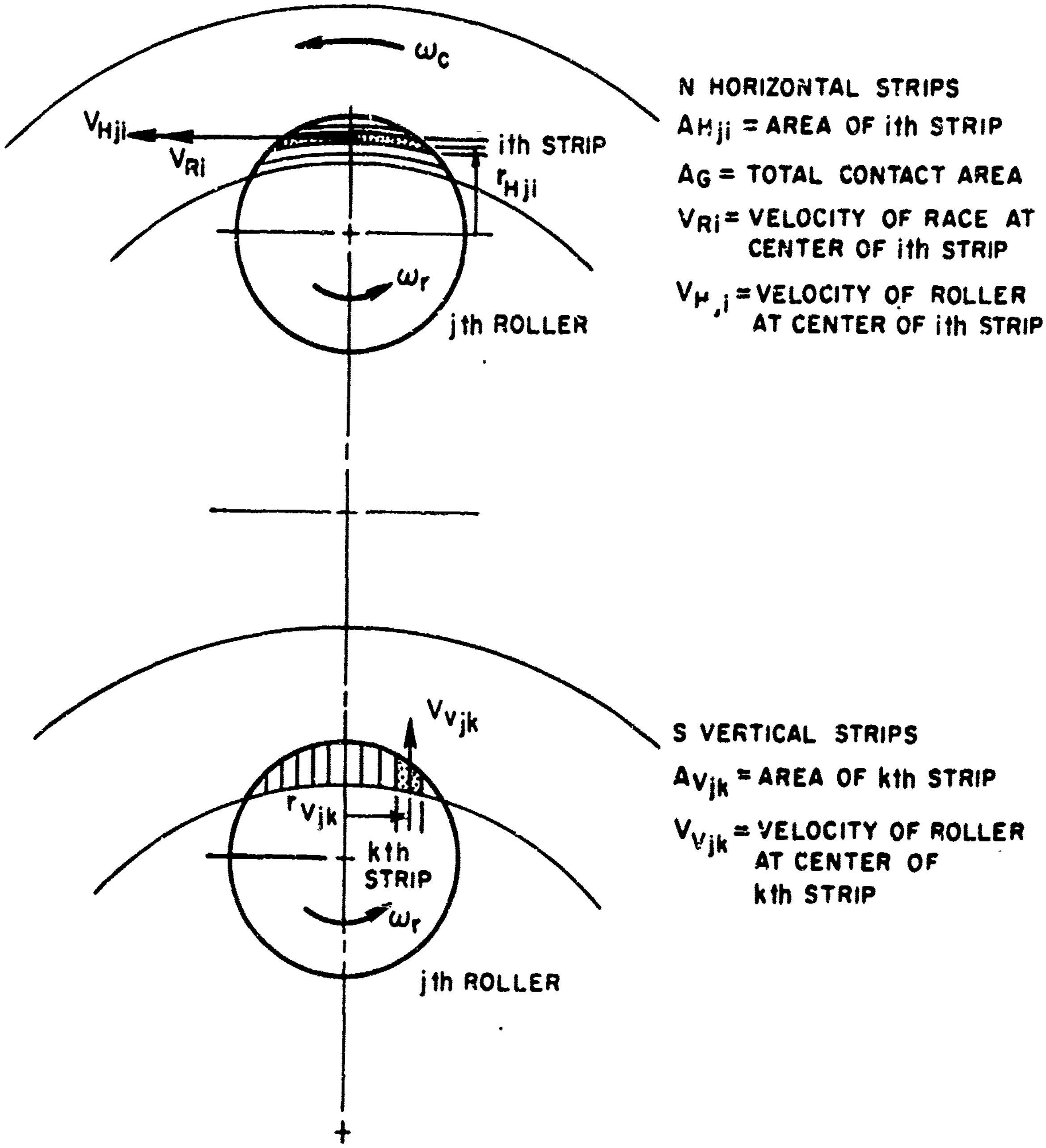

Figure 6. Mathematical Model of Horizontal and Vertical Relative Velocity Distributions in Roller-Shoulder Contact

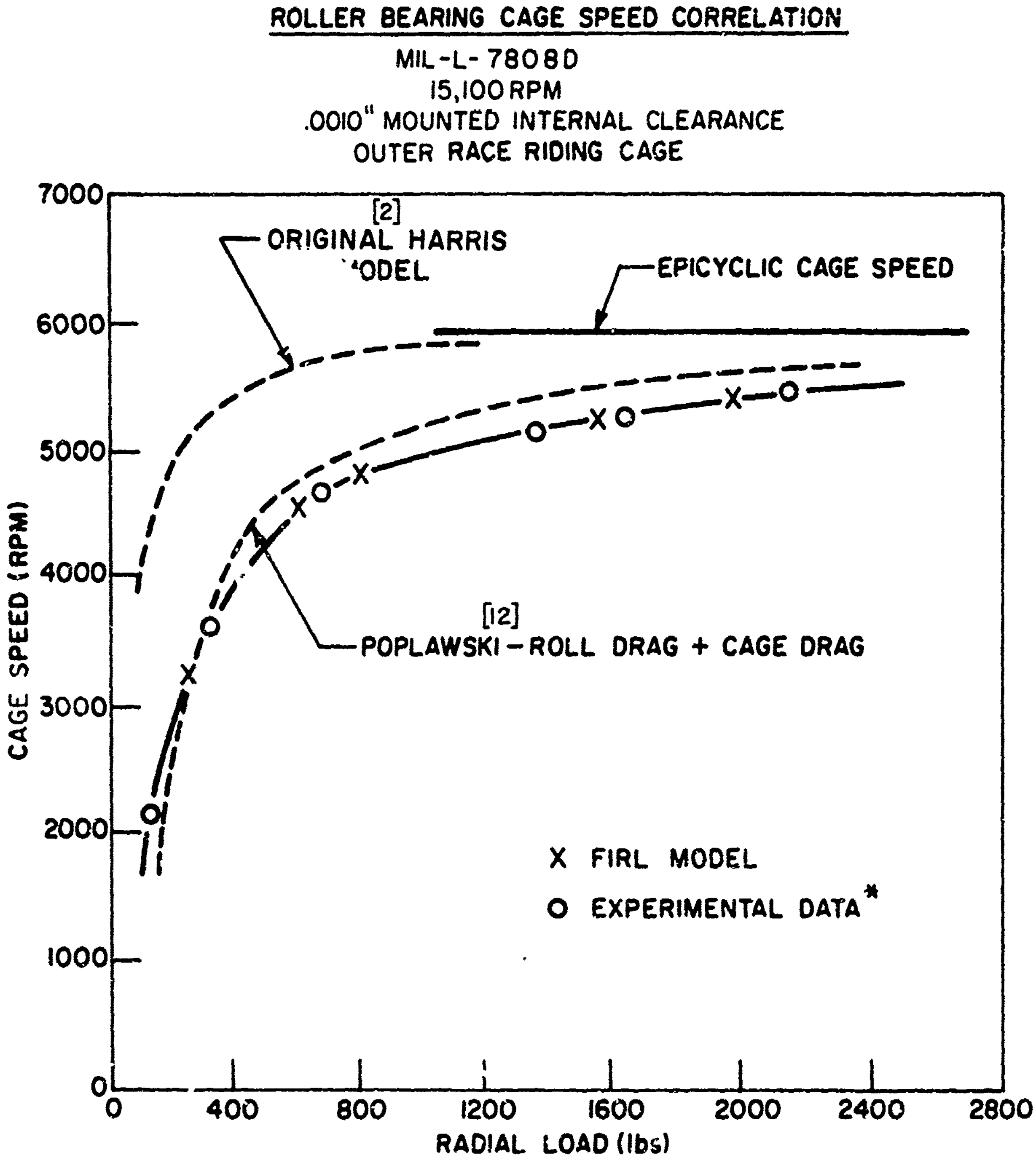

*DATA - *Courtesy of* BOEING COMPANY
VERTOL DIVISION
PHILADELPHIA, PA.

Figure 7. Roller Bearing Cage Speed Correlation

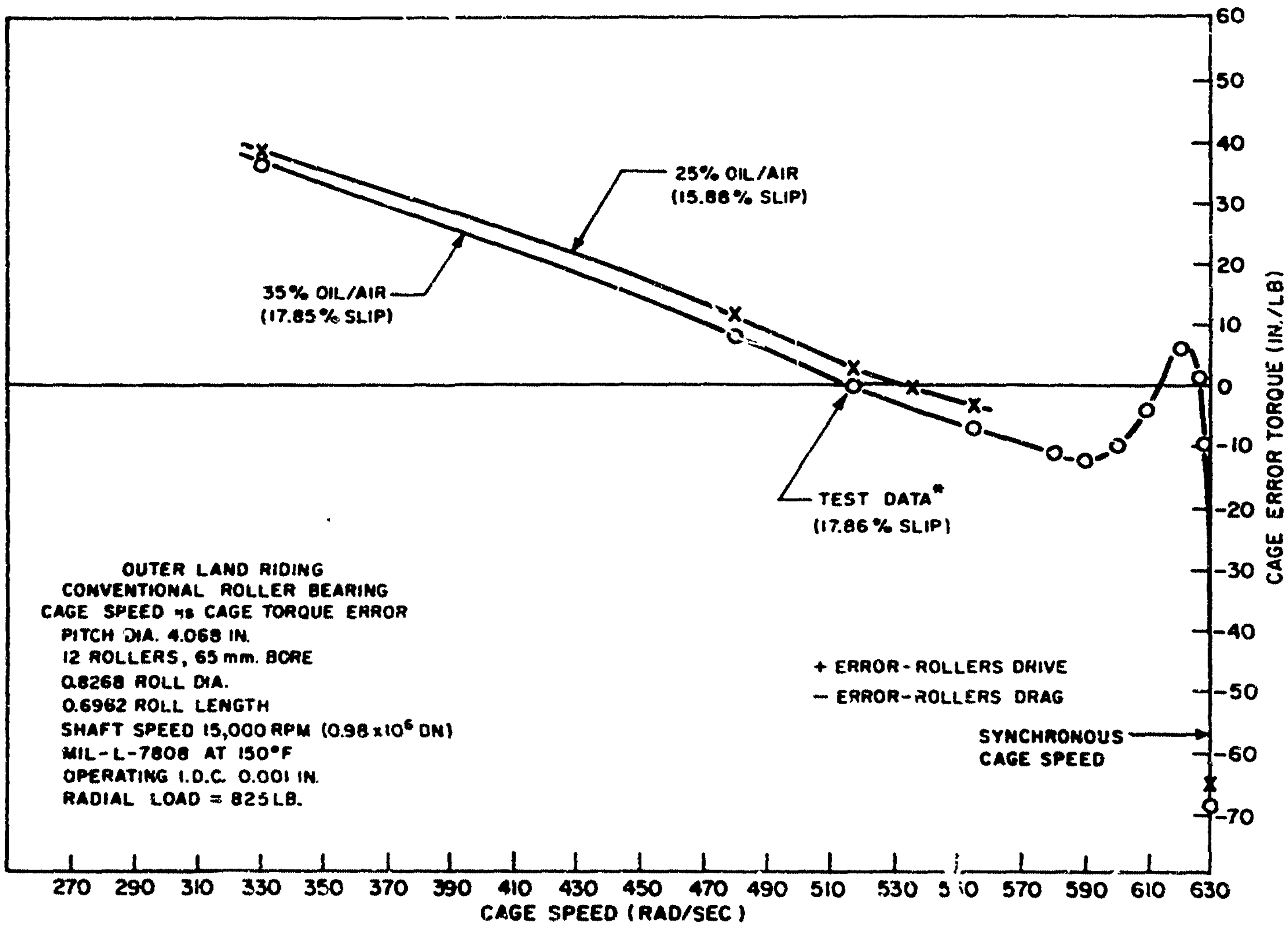

*COURTESY OF BOEING VERTOL DIVISION

Figure 8. Influence of Oil/Air Ratio on Each Solution

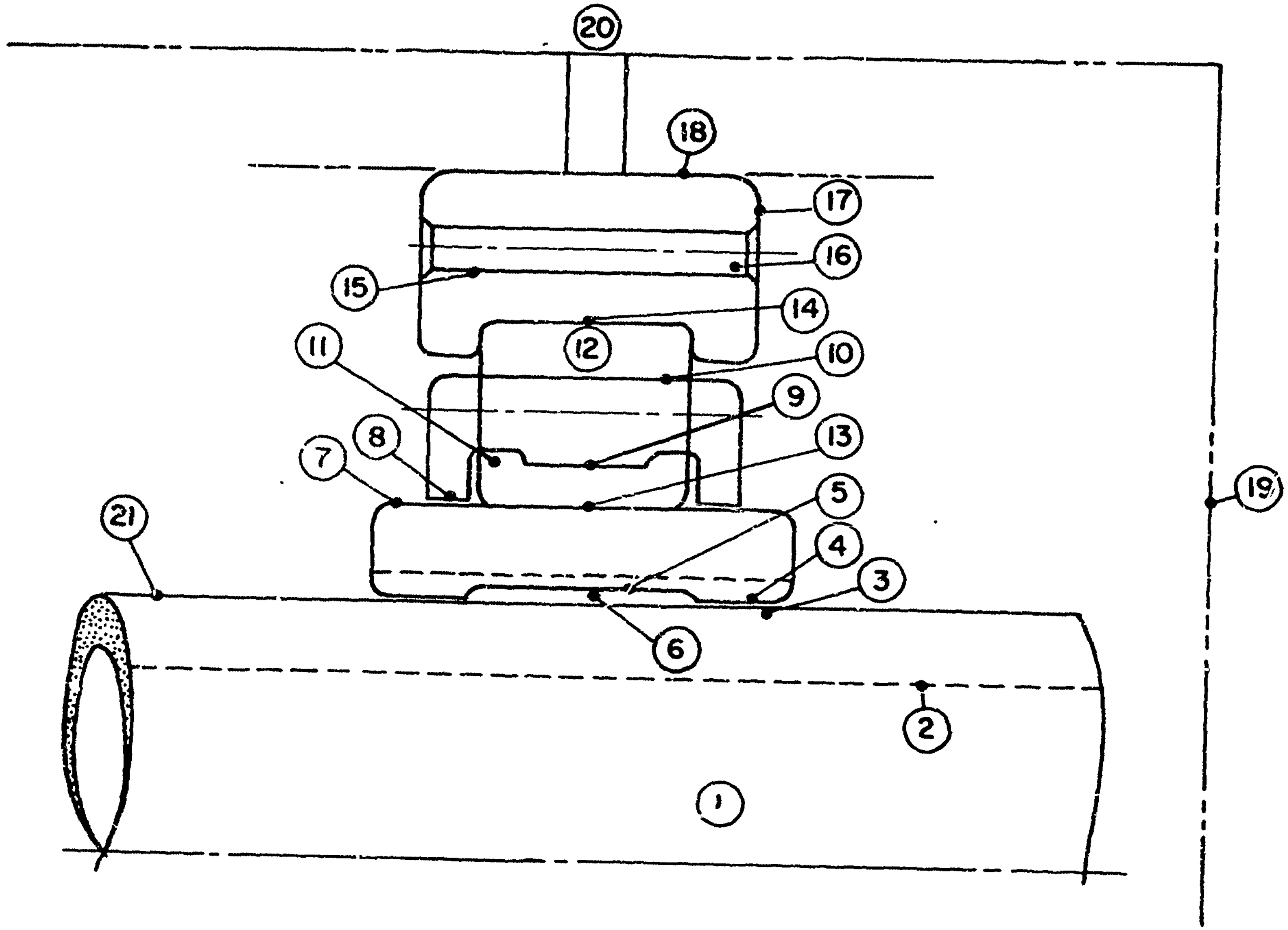

Figure 9. Nodes used in Thermal Analysis

TABLES

Table I

DIMENSIONAL MODELS
DIAMETER GROWTH DUE TO CENTRIFUGAL EFFECTS

Location	Model	Formula
Hollow Roller Outer Surface	Generalized Plain Strain	$\delta_{rot} = \frac{\rho_r \omega_r^2 r_o (1+\sigma_r)(3-2\sigma_r)}{2 E_r (1-\sigma_r)} \left[(1-\sigma_r) r_i^2 + \frac{(1-2\sigma_r)}{(3-2\sigma_r)} r_o^2 \right] + \frac{\rho_r \omega_r^2 r_o \sigma_r^2}{E_r} (r_i^2 + r_o^2)$
Solid Roller Outer Surface	Plane Stress	$\delta_{rot} = \frac{\rho_r r_o^3 \omega_r^2}{2E_r} (1-\sigma_r)$
Inner Race & Hollow Shaft Outer Surface	Plane Strain	$\delta_{IR_o} = \frac{\rho_{IR} \Omega^2 r_o (1+\sigma_{IR})(3-2\sigma_{IR})}{2E_r (1-\sigma_{IR})} \left[(1-\sigma_{IR}) r_i^2 + \frac{(1-2\sigma_{IR})}{(3-2\sigma_{IR})} r_o^2 \right]$
Inner Race Inner Surface	Plane Strain	$\delta_{IR_i} = \frac{\rho_{IR} \Omega^2 r_i (1+\sigma_{IR})(3-2\sigma_{IR})}{2E_r (1-\phi_{IR})} \left[\frac{(1-2\sigma_{IR})}{(3-2\sigma_{IR})} r_i^2 + (1-\sigma_{IR}) r_o^2 \right]$
Inner Land Riding Cage - Land Diameter	Plane Stress	$\delta_{C_L} = \frac{\rho_C \omega_C^2 r_L (3+\sigma_C)(1-\sigma_C)}{2E_C} \left[\frac{r_L^2}{(3+\sigma_C)} + \frac{r_o^2}{(1-\sigma_C)} \right]$
Outer Land Riding Cage - Land Diameter	Plane Stress	$\delta_{C_L} = \frac{\rho_C \omega_C^2 r_L (3+\sigma_C)(1-\sigma_C)}{2E_C} \left[\frac{r_i^2}{(1-\sigma_C)} + \frac{r_L^2}{(3+\sigma_C)} \right]$

ρ, mass density (lb-sec^2/in.^{4})

Ω, shaft angular velocity (rad/sec)

ω_C, cage angular velocity (rad/sec)

σ, Poisson's ratio

E, Youngs Modulus, (lb/in.^{2})

r_i, innermost radius (in.)

r_o, outermost radius (in.)

r_L, cage land radius (in.)

Table 2
DESCRIPTION OF THERMAL ANALYSIS BY NODES

Node	Location and Description	Heat Transfer Path: With Nodes	Heat Transfer Path: Type	Dissipative and External Energy Assignments	Remarks
1	Inner Shaft Coolant	2,21	CV	$Q_1 = \dot{m}_1 C_{p1}(T_{IN_1} - T_1)$	Coolant flow through hollow shaft.
2	Inner Shaft Surface	1 3,4(a),21(b)	CV C		a) for $\Delta \leq 0$ interference fit b) use average of T_2 & T_3
3	Outer Shaft Surface	4(c),6 2,4(a),21(b)	CV C		c) for $\Delta > 0$ loose fit on shaft
4	Outer Edges of Underside of Inner Race (In Contact with Shaft)	3(c),6(d) 2(a),3(a),5,21(a)	CV C		d) use average of T_4 & T_5
5	Middle Section of Underside of Inner Race	6(e)(d),6 4,7,13	CV C		e) sides of undercut
6	Under Race Coolant	3.4&5(d,e),5,18,19,21	CV	$Q_6 = \dot{m}_6 C_{p6}(T_{IN_6} - T_6)$	Oil flow cooling under inner race.
7	Outer Edges of Top Side of Inner Race	11 5,13 8(f)	CV C R	1/6 Q_{DIS}-Cage-Inner Surface 1/3 Q_{DIS}-Lands(f)	f) for inner land riding cage
8	Lands of Cage	11,11(h),11(i) 9 7(f),14(g)	CV C R	1/3 Q_{DIS}-Lands(f or g)	g) for outer land riding cage h) use average of T_8 & T_9 inner side surface i) use average of T_8 & T_{10} outer side surface
9	Inner Surface of Cage	11,11(h) 8,10 12,14	CV C R	1/3 Q_{DIS}-Cage-Inner Surface 1/2 $Q_{COUL}^{(j)} \left(\frac{V_C}{V_C+V_R}\right)$	j) dissipation due to Coulomb friction between roller and cage pockets. V_C = Cage Volume V_R = Roller Volume (Total)
10	Outer Surface of Cage	11(i),11 9 12,14	CV C R	1/2 $Q_{COUL}^{(j)} \left(\frac{V_C}{V_C+V_R}\right)$ 1/2 Q_{DIS}-Cage-Outer Surface	
11	Oil Within Bearing	7,8,9,10,12,13,14 8&9(h),8&10(i) 18,19,21	CV CV CV	$Q_{11} = \dot{m}_{11} C_{p11}(T_{IN_{11}} - T_{11})$ 1/3 Q_{DIS}-Cage-Inner Surface 1/2 Q_{DIS}-Cage-Outer Surface 1/3 Q_{DIS}-Lands 1/2 Q_{DIS}-Rollers 1/2 Q_{SLIDE}-Inner Race 1/2 Q_{SLIDE}-Outer Race $Q_{DIS}^{(k)}$	Oil flow through bearing k) Q_{DIS} is internal fluid energy dissipation not attributable to particular surfaces and = Shaft Power - Sum of Surface Dissipations. Q_{SLIDE} = EHD Traction x Sliding Velocity
12	Rollers	11 9,10,13,14	CV R	1/2 Q_{DIS}-Rollers $Q_{COUL} \left(\frac{V_R}{V_C+V_R}\right)^{(j)}$ 1/4 Q_{SLIDE}-Inner Race 1/4 Q_{SLIDE}-Outer Race	
13	Middle Section of Top Side of Inner Race (Roller Path)	11 5,7 9,12	CV C R	1/4 Q_{SLIDE}-Inner Race 1/6 Q_{DIS}-Cage-Inner Surface	
14	Inner Surface of Outer Race (Roller Path)	11 15 8(g),10,12	CV C R	1/4 Q_{SLIDE}-Outer Race 1/3 Q_{DIS}-Lands(g)	
15	Inner (Cooled) Surface of Outer Race	16 14,17	CV C		
16	Outer Race Cooling Fluid	15,17,18,19,21	CV	$Q_{16} = \dot{m}_{16} C_{p16}(T_{IN_{16}} - T_{16})$	Oil flow through outer raceway
17	Outer (Cooled) Surface of Outer Race	16 15,18	CV C		
18	Outer Surface of Outer Race	6,11,16,21 17,19,20 19	CV C R		
19	Chamber Wall	6,11,16 18 18	CV C R	$Q_{EXT_{19}}^{(l)}$ Q_{LOSS}-CV&R-Ambient Air	l) external energy input from other bearings, seals, etc.
20	Load Yoke Rest	18	C	Q_{LOSS}-CV-Ambient Air.	
21	Outer Shaft Surface Remote From Bearing	1,6,11,16(m),18 2&3(b),4(a)	CV C	$Q_{EXT_{21}}^{(l)}$	m) assumes all cooling oil flows mix at node 21 on way to common sump.

CV - Convection
C - Conduction
R - Radiation

Table 3
TYPICAL THERMAL ANSLYSIS

Bearing & Lubricant Data

Pitch diameter - 6.512 in.
Roller diameter - 0.5 in.
Operating IDC - .002 in.
Operating radial land clearance - 0.015 in.
Lubricant - MIL-L-7808D
Lubricant flow rates - 6 lb/min through bearing (both runs)
6 lb/min under race (2nd run only)
Lubricant inlet temperature - 250°F
Radial load - 333 lb
Shaft speed - 14,280 rpm
Oil/air ratio in bearing - 15%

Temperature Distribution (Ref. Fig. 9)

Node	Location	Temperature, °F No Under-Race Cooling	Temperature, °F Under Race Cooling
1	Inner shaft coolant	--	--
2	Inner shaft surface	361.5	295.8
3	Outer shaft surface at bearing	[illegible]	293.6
4	Inner race at shaft	[illegible]	310.7
5	Under-cut surface of inner race	362.5	314.6
6	Under race coolant	--	265.9
7	Inner race beyond roller contact	361.7	317.1
8	Cage at the land	380.8	370.3
9	Cage inner surface	393.1	383.1
10	Cage outer surface	392.9	383.0
11	Internal lubricant to bearing	330.7	318.3
12	Rollers	351.3	339.2
13	Inner race at rollers	367.5	324.8
14	Inner surface of outer race	329.9	30[illegible].2
15	Inner cooled surface outer race	329.9	307.[illegible]
16	Outer race lubricant	--	--
17	Outer cooled surface outer race	329.8	306.2
18	Bearing outer diameter	329.4	302.6
19	Chamber wall (inner side)	309.0	273.7
20	Loading bolt (strut) root	281.8	260.1
21	Shaft (external to bearing)	335.3	293.1

	No Under-Race Cooling	With Under-Race Cooling
Percent cage slip	32.5	33.7
Power dissipation, H_p	7.09	7.15
Initial shrink fit, in.	0.0082	0.0088
Machined IDC, in.	0.0097	0.0089
Mounted IDC, in.	0.0024	0.0011
Machined diametral land clearance, in.	0.0037	0.0035
Mounted diametor land clear...ce, in.	0.0029	0.0027
Mixed lubricant temperature at sump, °F	330.7	292.3

Table 4

TYPICAL EHD FILM THICKNESS AND TRACTION VALUES

4a

OUTER RACE CONTACT OF UNLOADED ROLLERS

Brg. DN $\times 10^{-6}$	% Cage Slip	V_{oj} in/sec	V_{sj} in/sec	P_{oj} lbs.	$f(To)_o$	Sliding Portion $\frac{\lvert V_{sj}\rvert}{V_{oj}} f(To)_o P_{oj}$ lbs.	Rolling Portion $-0.2\frac{h^{-0.7} ...}{g^{0.3}}$ lbs.	Traction T_{oj} lbs.	Oil Film Thick. h $\times 10^{6}$	EHD Contact Temp To °F	Oil Type	Bore mm	Ball Dia. in.	Cage Riding Land	Radial Load lbs.	Ratio $\lvert Rolling\rvert / T_{oj}$
1.0	10.0	1363	3.31	172.37	0.0098	1.508	- 0.401	0.907	33.2	150	MIL-L-7808	65	0.3360	Outer	825	0.70
1.36	0.087	1651	1.075	60.6	0.010	0.607	- 0.365	0.332	19.9	150	MIL-L-7808	115	0.500	Inner	3075	1.13
2.0	0.066	1552	3.133	34.71	0.016	0.347	- 0.132	0.435	[illegible]	150	MIL-L-7808	140	0.250	Inner	333	0.30
3.0	19.05	3021	2.623	66.0	0.0086	0.758	- 0.323	0.430	[illegible]	[illegible]	MIL-L-7808	140	0.125	Inner	333	0.75
4.0	0.0005	3112	1.000	130.07	0.0093	1.332	- 0.212	1.130	[illegible]	[illegible]	MIL-L-7808	140	0.250	Inner	333	0.19
4.0	30	2307	2.375	76.23	0.012	0.907	- 0.172	0.730	[illegible]	150	MIL-L-7802	140	0.250	Inner	100	0.23
4.0	0.006	3115	0.010	130.07	0.0070	0.965	- 0.133	0.814	[illegible]	500	5P4E	150	0.250	Inner	333	0.19

4b

OUTER RACE CONTACT OF MAXIMUM LOADED ROLLER

Brg. DN $\times 10^{-6}$	% Cage Slip	V_{oj} in/sec.	V_{sj} in/sec.	P_{oj} lbs.	$f(T_o)_{oj}$	Sliding Portion $\frac{\lvert V_{sj}\rvert}{V_{oj}} f(T_o)_{oj} P_{oj}$ (lbs.)	Rolling Portion $-0.2\frac{h^{0.7} ...}{g^{0.3}}$ (lbs.)	Total Traction T_{oj} (lbs)	Oil Film Thick. in $\times 10^{6}$	EHD Inlet Temp T_o °F	Oil Type	Bore mm	Ball Dia. in.	Cage Riding Land	Radial Load lbs.	Ratio $\lvert Rolling\rvert / T_{oj}$
1.0	10.0	1362	-3.10	375.0	0.0081	- 5.039	- 0.692	- 5.351	30.7	150	MIL-L-7808	65	0.3360	Outer	825	0.13
1.36	0.037	1633	-0.09	353.9	0×10^{-6}	- .004	- 0.364	- 0.368	11.3	150	MIL-L-7808	115	0.500	Inner	3075	3.99
2.0	0.066	1556	-0.46	247.0	0.010	- 2.342	- 0.130	- 2.071	6.7	150	MIL-L-7808	140	0.250	Inner	333	0.05
3.0	10.06	2023	-1.735	185.1	0.0042	- 0.781	- 0.323	- 1.103	13.0	150	MIL-L-7808	140	0.500	Inner	333	0.29
4.0	0.0005	3113	-0.0003	715.1	0.0030	- 2.776	- 0.212	- 2.988	7.7	150	MIL-L-7808	140	0.236	Inner	333	0.07
4.0	30	2305	-0.6×10^{-4}	130.5	3×10^{-6}	- .001	- 0.171	- 0.172	8.9	150	MIL-L-7808	140	0.250	Inner	100	0.99
4.0	0.006	3113	-0.6×10^{-4}	375.9	0.0030	- 1.097	- 0.153	- 1.250	2.1	500	5P4E	140	0.250	Inner	333	0.12

4c

INNER RACE CONTACT OF MAXIMUM LOADED ROLLER

Brg. DN $\times 10^{-6}$	% Cage Slip	V_{ij} in/sec.	V_{sj} in/sec.	P_{ij} lbs.	$f(To)_{ij}$	Sliding Portion $\frac{\lvert V_{sj}\rvert}{V_{ij}} f(To)_{ij} P_{ij}$ (lbs.)	Rolling Portion $-0.2\frac{h^{0.7} ...}{g^{0.3}}$ (lbs.)	Total Traction T_{ij} (lbs.)	Oil Film Thick. $\times 10^{6}$	EHD Inlet Temp To °F	Oil Type	Bore mm	Ball Dia. in.	Cage Riding Land	Radial Load lbs.	Ratio $\lvert Roll\rvert / T_{ij}$
1.0	10.0	1863	454.5	387.7	0.0190	7.886	- 0.687	7.179	35.0	150	MIL-L-7808	65	0.3360	Outer	825	0.10
1.36	0.087	3653	3.730	663.7	0.0081	1.030	- 0.365	0.692	11.3	150	MIL-L-7808	115	0.535	Inner	3075	0.50
2.0	0.066	3618	43	315.3	0.018	3.860	- 0.165	3.675	11.0	150	MIL-L-7808	140	0.50	Inner	333	0.04
3.0	19.05	3003	3	90.0	0.0315	2.136	- 0.306	1.713	11.6	150	MIL-L-7802	140	0.50	Inner	333	0.20
4.0	0.0006	6336	0.004	370.0	0.0067	3.000	- 0.360	4.732	5.5	150	MIL-L-7808	140	0.50	Inner	333	0.06
4.0	30	4610	2370	34.6	0.510	1.443	- 0.576	2.780	10.6	150	MIL-L-7808	140	0.50	Inner	100	0.31
4.0	0.0006	6306	0.02	140.9	0.610	2.733	- 0.156	3.130	2.3	500	Polyphenyl Ether 5P4E	140	0.50	Inner	333	0.05

NOMENCLATURE

Load & Speed Equilibrium

b	=	semi-width of Hertzian contact - in.
C_r	=	hollow roller ring deflection constant - in/lb.
CF^*	=	centrifugal force acting on roller - lb.
d	=	roller diameter - in.
E	=	pitch diameter of bearing - in.
E_{YM}	=	Modulus of elasticity - lb./in^2
E'	=	reduced Modulus = $E_{ym}/(1-\sigma^2)$
f(Te)	=	coefficient of traction at temperature T_e
Fddd	=	contact force on roller from guiding race shoulder (lb.)
F_c	=	cage to roller force - lb.
F_x	=	radial external load - lb.
G	=	material parameter = $\alpha E'$
G1,G2,G3	=	parameters to determine f(Te)

$G_1 = \dfrac{\eta_e V}{P_{hz} h}$ (Shear Rate Effects)

$G_2 = \dfrac{\beta_1 \eta_e V^2}{8K_f}$ (Thermal heating effects)

$G_3 = \alpha P_{hz}$ (Pressure viscosity effect)

h	=	lubricant average film thickness - in.
I_r	=	roller polar moment of inertia lb-in-sec^2
I_c	=	cage polar moment of inertia lb-in-sec^2
I	=	bending moment of inertia for hollow roller - in^4
K	=	roller to race deflection constant
K_f	=	thermal conductivity of lubricant, BTU/^oF-hr.-ft.
ℓ	=	effective length of roller contact - in.
m_r	=	roller mass - lb-sec^2/in.
M_c	=	cage fluid drag moment - lb-in.
M_r	=	roller fluid drag moment - lb-in.
P	=	roller load - lb
p	=	order of iteration
P_{HZ}	=	maximum Hertz contact stress - lb./in^2
Pd	=	diametral clearance - in.
Q	=	hydrodynamic pressure force - lb.
$\bar{Q}$	=	dimensionless form of Q $= Q/(\ell E'R)$
Q_m	=	dimensionless heating parameter $= 2\eta_e U^2/(K_f T_e)$
r	=	mean radius of hollow roller - in.
R	=	radius of an equivalent cylinder and plane - in.
t	=	thickness of hollow roller - in.
T	=	traction in an EHD contact - lb.
T_e	=	temperature of lubricant at entrance to EHD contact - °F
U	=	fluid entrainment velocity - in./sec.
$\bar{U}$	=	dimensionless form of U $= \eta_e V/(E'R)$

V	=	sliding velocity - in./sec.
$\bar{V}$	=	dimensionless form of V = $\eta_e V/(E'R)$
$\bar{W}$	=	dimensionless load = $P/(\ell E'R)$
X	=	radial displacement of inner race - in.
X_ϕ	=	deviation of races from true circular form - in.
Z	=	total number of rollers
α	=	pressure viscosity exponent - in^2/lb.
β	=	temperature viscosity coefficient - °F
γ	=	ratio of roller diameter to bearing pitch diameter
ψ_j	=	angular location of roller, deg.
ϕ_T	=	thermal reduction factor for EHD film thickness
Ω	=	angular velocity of inner race, rad/sec.
ω_c	=	angular velocity of cage, rad/sec
ω_r	=	angular velocity of roller, rad/sec.
η	=	lubricant absolute viscosity - lb.-sec/$in.^2$
μ	=	coulomb coeff of sliding friction
δ_o	=	roller - outer race deflection - in.
δ_i	=	roller - inner race deflection - in.
δ_{CF}	=	hollow roller deflection from CF^* - in.
δ_{ROT}	=	roller diametral expansion from ω_r - in.
δ_{TOTAL}	=	total deflection of an unloaded roller - in.
$\delta_{\phi j}$	=	relative movement of races at ϕ_j - in.
σ	=	poison's ratio

SUBSCRIPTS

i = inner race contact

o = outer race contact

j = roller number or location

u = an unloaded roller

e = entrance region of EHD contact

<u>Fluid Mechanics</u>

A	Surface Area in.^{2}
A_G	Total contact area between roller and guiding shoulders in.^{2}
A_{Hji}	Area of i^{th} horizontal lamina in.^{2}
A_p	Roller and cage surface area within typical crossflow passage exposed to crossflow in.^{2}
A_{Vjk}	Area of k^{th} vertical lamina in.^{2}
A_x	Cross sectional area of a typical crossflow passage in.^{2}
C	Radial clearance, in.
C'	Clearance of cage pocket and roller, in.
C_N	Laminar or turbulent correlation factor for disk rotating in a viscous fluid
F_{jG}	Contact force between roller and race guiding shoulder lb
f	Friction factor
f_L	Laminar friction factor
L	Bearing length
ℓ_p	Peripheral length of a typical crossflow passage in.
M_T	Moment about center line of a disk rotating in a viscous fluid in-lb.

N	Number of horizontal lamina
N_{Re}	Reynold's number (Defined in Text)
N_{Ta}	Taylor number (Defined in Text)
r	Reference radius in.
r_{Hji}	Distance from roller center to i^{th} horizontal lamina in.
r_i	Inner radius
r_o	Outer radius
r_{Vjk}	Distance from radial ray through roller center to k^{th} lamina in.
S	Number of vertical lamina
δ_p	Crossflow differential pressure lb/in.^{2}
T	Drag torque in.-lb
T_{add}	Moment contribution of contact force to roller drag moment in.-lb
T_{cland}	Fluid drag moment on cage lands in.-lb
T_{cside}	Fluid drag moment on cage sides in.-lb
T_{rend}	Moment contribution of roller ends to roller drag moment in.-lb
T_{rcyl}	Moment contribution of roller surface to roller drag moment in.-lb
U	Mass average velocity of fluid in./sec
$\overline{V}$	Peripheral crossflow surface average velocity in./sec
V_{Hji}	Velocity of roller at i^{th} horizontal lamina in./sec
V_{Ri}	Velocity of race at i^{th} horizontal lamina in./sec
V_{Vjk}	Velocity of roller at k^{th} vertical lamina in./sec
μ_c	Coulomb coefficient of friction between roller and race guiding shoulder
ν	Fluid Kinemetic visosity in.^{2}/sec
ρ	Fluid mass density lb sec^2/in.^{4}
τ_w	Wall shear stress, lb/in.^{2}

Thermal Analysis and Dimensional Model

a	roller inner radius, in.
B_k	energy rate constants in formulation of thermal problem, ref. equation (48), Btu/sec.
b	roller outer radius, in.
C	radial clearance between cylindrical surface - in.
c_{p_i}	specific heat of lubricant or coolent associated with i^{th} thermal node - Btu/lb°F.
$\bar{F}_{m,n}$	Radiation view factor between m^{th} and n^{th} surface
g	gravitational acceleration, 386.4 in./sec^2
H_{ij}	energy transfer between nodes i and j Btu/sec
h_k	convective conductance associated with k^{th} surface Btu/sec - in.^{2} °F
IDC	bearing internal diametral clearance - in.
k	thermal conductivity - Btu/sec in. °F
k_f	thermal conductivity of fluid - Btu/sec in. °F
ℓ_s	generic length of cylindrical surface - in.
m_i	lubricant or coolent flow rate of i^{th} thermal node - lb/sec.
N_i	total number of component dissipations, external energy inputs, energy transfer to coolent or lubricant flows, and losses at i^{th} thermal node.
N_i'	total subset of N_i not expiicity containing temperature.
$N_{Ta_{cond}}$	Taylor Number for pure conduction through a fluid.
$N_{Ta_{cr_\eta}}$	critical Taylor number at speed ratio η.
r_L	radius of inner race at land for an inner land riding cage or radius of outer race at land for an outer land riding cage - in.
T_{ave}	mixed lubricant temperature - °F

T_i	temperature of i^{th} thermal node - °F.
T_{ref}	initial uniform reference temperature of all bearing elements - °F
α	coefficient of thermal expansion - in./in. °F.
α_d	thermal diffusivity - in.^{2}/sec.
β	kinematic viscosity of fluid - in.^{2}/sec.
γ	coefficient of volumetric expansion - 1/°F.
ΔT_{ij}	Temperature difference between i^{th} and j^{th} thermal nodes, T_j-T_i, - °F.
Δt	absolute temperature difference between surface and fluid.
δ_{T_i}	thermal deformation of the i^{th} surface of a bearing member, (see Figure 1) - in.
ε_i	energy error function at i^{th} temperature node for Newton-Raphson solution of temperature field in bearing - Btu/sec.
ξ_m	emissivity of m^{th} surface.
μ	coulomb coefficient of friction between rollers and cage.
η	ratio of cage to shaft angular velocities.
ν	Poisson's ratio
σ	Boltzmann radiation constant - Btu/sec in.^{2} °R^4

12. Fritz, R. J., *Friction Factors for Use in Analysis of Journal Bearings with Vortex Turbulent Flow*, KAPL-M-6546, G. E. Knolls Atomic Power Laboratory, U. S. Atomic Energy Commission, Contract No. W-31-109 Eng-52.

13. Schlichting, Dr. H., *Boundary Layer Theory*, Fourth Edition, McGraw Hill Book Co., Inc., 1960.

14. Goldstein, S., *Modern Developments in Fluid Dynamics*, Vol. I and II, Dover Publications, Inc., 1965.

15. Ehrich, F. F., *Bistable Vibration of Rotors in Bearing Clearance*, presented at the winter annual meeting, ASME Machine Design Division, Chicago, Ill., Nov. 7-11, 1965.

16. Timoshenko and Goodier, "Theory of Elasticity," McGraw Hill Book Co. Inc., 1956.

17. Wang, "Applied Elasticity," McGraw Hill Book Co. Inc., 1953.

18. "New Departure Analysis of Stresses and Deflection," Vol. I, 1946. New Departure Division of G.M. Corp. Bristol, Conn.

19. Harris, T. A., "Rolling Bearing Analysis," John Wiley and Sons, Inc., 1966.

20. Eckert, E. R. G. and Drake, R. M., "Heat and Mass Transfer, Second Edition, McGraw Hill Book Co. Inc., 1959.

21. Bjorklund, I. S. and Kays, W. M., "Heat Transfer Between Concentric Rotating Cylinders," ASME Journal of Heat Transfer, Aug. 1959, Pages 175-186.

22. Jakob, M., Hawkins, G. A., "Elements of Heat Transfer and Insulation," John Wiley & Sons Inc., Second Edition, 1950.

23. Kays, W. M., "Corrective Heat and Mass Transfer," McGraw Hill Book Co. Inc., 1966.

SECTION VIII

REFERENCES

1. Rumberger, J. H., et.al., Gas Turbine Engine Mainshaft Roller Bearing - Systems Analysis", Submitted to Lubr. Div. ASME for publication in Trans. ASME, Jrnl. of Lubr. Tech. 1973.

2. Dowson, D. and Higginson, G. R., "Elastohydrodynamic Lubrication - The Fundamentals of Roller Gear Lubrication", Pergamon Press, New York, 1966.

3. Palmgren, A., "Ball and Roller Bearing Engineering", S. H. Borbank and Company, Third Edition, 1959.

4. McGrew, J. M., et. al., "Elastohydrodynamic Lubrication - Preliminary Design Manual", Technical Report AFAPL-TR-70-27, Air Force Aero Propulsion Laboratory, Air Force Systems Command, Wright Patterson Air Force Base, November 1970.

5. Nypan, L. J., et.al., "Optimal Speed Sharing Characteristics of a Series Hybrid Bearing", Trans. ASME, Jrnl. of Lub. Tech., Vol. 95, Series F, No. 1, January 1973, pp. 76-81.

6. Peacock, L. A., and Rhodes, W. L., "High Temperature Lubricant Screening Tests", SKF Industries, NASA CR 72615, September 1969, for NASA Lewis Research Center, Cleveland, Ohio.

7. Parker, R. J., Bamberger, E. N., and Zaretsky, E. V., "Bearing Torque and Fatigue Life Studies with Several Lubricants for Use in the Range 500° to 700°F", NASA Technical Note, TN-D-3948, May 1967.

8. Bamberger, E. N., Zaretsky, E. V., and Anderson, W. J., "Effect of Three Advanced Lubricants on High Temperature Bearing Life", ASME Jrnl. of Lub. Tech. Vol. 92, Series F, No. 1, January 1970, pp. 23-33.

9. Chasman, M. R., "Latest Avariable 5P4E High Pressure Viscometry Data", telephone conversation 10/1/71, Aero Propulsion Laboratory, WPAFB, Ohio.

10. Bamberger, E. N. - "Unpublished Information (1955) on reversed bending fatigue properties of Air Melt M-50 at 500°F" - Telephone Conversation - Nov. 1972.

SECTION VIII (Cont'd)

REFERENCES

11. FIRL **Computer Program,** *FEBOR, Finite Element Analysis Program for Bodies of Revolution Subjected to Axisymmetric Loading - Program No. 52-4.*